AUTOCATALYTIC DEPOSITION OF COMPOSITE COATINGS

MICHAEL IZZARD

Doctor of Philosophy

THE UNIVERSITY OF ASTON IN BIRMINGHAM

OCTOBER 1987

The University of Aston in Birmingham
Autocatalytic Deposition of Composite Coatings
Michael Izzard
Doctor of Philosophy
October 1987

The deposition and properties of electroless nickel composite coatings containing graphite, PTFE and chromium were investigated. Solutions were developed for the codeposition of graphite and chromium with electroless nickel.

Solutions for the deposition of graphite contained heavy metal ions for stability, with non-ionic and anionic surfactants to provide wetting and dispersion of the particles. Stability for the codeposition of chromium particles was achieved by oxidation of the chromium. Thin oxide layers of 200 nm thick prevented initiation of the electroless reaction onto the chromium. A mechanism for the formation of electroless composite coatings was considered based on the physical adsorption of particles and as a function of the adsorption of charged surfactants and metal cations from solution.

The influence of variables such as particle concentration in solution, particle size, temperature, pH, and agitation on the volume percentage of particles codeposited was studied. The volume percentage of graphite codeposited was found to increase with concentration in solution and plating rate. An increase in particle size and agitation reduced the volume percentage codeposited.

The hardness of nickel-graphite deposits was found to decrease with graphite content in the as-deposited and heat treated condition. The frictional and wear properties of electroless nickel-graphite were studied and compared to those of electroless nickel-PTFE. The self-lubricating nature of both coatings was found to be dependent on the ratio of coated area to uncoated area, the size and content of lubricating material in the deposit, and the load between contacting surfaces. The mechanism of self-lubrication was considered, concluding that graphite only produced an initial lubricating surface due to the orientation of flakes, unlike PTFE, which produced true self-lubrication throughout the coating life.

Heat treatment of electroless nickel chromium deposits at 850^{o}C for 8 and 16 hours produced nickel-iron-chromium alloy deposits with a phosphorus rich surface of high hardness. Coefficients of friction and wear rates were initially moderate for the phosphorus rich layer but increased for the nickel-iron-chromium region of the coating.

Key Words: Electroless nickel, composite coatings, self-lubrication, friction, wear.

ACKNOWLEDGEMENTS

I would like to thank the Science and Engineering Research Council and W. Canning Materials Ltd. for their financial support of this project. In particular I would like to thank Mr. S.J. Wake and Dr. A.J. Gould for their assistance and advice.

Sincere thanks are also due to Dr. J.K. Dennis, members of the staff and technicians of the Department of Mechanical and Production Engineering of Aston University for their assistance and valuable advice. A personal thanks also goes to Mr. John Foster and colleagues at BAJ Ltd.

Finally, I am indebted to my wife Gail, for her dedicated support and assistance in the production of this thesis.

CONTENTS

LIST OF FIGURES

LIST OF TABLES

CHAPTER I

INTRODUCTION

In recent years electroless, chemical, or more correctly termed autocatalytic nickel plating, has expanded into a multi-million pound industry as a wear and corrosion resistant coating. The reason for this growth can be explained by the ability of electroless nickel to overcome those problems which limit the use of electrolytically deposited nickel. Electrolytically deposited nickel has found wide use for its corrosion, erosion and fretting resistance, as well as its load bearing qualities. It does however, have certain disadvantages. For example, its wear resistance can only be described as adequate, because of its low hardness. Also the production of coatings with uniform thickness on complex geometries is difficult, even with the aid of complex and expensive jigging arrangements.

As stated, electroless nickel is able to overcome these problems. This easy to operate process produces coatings of uniform thickness on substrates of the most complex geometry. This offers considerable advantages for plating the inside of pipes and blind holes. As-plated, the coating is harder than electrolytic nickel, this can subsequently be heat treated to compete in hardness and wear resistance with hard chromium deposits.

Electroless nickel is a controlled chemical reduction process that takes place on the surface of the component which is immersed in the solution. The component must catalyse the reaction or else the reduction must be started by other means, for example, an applied potential. After the reaction has started it continues because the deposited metal continues to act as a catalyst and therefore the process is deemed autocatalytic. The removal of the catalytic surface stops the reaction.

Electroless nickel coatings are being used by industry as wear resistant coatings to increase the life of pumps, valves, dies and compressors and the improved corrosion resistance over electrolytic nickel makes it useful in containers, oil refineries and jet engines.

Although being superior to electolytic nickel, electroless nickel does itself have certain limitations. The hot hardness is lower than desirable for many purposes and exposure to elevated but relatively low temperatures for long periods gradually softens the coatings. Electroless nickel also has a tendency to galling particularly when in contact with other electroless nickel surfaces.

To overcome the deficiencies in mechanical properties, electroless nickel composite coatings have been developed. This involves the incorporation of a second phase, particulate material into the deposit during deposition. To improve hot hardness and further improve wear resistance, hard particles such

as silicon carbide, ceramics and diamond have been incorporated. These materials do not lose their properties over the desired operating temperature ranges and therefore improve the overall performance of the coating. The tendency for galling can be prevented by incorporating high pressure lubricants such as PTFE into the coating. This reduces the overall coefficient of friction of the coating. Unfortunately electroless nickel-PTFE coatings cannot be fully heat treated without the degradation of the PTFE. The coatings are therefore used essentially un-heat treated, and as a result have hardness values lower than conventionally deposited electroless nickel. The result of this can be high wear rates.

While a certain amount of work has been conducted into the techniques needed to introduce insoluble particles into electroless nickel coatings and some comparative measurements made of the wear resistance of these coating with other hard surfaces, eg. hard chromium, only recently has any significant industrial use of electroless nickel composite coatings been reported.

The aim of this work was to develop more suitable electroless nickel composite coatings for industrial use. The first objective was to produce a self-lubricating composite, similar to electroless nickel-PTFE, but with an improved wear resistance. The material considered for this function was graphite. Graphite containing coatings could be conventionally heat treated to produce a fully hardened matrix, and thus give

almost the wear resistance of heat treated electroless nickel, plus a self-lubricated suface with low coefficient of friction. The second objective was to incorporate metal particles into electroless nickel, which, after suitable heat treatment would produce metal alloy coatings. Such a technique would enable almost any nickel alloy to be produced, and thus its properties could be tailored to suit the application. For this work chromium metal particles were incorporated in order to produce a nickel-chromium alloy. Such nickel-chromium alloys were known to have extended wear, corrosion and oxidation resistances and provided a good basis for investigation.

To evaluate such coatings it was first necessary to develop plating solutions capable of depositing the desired composite systems. Having achieved this, those factors controlling particle incorporation were examined with a view to understanding the mechanism of particle incorporation. Once the production of composites was understood coatings were produced and evaluated for their wear and frictional properties.

CHAPTER II

FRICTION, WEAR AND LUBRICATION - LITERATURE REVIEW

2.1 FRICTION

Friction is the resistance to motion which exists when a solid object is moved tangentially with respect to the surface of another with which it is in contact, or when an attempt is made to produce such motion. The importance of friction can be seen by the very substantial amounts of energy lost in overcoming frictional losses during sliding. Reduction of friction, either through improved design or through the use of more suitable contacting materials, and the application of better lubricating substances, is thus an extremely important problem of modern technology.

It must not be overlooked, however, that very many processes of everyday life are dependent for their effectiveness on the presence of friction in significant amounts. Hence the provision, when required, of sufficiently high friction is also of great importance, for example: walking, driving a car (with regard to starting, stopping and cornering) and gripping objects in our hands, cannot be readily carried out if friction is too low.

Examples of friction are many. However, it is clear that from the tribological point of view, a detailed

understanding of friction is necessary because of both its positive and damaging roles in the relative motion of components.

2.1.1 Laws of Friction

Elucidation of the science of friction is attributed to Leonardo de Vinci in the 15th. Century. He observed that:

(1) the frictional resistance F is proportional to the weight W of the object which is being moved, and

(2) the frictional force is independent of the apparent area of contact.

The above two observations are known as Amonton's laws of friction which were stated fully in 1699. There is a third law which states that the interfacial resistance between two surfaces is independent of the velocity of sliding. This law is attributed to Coulomb who enunciated it in 1780, but it only holds true over a limited range of speed. Amonton's two laws are followed quite closely although do require some qualification today.

The proportionality of F on W giving a characteristic value of the static coefficient of friction, μ_s, and kinetic component, μ_k, are probably true, in a very broad sense, in ambient atmosphere. It must be stated however that μ is not an intrinsic property of a material but depends on the solids constituting the friction couple. Other things being equal, the frictional resistance is independent of the apparent area of contact because it is the true area established at the interface

between asperities which determines the frictional bonds. Experimental evidence has shown that the 3rd law of friction can only be taken as constant within a limited speed range. The range varies for metals but, for example, titanium sliding on itself has a speed range of 10^{-8} to 10^{2} cms^{-1} where friction shows only a very slight negative slope. If the relative movement is inordinately high, the coefficient of friction is known to fall considerably because of incipient fusion of the contact points thus providing a layer of viscous lubricant.

2.1.2 The Theory of Friction

When two surfaces are put under a load, the interface opposes the intended function and an amount of the total energy is not available as useful work. It has been established that this non-useful energy at a tribological interface is dissipated into one or more of the following phenomena:

(i) elastic hystersis.

(ii) plastic deformation.

(iii) fracture and creation of new surfaces.

(i) Friction in Terms of Elastic Deformation

This hypothesis was proposed by Archard[1-3] who made plausible assumptions regarding the contacting asperities. Archard applied the theory of single (elastic) spherical contacts on a flat surface to the multiple contact of real surfaces, to

show that the first law of friction, $f = \mu W$, could be explained in completely elastic deformation terms.

Before any such interactions can be considered it is first necessary to look at the nature of the surfaces which come into contact. It is almost impossible to make a surface perfectly smooth; even the smoothest surface is comprised of many "valleys and hills". The best engineering surfaces, prepared by grinding and polishing, have roughnesses in the order of 2500 nm. This seems very smooth in ordinary terms however 2500 nm is approximately 100 atomic spacings, clearly on an atomic scale the surfaces are rough. Most engineering surfaces are considerably rougher, hence when two specimens are in stationary contact over an apparent area of contact they are, in fact, in contact only where the tips of the asperities of both surfaces touch. Obviously this must be an area less than the apparent area of contact and is called the "real area of contact".

The first consideration is the area of contact for the ideal case of a single point contact of a hemispherical, smooth asperity against a smooth flat surface. Let E_1 and E_2 be the Young's moduli for the asperity and flat surface which is made of softer material than the asperity. If they are now brought into contact under load W, they will deform elastically at first according to the relation:

$$a = 1.1 \left\{ \frac{WR}{2} \left[\frac{1}{E_1} + \frac{1}{E_2} \right] \right\}^{1/3} \qquad (1)$$

a is the radius of the circle bounding the region of contact and

R is the radius of the asperity. We can see that the area of contact due to elastic deformation is proportional to $W^{2/3}$.

i.e. $A_s = \pi a^2 \propto W^{2/3}$ (2)

Suffix s denotes A is the area of a single contact deformed elastically. Thus the elastic deformation theory had previously been discounted as the elastic deformation of a single contact, which gives an area of contact $\propto W^{2/3}$, and hence a kinetic friction force $\propto$ to $W^{2/3}$ was not the direct proportionality expressed in the first law ($F \propto W$). Archard, however, had found experimentally that the plastic deformation hypothesis (explained in the next section) was not valid for all conditions of sliding between surfaces, especially metallic surfaces. This prompted Archard to look for an alternative approach.

Archard tried to assume a more realistic surface model, as in Figure 1. As the load is increased the contacting area increases in size and more asperities come into contact.

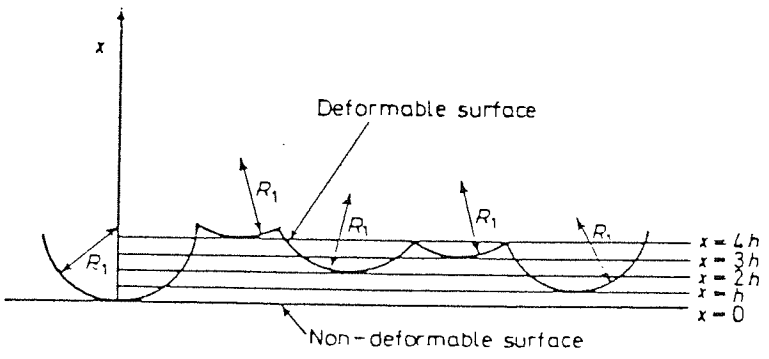

Figure 1. Multiple areas of contact model [1-3]

Thus an increase in load increases both number and size of contact areas. It then follows automatically, that these contact areas have a size distribution. It is assumed that the

asperities are evenly distributed in depth (in the x direction), i.e. there is one asperity at each x co-ordinate, $x = 0, h, 2h, 3h$, etc. When a load is applied the total area of multiple contact deformed elastically, A_m, resulting from a movement of distance $x = Nh$ (i.e. bringing N asperities into contact) is given by:

$$A_m = \sum_{r=1}^{r=N} A_r \tag{3}$$

where A_r is the contribution to the total contact area from the asperity of the r^{th} level. When a spherical asperity is deformed elastically through a distance rh, the contact area is:

$$\delta A_r = 2\pi R_1 rh \tag{4}$$

(from the Sagittal formula $(2R_1 - rh)rh = a^2 r$ where $rh << 2R_1$. a_r is the radius of contact area). From (3) and (4) we get:

$$A_m = 2\pi R_1 h \sum_{r=1}^{r=N} r \tag{5}$$

For large values of N, equation (5) becomes:

$$A_m = \pi R_1 h N^2 = \pi R_1 \frac{x^2}{h} \tag{6}$$

If the number of asperities per unit depth is M, which equals 1/h, equation (6) becomes:

$$A_m = M\pi R_1 x^2 = Bx^2 \tag{7}$$

where $B = M\pi R_1$. Using equation (1) and an analysis similar to the above, it is possible to deduce an expression for the load W_m, which can be supported elastically by the multiple contact area A_m, ie.

$$W_m = 0.86\, E R_1^{1/2}\, M x^{5/2} = C x^{5/2} \tag{8}$$

where $C = 0.86\ ER_1^{1/2}$ and $E = E_1 = E_2$ (for simplicity). From equations (7) and (8) it is possible to obtain a relation between W_m and A_m, namely:

$$A_m \propto W_m^{4/5} \tag{9}$$

In a later paper [2] Archard considered the same surface again but covered it with protuberances of radius R_2 ($R_2 << R_1$). Archard then showed that the relationship between load and the area capable of supporting the load elastically was :

$$A_m \propto W_m^{14/15} \tag{10}$$

By further considering that protuberances of radius R_2 were covered with spherical protuberances of radius R_3 where $R_3 << R_2$ Archard showed that:

$$A_m \propto W_m^{44/45} \tag{11}$$

Thus, the more realistic Archard made the model the closer the relationship reached proportionality between load supported elastically and the contact area, as is the case in practice.

If it is accepted that frictional force should be proportional to the real area of contact, Archard's model leads to the possibility that the frictional force between real surfaces will still be proportional to load even if all the deformations are elastic.

A serious limitation of the theory however is that if contact is elastic there will be no surface damage when a solid is placed upon another and then lifted for examination. It is common experience that some form of mechanical change in the

interface occurs, such as metal transfer or work hardening due to the tribological interaction.

(ii) **Friction in Terms of Plastic Deformation**

The theory proposed by Bowden and Tabor[4,5] explains friction in terms of plastic deformation of the surface. As with Archard's elastic thoery it is limited in that it is based on metallic friction, however, this theory is generally given more prominence as it offers the most satisfactory physical explanation for metallic friction.

For the plastic deformation hypotheses it is necessary to first know the compressive stress σ across a single contact of radius "a":

$$\sigma = \frac{W}{\pi a^2} \tag{12}$$

From this definition and equation (2) we see that:

$$\sigma \propto W^{1/3} \tag{13}$$

for completely elastic deformation. When the load is increased beyond the elastic limit of the softer material it will begin to deform plastically at a point 0.6a below the surface when $\sigma = 1.1Y$[6]. As the load is increased the material around the point becomes plastic and yields irreversibly until the region around the original point of contact is deformed plastically to such an extent that the new area of contact is able to support the load. At this stage $\sigma \approx 3Y$ and is the condition for full plastic flow. σ is independent of load once full plasticity is attained. Any further increases will increase the area of contact σ remaining

PAGE 32

MISSING

It was shown for a single contact that, σ = (mean yield stress) was independent of load W. Provided assumptions (a) and (b) are valid for multiple contact the real area is porportional to the load and inversely proportional to the mean stress required to produce plastic flow at the contacting asperities. This means that when two surfaces come into contact, the harder material sinks into the softer material until the real area of contact is sufficient to support the load W. Under stationary conditions, this results in cold welding of the mating asperities, especially in the case of metals. Bowden and Tabor maintain that the force required to shear the welded junctions is directly related to the static frictional force F_{stat}. They also claim that the junctions still weld together when the surfaces are slid over one another under normal conditions of sliding contact between specimens. The force required to maintain a constant sliding speed whilst making and breaking the welded asperity contacts is the kinetic force F_{kin}, provided it is assumed that the force required to "plough" out the softer material (the ploughing term) is negligible, which Bowden and Tabor state is true for most cases. The kinetic frictional force can be expressed as:

$$F_{kin} = (A)m.\tau \qquad (16)$$

where τ is the mean tangential shear stress, the stress required to shear the welded junctions. Combining with (15):

$$F_{kin} = W\tau/\sigma \qquad (17)$$

This embodies the empirical laws of friction, namely that the frictional force is proportional to the applied load W and is independent of the apparent area of contact. The coefficient of

kinetic friction u_{kin} is then:

$$\mu_{kin} = \frac{F_{kin}}{W} = \frac{\tau}{\sigma} = \frac{\text{Shear strength of the junctions}}{\text{Yield stress of the softer material}} \quad (18)$$

As shearing often takes place in the softer material, Bowden and Tabor described μ_{kin} as:

$$\mu_{kin} = \frac{\text{Shear strength of the softer material}}{\text{Yield stress of the softer material}} = \frac{\tau_m}{\sigma_m} \quad (19)$$

This is a ratio of the strength properties of the same material. It could, therefore, be expected that μ_{kin} would be approximately the same for a wide range of materials. Bowden and Tabor also pointed out that the shear strength and yield stress will vary together as temperature is varied, therefore, μ remains constant; a prediction often confirmed by experiment.

Bowden and Tabor later [5] re-examined the assumption leading to equation (18). They questioned the validity of assuming that the shear strength of the junction is the same as the shear strength of the softer material and that the shear strength and yield stress are both independent of strength properties. They suggested that the coefficient of friction should more correctly be:

$$\mu_{kin} = \frac{\text{Critical shear stress at the interface } \tau_i}{\text{Plastic yield stress of the underlying material } \sigma_m} \quad (20)$$

The interface, they maintained, is not usually one between metal and metal since a realistic surface more often consists of oxide films or thin films of boundary lubricants, therefore it is incorrect to take the critical shear of the underlying material τ_m instead of τ_i the interface shear stress.

For Archard's theory, the frictional force between sliding surfaces is that required to deform the real area of contact elastically. With plastic deformation the force of friction is mainly due to the force required to break the welds formed between such surfaces. In practice probably both can be considered to have some relevance. As asperities come into contact the juctions may be considered elastic in nature if junctions completely disappear once the load is removed. Archard's theory could then be applied. If plastic deformation occurs, ie. under higher loads, the junctions produced will then adhere more permanently to the flat surface and can be considered in terms postulated by Bowden and Tabor.

2.1.3 Junction Growth.

Experiments[7,8] have shown that the combined effect of a normal stress and an applied tangential pull is to increase the area of contact, generally in the direction of motion. As the applied tangential force is increased steadily, there is a progressive increase of the area of the junction, until at the onset of macroscopic sliding the junction area has reached a maximum steady value and the coefficient of friction is equal to the static component μ_{stat}. The yield criterion for junction growth is then:

$$\sigma^2 + \alpha\tau^2 = \sigma_y{}^2 \qquad (21)$$

where σ is the applied normal stress and τ is the applied tangential stress, α is a constant and σ_y is the yield stress of the material forming the junction. At most values of

yielding of some asperities will occur and junctions will form having a potential value of instantaneous coefficient friction, μ_i. As τ increases, according to the yield criterion for junction growth Eq. 21. σ decreases. To maintain plasticity therefore, τ must be increased with a concommitant increase in area and a decrease in σ . This continues until τ is large enough to overcome the static coefficient of friction and large scale sliding begins, thus, the model is that as an asperity is squashed to form a junction, there will be a small, but finite, amount of friction. This will continue to increase as the area increases because the instantaneous frictional resistance F_i is related to the instantaneous area A_i as $F_i = \tau_c A_i$, where τ_c is the critical shear stress of the material forming the junction. At gross sliding $\mu_i \rightarrow \mu$ as the level of contact increases and $\tau \rightarrow \tau_c$.

2.1.4 Work Hardening

In the postulates where yield is considered[4,5] it is assumed to be completely plastic. Plastic yielding results because of a compressive stress, but the use of σ in Eq. 11 to express μ can be misleading. This is because not all the compressive stress is available for plastic yielding. The true area of contact A_t due to plastic interaction is:

$$A_t = W/3\sigma_y \tag{22}$$

Since the hardness of the material is $H = 3\sigma_y$

$$A_t = W/H \tag{23}$$

and $$\mu = \tau_c/3\sigma_y \quad \text{or} \quad \mu = \tau_c/H \tag{24}$$

It could be argued that work hardening will result in an increase in the value of τ_c of the junction and hence a rise in the magnitude of μ. However, the hardness or the yield of the material will increase as well so that μ remains relatively unchanged as expressed by Eq. 24.

2.1.5 Slip Stick

The trace of μ, unlike that of wear, does not produce a steady, smooth line but fluctuates instead about a mean value as sliding continues[9,10]. An idealised pattern of the variations in μ has the appearance of a saw-tooth as shown in figure 2. As the motion commences the coefficient of friction rises from A to B, the surfaces stick together and at B the coefficient is a maximum. The value B is the maximum value of the static coefficient of friction.

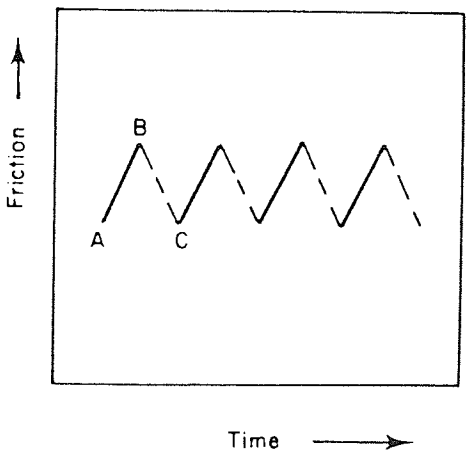

Figure 2. Schematic variation of friction with time, Bowden et al[9,10]

The static component of friction disappears at B because it is then that the two surfaces separate, that is the interface slips so that the falling coefficient tends to assume the value of the kinetic component at C. The nature of the surfaces are such that the interface sticks and repeats the process.

Measurement of the electrical resistance between the surfaces shows that the area of contact of the junctions increases from A to B. Recalling the combined effect of a normal and tangential force at an interface is to cause an increase in the area of contact, μ is then also increased. The period B to C is of course that when the top surface slides relative to the bottom, so that the interfacial area slips and sticks again. The period between peaks will then vary according to the mating materials and to the friction test machine used.

If the speed of the machine used to produce the trace in figure 2 is increased, the interval between A and B becomes smaller and the overall magnitude of the coefficient of friction is also diminished. Thus with very rapid relative interfacial movement, the distances between the process of stick and of slip become less accentuated and $\mu \rightarrow \mu_k$ until sticking and slipping of the asperities is indistinguishable and the machine will run smoothly. It must however be noted that μ may tend not to be similar to μ_k at all speeds for all combinations of metals or for all types of machines.

2.1.6 Real Surfaces

So far we have mainly been concerned with theoretical surfaces. Real surfaces are covered with undulations so that if one solid approaches another contact will only occur between the appropriate summits of the opposing components Figure 3. With most metals, the first area thus produced would continue to yield laterally and increase in size, other asperities may then come into contact, until the sum of these discrete areas thus produced is large enough to support the load W, and plastic flow will cease.

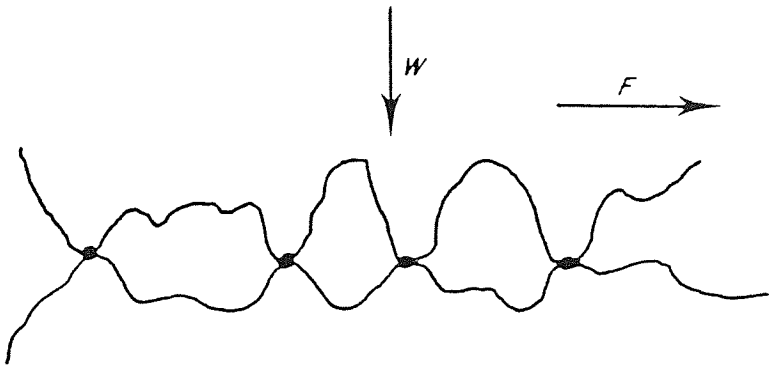

Figure 3. Two rough surfaces making contact at four points (W = normal load; F = load applied tangentially)

This increase in area is entirely due to the static load and should not be confused with junction growth due to tangential stress. The area supporting the load is then the true area of contact A_t as opposed to the apparent area A. Thus $A_t = A_1+A_2+A_3+A_4+....A_n$, and $A = W/3\sigma y$ or $A_t = W/H$. Similarly, all previous effects such as junction growth apply in addition to the

additive process of all the interacting asperities. The true area of contact can be evaluated experimentally[11] and it has been shown $A_t << A$.

Other points to be considered with real surfaces are contamination and temperature increase. Contamination, in the form of oxide films, is often beneficial and is caused by increased temperatures due to high sliding speed. This should facilitate creep, but low friction is still the case because of one or both of the phenomena of low yield stress and oxidation. A low yield stress will increase the area by creep but the applied tangential stress necessary to rupture the junctions will be low. Increased temperature also results in oxidation of the surfaces. Oxide films often have low shear stress and are thus very effective at lowering the frictional resistance of the surface.

2.2 WEAR

Wear is one of the three most commonly encountered industrial problems leading to the replacement of components and assemblies in engineering; the other problems being fatigue and corrosion. Wear is rarely catastrophic, but it reduces operating efficiency by increasing power losses, oil consumption and the rate of component replacement. Wear is not an intrinsic property, but a characteristic of the engineering system. Any change in load, speed or environment can cause a dramatic change

in the wear rates of one or both of the contacting surfaces.

2.2.1 Mechanism of Wear

Widely varying conditions cause wear and many mechanisms contribute to the damage caused. Wear encountered in industrial situations can be classified broadly as below (although there are of course situations where one type changes to another, or where two or more mechanisms operate together):[17]

- Abrasive 50%
- Adhesive 15%
- Erosive 8%
- Fretting 8%
- Chemical 5%

(i) Abrasive Wear

Abrasive wear occurs when hard particles indent, penetrate and groove a surface and displace material from that surface. The degree of penetration can be given by:

$$\frac{\text{Load on the particle}}{\text{Hardness of the surface}} = \frac{W}{Hv} \qquad (25)$$

and $$\text{Wear Volume} = \frac{W}{Hv} A L \qquad (26)$$

where A = area of cross section of groove and L = length of groove.

Volume wear usually increases linearly with load and sliding distance. The highest wear rates are caused by attack

angles between 80^{o} and 120^{o}. If deviations occur they are usually due to reduction in particles size of the abrasive or clogging of the surface.

Abrasive wear can be expressed in terms of relative wear resistance, R[13], where:

$$R = \frac{\text{linear wear of a standard}}{\text{linear wear of material under test}} \qquad (27)$$

This is the ratio of the wear rate of the material under investigation to that of a standard sample. An advantage with this approach is that variables such as load and speed can be arbitrary, provided that they are identical for both materials. A plot of relative abrasive wear resistance of materials against their corresponding values of hardness produces a linear relationship from which an empirical relationship can be obtained:

$$R = K_1 H + K_2 \qquad (28)$$

where H is the hardness of the material under investigation and K_1 and K_2 are empirical constants. Denoting the applied stress by σ and using a range of commercially pure metals and some alloys all in their fully annealed state, a plot of R against the annealed hardness H produces a linear curve which passes through the origin. Values of R for a range of metals have been obtained and the empirical law changes as follows where K is a constant:

$$R = K.\frac{H}{\sigma} \qquad (29)$$

Relative wear resistance is then proportional to hardness although this relationship becomes somewhat more complex with microstructure, figure 4.

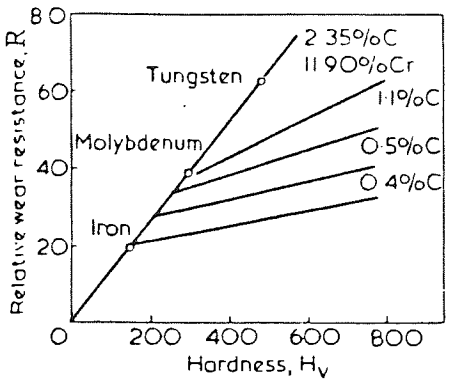

Figure 4. Relative wear resistance, R, as related to hardness

It is also necessary to take into account the hardness of the abrasive particles[14]. The hardness of the surface resisting must be greater than half the hardness of the abrasive if any real improvement in wear resistance is to be achieved figure 5.

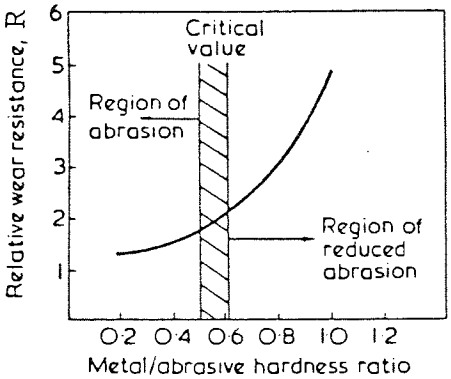

Figure 5. Relative wear resistance, R, as related to the ratio of metal to abrasive hardness

This illustrates that there is no simple relationship between hardness and wear resistance and that the hardness of the material must exceed some critical value K_t to bring about any significant improvement.

$$K_t = \frac{H_V \text{ of the surface}}{H_V \text{ of the abrasive}} \qquad (30)$$

K_t must be greater than 0.5. However, it is unnecessary to

increase hardness of the material beyond 1.3 times that of the abrasive because no further significant improvement will be obtained. If the surface is made too hard it may also become too brittle. Cracking may occur adjacent to the critical region and relatively large flakes of material may fall out of the surface resulting in severe wear.

In sliding of metals the main cause of abrasion is hard particles that may be present in one of the surfaces (eg. carbides or inclusions in steel), work hardened wear fragments or the formation of very hard oxide films ie. Al_2O_3.

(ii) **Adhesive Wear**

Adhesive wear occurs when surfaces slide against each other and the pressure between the contacting asperities is high enough to cause local plastic deformation and adhesion, as was realised in the theory proposed by Bowden and Tabor[5]. Adhesion is favoured by clean surfaces, non-oxidising conditions and by chemical and structural similarities between the sliding couple.

Adhesion occurs between asperities which come into contact under an increasing load, figure 6. The top hard asperity sinks into the softer bottom asperity, then under tangential pull the two separate at the weakest point, usually in the softer material, thus resulting in material transfer. Wear decreases if both asperities are harder because the contact area is lower (area of contact being inversely proportional to hardness). Adhesive wear increases if asperities are chemically

clean, as bonding and welding are much more likely to take place.

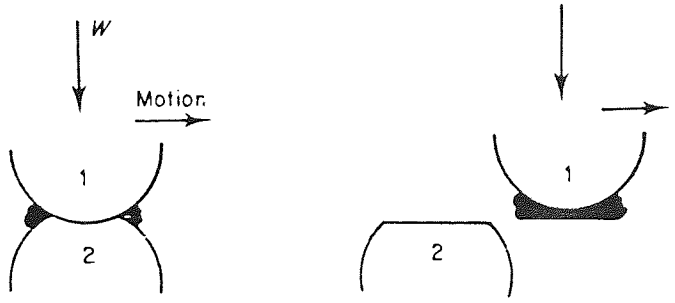

Figure 6. Asperity 1 sinks and causes plastic flow in 2 which is soft. 1 moves on carrying with it adherent wear debris

Likewise, wear increases if the metals comprising the wear couple are mutually soluble[15]. Transferred particles and wear debris may also become considerably harder due to work hardening, this can lead to abrasive wear.

A law for wear was proposed by Archard[1] which expressed the volume of metal lost V in terms of sliding distance S, the applied load W, and the yield stress σ of the wearing surface:

$$\frac{V}{S} = \frac{K\,W}{3(3\sigma y)} \tag{31}$$

since $3\sigma y \approx H$ $$\frac{V}{S} = K\frac{W}{3\,H} \tag{32}$$

The wear constant K represents the property of the friction couple and is the probability of junction interaction. Numerous values of K have been found for different materials, but it only has any real meaning provided that the wear mechanism does not change.

Wear under adhesive conditions, unlike abrasive wear, is subject to sharp transitions in behaviour. Variation in load and speed may bring about marked thermal changes which precede and cause wear change[16]. Figure 7 illustrates this transition of wear from mild wear (oxidation) to severe wear (metallic). Below T wear occurs by the removal of oxide debris from an oxidised surface supported on a work hardened substrate. T_1 is a transition to severe wear instigated by the breakdown of the protecting surface oxide produced at lower loads. Plastic deformation of the substrate occurs, caused by a higher bulk temperature, and the wear rate increases considerably with the production of metallic debris. Between T_1 and T_2 severe wear occurs.

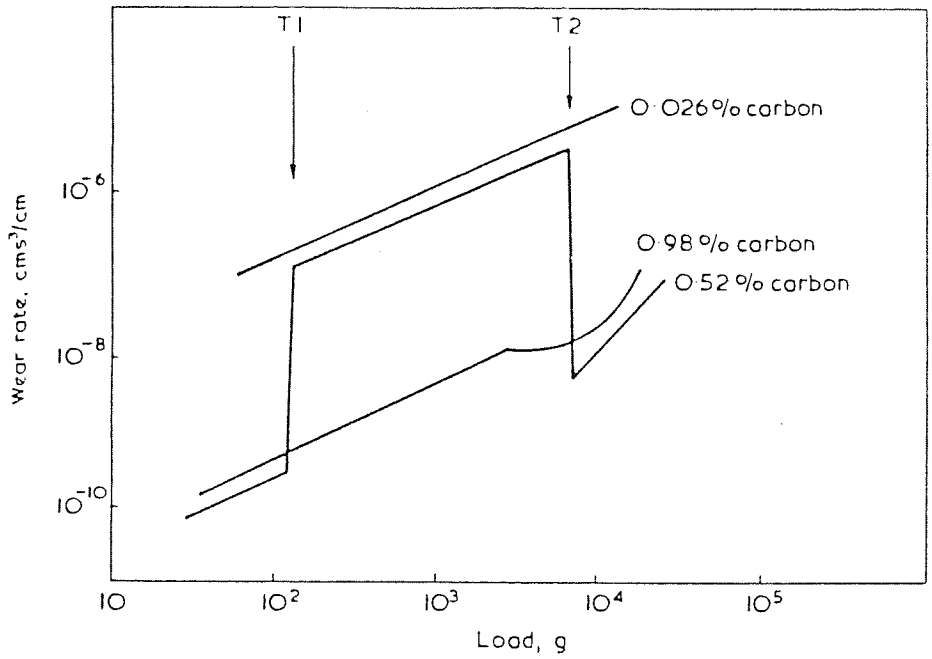

Figure 7. Transition wear behaviour of different steels[16]

At T_2 the surface temperature is high enough to enable an oxidised surface once more, and the wear rate is now reduced considerably. It is possible, however, to suppress the transition provided the steel is of sufficient initial hardness.

Figure 7 is based on constant sliding speed, which itself has an affect on both the wear rate and the transition loads. Figure 8, based on both load and sliding speed illustrates that below the transition line a mild wear mechanism will operate and above it a severe wear mechanism will be responsible for a much higher wear rate[17]. Actual wear results for two loads are superimposed on this diagram to show how it has been constructed.

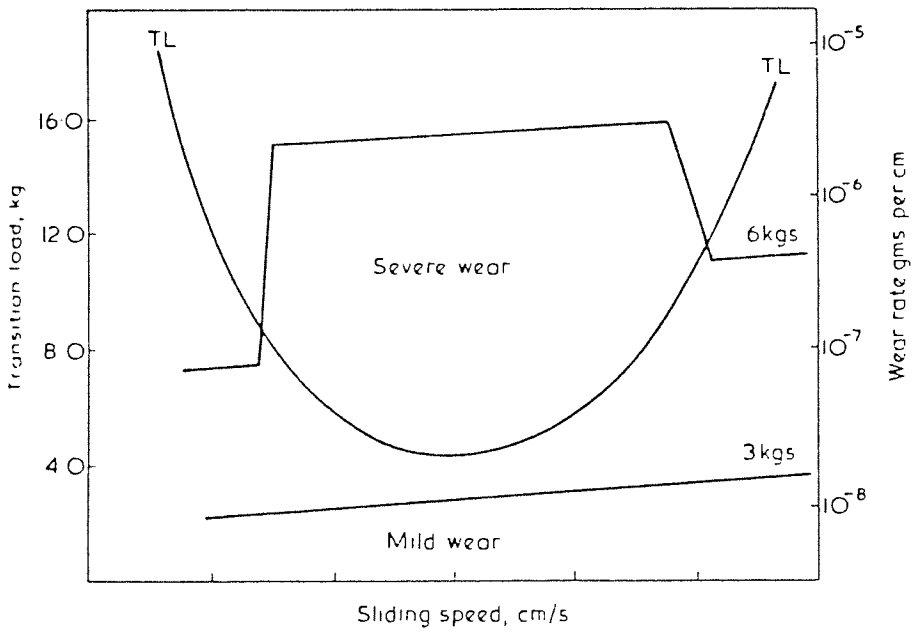

Figure 8. Transition from mild to severe wear for nodular cast iron as a function of load and sliding speed. TL = Transition Load [17]

(iii) Delamination Theory

The delamination theory was proposed by Suh[18] and is only applicable to low speed sliding so that the bulk temperature of the interface does not rise appreciably. The theory suggests that as a rider moves over a surface and the latter is plastically deformed, dislocations are generated within the material. The dislocations from the surface region are

eliminated by what is called the "image force" created by the free surface. As sliding proceeds, fresh dislocations are generated which move until they pile up at obstacles such as grain boundaries. This results in the formation of voids which coalesce in time by growth and also due to the applied shear stress at the interface. The next stage is for the agglomerate of voids to assume the form of a crack, parallel to the surface which will propagate to form a wear particle.

(iv) **Surface Fatigue**

Fatigue wear is the removal of surface layers by spalling. This is a common cause of failure observed with rolling bearings[19]. Continuous rolling produces a local loading and unloading of the races this repetitive stress results in fatigue of the surface and substrate layers. Ultimately, this can lead to fracture and removal of material from the surface. Spalling, or fatigue wear, is even experienced under fully developed elasto-hydrodynamic lubrication. Wear occurs as a result of induced normal and tangential stresses through the lubricant film and so direct physical contact between asperities is unnecessary.

(v) **Erosive Wear**

Erosive wear is a form of abrasion which is generally treated rather differently because the contact stress arises from the kinetic energy of particles flowing in an air or liquid stream as it encounters the surface. The particle velocity and impact angle, combined with the size of the abrasive, give a

measure of the kinetic energy of the erosive stream and are thus important parameters of erosive wear[20].

One method of categorising erosive wear is by the damage number[21] defined as:

$$\text{Damage Number} = \rho v^2 / \sigma y \, g \qquad (33)$$

where ρ = density of the target material, v = velocity of the normal impact, σy = flow stress of the target material and g = acceleration due to gravity. The dependence on velocity can be seen. When the impact angles are small, cutting wear prevails and the hardness of the surface resisting wear is the critical factor. At large angles, wear is due to deformation, the solution is more complex and a softer material may then be suitable[22] figure 9.

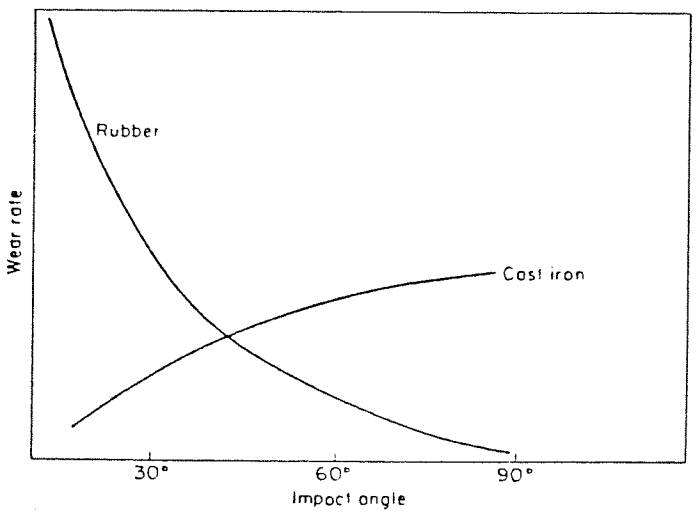

Figure 9. Erosive wear as a function of impact angle[22]

Natural and synthetic rubbers produce good results due to their low modulus of elasticity. There would also appear to be a good correlation between erosive wear resistance and ultimate resilience.

$$U.R. = \frac{1/2(\text{tensile strength})^2}{\text{elastic modulus}} \quad (34)$$

This expresses the amount of energy that can be absorbed before deformation or cracking occurs.

A solution to an erosive wear problem may often be found by changing the angle of attack, reducing the velocity of flow or by choosing a more suitable material.

(vi) **Fretting**

This is a wear phenomenon occurring between two surfaces having oscillatory relative motion of very small amplitude[23] only of the order of 100μm. The surfaces are never brought out of contact and, therefore, there is little opportunity for the products of the action to escape. Seizure may then occur because of the prevention of lubrication. During fretting, there appears to be three basic processes:

(1) Mechanical action disrupts oxide films on the surface, exposing clean, and possibly strained, metal. This will be reactive, and in the presence of the atmosphere would oxidise rapidly during the half cycle after disruption. This is, again, disrupted on the return half cycle.

(2) The removal of metal particles from the surface in a finely divided form by a mechanical grinding action or by the formation of welds at points of contact. These welds are subsequently broken at a surface other than the original surface, either by shearing or by a local fatiguing action. The atmosphere only plays a part in this process when fatiguing occurs because it can introduce an element of corrosive fatigue.

(3) Oxide debris resulting directly from (1) or as a result of the oxidation of the metal particles in (2) is an abrasive powder which continues to damage the surface.

Fretting often occurs when there is vibration. Removal of the source of vibration can often eliminate the problem. Surrounding the contact area with lubricant effectively reduces friction, and thus reduces adhesion. At the same time, oxygen may be eliminated which prevents the formation on oxides. Adequate sealing can, therefore, often prevent fretting.

(vii) **Corrosive Wear**

Corrosive wear is a form of wear which results from the interaction of corrosion and the relative sliding motion of the surface. In a corrosive environment a surface will be attacked and corrosion products will be formed. This often reduces the rate of reaction, and may stop it completely. If, however, the products do not adhere to the surface, or the film is porous, the chemical reaction proceeds independently of any sliding and the process is one of pure corrosion. In a corrosive wear situation the protecting film is removed by the sliding of the mating surfaces. This then exposes the original surface and the chemical attack continues at the initial rate of reaction and so the process continues. If the film is resistant, the basic surface may actually be protected. This may not last long though, if the film is brittle and breaks away.

Some films, formed as the result of chemical action, give low rates of wear. Examples are the films formed by oil

additives, eg. metallic chlorides, sulphides and phosphates acting as boundary lubricants.

2.3 LUBRICATION

One of the main methods of reducing wear and ensuring long life, is to physically separate the interfaces with a lubricant so that the components are unable to interact directly. The reduction of friction by lubrication can be divided into hydrodynamic, elasto-hydrodynamic, boundary lubrication and solid lubrication.

(i) Hydrodynamic Lubrication

With hydrodynamic lubrication a thin film of lubricant is maintained between the surfaces, completely separating them and thus preventing contact. All of the friction now arises from the shearing of the lubricating film, this makes the viscosity of the film all important[24]. The thinner the oil, the lower the friction. Friction as low as $\mu = 0.001$ can be obtained, and in the ideal case, there is no wear of the moving parts. If the viscosity of the oil is too low, the distance between surfaces may become smaller than the height of the surface irregularities. The film may then be penetrated with a consequent increase in the friction and wear.

(ii) Elasto-Hydrodynamic Lubrication

This involves the elastic deformation of the surface without the oil film actually breaking down inbetween the

surfaces[25], ie. a steel shaft in a rubber block, figure 10. In such situations, the rotating shaft can set up a hydrodynamic film which can support the applied load. The pressures, however, are sufficient to modify, by elastic deformation, the shape of the rubber surface. Such a system is very useful as a low friction shaft seal.

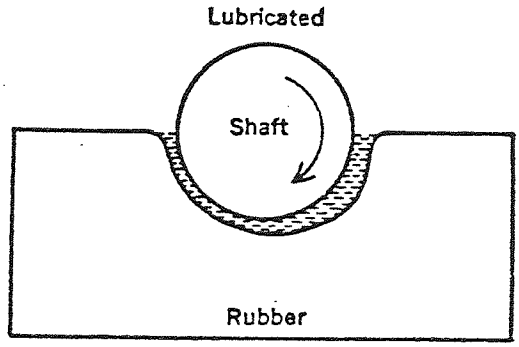

Figure 10. Elasto-Hydrodynamic Lubrication

(iii) **Boundary Lubrication**

If loads are too high, the running speed low or the surface roughness too great, penetration of the lubricant film will occur. Contact can then take place between the asperities; friction will rise and wear will take place. To overcome this active organic compounds are added to the mineral oil. These additives may have little effect on viscosity but work by forming surface films of one or two molecules thick which are able to prevent metal to metal contact. The best boundary lubricants are long chain molecules with an active end group to bond to the metal, typically an alcohol, an amine or a fatty acid[26]. The attraction between chains is strong and therefore difficult to penetrate, thus two surfaces tend to slide over each other rather than penetrate. The best such films break down at 200-250 ^{o}C

allowing metal to metal contact. Above this temperature extreme pressure lubricants must be used. Essentially these are able to withstand the temperatures caused by the sliding surfaces. Other additives to lubricating oils are compounds containing phosphorus, chlorine and sulphur. These function in a similar way by reacting with the metal surface to from a surface film which again prevents metal to metal contact.

(iv) **Solid Lubrication**

As an alternative to fluid lubricants a solid film of low shear strength can be used. These films are useful where fluids cannot be used. Solid lubricants are essentially boundary lubricants giving coefficients of friction of approximately 0.1 under heavy loads. When this is contrasted with the best hydrodynamic conditions where $\mu = 0.001$, it will be appreciated that they are not substitutes for mineral oils. They have many uses in hostile conditions where liquid based lubricants cannot be used, eg. in space and in vacuums, reactors where high temperatures and radiation are expected, gas turbines and other engines where temperatures are again too high and in pressure situations where other lubricants would be forced out.

Solids typically used as such lubricants are graphite, PTFE and molybdenum disulphide. Graphite and molybdenum disulphide both have a lamellar crystal structure which is easily sheared figures 11 and 12. A thin film on a supporting metal, ie. hard to prevent ploughing, provides a low coefficient of friction.

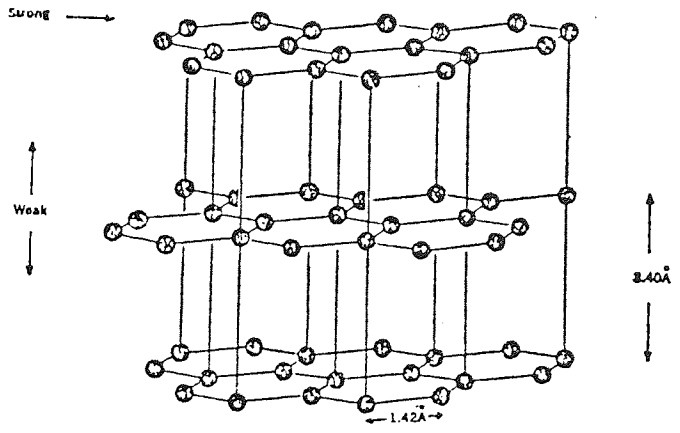

Figure 11. The structure of graphite

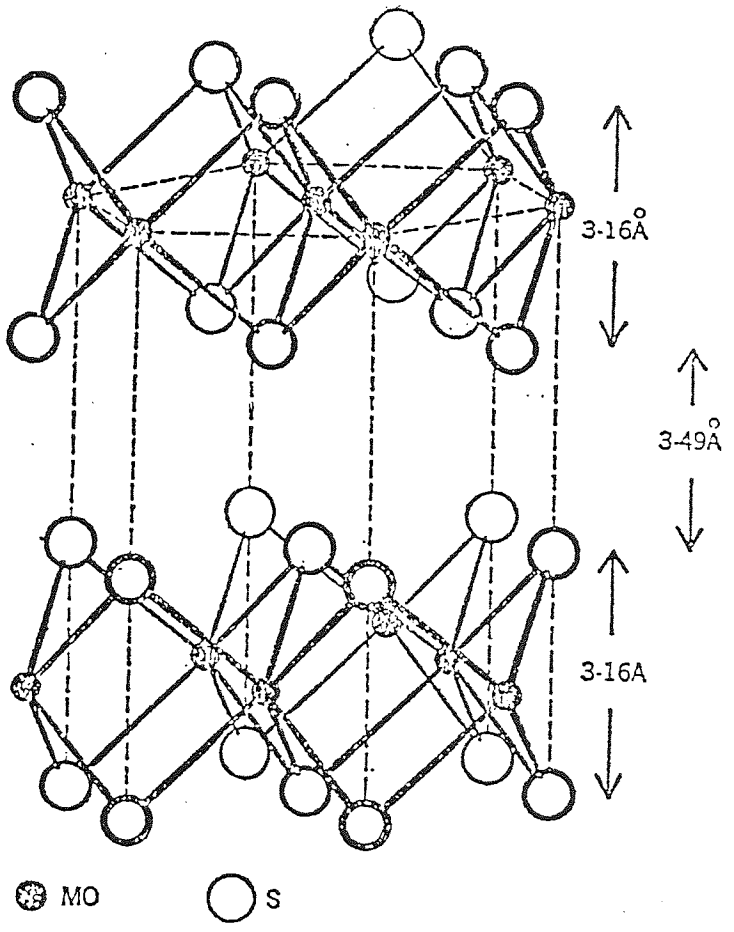

Figure 12. The structure of MoS_2. Both graphite and MoS_2 are strong in compression but weak in shear

Numerous theories have been advanced on the actual mechanism of lubrication of graphite. These can be divided into two main groups.

First there is the original structural theory based on the anisotropic nature of graphite. Bragg[27] discovered that the relatively large distances separating the layer planes were sources of weakness in the mutual attraction between these planes and, in turn, gave rise to the interplaner mechanical weakness of "slip action" associated with graphite. This explanation is however too simple and it is more likely that the key to this movement lies in the presence of dislocations or areas of atomic disorder which weaken the binding forces. The presence of such dislocation was reported by Tsuzuku [28], and the behaviour of these dislocations have been further studied by Amelink and Delavignette [29] and by Boswell [30].

The second theory of the mechanism of lubrication of graphite is based on the adsorption of oxygen and certain condensable vapours. This was developed by Savage [31][32] who measured the coefficient of friction and wear rate of graphite in a system which was thoroughly degassed and operated under high vacuum. Under such conditions the coefficient of friction and wear rate were high (μ=0.8), however the admission of water vapours at low pressures reduced the wear rate by a factor of a thousand and the coefficient of friction to μ=0.18. The introduction of oxygen showed a similar decrease whereas nitrogen and hydrogen did not show such an effect. As the graphite was

subjected to wear conditions it was considered that aggregates of graphite were broken into discrete crystallites with their long axis oriented in the direction of motion followed by adhesion and bonding to the mating surface. Whether this is permanent and provides lubrication depends on several factors. Firstly the breaking of the aggregate will expose crystallite edges with free valencies which will promote the continual reformation of irregular aggregates. These may act as abrasive wear particles in that they repeatedly break up the film of graphite formed on the surface. Secondly, lubricating conditions will only occur if the force of adhesion to the metal exceeds the shear stress of adhesion between the graphite layers.

Under wear therefore, the admission of oxygen would satisfy the edge valencies of the broken crystallites by chemisorption thereby greatly reducing any tendency to reaggregate. Furthermore, the chemisorption would lower surface energy of the edge of the graphite layer. By this it is meant that the edge forces would also be decreased, thereby making it easier for the graphite to shear along the lattice planes. The action of condensable vapours would be similar. Nitrogen does not have any effect in reducing the wear rate because of its inability either to be chemisorbed or physically adsorbed since it is not a condensable vapour at room temperature.

In practice then the anisotropic nature is important, but is not the complete answer. Summarising Savage's work, it can be seen that lubricating conditions prevail when either the

shear strength of the graphite between the layers, or the adhesion between already separated layers, is reduced, and when the reaggregation of the wear debris is prevented by the absorption of oxygen or condensable vapours. Further work by Rowe, Campbell and Kozak [33] has shown that provided the graphite is adhered securely to the surface, it will lubricate under atmospheric conditions even in the absence of adsorbed films of condensable gases, but if the surface bond is weak then the shear strength of the graphite must be reduced by the adsorption of gases below that of the metal/graphite interface.

Molybdenum disulphide is another material with a layer-like structure. Its mechanism of protection can be extended from that of graphite with the embedment of platelets into the surface and the build up of surface films approximately 1-5um thick. Also like graphite this is an over-simplification of the mechanism as molybdenum disulphide is a much more chemically active substance. Thus as a lubricant molybdenum disulphide acts in reverse to graphite, it is good in nitrogen and carbon dioxide but considerably worse in oxygen and poor in wet air. It is thus one of the best lubricants in a vacuum. It also suffers from excessive oxidation in air at elevated temperatures limiting the working temperature to 350 ^{o}C[34]. Above 800 ^{o}C in a vacuum molybdenum disulphide decomposes to leave metallic molybdenum and the friction rises to that of the clean metal.

Polytetrafluoroethylene or PTFE is a relatively hard plastic material with an unusually low coefficient of friction (0.05-0.1). However PTFE is the polymer that reveals the highest wear among the crystalline polymers.

PTFE is anisotropic in nature like graphite or other lamellar solid lubricants. At low speeds or moderate temperatures the friction is low and a film of PTFE is drawn over the counterface[35]. The film is adherent with a highly orientated fibrous structure with a thickness of between 1000 and 4000 nm. The low friction is attributed to the easy shear of these thin layers under tangential traction. Obviously, transfer of films means that the PTFE wears by that amount and attempts have been made to establish the mode by which the polymer layers detach from the bulk[36]. Firstly, the banded structure of PTFE is destroyed with the progress of sliding and long fibres, each with a thickness of about 2500 nm, from the surface of the PTFE. These connect laterally to produce a film over the contact face and this is then transferred on to the counterface. As sliding progresses, the film continues to form and then moves on to the counterface giving the transferred polymer a layer-like deposit, each layer being about 2500 nm thick.

At high speeds or low ambient temperatures the friction is high, possibly because of the resistance offered by the viscous polymeric film deposited on the counterface. A second reason is that the interfacial interaction is now between the polymer and its film which has been deposited. Polymers are

viscoelastic in nature so that the higher the speed of the counterface, the greater the rate of shear at the interface, which will result in correspondingly high resistance to shear. Transfer of such films occurs on a massive scale and they can be observed in the form of sheets, ribbons or humps with thicknesses in the order of a few tenths of a micron.

Despite the very low coefficient of friction of PTFE up to about 300^{o} C it has four major defects as a practical bearing material:

(a) It is mechanically weak.

(b) It is a poor conductor of heat.

(c) It has a high coefficient of thermal expansion.

(d) At high speeds μ - 0.3.

Accordingly, if PTFE was used directly as a bearing material, it would become hot, expand, stick and result in high friction and wear. In order to obtain long life and low friction, fillers must be used with PTFE. Usually copper, bronze or glass-fibres are used in the proportions of 15-20%. With these limitations its overall performance is comparable with that of MoS_2. When vacuum conditions apply, however, there is no known material which can give a performance comparable with that of molybdenum disulphide.

The main difficulty with all these lubricating materials is applying and maintaining the material on the surfaces as all are subject to high wear rates by smearing. One method is to bond layers on with a suitable resin. Another approach is to use a sintered porous metal and incorporate the

graphite, PTFE or MoS_2 into the pores. In a similar way, lubricating particles can be incorporated into electrolytically or electroless deposited metal. Based on a metal such as nickel a good percentage of lubricating material can be incorporated throughout the coating to give a constant supply of lubricant and the metal will give a good wear performance and corrosion resistance. In this way the two enhance each other to produce a coating which has the mechanical and thermal properties of the metal but also has the surface frictional properties of the lubricating material incorporated.

Composite low-friction surfaces of this type are being increasing applied under conditions where conventional lubricants are ineffective and undesirable[37]. It is one of the objects of this work to investigate such a system.

2.4 WEAR AND FRICTION TESTING

Physical properties of materials such as hardness or viscosity of lubricants are not enough to describe their performance under wear situations. Operational tests can be very expensive and involve many variables with consequent uncertainty in interpreting results. Attempts have therefore been made to evolve simple tests which would be able to be reproduced and would simulate practical conditions, as far as possible, while reducing the number of variables to a minimum and providing carefully controllable running conditions.

Because there are no specific laws of wear to use in devising a standard test, numerous methods of assessing wear have been developed. All the tests are comparative, ie. one metal or coating is compared to a similar metal or coating or any other material on a particular test. The tests do not measure any specific property. Each test provides comparative rubbing in different ways and therefore evaluates properties unique to that test method. Although the overall pattern of performance may remain the same for materials from test machine to test machine, the quantitative results for each machine are not comparable. The results from one machine only cannot be used as a property of wear resistance. Wear tests only give an idea of properties and as wear can change so much with conditions, wear rates in practical systems can be quite different, and certainly they are from test to test.

Figure 13 shows some of the test piece shapes devised for assessing lubrication films. The four ball and Timken are the most popular. Some tests are also capable of comparative wear testing ie. falex, but are primarily designed to maintain a lubricant film for its evaluation. These tests are described more fully in Practical Lubrication[38]. Figure 13 also shows some of the tests developed for the fundamental study of wear.

The simplest and most convenient method is the pin and disc assembly. It consists of a horizontal rotating disc on which is superimposed the material or coating to be tested. The pin is of similar hard or coated material mounted on a balance

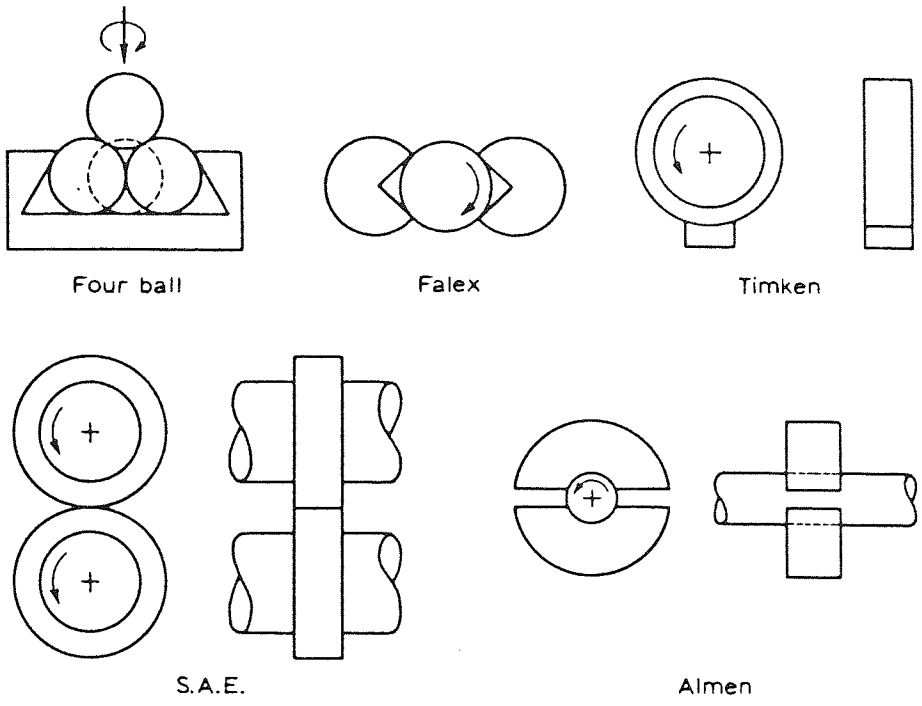

(a) Test-piece shapes for commercially available lubricant testing machines

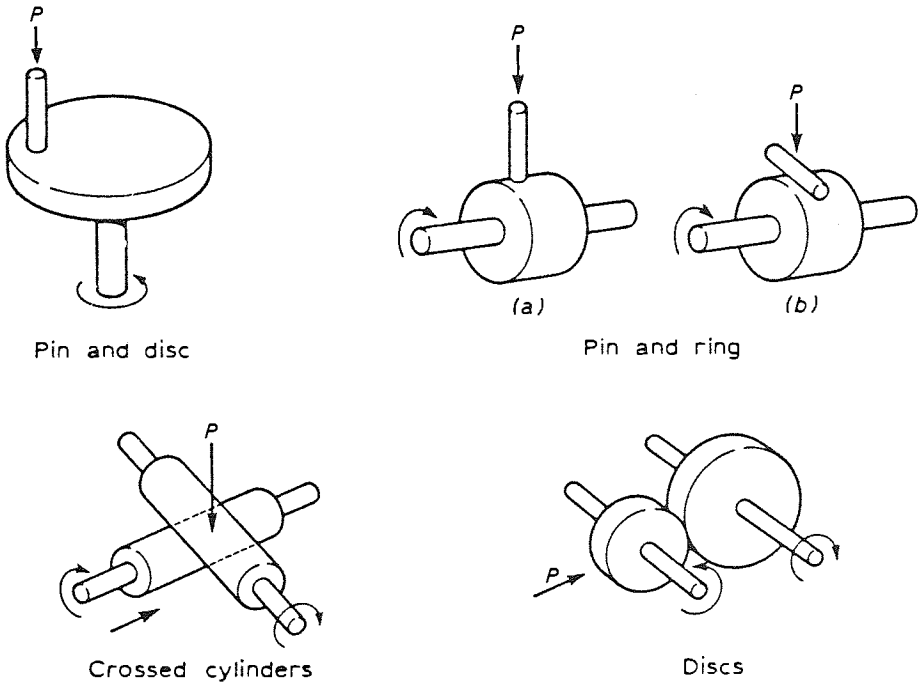

(b) Test-piece shapes for commercially available wear testing machines

Figure 13. Test-piece shapes for the evaluation of wear and coefficient of friction

lever arm and loaded aginst the rotating surface. The relative sliding velocity can be varied according to the radius between the centre of the disc and the contact point. Frictional force can be measured by strain gauges mounted on the vertical sides of the lever arm so as to record the horizontal bending stresses induced in the arm. Contact temperatures can be approximately determined by thermocouples in the pin and disc. Measurements with the pin and disc cannot be regarded as precise, although they are reliable and broadly consistent. The most serious difficulties arise from vibration of the arm and grooving of the disc after a relatively small number of revolutions. Vibration can be overcome by mechanical dampers and applying loads through hydraulic cylinders. Electrical filters diminish the spread of the dynamic trace from the strain gauges. The grooving effect can be minimised by limiting the number of revolutions, or movement of the pin, to give a continually decreasing radial distance from the disc centre to the contact point. One drawback is the curved path of the points on the surface of the pin and disc as they make contact. To avoid consequent deformation, the area of contact must be quite small. It is also impossible to maintain lubricant films because of centrifugal forces. Wear can be assessed by weight loss, loss in height of the pin or measurement of wear scars. A research machine of this type has been marketed commercially[38].

With the pin and ring contact can either be end-on or side-on. If the ring takes the form of a grinding wheel and the pin is end-on, this position gives a simple grinding set up to

study abrasive wear[39]. Side-on simulates sliding wear. With a metallic ring (approx. 25-30mm ϕ) and a pin (approx. 6mm ϕ) various types of wear can be reproduced by varying operating conditions, ie. sliding speed, load and lubrication.

The Taber Abraser, figure 14, consists of two rotating rubber wheels under a 1000g load which produces a circular wear track on the test panel. The weight loss in mg/1000 cycles is measured and expressed as the Tabor Wear Index (TWI). The lower the TWI the better the wear resistance.

The Taber Abraser uses no lubricant and determines wear under dry friction conditions. Rotating wheels of different hardness and composition are available. As the test is continued, the TWI gradually decreases, apparently due to increasing surface smoothness.

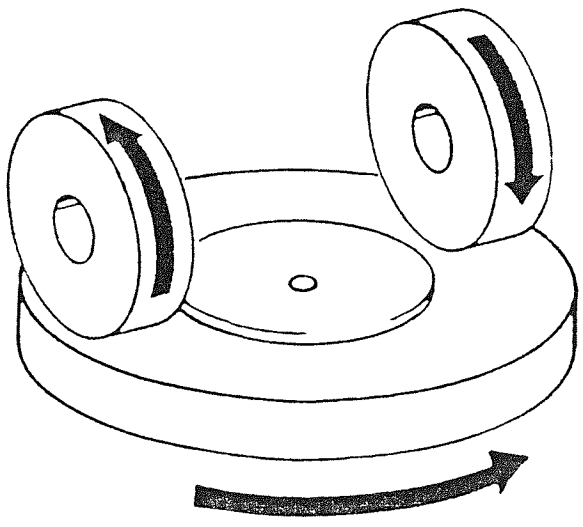

Figure 14. The Taber Abraser

The Falex lubricant tester can also be used to measure wear. A 1/4" ϕ pin is rotated at 290 rpm between two stationary

V-ground blocks under variable loads (ASTM D2670-67). The blocks are sprung loaded in a jaw mechanism, figure 15. The total jaw load can be increased to any desired load up to 1812 Kg (4000 lbs). The friction generated between the pin and V-block is calculated by a torque pressure gauge. Any standard lubricant oil can be used. The wear is determined by the weight loss of the pin and V-blocks and by the number of advancements of the ratchet mechanism used to maintain constant load during the test.

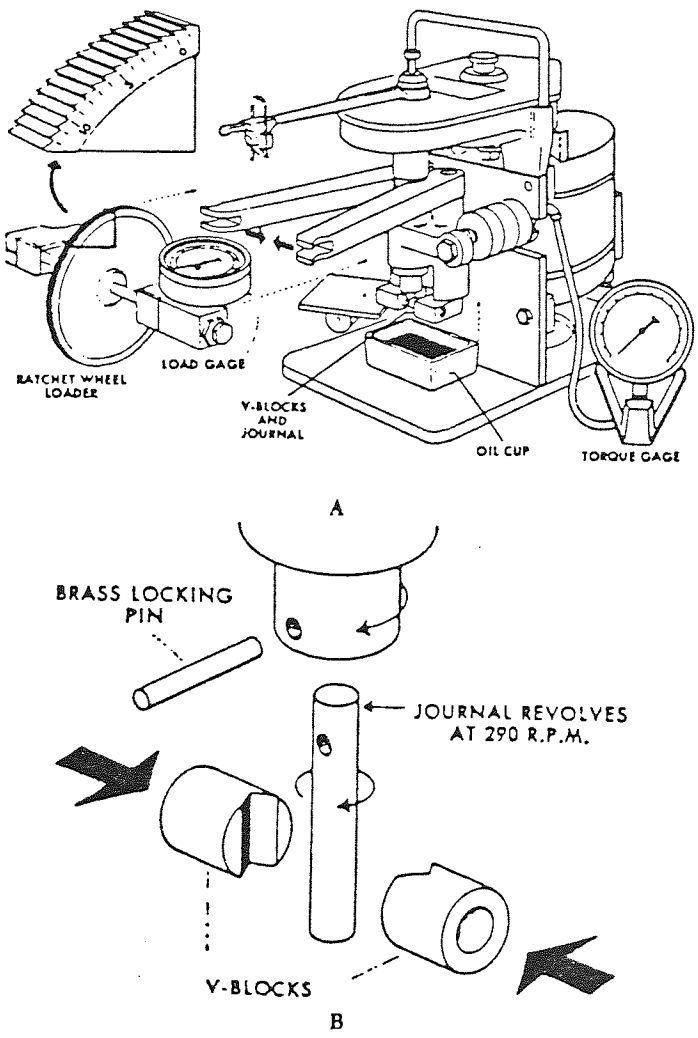

Figure 15. The Falex lubricant tester

In the Alpha Model LFW-1, figure 16, a ring rotates against a stationary block making line contact under a load. A

variable load is applied by dead weights through a lever system. Static and dynamic friction coefficients are calculated from the friction force indicated on a gauge. The weight loss and wear scar of the test block can be measured. The weight loss of the rotating ring is also determined (ASTM D2714-68).

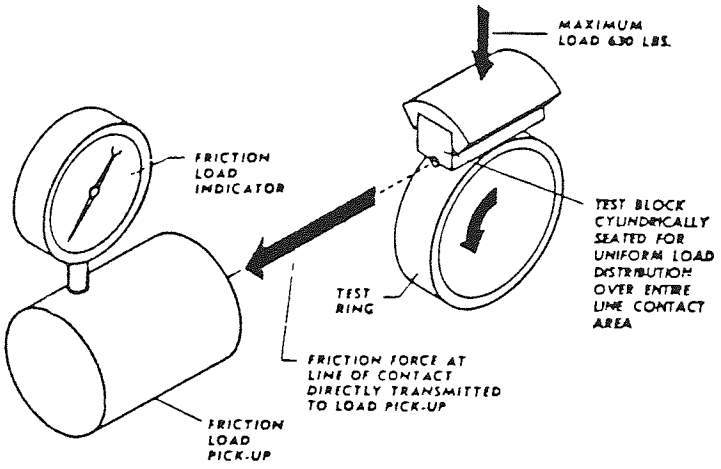

Figure 16. The Alpha LFW-1 testing machine

With cross cylinder machines geometrically the contact conditions are similar to those between balls, but more scope is offered in the variation of the ratio of rolling to sliding when each cylinder can be driven independently. In variations of this test type, one of the cylinders can be reciprocated in various directions. Cross cylinder machines are particularly suitable for the study of scuffing surfaces. Scuffing is connected with concentrated loads and high sliding velocities which this machine is able to produce.

In the simple two disc machine, one disc is mounted in a bearing supported in a loadable swinging arm, while the other is held in a rigid bearing. The first machine was introduced by

Merritt in 1953 [40] to simulate gear conditions and has found use in this field since.

Most experimental methods of measuring friction use relative tangential sliding as their mode of operation. In contrast the four-ball machine, figure 13, causes continuous rolling between the surfaces. It is known that a common type of failure in rolling elements is pitting fatigue, and this can be investigated satisfactorily with the four-ball device.

There are also numerous other methods of measuring wear, friction and lubrication. Those just described are among the most popular methods.

CHAPTER III

ELECTROLESS NICKEL - LITERATURE REVIEW

3.1 INTRODUCTION

Wear is principally a surface phenomenon, therefore, to increase the wear resistance of a component the surface properties must be improved. This can often be achieved by using alloyed materials and heat treating the whole component. However, the most economical method is to apply some form of surface treatment. For example, the deposition of a metallic coating possessing much improved wear properties than the original substrate material. Metallic coatings such as electroplated nickel, hard chromium and electroless nickel are well known for this application.

Electroless nickel is the deposition of nickel ions from solution by means of a chemical reducing agent. The reaction is catalysed by the deposited nickel and is thus an autocatalytic chemical reduction process.

Since gaining commercial use in the 1950's electroless nickel plating has grown rapidly and is now an established industrial process. Currently, hot acid hypophosphite reduced baths are the most frequently used to plate steel and other metals for wear and corrosion resistance. Warm alkaline hypophosphite baths are used for the plating of plastics and non-

metals for wear resistance and to produce a conducting surface for further electroplating i.e. printed circuit boards. Borohydride reduced baths are also used to plate iron and copper alloys.

The subject of this review is the reduction of nickel ions using sodium hypophosphite as the reducing agent, the most important system for wear resistance. This produces a nickel-phosphorous alloy, the structure and mechanical properties of which are dependent upon the formulation of the plating bath, the plating conditions and the post plating heat treatments.

3.2 HISTORICAL DEVELOPMENT

The deposition of nickel by a chemical reducing medium was first noticed by Wurtz[41] in 1844. Despite interest, most workers could only produce nickel powder within the solution, but a few succeeded in producing a mirror finish on the walls of the reaction vessel. The first patent for chemically reduced nickel was registered in 1916 by Roux[42]. It describes the manufacture of nickel coatings by immersing aluminium in hot solutions of nickel nitrate, hypophosphite, citrate and ammonia. The major problem with these early solutions was that they decomposed spontaneously on both work piece and reaction vessel. These problems were not overcome and not surprisingly the solution found little use and was soon disregarded.

In 1946 Brenner and Riddell[43,44] investigating the electrolytic deposition of nickel tungsten alloys from a solution of citrates, added a number of reducing agents. This resulted in an apparently greater than 100% current efficiency. They identified the reducing action of hypophosphite and established the autocatalylitic nature of the process. They went on to develop both acid and alkaline baths capable of producing nickel phosphorous deposits.

The first commercial electroless nickel bath was later developed by the General American Transportation Corporation (G.A.T.C.) who installed an experimental automatic plant in 1955. This led to the first industrial non-electrolytic nickel plating process under the trade name of "Kanigen"[45].

Since then much research has been carried out into most aspects of electroless nickel and although hypophosphite remains the most widely used reducing agent, others such as sodium borohydride, hydrazine and dimethyl amino borane (DMAB) have also been successful at producing nickel deposits. As mentioned this review will concentrate on hypophosphite reduced deposits as this type of solution was used during this particular research.

3.3 CATALYTIC NATURE

Electroless nickel deposits are produced by the chemical reduction of nickel ions by sodium hypophosphite onto a catalytic surface. The deposit itself is catalytic to the

reduction and so the reaction continues as long as the surfaces remain in contact with the electroless solution, hence autocatalytic chemical reduction. The catalysts for chemical reduction of nickel from hypophosphite solutions are the elements of the eigth group of the periodic table. However, only nickel, cobalt, rhodium and palladium are truly catalytically active[46] and can be directly non-electrolytically plated. As with nickel, these elements will continue the reaction until removed from the solution. In the case of non-catalytically acting metals, in order for the reaction to proceed, a catalytic surface must first be formed. Metals less noble than nickel, ie. Fe or Al, when dipped into the solution have metal nuclei deposited on the surface by exchange of electric charge, ie. galvanic action. The nickel acts catalytically and the process continues. Non-catalytically acting metals which are more noble than nickel, eg. Cu, Ag, Au, Cr and also carbon, can be activated by a short cathodic impulse or by contact with a less noble metal forming a galvanic cell. Autocatalytic nickel is then deposited on the surface and the process continues. Gutzeit[46] asserts that deposition is not possible on lead, cadmium, zinc, bismuth, arsenic, antimony, molybdenum, tin and tungsten. Such metals require a nickel strike in order to be electroless plated.

3.4 THE HYPOPHOSPHITE ELECTROLESS NICKLE PLATING SOLUTION

Electroless nickel plating solutions are a blend of different chemicals each performing an important function.

Electroless nickel plating solutions consist of:[47][48]

(a) A source of nickel ions.

(b) A reducing agent.

(c) Complexing agents/buffering agents.

(d) Stabilizers.

(e) Accelerators.

(f) Brighteners and wetting agents.

(a) **Nickel ions :** The nickel ions are supplied by nickel salts, ie. nickel chloride for alkaline baths and nickel sulphate for acid baths.

(b) **Reducing agent :** A number of different reducing agents have been used in preparing electroless nickel baths as previously mentioned. The majority of electroless nickel used commercially is deposited from solutions reduced with sodium hypophosphite. Apart from being a powerful reducer it has the advantage of lower cost, greater ease of control and better corrosion resistance of the deposit than those produced by using boron compounds or hydrazine.

(c) **Complexing agents :** To avoid spontaneous decomposition of the electroless solutions and to control the reaction so that it occurs only on the catalytic surface, complexing agents are added. These are organic acids or their salts, added to control the amount of free nickel available for reaction. They act to stabilise the solution and to retard the precipitation of nickel phosphite.

Complexing agents also buffer the solution and prevent the pH from decreasing too rapidly due to the increase of hydrogen ions liberated by the reduction reaction.

Early electroless solutions were complexed with the salts of glycolic, citric, malic or acetic acid. Later solutions were prepared using other polydentate acids including succinic, glutaric, lactic, propionic and aminoacetic.

(d) **Accelerators :** Complexing agents reduce the speed of deposition and can cause the plating rate to become uneconomically slow. To overcome this, organic additives, called accelerators or exultants, are often added to the plating solution in small amounts. Accelerators are thought to function by loosening the bond between the hydrogen and phosphorous atoms in the hypophosphite molecule, thus allowing it to be removed more easily and adsorbed into the catalytic surface. Accelerators include, succinic acid, saturated mono-carboxylic acid, amino-carboxylic acid and non-substituted dicarboxylic acid or their salts.

(e) **Stabilisers :** The reduction reaction of the electroless plating bath must be controlled so that deposition occurs at a predictable rate and only on the substrate to be plated. To accomplish this stabilisers, also known as inhibitors, are added. Even with the most carefully balanced solution there is a tendency for spontaneous decomposition. Decomposition is usually initiated by the presence of foreign

matter, such as dust or precipitates generated in the solution as the concentration of orthophosphite exceeds its solubility limit.

Spontaneous decomposition can be controlled by adding trace amounts of catalytic stabilisers to the solution. These stabilisers are adsorbed onto colloidal particles present in the solution and prevent the reduction of nickel on these surfaces. Stabilisers used with hypophosphite reduced nickel have been a) sulphur compounds, such as thiourea, b) oxy anions, such as molybdates or iodates and c) heavy metals, such as lead, bismuth, tin and cadmium.

Stabilisers can have a harmful as well as beneficial effect on plating and the deposit. In small amounts some stabilisers increase rate of deposition and/or the brightness of the deposit. Others, especially metals or sulphur compounds, increase internal stress and porosity, and reduce ductility.

The amount of stabiliser added is critical. The presence of only about 1mg/l of HS^- ions completely stops deposition. However, at concentrations of 0.01mg/l, HS- is an effective stabiliser. Baths containing less than 0.1mg/l Pb^{++} decompose rapidly, whereas solutions containing higher concentrations are stable.

(f) **Brighteners/wetting agents :** As with the galvanic process similar organic addition agents can be used to give rise to bright, lustrous electroless nickel deposits. Similar wetting agents can also be used.

3.5 THE PLATING MECHANISM

The mechanism involved in the hypophosphite reduction of nickel ions has given rise to much speculation for although the reaction can be generally represented by the following equation:

$$Ni^{2+} + (H_2PO_2)^- + H_2O \longrightarrow Ni + 2H^+ + H_2 + H_2PO_3^- \quad (35)$$

with hydrogen gas attributed to:

$$2[H] \longrightarrow H_2 \quad (36)$$

the details of how this reaction occurs have not yet been explained completely satisfactorily.

Brenner and Riddell[43] proposed two possible mechanisms, one electromechanical and the other involving atomic hydrogen. The electrochemical explanation of the process has been supported by Machu and El Gendi[49], Muller[50] and Ishibashi[51]. However, it is the second theory that is now more commonly accepted[43,44,45,52-56].

This suggests that nickel ions are catalytically reduced by active hydrogen adsorbed onto the catalytic surface formed from the reaction with hypophosphite and water, with the simultaneous formation of orthophosphite and hydrogen ions.

$$H_2PO_2^- + H_2O \longrightarrow H_2PO_3^- + 2[H] \text{ on the catalytic surface} \quad (37)$$

$$Ni^{2+} + 2[H] \text{ on catalytic surface} \longrightarrow Ni + 2H^+ \quad (38)$$

This gives the overall reaction in Eq. (35), with the reduction of hypophosphite ions to elemental phosphorous being attributed to the reaction:

$$H_2PO_2^- + [H] \longrightarrow P + OH^- + H_2O \quad (39)$$

Although this reflects the final result, the theory fails to explain the simultaneous reduction of nickel and hydrogen and the low values of the yield of hypophosphite.

Lukes[57] prposed that the reaction between hypophosphite and water leads to the formation of a hydride ion H^-, which with respect to nickel ions is a reducing agent. The hydride ion is oxidised to atomic hydrogen which recombines to evolve a gas.

$$H_2PO_2^- + H_2O \longrightarrow HPO_3^{2-} + 2H^+ + H^- \quad (40)$$

$$Ni^{2+} + 2H^- \longrightarrow Ni + 2H \quad (41)$$

$$H^+ + H^- \longrightarrow H_2 \quad (42)$$

This gives a satisfactory explanation of the laws of a coupled reduction of nickel and hydrogen.

Nikiforova and Sadakov[58] believe that the reaction between hypophosphite and water is accompanied by a decomposition of water molecules:

$$H_2O \longrightarrow H^+ + OH^- \quad (43)$$

This leads to the production of an electron and atomic hydrogen

$$H_2PO_2^- + OH^- \longrightarrow H_2PO_3^- + [H] + e \quad (44)$$

Hydrogen is produced according to the reaction:

$$H^+ + H + e \longrightarrow H_2 \quad (45)$$

in equal parts with the overall reaction being:

$$H_2PO_2^- + H_2O \longrightarrow H_2PO_3^- + H_2 \quad (46)$$

Reaction (44) shows that two sodium hypophosphite molecules are required to reduce one nickel ion. The total

reaction can be written as:

$$Ni^{2+} + 2H_2PO_2^- + 2H_2O \longrightarrow Ni + 2H_2PO_3^- + 2H^+ + H_2 \qquad (47)$$

with acidification of solutions due to the decomposition of water.

For the accompanying phosphorus deposition it is believed that one electron is needed for the reduction of one ion of hypophosphite to elemental phosphorus according to the reaction:

$$H_2PO_2^- + e \longrightarrow P + 2OH^- \qquad (48)$$

the kinetics of which are favoured by an acid condition. The overall reaction being:

$$2H_2PO_2^- \longrightarrow H_2PO_3^- + P + OH^- + [H] \qquad (49)$$

These theories[57-59] have helped to explain the experimentally found regularities of the reaction.

3.6 FACTORS INFLUENCING THE DEPOSITION RATE AND COMPOSITION OF DEPOSITS.

There is no simple relationship between components of the solution and the plating rate. Much work has been done on the conditions and components of the working solution, the results of which have sometimes contained contradictions. This fact can be understood when we realise the number of factors which affect the speed of reduction.

Gawrilov[60] expressed these factors as:

$$\text{Plating rate} = f(T, pH, [C_{Ni}2+], [C_{H_2PO_2}-], [C_{HPO_3}2-], S/V, C, A, S, n_1, n_2.....)$$

whereby T = temperature,

pH = pH value,

$C_{Ni}2+$ = concentration of nickel,

$C_{H_2PO_2}-$ = concentration of hypophosphite,

$C_{HPO_3}2-$ = concentration of phosphite,

S/V = relationship of surface to volume,

C = nature and concentration of the complexing agent,

A = nature and concentration of the accelerator,

S = nature and concentration of the stabiliser,

n_1, n_2 = additional factors such as pressure, speed of agitation etc.

Before considering the major factors individually it can be noted that, with a correctly balanced plating solution, as the plating process continues the composition of the solution will change if left uncorrected. The concentration of stabilisers and nickel and hypophosphite ions will reduce, whilst the concentration of phosphite and hydrogen ions will increase. This will result in a steady decrease in the rate of deposition and an increase in the phosphorus content of the deposit[61].

(a) **Temperature:** The amount of energy, in the form of heat, present in a hypophosphite electroless nickel solution is one of the most important variables affecting deposition rate.

The part reactions only start at around 40-50 ^{o}C so a higher than normal (ie. electrolytic) operating temperature is required. The deposition rate is thus very slow at temperatures below 65 ^{o}C but increases rapidly with increased temperature[62], figure 17, to the usual operating range of 90-98 ^{o}C. At temperatures above 100^{o}C however the solution may decompose. Baldwin and Such[62], have also shown that the phosphorus content of the deposit will fall slightly from 7.5 to 6 wt% phosphorus with an increase in temperature from 70 ^{o}C to 90 ^{o}C.

Figure 17. The effect of temperature on plating rate[62]

(b) **pH value:** Early electroless nickel formulations were ammoniacal and operated at high pH. Later acid solutions were found to have several advantages over alkaline solutions, such as higher plating rate, better stability, greater ease on control and improved deposit corrosion resistance. Accordingly

most hypophosphite reduced electroless nickel solutions are operated between 4 and 5.5 pH.

It was seen from reaction (44) in section 3.5 that the concentration of hydrogen ion increases with the reduction of nickel ions[46,50,63]. The resulting acidification of the solution can be partially offset by buffer systems, however, when changes in pH do occur they have significant effects. A decrease in pH will produce an increase in the level of phosphorus content[62,63] of the deposit, figure 18.

Figure 18. The effect of solution pH on alloy composition and plating rate[62]

Low pH can also prevent separation of basic salts and hydroxides and a reduction in the reducing properties of the hypophosphite. A rise in pH will increase the speed of reduction[62], until the hypophosphite reaction changes from one of catalytic to homogeneous, leading to spontaneous dissociation of the solution. A rise in pH will also reduce the solubility of nickel phosphite, the precipitation of which can initiate dissociation and produce rough coatings.

(c) **Nickel concentration:** A typical acid electroless nickel plating solution containing 4-16 g/l of nickel is virtually uneffected by concentration of nickel ions in solution.[62]. An increase in the concentration of nickel ions from 4-10 g/l does however produce an increase in nickel content of the deposit, any further increase has little effect.

(d) **Hypophosphite concentration:** Brenner and Riddell[43] found no significant influence of the concentration of hypophosphite on the speed of reaction of glycolate solutions. Gorbunova and Nikiforova[64] with a similar solution containing less glycolic acid found a maximum speed at 10g/l sodium hypophosphite. Baldwin and Such[62], showed that the plating rate increases with the hypophosphite content until appoximately 10g/l, after which, hypophosphite has little effect on plating rate. They also showed that the phosphorus content of the deposit will increase in almost linear fashion with hypophosphite content. According to Gutzeit and Krieg[65] it is more important to maintain the optimum Mol ratio $Ni^{2+}/(H_2PO_2)^-$ in the range 0.25 to 0.6 or even more accurately 0.3 to 0.45.

(e) **Complexing agents:** Complexing agents act in two ways: they buffer the solution and also reduce the concentration of free nickel ions in order to prevent precipitation of nickel phosphite. The solution is stabilised but the formation of these complexes normally causes a slowing down in the speed of deposition. It has been shown[53] that the speed of deposition reaches a maximum at a certain concentration of acid after which

slowing down is considerable as the availability of nickel ions is severely reduced.

3.7 STRUCTURE AND PROPERTIES OF ELECTROLESS NICKEL

Hypophosphite reduced electroless nickel has been shown[60,66-69] to have markedly different properties from those of electrolytic deposited nickel. As applied, the nickel-phosphorus deposits are uniform, hard, relatively brittle, easily solderable and highly corrosion resistant. Because of their alloy nature they can be precipitation hardened to very high levels through the use of low temperature treatments, producing wear resistance equal to that of commercial hard chromium coatings. This combination of properties makes the coating well suited for many severe applications.

3.7.1 Structure

The microstructure of an as-deposited electroless nickel phosphorus alloy is a pore free, amorphous, banded or lamellar structure with, in certain instances, evidence of columnar growth[61,70]. Many authors believe the morphology is due to the periodic change of the phosphorous content of the deposit, however, this is still subject to discussion.

Goldstein[70] and his co-workers[71] carried out x-ray analysis on coatings of 7-10% phosphorous. They concluded that

such coatings were amorphous or "liquid-like" structures. However, coatings with phosphorus contents below 7% exhibited a crystalline structure[61].

A different viewpoint was presented by Graham, Lindsay and Read[61]. They considered layers with 4.6-9.4% phosphorus, as super-saturated solid solutions of phosphorus in crystalline nickel, whereby the layers showed a pronounced fibrous structure in the (111) direction. The grain size was dependent on the content of phosphorus[61] and in nickel layers with 9.4% phosphorus it was only about 160 nm. Wiegand et al[72] estimated the size of crystals to be 600 nm whilst Pai et al[73] suggested that the size is even smaller, from 100 to 200 nm.

From the phase diagram, figure 19, it can be seen that a number of forms of nickel phosphide are possible in phosphorus rich layers. Randin[74,75] and co-workers have shown the presence of the phase Ni_2P, and assumed that the entire phosphorus content was present as nickel phosphide, Ni_2P, and that only very little was present in its elemental state. During heat treatment Ni_2P became Ni_3P and the latter compound was built into the nickel matrix.

During heat treatment the structure undergoes significant changes. According to Goldstein[70] heat treatment at 200 ^{o}C for 20 hours does not lead to any changes in structure. Heat treatment at 400 ^{o}C[76] precipitates Ni_3P out and the boundaries between lamellar become less pronounced and will

disappear after treatment at 600 ^{o}C for one hour. Further treatment at increased temperatures (600-800 ^{o}C) leads to re-crystallisation.

Figure 19. Nickel phosphorus binary phase diagram
(Hansen, Constitution of Binary Alloys, McGraw-Hill)

Graham[61] believes the crystallisation of the phase Ni_3P in the solid solution is initiated on the basis of nickel on a surface of the crystal lattice of nickel in which the position of the atoms is similar to that in the crystal lattice surface of Ni_3P.

Goldstein[70] who postulated the amorphous structure assumes the structure first changes to a super-saturated crystalline solid solution which then decomposes under segregation of the phase of the intermetallic compound Ni_3P.

Alloys containing 8.5 or 9.0% phosphorus are considered as nickel dispersed in a Ni_3P matrix phase. For alloys containing less than 7% phosphorus, Ni_3P is dispersed in the nickel phase[61]. This change in structure at about 7% phosphorus is associated with the changes that occur in the strength and ductility of electroless nickel at this phosphorus content (see figure 20).

3.7.2 Properties of electroless nickel

As this work is primarily aimed at developing coatings for wear applications this review is directed at those properties of electroless nickel which are relevant to its performance in wear situations.

(i) Strength and ductility

Electroless nickel deposits have high strength with limited ductility and a high modulus of elasticity. The ultimate tensile strength of commercial coatings exceeds 700 MPa and allows the coating to withstand a considerable amount of abuse without damage. These properties are influenced considerably by phosphorus content of the deposit[61]. Both properties reach a maximum at about 7% phosphorus and then remain relatively

constant, figure 20. With deposits containing metallic or sulphur impurities ductility is greatly reduced and may approach zero.

The change in structure by heat treatment reduces both the strength and ductility of deposits[61,72]. Below 600 ^{o}C the strength and ductility are both reduced, ductility almost to zero, figure 21. Heat treatment at 750 ^{o}C, however, will increase the strength and ductility of the deposits with phosphorus contents below 7%. The difference in properties of the deposit below and above 7% are quite significant. As mentioned, links have been drawn between this and the considered change in structure at about 7% phosphorus.

Figure 20. Influence of phophorus content on the strength and strain at fracture of electroless nickel[61]

Figure 21. The effect of heat treatment on the ductility of a 6% phosphorus electroless nickel[61]

A decrease of 10% to 46% in the fatigue strength of high speed steel, as a result of plating with electroless nickel, has been reported in several investigations[69].

(ii) Hardness

The hardness of as-deposited electroless nickel is significantly higher than that of electrolytically deposited nickel. As-deposited, the hardness is about 500-600 Hv. There is little significant change in hardness with phosphorus content between 2-11%; though a slight decrease has been reported[61,63] in hardness with phosphorus, quoting a minimum at 7%. Alloys containing 13-19% phosphorus are much softer at 300-375 Hv.

The ability to heat treat electroless nickel and cause age hardening by precipitation of nickel phosphide enables the hardness of the coating to be considerably increased[50,61-

63,77,78). Alloys of 4-11% phosphorus can be increased to 900-1100 Hv by heat treatment for 1-2 hours at 400-450 °C, figure 22.

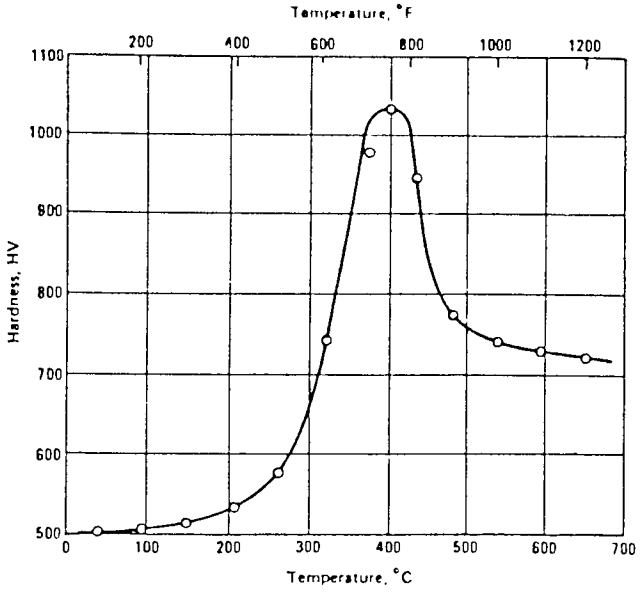

Figure 22. The effect of heat treatment temperature on the hardness of electroless nickel deposits(50,61-63,77,78)

Hardness after heat treatment at 400 °C does not appear to vary appreciably with phosphorus content. Some deposits, however, containing 13-19% phosphorus have a tendency to be much softer, 350-450 Hv after similar heat treatment. This can be improved for these alloys by heat treatment at higher temperatures(63). These alloys will also retain a higher hardness after heat treatment at much higher temperatures, than deposits of lower phosphorus content(63).

Up to about 300 °C the hot hardness of electroless nickel is equal to or better than that of hard chromium coatings. As deposited coatings also retain their hardness to this temperature, although at a lower level. Above this temperature

the hardness rapidly decreases and hard chromium is superior. Figure 23.

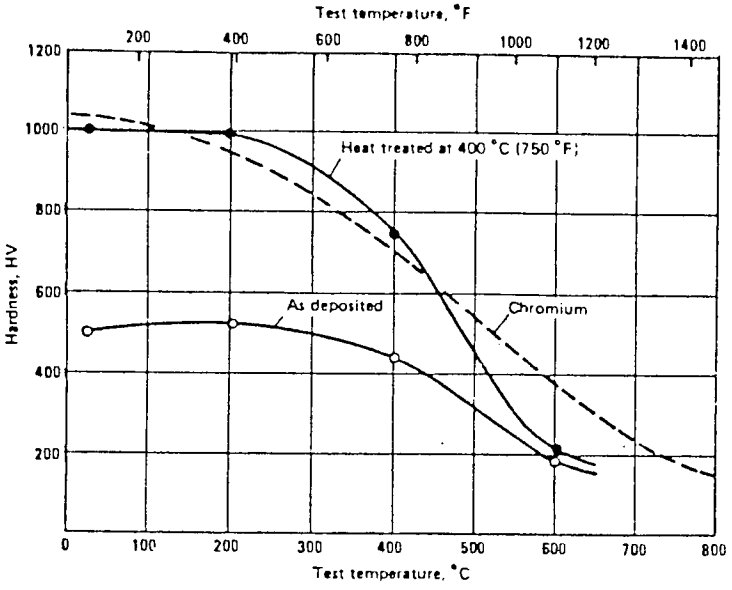

Figure 23. The hardness of electroless nickel-phosphorus alloys at elevated temperatures (10 % Phosphorus)

(iii) Internal stress

The internal stress in electroless nickel deposits is a function of composition and substrate material. As illustrated in figure 24, stress in coatings on steel containing 10 % phosphorus is neutral or compressive[79]. With lower phosphorus deposits, however, tensile stress develops.

Figure 24. Effect of phosphorus content on the internal stress of electroless nickel deposits[79]

Stresses develop on different substrate materials because of the difference in thermal expansion between the deposit and the substrate. The stress in nickel on brass or aluminium, which have a high coefficient of expansion, tends to be compressive when the phosphorus content exceeds 6% to 7%. However, nickel-phosphorus alloys on metals such as titanium, beryllium or steel , which have a low coefficient of expansion, are stressed in tension when the phosphorus content is less than 11%[79]. Minimum stress can therefore be achieved by control of the plating process to give the desired levels of phosphorus for the substrate used. To retain a compressive stress in heat treated coatings on substrates with low coefficients of expansion, ie. steel, the coating as-deposited must have at least 11.5% phosphorus.

The structural changes during heat treatment at temperatures above 220 ^{o}C cause a volumetric shrinkage of electroless nickel deposits of up to 4-6%[80]. This increases tensile stress in the coating. Stress can also be increased by the codeposition of orthophosphite or heavy metal ions as well as by the presence of excessive complexing agents in the plating solution. High levels of internal stress also reduce the ductility of the coating often promoting cracking. Addition agents such as saccharin and other organic sulphur compounds, as with electrolytic solutions, have been reported to reduce stresses in electroless nickel deposits[81].

(iv) **Wear resistance**

Because of their high hardness, electroless nickel deposits have excellent resistance to wear and abrasion, both in the as-deposited and hardened condition. Work by numerous authors using different methods of assessing wear have confirmed this[52,63,72,78,84]. In the as-deposited condition electroless nickel lies between that of hard chromium and electrolytically deposited nickel. Heat treatment however, can improve the wear resistance to equal that of hard chromium.

Randin and Hinterman[63] examined the influence of the phosphorus content upon the value of wear. The greatest wear was established in the as-deposited condition at a phosphorus content of approximately 7%. With increasing hardening temperature wear is decreased. Maximum wear resistance was found at a hardening temperature of 400 ^{o}C for 1 hour, with the resistance increasing with phosphorus content, figure 25 . For low temperature heat treatments, wear at first increases with phosphorus content but above 7% it begins to decrease again. High temperature heat treatments also reduce the wear resistance. Parker[83] used a number of wear testing methods and also concluded that heat treatment improved the coating's wear resistance.

Wiegand[72] and his co-workers showed that the connection between hardness and abrasion resistance cannot be extended either for conditions of wear by furrowing or by lapping. Furrowing wear is constant for the entire range of

hardness. This shows the complicated nature of wear and the difficulty in fully assessing a coating's wear properties.

Figure 25 . Wear resistance as a function of heat treatment and phosphorus content [63]

Work by Gould[85] showed that the fretting wear resistance of components can be improved by electroless nickel, the improvement increasing with the heat treatment.

The frictional properties of electroless nickel are generally quite good, the phosphorus content providing a degree of natural lubrication. Table 1 gives an indication of values that can be expected for sliding friction for various pairings. Frictional values for electrodeposited chromium are lower than those of electroless nickel. Against itself or electrolytic nickel high values of friction occur because of the high degree of mutual solubility between the two surfaces. This can lead to complete seizure.

Table 1. Coefficient of friction of electroless nickel-phosphorus[60]

Paring of substances	Coefficient of friction	
	Dry	Lubricated
Nickel-Phosphorus-Nickel	Seizure	0.26
Nickel-Phosphorus-Nickel	0.45	0.25
Nickel-phosphorus/Nickel-Phosphorus	0.43	0.30
Nickel-Phosphorus/Chromium	0.38	0.21
Nickel-Phosphorus/Cast Iron	0.16	0.08
Chromium/Chromium	0.43	0.26
Chromium/Steel	0.21	0.15

(v) Uniformity

One especially beneficial property of electroless nickel is a uniform coating thickness. With electroplated coatings thickness can vary significantly depending on the shape and proximity of the part to the anodes. With electroless nickel the plating rate and coating thickness are the same on any section of the part exposed to fresh plating solution. Grooves and blind holes then have the same amount of coating as the outside sections.

(vi) **Adhesion**

Adhesion of electroless nickel coatings to most metals is excellent. The initial replacement reaction, which occurs with catalytic metals, together with the associated ability of the baths to remove submicroscopic soils, allows the deposit to establish metallic as well as mechanical bonds with the substrate. The bond strength of the coating to properly cleaned steel or aluminium substrates has been found to be at least 300-400 MPa. With non-catalytic or passive metals proper pre-treatment and activation can produce adequate adhesion although at reduced levels, approximately 140 MPa[60,86].

Baking can be of assistance if pre-treatment has been less than adequate, but with properly applied coatings, baking has only a minimal affect on bond strength. Baking does however reduce hydrogen embrittlement of the coating.

(vii) **Corrosion resistance**

Electroless nickel is a barrier coating, protecting the substrate by sealing it off from the environment, rather than using sacrificial action. Because of its amorphous nature and passivity, the corrosion resistance is excellent and in many environments, superior to that of pure nickel or chromium alloys[60,80].

The corrosion resistance of an electroless nickel coating is a function of its composition. Alloys containing more than 10% phosphorus are more resistant to attack than those with lower phosphorus contents[80]. Heat treatment of nickel-phosphorus deposits precipitates nickel phosphide particles, reducing the phosphorus content of the remaining material. This reduces the corrosion resistance of the coating. The particles also create small active/passive corrosion cells, further contributing to the corrosion of the deposit. Heat treatment also shrinks the deposit as it hardens, this can crack the coating and expose the substrate to attack.

CHAPTER IV

COMPOSITE COATINGS - LITERATURE REVIEW

4.1 INTRODUCTION

Despite the advantages of coatings such as nickel, and especially electroless nickel, as wear resistant coatings, there is still a need to improve the performance of such coatings in the more extreme wear situations. Accepting this fact, research was carried out to improve the wear resistance, in the first place of electroplated deposits , and later of electroless deposits as the process became commercially developed. The technique used involved producing composite coatings by incorporating into the metal coating a second phase of insoluble particles having an abrasive, refractory or lubricating nature. In this way the two materials were combined and the desirable properties of one were enhanced by those of the other, resulting in the production of a single composite system possessing both extended mechanical and physical properties.

For example, the incorporation of hard particles into a nickel coating significantly increased hardness, wear resistance and hot hardness of both electrolytic and electroless nickel, the degree of improvement depending on the type of second phase used. Better properties were produced with electroless nickel because of the all round superior properties of the matrix.

4.2 MATRIX MATERIAL

The matrix, or binder phase, should be designed to put the good and desirable properties of the particles to full use. This means it must be: mechanically strong, to withstand the load acting on the particles; have a high abrasion resistance; be corrosion resistant, so that the particles do not get undermined and lost from the coating prematurely; and be economic. As is often the case a compromise is inevitable and it is the economic factor in particular that often takes priority.

The above basically defines a good coating system. It is therefore not surprising that electroplated nickel, which has evolved as a good all-round coating, should also possess the properties of a good matrix for composites. Electroplated nickel was the initial basis for commercial composite developments and resulted in considerably improved wear resistant properties. Electroless nickel is even more suitable for supporting incorporated particles and producing composite coatings with further improved properties than electrolytic nickel composites.

Other matrix materials and particle combinations may possess better properties, however such improvements often minimal can be costly, and are thus not economical for everyday use. But there are situations where cost is not such an important factor eg. aerospace applications. Here it is possible to use relatively expensive to produce coatings, such as cobalt/chromium carbide, which has very good wear resistance and

hot hardness. The process of composite coatings is of course limited to those metals which can be electro or electroless plated, but has included copper[87], iron[88], gold[89], silver[90], lead[91], rhodium[92], chromium[92], platinum[92], tin[93], zinc[94] and cobalt[95].

4.3 PARTICLE CLASSIFICATION

Table 2[96] shows the type of material suitable for codeposition in electrolytic and electroless coatings. Many varieties of composite coatings are made possible by substituting different particles into different matrices. In this way, different second phase material ie. in size, shape and composition, can be selected for specific purposes.

Table 2. Powders applicable for codeposition[96]

Kaolin	Glass	Talcum
Graphite	Plastics	Diamond

Oxides, carbides, borides, nitrides, silicides, sulphides, silicates, sulphates, carbonates, phosphates, oxalates and fluorides from:

Aluminium	Tantalum	Barium
Boron	Vanadium	Strontium
Chromium	Tungsten	Cerium
Hafnium	Zirconium	Iron
Molybdenum	Manganese	Nickel
Silicon	Magnesium	Titanium
Calcium	Graphite	

Metals and alloys from:

Boron	Titanium	Zirconium
Chromium	Tantalum	Hafnium
Vanadium	Molybdenum	Tungsten
Stainless Steel		

One characteristic common to all these substances is that they are insoluble, or only slightly soluble, in the plating solution. If they are slightly soluble the dissociated ions must not affect the metal deposition mechanism.

The type of particle incorporated, ie. abrasive, refractory, metal or lubricant, dictates the properties of the composite coating. Taking the range of particles that can be incorporated, it is possible to divide composite coatings into three basic categories according to the properties imparted into the coating by the particle phase:

(a) Wear resistant coatings.

(b) Dry lubricant coatings.

(c) Heat treatable metal alloys.

The following sections describe these coatings.

4.4 ELECTROLYTIC COMPOSITE COATINGS

The technique of producing electrolytic composite coatings was first used by Fink and Prince[97] in 1928 to deposit finely divided graphite with copper. It has since been employed, not only in the production of wear resistant coatings, but also in producing bright or semi-bright nickel layers for obtaining microphous chromium deposits and semi-bright coatings with a satin effect[98].

Commercially, diamond dust and grit were the first solids to be incorporated into a nickel electrodeposit in order

to manufacture diamond tools[99-101]. Synthetic polycrystalline diamonds, formed by the shock wave method, have a rough surface which offers a greater degree of mechanical keying than the smooth natural diamonds. Natural diamonds however have superior performance. Du Pont coat a number of items with diamond composites includng drill tips and tools for microfinishing profile sections. These coatings are abrasive and must be so in order to function correctly. For most other industrial purposes, such as wear resistance, hard but less abrasive composite coatings are desired and so non-metallic particles such as silicon carbide are generally used.

The technique adopted to produce such coatings is simply to deposit nickel or cobalt under standard conditions from conventional plating baths in which are contained solid particles kept in suspension by agitation. Agitation of the slurry is one of the most important factors in composite plating. This is required to provide an even distribution of particles throughout the electrolyte, necessary for the formation of a homogeneous coating. The most developed methods are those used for the production of cobalt chromium carbide composite coatings, where circulating liquid/air units and plate pumping systems are used[95,102-106].

4.4.1 Wear Resistant Electrolytic Composite Coatings

Wear resistant coatings are produced by incorporating hard, abrasive or refractory particles. In general it can be

resistance of the coating. Likewise, the harder the matrix the better the wear resistance of the composite. Larger particles seem to provide somewhat better resistance to abrasion but experience has shown that they produce a more aggressive finish which abrades the mating material unless lapped or polished smooth before use[107]. Therefore small hard particles, between 1-12 μm in size in a hard matrix are more versatile and the most practical combination for general use. Other considerations are cost and availability of material in the desired shapes and micron sizes. Typical particles include oxides, eg. SiO_2, Al_2O_3, TiO, ZrO_2, or carbides, Cr_3O_2, WC, SiC, diamonds and other such hard non-metallics.

The original wear model was based on the concept that when the composite coating was brought into contact with a sliding counterface, wear would continue until sufficient hard particles were exposed for the wearing load to be completely supported by the additive. Consequently, provided that the wearing load did not exceed the compression yields strength of the composite, the wear pattern would be dictated mainly by the tribological properties of the hard particles. Practice has shown this not to be strictly true, in that there is always contact between the matrix and the counterface. Consequently, for the composite coating to have usable wear properties, the matrix must also have good wear resistance in its own right.

Composite coatings are usually assessed by comparing the performance of coated metal against some standard material in an

engineering situation, or in an accelerated test, (see Wear Testing, Chap. 2). Such tests show wear rates of electrolytic composite coatings to have significantly greater wear resistance than conventional electrolytic coatings, particularly at temperatures greater than 300° C up to 800° C. The hardness of these coatings is also considerably increased although this cannot always be relied on as an indication of wear resistance. The tendency for cold welding is also decreased.

The use of electrodeposits in conjunction with wear resistant hard particles was patented in 1962[108] by Grazen. One of the first major applications of a composite coating for a wear application was an electrodeposited nickel and silicon carbide composite coating applied to the Wankel trochoid surface rotary engines in Germany[109]. Nickel-silicon carbide is now used to coat cylinder liners of aluminium engines, for extended wear life, and numerous other applications. Many more composite coatings have since followed involving a variety of hard particles and several different types of matrices.

A composite coating, that has been a great success and is still finding new applications, is that of cobalt-chromium carbide. The coating known as "Tribomet" has been extensively examined by Kedward et al[95,102-105] and Cameron[106] and has been shown to have excellent wear and oxidation resistance up to 800°C. The coating has found many applications particularly within the aerospace industry.

Although many combinations of particles and matrices have been considered (Section 4.2 Matrix Material) the most work by far has gone into wear resistant coatings of electrolytic nickel, as this type has found the most applications. Particles of hard materials, ie. carbides, oxides, and diamond, have been successfully incorporated in both Watts[110-112] and sulphamate[113] baths.

The proportion of incorporated particles in the nickel coatings can vary between 1% and 50% by volume, although around 5% to 30% by volume is normally used in practice. This content is achieved by adding concentrations of between 25 and 150 grams per litre to plating solutions; more than the latter has little effect on the volume included in the coating.

Nickel-TiO_2 deposits have hardness values of 350 Hv dependent on plating variables[114,115]. They are softer than nickel-alumina composites (hardness 500 Hv[116]) even though the amount of TiO_2 codeposited is double that of alumina. Nickel-silicon carbide coatings have been deposited from sulphamate baths with hardnesses of 600 Hv[113] and high abrasion resistance.

Ishimori[117], working for the Suzuki Motor Company, applied a nickel silicon-carbide coating to the cylinder liners of a two stroke engine and found a sixty per cent reduction in wear loss over cast iron cylinder liners.

Viswanethan et al[118] produced electrolytic nickel-silicon carbide composites by a technique of "sediment codeposition" where particles were allowed to fall onto an upward facing cathode. Particle contents as high as 40% were reported by this method. The process was however more suited to codeposition of expensive particles such as diamond, as only very small quantities of powder were required.

The nickel-boron carbide[115], nickel-tantalum carbide, and nickel-titanium carbide coatings[119], produced by the electrolytic technique, have been reported to be oxidation resistant, corrosion and wear resistant, with high tensile strength. Other materials such as uranium oxide, iron oxide, boron nitride[120] and zirconium boride have also been successfully incorporated into the metal matrix[118]. Electrodeposited nickel can also be reinforced by fibres[121]. This technique was aimed at producing stronger electroforms than would otherwise be obtainable.

The properties of a metallic coating can be modified by the inclusion of sub-micron particles to give a dispersion-strengthened material. Such composites have a hardened structure and therefore, generally, an improved wear resistance. They can easily be fabricated by codeposition.

One of the earliest publications on dispersion-strengthened composites was by Sauter[122] who briefly evaluated both the conditions of formation and the properties of nickel-

alumina composites. Sauter found that the sub-micron particles increased the room temperature yield strength from 8 kg/mm^2 for pure nickel to 15 kg/mm^2 for nickel-alumina containing 3.5 to 6.0 volume per cent alumina. In addition he found yield strength increased with particle concentration.

Nickel cermets (the name given to nickel and ceramic particles) are generally heat resistant up to 800°C. Nickel-boron carbide coatings showed no change in the surface structure of the deposit after heat treatment at 375°C. Nickel-alumina composites showed no change in the microstructure up to 750°C[113] but at temperatures of 1110°C the oxide particles were dissolved and large crystals of nickel aluminate were formed. Nickel titanium dioxide composites when heat treated in a hydrogen atmosphere, showed no change up to 800°C but at 1000°C there was a change in the structure attributed to either the partial reduction of TiO_2 to Ti_2O_3, or the redistribution of the particles[114].

4.4.2 Dry Lubricant Electrolytic Composite Coatings

Coatings with the inclusion of dry lubricating particles find applications where adhesion between contacting surfaces is a significant factor. As proposed in the review of friction (chapter II), most surfaces, even those which feel smooth and give good reflection, are rough and when placed in contact touch only at the tips of their asperities. At these points of contact, if the surfaces are clean, adhesion or cold welding

(galling) will occur. Sliding can then only occur when sufficient force is applied to shear the junctions of contact.

The most effective way of reducing contact between the two metal surfaces, and reducing friction, is by introducing a fluid lubricant. However, in many sliding situations fluid lubricants cannot be used. In such situations, films of lamellar solids which generate a low shear strength surface film, can be applied. These films are very thin, and wear rates are high unless filled with harder material to prolong the wear life.

An alternative, especially in the case of nickel coatings which have a significant tendency to galling in dry wearing situations, is to incorporate such lamellar solids into the coating in order to lubricate the surface. Throughout the life of the coating, lubricating particles are continuously exposed supplying a constant coating to the surface. Such coatings confer release (non-stick), non-galling, dry lubrication, lower coefficient of friction and improve the bearing capabilities of the coating. Materials capable of performing as dry lubricating solids in nickel coatings are typically graphite, molybdenum disulphide and PTFE.

The codeposition of a lamellar solid is more difficult than the codeposition of ceramic particles. However, materials such as graphite, mica, PTFE and molybdenum disulphide can all be codeposited.

Nickel-molybdenum disulphide systems have a low inclusion content but it is sufficient to generate a low shear strength surface film under low load conditions[123,124]. Lowering the pH and the current density raises the volume per cent of the $MoSO_2$ in the coating. The same behaviour is observed in the codeposition of graphite, mica, and PTFE. This effect is attributed to the adsorption of hydrogen ions on the particle surface[125], but is more likely to be connected to the reduced plating rate. Vest et al[126] examined the use of a nickel-molybdenum disulphide coating as a dry lubricant for applications within the spacecraft industry. They found the coefficient of friction of the coating to be sufficiently low but were hampered by poor adhesion of the coating onto aluminium and the poor load bearing capacity of the coating.

Nickel-boron nitride composites have similar properties to nickel-molybdenum disulphide but possess high oxidation resistance and are used to overcome the problem of fretting corrosion. Barium sulphate in nickel has also been studied to improve sliding contacts because of their anti-stick properties[127].

Graphite can be included in nickel matrices either as fibres or powder[125,128] to produce dry lubricating surfaces. Finks and Prince[97] who were the first to record work within the field of composites, examined the codeposition of graphite powder from an acid copper sulphate bath. They conclude that it was quite feasible to produce such wear resistant coatings although

no wear results were reported. Graphite coatings were also produced by Mitchel[129], Williams and Martin[130] and by Faust et al[131]. The latter workers codeposited graphite with both zinc and nickel. Zinc-graphite deposits have also been investigated by Donakowski[132] who showed the deposit to have good anti-galling properties. Ghouse et al[133] showed a reduction in the coefficient of friction by the inclusion of graphite into both nickel or copper.

Composites of copper and nickel containing graphite fluoride particles were produced by Yuco Tsuya et al[134]. Graphite fluoride was chosen for its ability to withstand chemical breakdown at temperatures where other powders, such as molybdenum disulphide, would decompose. After a detailed study they concluded that a copper-graphite fluoride composite was a more wear resistant coating than the similar nickel composite.

Polytetrafluoroethylene (PTFE) is a substance with a very low coefficient of friction and has therefore been the subject of a number of investigations. However, this material is difficult to codeposit without the use of suitable wetting agents, this was overcome in a Swedish patent by Akzo[135]. Work was carried out by both Plastique[136] and Boyer[137] on the codeposition of PTFE powder. Similarly, a patent by Vandervell Products Ltd[138] described the codeposition of PTFE with lead for particular use as a bearing material. They suggested that graphite or indium could also be substituted for the PTFE powder.

4.4.3 Metal Alloy Electrolytic Composite Coatings

This third type of coating is produced by incorporating inert metallic particles into the coating. Subsequent heat treatment will produce an alloy coating. The metallic particles can be chromium, molybdenum, tungsten, titanium, vanadium, zirconium, hafnium, niobium, tantalum or alloys of metals, eg. stainless steel[96]. Such coatings can be heat treated to develop high temperature corrosion and oxidation resistant coatings, with considerable hardnesses.

Electrodeposition in the presence of conducting particles, such as metal powders, generally leads to a dendritic-like growth and porous deposits. However, chromium powder has been codeposited with nickel and heat treated above 1000°C to produce nickel-chromium alloys[140,141] for electroforming. Bazzard[140], who produced the nickel-chromium alloys, controlled dendritic growth by mechanical methods. Bazzard also reported that the chromium content was controlled by the concentration of particles in suspension rather than current density.

An alternative method of producing Ni-Cr alloy coatings was suggested by Wearmouth[141]. In this technique Cr_2C_3 was codeposited into a nickel matrix. Subsequent heat treatment under controlled atmospheres resulted in a breakdown of the carbide. The chromium diffused into the nickel matrix, whilst the carbon was lost to the substrate and the atmosphere, leaving a nickel-chromium alloy coating.

A quaternary alloy of Ni-Co-Cr-Zr was produced by Sova[142]. Here a zirconium powder was codeposited with a nickel-chromium matrix and overlayed with chromium. Subsequent heat treatment at 1100°C produced the alloy coating. Similar highly alloyed coatings have also been produced by plating with a mixture of powders or with alloyed powders.

Newnham and Foster[143] produced alloys similar to stellite and X40 (Cr-W-Co-C alloys) by the incorporation of chromium carbide and tungsten carbide into a cobalt matrix. By heat treating in an argon or hydrogen atmosphere this produced a cobalt, chromium, tungsten and carbon alloy of the desired alloy content. More complex alloys can be produced by the addition of highly alloyed particles such as chromium, aluminium and yitrium to nickel-cobalt to give the well known MCrAlY type coatings after heat treatment[144]. These, and similar alloys, are finding many applications as overlay and thermal barrier coatings and in the electroforming of components mostly for the aerospace industry.

Other metal composite coatings include the use of nickel matrix layers produced by the codeposition of nickel powder in a nickel matrix for electron tubes[145]. Such a matrix improves heat or electrical conductivity, adherence to the base metal, decreases the interfacial resistance and minimises the electrical effects of high voltage sparking.

Nuclear materials such as UO_2 or ThO_2 have been codeposited with nickel to be used as fuel elements or as radiation detectors. Neutron adsorbing materials, like boron and its compounds, have been codeposited with nickel to produce reactor coating materials. Efforts have also been made to include luminescent phosphorus in the metal plating which can be used in the decorative field in name plates and traffic signals[113].

4.5 MECHANISM OF FORMATION OF ELECTRODEPOSITED COMPOSITE COATINGS

In explanation of the mechanism of codeposition a number of models have been put forward,these have essentially involved:

1. The electrostatic attraction of the particle for the cathode;
2. The mechanical entrapment of the particle by metal deposition;
3. The adsorption of the particle onto the cathode surface;
4. The adsorption of reducible metal ions onto the particle followed by their reduction to form a solid connection between the particle and the cathode.

The first stage of codeposition can be considered to be the movement of the particle to the cathode. It was suggested by

Tomaszewski[127] that this occurred by electrophoresis. This idea was opposed by Guglielmi[146] who considered that for liquids of high ionic strength, the majority of the potential gradient through the electrolyte occurred at the electrodes and there would therefore be little potential gradient through the bulk solution. In agreement with this Snaith[147] proposed that hydrodynamic transportation, by movement of the electrolyte, brought the particle into close proximity with the cathode, that is the outer Helmholz plane. It has been calculated by Snaith that transportation by electrophoresis will be in the order of $5x10^{-5}$ cms^{-1}, compared to that measured for hydrodynamic transportation of about 5 cms^{-1}. Clearly electrophoresis will not be the primary mode of transportation of particles to the cathode in a well agitated solution. This has also been supported by numerous other workers.[148-154]

It has been suggested [155,156] that particles reaching the cathode surface, by hydrodynamic transportation, will result in mechanical entrapment of particles as they are engulfed by the growing metal interface. This however fails to account for solutions which do not codeposit particles into a matrix and has therefore been discounted by most authors on the subject.

Any particle in solution will carry a charge relative to the liquid. It has been proposed by numerous workers[127,147,149,152,154,157-159] that a particle will acquire a further charge from solution by adsorption of electrolyte cations, such as nickel ions. This adsorbed charge on the

particle is expressed as the zeta potential. As the concentration of cations in solution increases so the adsorption onto the particle also increases. For an initially negatively charged particle, as concentration increases so the build up of positive charge equals, and overcomes the negative charge producing a particle with a net positive zeta potential. Such a particle is considered to be able to experience electrostatic attraction to the negatively charged cathode.

Although hydrodynamic transportation brings the particles to the cathode the second stage of codeposition at the cathode surface was considered by most authors, who investigated the influences of zeta potential, to be one of electrostatic attraction. The positively charged particles, close to the cathode at the outer Helmholtz layer, are under the influence of a strong electric field and are moved towards the cathode surface and held firmly against it. The third stage of codeposition then follows, one of mechanical keying, where the particle, held against the cathode surface by electrostatic attraction, is permanently secured in place by deposition of metal.

Foster[149,150] also suggested that the adsorption of metal ions onto the particle not only produced a positive charge, but also, by their reduction at the particle-cathode interface, formed an efficient mechanical bond between the particle and cathode. In addition Foster et al considered that the time required to form such a mechanical bond, capable of withstanding the forces of agitation, was small being in the order of twenty

milliseconds for a one micron particle, although this would depend on the current density.

Tomaszewski[127] supported the mechanism of electrostatic attraction and mechanical keying and considered that additives such as thallium and TEPA, which promoted codeposition from acid copper baths, functioned by increasing the attraction between particles and the cathode. This was supported by Foster[149].

Brandes[151] noticed that particles could be swept along ahead of the metal-electrolyte interface without codeposition and suggested that the microthrowing power of the electrolyte might influence this movement. Good throwing power would result in metal deposition behind the particle whereas poor throwing power would result in the build-up of metal around the particle and would therefore entrap it.

A model was proposed by Guglielmi[146] based on electrostatic attraction and mechanical keying but involved a two-step adsorption mechanism. The first stage was considered to be the "loose adsorption" of particles onto the cathode and was substantially physical, with a high surface coverage. The second adsorption step was the so called "strong adsorption" of the particle where, under the action of the field, the particle was stripped of its adsorbed ions and water molecules and held firmly against the cathode. An important distinction however was made at this stage as it was considered that particles were

irreversibly adsorbed before metal had been deposited. The deposition of metal simply covered the adsorbed particles.

Based on the above mechanism, Guglielmi derived a mathematical expression that related the concentration of particles in the deposit to the concentration of particles in suspension and to the cathode overpotential.

$$\frac{C}{\alpha} = \frac{Wi_o}{nFdV_o} e^{(A - B)\eta} . (1/k + C) \qquad (50)$$

where C = the concentration of particles in solution.

α = volume fraction of particles in the deposit.

W = atomic weight.

i_o = exchange current density.

n = valency

F = Farady constant

d = density of the metal

η = overpotential for metal deposition.

A,B,Vo,k = constants

In a more recent study White and Foster[161] concluded that electrostatic attraction was not significant in the adsorption process. They considered that particles were physically adsorbed onto the cathode with the rest time upon the cathode dependent on agitation and the properties of the particle such as size, density and shape. Particles were then permanently secured to the cathode by the creation of a particle-cathode interface. The rate of formation of this bond being controlled by the metal ion adsorption on the particle, current density, pH and

temperature and was strongly influenced by inhibitors. Inhibitors, it was concluded, combine with the adsorbed metal ions on the particles and prevented formation of the particle-cathode bond. This produced riding of the particles ahead of the metal surface during deposition as was experienced by Brandes[151]. The addition of agents such as thallium was considered not to promote increased zeta potential, as suggested by Foster and Kariapper[157], but instead to combine with the inhibitors in solution leaving the adsorbed metal ions on the particle surface free to form the particle-cathode bond. This mechanism of codeposition has also been supported by Celis and Roos[162].

Foster[143,163] carried out composite plating in a barrel system which produced saturation conditions of powder at the surface when a critical concentration was exceeded. Under these conditions and assuming the mechanism of codeposition above, Foster was able to produce an expression based on the settling rate of the particles in terms of Stoke's law and the plating rate in terms of Faraday's law:

$$KC = \frac{I\alpha}{(1-\alpha)} \qquad (51)$$

Where C is the concentration of particles in solution, α is the particles codeposited, K is a constant and I is current density.

Also under these conditions the importance of agitation, particle size and current density can be realised. Newnham and Foster[143] concluded that the composition of the

deposit was related to the apparent density of the powder sediment formed on the cathode surface. As this is related to particle size, at saturation, the composition of the deposit could then best be controlled by varying particle size. White and Foster[161] showed that with current density particle content increased to a maximum until the metal deposition rate exceeded particle arrival rate after which the particle content of the deposit decreased. For these relationships to be followed the surface had to maintain its saturated condition, this showed the importance of agitation which could reverse the relationships under different agitation conditions. This may explain some of the contradictory results that have been published on this subject.

4.6 ELECTROLESS COMPOSITE COATINGS

Encouraged by the successful development and industrial application of electrodeposited composite coatings, Metzger[164], investigated the idea of codepositing hard particles by chemical reduction. The benefits of having incorporated hard particles into the coating could then be exploited in addition to the advantages that electroless nickel had over electrolytic nickel, namely, inherent uniformity, corrosion resistance and most importantly for wear resistance, the ability to be hardened. Metzger began work in 1966 and patented the idea in 1971 [165].

The addition of inert solids to electroless nickel solution appears at first to have been inadvisable as all the

relevant literature states that pollution of chemical electrolytes with solid particles should be avoided because of the risk of spontaneous autocatalytic deposition. Nevertheless the advantages gained by using electroless nickel made it worth investigating.

The first coatings Metzger produced incorporated alumina particles into a nickel matrix. The particles were 3-6 um in size and produced an even distribution of particles throughout the matrix. This provided the impetus for extensive research to establish conditions which would enable the process to become suitable for practical application.

Metzger achieved steady, reliable plating conditions by the further addition of suitable stabilisers beyond the normal quantity and also by modifying the operating conditions. These solutions enable 15-20 um/h to be deposited during continuous operation.

Particles such as carbides, oxides, borides and nitrides, all have potential use with the electroless process. Metzger and the other initial workers, Heinke [166], and Wagner[167], mainly examined nickel-silicon carbide and nickel-alumina following their successful application as electrolytic coatings. Since then a wide range of combinations has been considered.

Essentially the same particles can be used with electroless nickel as with electrolytic nickel, but in the case of metal powders those metals which are active as catalysts for electroless deposition or more electro-positive than nickel are unsuitable [166] for incorporation. A metal more electro-positive than nickel would become coated with nickel by electrochemical displacement and then the autocatalytic deposition would continue and the solution would be destroyed.

Commercially, silicon-carbide has received the most attention. It is among the hardest of materials and experience with electrolytic coatings has shown it to provide excellent wear resistant properties. It is also readily available in a wide range of micron sizes in relatively unchanged quality and the cost is good considering the increase in wear resistance. Incorporation of tungsten carbide for example, produces a minimally better wear resistant coating than silicon carbide but at a much higher cost.

4.6.1 Electroless Wear Resistant Composite Coatings

Electroless nickel wear resistant composite coatings, like their electrolytic counterpart, derive their wear resistance from the particles included in the matrix, with the properties dependent on nature, size and volume per cent codeposited. Coating performance is also influenced by hardness of the matrix and thus the ability to heat treat and harden electroless nickel further improves the coating performance.

Parker[166] has published considerable data on the wear resistance of electroless nickel composite coatings. These results demonstrated a considerable increase in wear resistance due to the embedded particles in the electroless nickel coating. It was shown how heat treatment also improves wear resistance. These two effects combined, improved on the wear resistance as indicated by test on nickel-silicon carbide and nickel-boron carbide coatings. As compared to hard chromium wear resistance was increased by seven times through the incorporation of silicon carbide and twenty times by incorporating boron carbide. This shows the very high wear resistance of electroless nickel composites.

The effect of increasing content of silicon carbide particles on wear resistance was measured by Gawrilov[167] using the Skoda-Slawin machine. The results showed a strong decrease in weight loss by increasing the silicon carbide content of the electroless nickel coating from 0 to 4% by weight.

Parker[166] also examined coatings using the Alpha LFWI test machine and the Falex wear tester. These results and other results by different workers with other test machines, if not directly comparable, are all in general agreement about the improvements made by heat treatment and composite coatings.

Lukschandel[168] reported on the incorporation of diamonds into electroless nickel. The coating was again an improvement on the electrolytic version because of the improved

properties of the electroless nickel. This coating had good wear resistance but was rather abrasive for normal applications. In highly abrasive situations the coatings performed well as the mating surface was now as abrasive, if not more, than the diamond coating. Because of the nature of the coating it can be applied where surfaces of good grip traction are required. The coating can also be adjusted to give the required coefficient of friction. Electroless diamond coatings are a significant improvement over electroplated diamond coatings for machine/surface finish tools because of the uniformity of the coating. This enables very accurate, profiled tools to be made that would normally be too expensive for electroplating.

From field experience[109] some very good improvements in wear resistance have been achieved with electroless nickel silicon carbide coated dies. Moulds for glass fibre reinforced thermoset plastic normally last for 10,000 parts. Coated dies produced 450,000 parts. With metal forming dies life was increased from 3,000 to 400,000 hits and for foundry sand core moulds life increased from 2,000 moulds to 25,000 moulds.

4.6.2 Electroless Self-Lubricating Composite Coatings

The only case of lubricating particles being incorporated into electroless nickel that has been reported to any extent is the recent development of PTFE electroless nickel coatings[37].

The electroless nickel PTFE coating consists of as-deposited electroless nickel with sub-micron size particles of PTFE incorporated. The technique for deposition of the composite is dependent on the right mix of surfactants in order to maintain a dispersion of the sub-micron PTFE particles in the plating solution. Provided this is maintained with adequate agitation, successful composites can be produced to achieve a coating with a low coefficient of friction. This composite has found numerous applications as a low coefficient of friction surface in the automotive industry, on butterfly valves and on many different parts of machinery where the coating has eliminated slip-sticking and facilitated smooth operation of the equipment.

The overall hardness of electroless nickel-PTFE deposits is around 250Hv, a combination of as-deposited electroless nickel, approximately 500Hv, and the very soft PTFE. Normal electroless nickel heat treatment of 400 ^{o}C for one hour to improve hardness and wear resistance only increases the hardness of the deposit to around 400Hv. This results in only a moderate improvement in wear resistance. Heat treatment at 400^{o}C does however have an adverse effect on the coefficient of friction. At temperatures of around 325 ^{o}C PTFE decomposes and is therefore lost as a lubricant. Electroless nickel-PTFE coatings are therefore generally only used in the as-deposited condition although treatments of 300 ^{o}C for 4 hours have been found to be useful for wear resistance without affecting coefficient of friction.

4.6.3 Metal Alloy Electroless Composite Coatings

Very little work has been published in this area. Parker[166] mentions such coatings in his works and in a patent[169]. The metal particles which can be incorporated are shown in Table 2 taken from Parker's patent. The metal particles must not act as a catalyst for the electroless reaction, this therefore limits the metals capable of being incorporated. The particle size can be within the range of 0.1 um to about 50 um. According to the patent specification, the incorporation of metal particles can reach 56% by volume.

Sheikh [170] examined coatings of electroless nickel and chromium particles. The resulting Ni, P, Cr composites were very hard coatings in the order of 1650 Hv after heat treatment for one hour at 400 ^{o}C. They were evaluated in a hot forging test but did not perform as well as might be expected. Post-plating heat treatment at higher temperatures and for longer periods showed enable similar diffused alloy coatings to those produced with electrolytic systems. The presence of phosphorus however may not be very desirable for most alloys. However, if such hardnesses as reported by Shiek are posssible they may well have considerable potential in many situations.

Kiowa and Osaka[171] have also incorporated very small chromium particles, 7000 nm in diameter, into electroless nickel boron deposits in an attempt to produce new types of resistive films.

4.6.4 The Mechanism of Formation of Electroless Composite Coatings

The mechanism of codeposition of particles in electroless nickel is quoted in most works as being developed mechanically by the effect of settling and impinging of the particle on the surface of the workpiece and the subsequent envelopment of the particle by the matrix as it is deposited. No indepth studies have been carried out on the subject as has been the case with electrolytic codeposition. Metzger and Florian[95] have reported that additions such as thallium, which increase codeposition in electrolytic systems, had no effect on electroless solutions. They used this as evidence of a non-electrical theory. White[161] and Celis[162] however showed that these additions do not act on the particle but combine with inhibitors which would prevent reduction of metal ions on the particles. It is most likely that these inhibitors are not present in electroless systems and therefore the addition of thallium, for example, would have no effect.

Codeposition has been shown to be dependent on concentration by Hubbel[109] and Gawrilov[167]. Figure 26 by Gawrilov showed codeposition increased with concentration to a maximum beyond which codeposition decreased. An increase in temperature also produced a decrease in codeposition over the complete concentration range. This was attributed to an increased plating rate where either, metal deposition exceeded particle arrival rate, or the increased hydrogen liberation, as a result

of increased plating rate, hindered particle arrival at the plating surface.

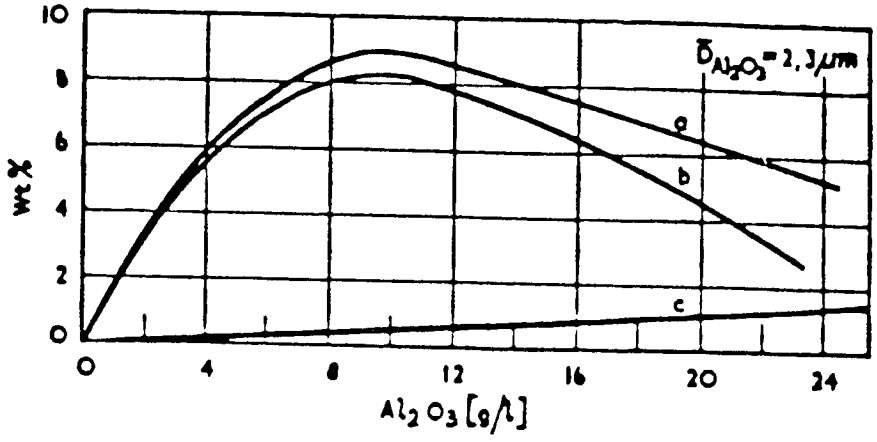

Figure 26. Codeposition of alumina with the concentration of alumina in solution (a) 83°C; (b) 93°C; (c) galvanic[167]

CHAPTER V

EXPERIMENTAL PROCEDURE

5.1 INTRODUCTION

From the literature review on composite coatings it was seen that the most developed group of electroless nickel composite coatings was that based on the incorporation of hard particles, such as silicon carbide, to improve wear resistance. Of the alternative electroless nickel composite systems i.e. those coatings containing metal particles to produce metal alloy coatings or lubricating particles to produce dry self-lubricating coatings, only the latter group, in the form of electroless nickel-PTFE, has received any real attention and commercial success.

Electroless nickel-PTFE coatings have a low coefficient of friction, but can suffer from higher wear rates than conventional electroless nickel in certain circumstances. This is because the inclusion of PTFE produces a softer deposit more subject to wear, and because the electroless nickel matrix cannot be heat treated without significant degradation of PTFE and consequent rise in friction values. This also makes the coating unsuitable for any application at higher than ambient temperature, otherwise a similar degradation of PTFE will again occur. It is also necesary to produce deposits from a solution containing large amounts of surfactants and stabilisers, making the solution complicated and producing a slow rate of deposition.

The requirements of a material to produce a self-lubricating composite coating based on electroless nickel is then a solid material which possesses lubricant properties but which will also withstand the heat treatment of electroless nickel, so that both frictional values, and matrix material can be optimised. Graphite was considered to be the material most appropriate to meet these requirements. It is well known as a lubricant material and is capable of withstanding temperatures up to 2000^{o}C. The ability of graphite to provide lubrication where it is the second phase within a matrix is also well known. For example, the incorporation of graphite into sintered bearings, this also shows the ability of graphite to withstand high processing temperatures[172]. The coefficient of friction of cast irons has also been shown to be reduced by the presence of flake and nodular graphite [173]. Such a graphite based coating could also be considered as a high temperature lubricating coating.

Metal alloy coatings based on electrolytic systems are under current development[144], but with the exception of the work by Shiek[170] little has been carried out in the area of incorporating metal particles into electroless nickel. Such a coating would have the properties of the many possible alloys that could be produced plus the advantages of the electroless system i.e. uniformity of coating.

The object of this work was aimed at investigating the production of two electroless nickel composite coatings. A self-lubricating coating based on graphite and a metal alloy

coating incorporating chromium to produce a nickel-chromium alloy deposit. The lubricating properties of the graphite deposit were also compared to those of deposits containing PTFE.

The properties of electroless nickel composite coatings clearly depend on the type of particles incorporated, the concentration of particles in the coating and any effect the particles may have on the matrix material. Having defined the type of particles to be incorporated, the next step was to examine the factors that control the concentration of particles in the coating. However, before this and the properties of the coatings could be examined it was first necessary to develop electroless nickel solutions capable of codepositing chromium and graphite particles.

5.2 EXPERIMENTAL TECHNIQUES

5.2.1 Graphite and Chromium Powders

(i) Graphite Powder

Natural Sri Lankan graphite powder (supplied by A. Branwell Ltd.), was used throughout this work. For the majority of the work, 2 micron nominal particle size was used. However to study the effect of particle size on codeposition and properties, a range of different size powders was required. As only two grades of graphite powder were available, 2μm and 20μm nominal size, it was necessary to produce the range of particle sizes by

ball milling of the 20 μm grade. Analysis of powders was carried out by Coulter Ltd. using Coulter analysis.

(ii) **Ball Milling of Graphite Powder**

The mill was constructed of stainless steel and was charged with ball bearings of varying sizes. When rotated the violent contacts of the metal surfaces, caused by the rolling motion of the balls inside the mill, effect the milling of the solid.

The milling process can be carried out in two ways depending on the nature of the final product required. The production of a dispersion of solid particles of colloidal dimensions in a liquid is achieved by "wet milling". The mill is charged with a slurry of the solid and liquid and the mixture milled until a stable colloidal suspension is obtained. If however, it is merely required to reduce the particle size of a solid, "dry milling", that is milling of the solid alone, is employed. Both methods were used to attempt to reduce the particle size of the graphite.

To achieve optimum efficiency of ball milling a number of factors must be taken into account[174]:

(a) **Volume of Balls.** Normal practice followed in milling indicates that the mill should be filled to 33-50% of its

volume with balls. Generally if the mill is filled with balls to the centre line, reasonable efficiency will result.

(b) **Total Charge.** Taken in conjunction with other variables, the optimum efficiency will be achieved when the mill is filled to between 60 and 70 per cent of its volume. The total charge is the sum of the ball charge and the batch charge. When calculating the batch charge sufficient solid is required to fill the interstices between balls (approximately 40% of the total volume occupied by the balls) and give a layer of 10-20% volume of the mill above balls.

(c) **Size of Ball.** It can be seen that the milling efficiency depends directly on the number of point contacts per unit volume occupied by the balls. The size of the balls should therefore be the minimum size capable of performing the grinding action. The surface area of a given volume of balls varies inversely to the diameter. Thus, by replacing balls with others half their size, the effective surface area is doubled. A grading of three different size balls was therefore used: 1";3/4";1/2" diameter. In dry grinding, the action is mainly shattering and size grading of the balls is relatively unimportant. In wet grinding, where abrasion is the main grinding action, a careful grading of balls will give a maximum abrasive surface. Grading can be either by weight or volume and in equal proportions of two or three different sizes.

(d) **Speed of Rotation.** This factor has the greatest effect on grinding efficiency. This can be demonstrated by examining what happens in the mill as the speed of rotation is increased.

As the speed of rotation of the mill is slowly raised from zero the first stage observed is "slipping". This involves the complete mass moving as a unit with the mill until it is sufficiently elevated to overcome the frictional force, it will then slip to the bottom again. This cycle is repeated continuously, and, since it results in very little change in the relative position of the balls, it is very inefficient as a milling process. Slipping is detectable aurally, since it is a comparatively quiet process. A further increase in speed results in the onset of "cascading".

Cascading describes an even tumbling motion of the grinding media. Each ball, on coming clear of the mass, rolls to the bottom and is carried up again by the motion of the mill. The graphite powder, being more mobile than the balls, tends to run out from the interstices, thus leaving the top of the ball mass clear of the powder and enabling the descending balls to gain momentum before falling into the graphite bed below. Cascading affords the most efficient milling and can be recognised by the dull continuous roar emitted.

The importance of having an amount of powder in excess of the volume of the interstices of the balls becomes apparent.

If it is insufficient the balls will fall directly onto the mill side resulting in wear of the mill, inefficient grinding and contamination of the powder.

If the speed of rotation of the mill is raised still further "cataracting" occurs. This involves balls being thrown clear of the main mass and striking the top of the mill. The proportion of the balls cataracting increases with the speed. The milling efficiency is below that of cascading and the wear is considerable. The process is marked by a harsh rattling noise superimposed on the normal sound of cascading.

If the speed is increased above that of cataracting the centrifugal force of the motion causes the mass to revolve with the mill; there is no relative motion between particles and balls. This process is known as "centrifuging" and the speed at which this just occurs is known as the critical speed. It results in very inefficient milling and is marked by almost complete quiet running.

The critical speed is usually quoted as 76.6/(dia. of mill in feet). The actual operating speed can vary between 50 and 75 per cent of the "critical" speed, depending on other variables. For dry grinding, the speed should be 62/(dia. of mill in feet). If grinding efficiency is not as high as expected, an improvement can be effected by increasing the speed or decreasing the batch charge. For wet grinding, the speed should be 43/(dia. of mill in feet). If grinding efficiency is

not as high as expected, the speed should be decreased or the batch charge increased.

(e) **Viscosity of Batch.** It is difficult to state a figure in this case, as each operation should be treated on its merits. Generally, viscosity should be as high as possible without allowing the grinding balls to stick. With a charge of high viscosity, the speed should be reduced. Higher viscosity will lower the amount of wear on the balls and lining.

(f) **Initial Particle Size of Charge.** Depending upon the relative hardness of the grinding medium, the initial particle size of the charge should not exceed the size of the largest ball. Hard materials should be reduced to smaller sizes by other means before ball mill grinding. The largest particle should be capable of being broken by the kinetic energy contained in the largest ball falling through a distance equal to three-quarters of the diameter of the mill.

Ball milling of the graphite was carried out both wet and dry; in both cases the same ball mill was used. The mill diameter was 13.2cm this gave a speed of rotation for dry grinding of 94 r.p.m. and a speed of rotation for wet grinding of 65 r.p.m.. The mill was charged to the centre line with balls, this gave an available batch charge volume of 853ml. In the dry condition the bulk density of the graphite powder was 0.3g/ml thus the batch charge weight was 256 grams. For wet milling, a slurry was produced that just allowed sufficient movement of the

balls. This was made up of 383g of graphite to one litre of distilled water, to which was added a surfactant to maintain dispersion of the particles during grinding. Slurry was then introduced into the mill to the same volume as above, 853ml, and the mill run continuously. Samples were taken on a regular basis and analysed.

Initially the graphite was ball milled wet, as doubts were expressed over the ability of the ball medium to break down the graphite dry, and also whether the particles once broken down would remain as discrete particles. Experiments with dry ball milling also highlighted another problem. The natural lubricity of the graphite prevented the balls from being picked up by the rotating drum, thus the charged mass was observed to "slip" at all speeds of rotation preventing the onset of efficient grinding.

It was therefore thought necessary that ball milling had to be carried out wet and that a surfactant solution would be required to maintain the broken down particles as a dispersion. A slurry was thus produced containing the graphite and a surfactant solution for ball milling. After 24 hrs. a sample was taken from the drum and added to an electroless nickel plating solution. A deposit was produced containing graphite particles of size 1 μm. The slurry was then removed from the ball mill and dried. Subsequently when this graphite was added to a plating solution it could not be incorporated into the coatings. Also repetition

of the original wet milling procedure and production of a graphite containing coating could not be achieved.

A further more detailed study of the literature concerned with ball milling was then made with particular reference to the ball milling of graphite. The desired information was found in a thesis by Hankin[175], where the object of his work was the ball milling of graphite. In Hankin's work, ball milling of the graphite was carried out dry and as in this case slipping of the charge mass was observed. However, Hankin allowed his mill to run on and after 120 hours of milling the "slipping" stopped and "cascading" started along with the effective size reduction of the graphite. Initial attempts to dry grind in this present work had not been run as long as 120 hours, consequently the onset of cascading had not been reached. Having observed Hankin's results the mill was again charged dry and this time left running. After 130 hours cascading started; the mill was then allowed to run on for a further 36 hours during which time effective reduction of the graphite occurred. Samples were taken at intervals during this time and analysed by Coulter analysis.

(iii) **Chromium Powder**

Chromium powder supplied by Johnson Matthey Ltd. graded at 2 μm nominal particle size was used for all the work on electroless nickel-chromium composite coatings. The particle size range was checked by Coulter analysis and S.E.M. measurements.

5.2.2. The Plating Cell

The addition of inert particles into a plating solution requires adequate agitation in order to maintain the particles in suspension. There are a number of ways of doing this and in order to identify the most suitable methods Shiekh [170], in a previous study at Aston University, investigated six possible methods: (i) air agitation, (ii) bath circulation, (iii) liquid air process, (iv) plate pumper process, (v) ultrasonics, and (vi) mechanical stirrer.

The essential criterion looked for in each case was a uniform coating thickness with constant particle concentration throughout. Sheikh concluded that agitation by plate pumper, liquid air process, and air agitation (especially if air was supplied at the bottom of a conical vessel) resulted in homogeneous composite deposits. Subsequently, Shiek used air agitation throughout his work on electroless composite coatings. It was therefore decided to use the same system for this work. The vessels used were 1 and 4 litres in size and conical shaped at the base to prevent any settling of the particles. Clean compressed air was then introduced through the bottom of the container to provide agitation, figure 27. The pressure of air supplied was controlled to prevent spillages and was maintained at constant pressure with the aid of a U-tube pressure gauge.

It was feared initially that air agitation would cause excessive foaming with the use of surfactants. However, the

particular surfactants used for plating did not foam excessively and by keeping the concentration of free surfactants in solution to a minimum, foaming was not a problem.

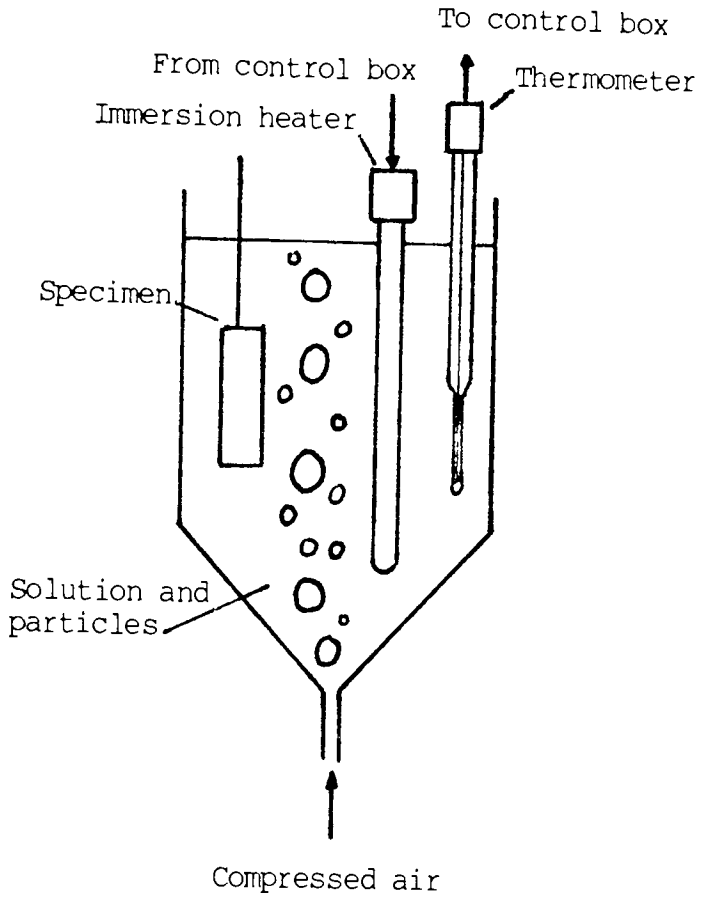

Figure 27. Schematic diagram of the plating cell

Experience showed that it was necessary to jig the steel panels rigidly in the vertical plane if uniform deposits were to be produced. It was realised that agitation effects were being experienced and so the degree of air agitation was studied by varying the volume of air blown through the solution and right angle shaped specimens were plated to assess any settling effects that may occur. Temperature was controlled in the case of the 1 litre vessel by placing it in a thermostatically controlled water bath. The 4 litre vessel was heated by immersion heater

thermostatically controlled by a contact thermometer placed in the solution.

5.2.3 Specimens

The electroless plating technique requires the surface of the component to act as a catalyst to initiate the deposition process. If the substrate does not meet this requirement deposition must be induced by the use of surface activation agents or by an applied potential to produce a flash coating of nickel.

Since mild steel acts as a convenient catalyst, has a relatively simple pre-plating cleaning sequence and is readily available in sheet form, it was used as the substrate material to investigate the deposition of electroless nickel-graphite composite coatings. The rolled mild steel sheet (1mm thick) was cut into panels which gave a ratio of total surface area to volume of plating solution within the range recommended by the manufacturers, this being $0.005m^2/l$. This provided samples of adequate size and put minimal demand on the solution. For wear testing suitably heat treated EN31 steel was used.

5.2.4 Specimen Pre-Treatment

For plated coatings to perform as wear and corrosion resistant surfaces they must have good adhesion to the

substrate. It is thus important to have an effective pre-treatment procedure to remove surface contaminants and prepare the surface for acceptance of the plated metal. The following pre-treatment procedure was employed:

1. Degrease in acetone.
2. Anodic cleaning in an alkaline cleaner at a current density of 4 A/dm^2 for 4 minutes at $70^{o}C$.
3. Rinse in water.
4. Dip in 50% hydrochloric acid for 15-30 seconds.
5. Rinse in water.
6. Anodic cleaning in a cyanide cleaner at a current density of $4A/dm^2$ for 2 minutes.
7. Rinse in water.
8. Dip in 20% sulphuric acid for 10-15 seconds.
9. Rinse in water.
10. Immediate transfer to the plating solution.

5.2.5 Optical and Electron Microscopy

For the examination of cross-sections using optical and electron microscopes, samples were first guillotined from the specimen panels. The samples were then mounted vertically in conducting bakelite using sample clips. The guillotining process can lead to break up of the coating, this can be prevented by overplating with watts nickel or cyanide copper. Alternatively, grinding the mounted specimen well back can remove most of the damaged area. Metallographic preparation was achieved by the

normal grinding and polishing procedures. Coatings were usually examined in the unetched condition. However, in order to ensure a clear boundary between the coating and steel substrate a 5% nital solution was used to etch the steel and leave the unetched coating distinct from the steel. The coatings could be etched with a 50% acetic acid-nitric acid solution. Samples were examined optically and using a Cambridge scanning electron microscope combined with a Link system for x-ray analysis. Electron probe micro-analysis (EPMA) was used to establish the phosporus content of the electroless nickel deposits and to study the inter-diffusion of elements on heat treatment of composite coatings containing metal particles.

5.2.6 Plating Rate Determination

The plating rate was determined by direct measurement of the thickness on the cross-section using a microscope and micron scale. This method is subject to possible discrepancies if the specimen is not mounted vertically. The use of specimen clips however, maintained the sample in the vertical position and results were averaged from a number of similarly mounted samples from the same specimen.

5.2.7. Assessment of Particle Content

To provide a value of particle content of each deposit a number of techniques were considered, these included:

gravimetric analysis; standard point counting technique; and image analysis.

By dissolving the coating and suitably weighing the specimen and undissolved particles a figure for the overall weight per cent of the particulate material in the coating could be found. However, it was known agitation effects were being experienced in practice, this left areas of the coating vacant of particles. Gravimetric analysis could not distinguish between these areas and could only give a figure averaging out the particle rich and low areas. As the effect of agitation was not particularly predictable gravimetric analysis could not be relied upon to accurately distinguish between the other plating parameters. Point counting, although a long established technique, is however, a long and tedious process and can more easily be carried out by image analysis; a system produced by Microsight and connected to a IBM PC was used. A video camera connected to a microscope captured an image of the micro- cross section of the composite deposit and entered it into the computer memory. This could then be analysed by the PC for the number of particles per unit area and area percentage. This could then be related to volume and weight per cent as required.

5.3 THE ELECTROLESS NICKEL-GRAPHITE PLATING SOLUTION

It is possible to produce plating solutions capable of depositing composite coatings such as electroless nickel-silicon carbide by simply adding silicon carbide particles to standard

electroless nickel solution. Stability of such a solution may be a problem but particles will be incorporated into the growing nickel coating. In the case of graphite however, the situation is not as straight forward. When graphite particles are added to the solution they are not naturally wetted. However, they do adsorb onto their surface the small quantities of organic wetting agent and stabilisers already present in the solution. Due to the large surface area of the graphite powder, approximately 400 m^2/g, the small amount of wetting agent present in the solution is insufficient to wet all the particles; they therefore remain essentially unwetted by the solution and are not incorporated into the coating. Also, as the stabilisers have been adsorbed the solution will be inherently unstable and likely to decompose spontaneously.

If composite coatings were to be produced, problems such as wetting of the graphite particles and the stability of the solution had to be overcome. The first priority was to increase the stability of the electroless nickel solution, this had to be achieved before any experiments on codeposition and wetting of the particles could be considered.

5.3.1 The Electroless Nickel Solution

The electroless nickel plating solution used to develop the composite plating systems was a commercial acid hypophosphite formulation, Nifoss 3000, supplied by W. Canning Materials Ltd. The solution contained nickel sulphate, sodium hypophosphite as

the reducing agent, buffers, complexants, stabilisers, brighteners and wetting agents. This was prepared according to the manufacturer's instruction. See Appendix A.

The electroless solution, unlike electroplating systems which have an external supply of electrons and an anode to maintain the metal ion concentration of the solution, contains the chemical reducing agent and the reservoir of metal ions to be deposited. Thus, in order to maintain the composition and performance of the solution, the bath must be analysed regularly and maintained with the appropriate additions (see Appendix A). The operation of the solution at temperatures approaching 100^{o}C also leads to rapid evaporation of water and thus required constant addition of deionised water.

The adjustment of pH was achieved by the addition of either 10% sulphuric acid or 10% sodium hydroxide solution. The pH was measured using a saturated KCL reference electrode and a digital reading pH meter with temperature compensation.

5.3.2 The Measurement of Stability

As previously mentioned, the addition of particles to electroless nickel solutions can induce instability resulting in spontaneous decomposition of the solution onto the particles. It was therefore necessary to increase the stabiliser content of the solution to prevent decomposition occurring.

Very unstable solutions typically required no measure of stability, the decomposition of the solution was clearly visible. Over-stable solutions would not plate. A more representative measure of stability of the electroless nickel-graphite plating solution was however required to narrow down the range of stabiliser addition.

The technique used was to determine the potential of a steel plate in the solution. This was achieved by measuring the potential difference between the specimen and a saturated calomel electrode (SCE). The SCE was connected via a salt bridge to a Luggin capillary which was placed close to the surface of the substrate within the plating solution. The potential was then read using a digital volt meter.

Measurements were first taken in electroless nickel solution with no additions as a standard. A figure of -700mV was typically obtained. If excess stabiliser was then added to the nickel and graphite solution, this would cause a rapid fall in potential as the plating reaction is poisoned. This technique could then be used to find the point at which the level of stabiliser in solution no longer caused a fall in potential. Such a solution would be stable to the graphite yet still allow normal plating to occur.

The procedure used was to place a volume of electroless nickel solution with excess stabiliser and 20g of graphite into a large container and agitated with air. The potential of a steel panel in the solution was then determined. If the value obtained

was below the standard value, the solution was over stabilised. The solution was then diluted by adding known volumes of standard electroless nickel solution this reduced the concentration of the stabiliser content in the original solution. A potential measurement was again made. This was continued until the correct value for plating of -700 mV was achieved. Knowing the original addition of stabiliser and the degree of dilution a figure for the amount of stabiliser required to produce a stable solution for the weight of graphite and volume of solution could be found. Both organic and heavy metal ion stabilisers were evaluated by this method.

5.3.3 Analysis of Stabilisers

Once it was considered that an approximately stable working solution had been found by the above procedure a more accurate technique was used to refine the stabiliser addition. To do this it was necessary to analyse accurately the content of stabiliser in solution. This was done by polarography which is a commonly used method for determining metal ions and electro-active organic compounds at low concentration ranges.

The method involves applying a varying voltage between a reference electrode and a dropping mercury micro-electrode. As the voltage reaches that of a half reaction, of say a metal ion in solution, a micro-current is produced as the metal ions are reduced onto the mercury drop. This current is limited by the

diffusion rate of the ions and thus directly proportional to the bulk concentration.

Once an approximately stable solution had been found, it was analysed for the concentration of stabiliser in the solution. The difference between the stabiliser content of the solution and the amount added, then gave a measure of the adsorption of the stabiliser onto the graphite. As the correct stabiliser concentration for the Nifoss 3000 electroless nickel solution was supplied by the manufacturer, the amount measured in solution could then be adjusted to give this concentration by increasing or reducing the stabiliser addition. A correctly stabilised solution then resulted.

5.3.4 The Addition of Surfactant

Having achieved a stable solution the next step was to provide wetting of the graphite particles and to investigate whether codeposition could be made to occur.

The Nifoss 3000 solution was used as before with 25g/l of 2μm graphite added, agitated by air and stabilised. To this solution known amounts of non-ionic, anionic and cationic surfactants were added.

The amount of surfactant required in solution to provide complete wetting of the graphite particles was assessed by measuring the surface tension of the solution. The surface

tension of the particle containing solution remained unchanged with surfactant addition until the particles were effectively saturated with adsorbed surfactant. Continued addition produced a significant decrease in the surface tension, as the surfactant now remained in solution. A critical concentration is then reached from which the amount of anionic, non-ionic and cationic surfactant required for the surface area of the particles could be deduced, the adsorption being different for each surfactant.

The surface tension was measured using commercially produced equipment based on the ring method. The surface tension of a solution was determined by measuring the force required to detach a ring of platinum wire from the surface of the solution. Pre-calibration gave direct readings of surface tension in Dynes/cm.

The determination of the correct surfactant additions was necessary in order to prevent excess amounts of the surfactants in solution. This was required as surfactants are known to affect plating rate and also with air agitation excess surfactants could have caused considerable foaming.

Having established the adsorption characteristics of each surfactant and combinations of surfactants, correct additions were made to suitably stabilised electroless nickel-graphite solutions and specimens plated to assess for codeposition of graphite. Cross-sections of samples were examined under an optical microscope for evidence of graphite incorporation.

5.4 THE ELECTROLESS NICKEL-CHROMIUM PLATING SOLUTION

The production of electroless nickel chromium composite coatings, like electroless nickel graphite, is also not straight forward. The problem associated with the addition of chromium metal particles, is that as a metal, it is above nickel on the activity series and thus galvanic exchange of ions will occur between the chromium metal and nickel ions in the solution. The result will be an atomic layer of nickel capable of catalysing the electroless reaction, thus the solution will plate out on the chromium particles. The surface area of the particles is extremely large and therefore depletion of the solution components is rapid and leads to an unstable solution.

If an electoless nickel chromium composite is to be produced then the chromium particles must be made stable in the electroless solution. The object is to prevent the initial exchange of ions. This can be done by placing a barrier of some form around the chromium particles, two possible methods for this were considered.

One method was to add excess stabilisers to the plating solution to cover all the particle surface area. The problem was again to add sufficient stabiliser to cover all the particles yet not to add too much as to over stabilise the electroless reaction.

An alternative, and easier answer in this case, was to transform the surface of the chromium into a surface inert to the

solution by the promotion of the oxide film covering the surface. To the solution then, the particles would appear as inert particles just as in the case of Cr_2O_3, yet once in the coating the particles would behave as chromium metal particles. The oxide film could simply be promoted by heating at suitable temperatures in air.

The problem with this method was to what extent the oxide film would prevent inter-diffusion of nickel and chromium during heat treatment and also whether the presence of oxygen would have an effect on properties.

5.4.1 Stabilisation of Chromium Powder in Electroless Nickel Solutions by Oxidation

The object was to determine the minimum degree of oxidation that prevented deposition of the electroless nickel onto the chromium particles. To achieve this, chromium powder was oxidised to varying degrees, added to electroless nickel solutions and the stability tested for.

(i) Oxidation of Chromium

The powders were oxidised by heating in a normal muffle furnace at the required temperatures. To assess the amount of oxidation, exactly 25g was weighed out to be oxidised. The balance used was accurate to five decimal places. Powders were

then heated for increasing times at 400°C and 600°C. After the prescribed time, samples were taken out, cooled and re-weighed.

(ii) Measurement of Stability in Solutions

After heat treatment each powder to be tested was added to a 1 litre solution of electroless nickel which was at a temperature of 90°C and a pH of 5.0. Before addition the solution was analysed for Nickel Base Solution content and then again after 1 hour. If the chromium powder reacted with the electroless nickel then after one hour the nickel content of the solution would have changed as the nickel would have been deposited onto the powder. The method of nickel analysis was the standard method used for Nickel Base Solution analysis during the maintenance of solution (see Appendix A). The powders used were those heated at 400°C for 5,10,20,40,60, and 120 minutes.

5.5 FACTORS AFFECTING PARTICLE INCORPORATION

Once solutions had been developed that could codeposit graphite and chromium with electroless nickel the conditions which control the codeposition could be examined more fully.

Despite having a significant importance on the properties of the coating little has been published with regard to the effect of electroless plating condition on particle incorporation. The majority of the literature is primarily concerned with the wear properties of the coatings with respect

to the differing types of particle. It was therefore necessary to start by examining the basic parameters that could effect particle incorporation. A series of experiments was carried out to study the effect of (i) particle size, (ii) plating rate and (iii) particle concentration in solution.

5.5.1 Experimental Procedures for Investigating Graphite Deposition

The plating solution used was that evolved in the previous section. To the standard Nifoss 3000 solution anionic and non-ionic surfactants were added to wet and disperse the graphite while heavy metal ions were used to give stability. Surfactants were added to the levels determined in section 5.3.4. Results showed that provided the amount of surfactant added was sufficient the addition was not critical as the extra surfactant could easily be tolerated in solution. Steel panels were used as before and deposits were examined using an optical microscope. Plating rate was determined as in section (5.2.6).

As mentioned previously, the object of this section was to investigate those factors which influence the incorporation of particles into the growing electroless nickel coating. It had been found that agitation could affect codeposition but the other main factors considered to influence incorporation were particle size, plating rate, and concentration of graphite in solution. The series of tests performed to investigate these factors was as follows:

(i) To study the effect of particle concentration in solution on particle incorporation rate.

(ii) To study the effect of increased plating rate on particle incorporation rate.

(iii) To study the effect of decreasing particle size on particle incorporation rates.

(i) The Effect of Particle Concentration in Solution

To study the effect of graphite concentration in solution on particle incorporation rates, graphite was added with suitable amounts of addition agents over concentrations ranging from 5 to 60 g/l. Two particle sizes, 2μm and 6μm, were used over this range. The specimens were plated for 1 hour at each concentration, the solution temperature was 90°C and pH 5.0. Samples were then sectioned and graphite content determined.

(ii) The Effect of Plating Rate

To study the effect of plating rate on the particle incorporation rate a solution of electroless nickel, plus additives and 25 g/l of 2 μm graphite, was plated over a range of temperatures and pH for one hour periods. The samples from each temperature and pH were sectioned and the graphite density and plating rate determined.

(iii) **The Effect of Particle Size**

Once a range of particle sizes had been achieved by ball milling, experiments could be carried out on the incorporation rates of the different particle sizes. The selected particle size was added at a concentration of 25g/l to an electroless nickel plating solution which contained suitable levels of surfactants and stabilisers. This solution was plated for 1 hour at a temperature of 90^{o}C and pH 5.0. The resulting coatings were sectioned and the graphite content and number of particles codeposited were determined.

5.5.2 Experimental Procedure for Investigating Chromium Deposition

As only one size of chromium powder was available only the effects of increasing concentration and plating rate could be examined. Having established the degree of oxidation required for primary stabilisation of chromium powder, additions in increasing amounts, over the range from 3-24 g/l, of the oxidised chromium powder were added to an electroless nickel solution at 90 ^{o}C and pH 5.0. Chromium powder was also added over the same range, but with the solution temperature at 85 ^{o}C and pH 5.0 in order to show the influence of plating rate.

5.6 THE EVALUATION OF COATING PROPERTIES

5.6.1. Introduction

Having established the basics of producing graphite containing coatings the question remains as to whether (1) the presence of the graphite in the electroless nickel coating actually provides solid lubrication and enhances the properties of the coating in a wear situation and (2) whether Ni-Cr-P alloys can be produced with high hardness and improvements in wear properties. The properties therefore, that are of most interest and will be examined for are: the coefficient of friction; wear resistance and hardness.

5.6.2 Measurement of Hardness

The hardness of a coating was measured using a Vickers Micro Hardness Tester. Using low loads this tester is able to place hardness impressions onto very thin coatings. To obtain measurements of high accuracy on cross sections the coatings must be thick enough for the load employed. Generally a coating thickness about three times the size of the hardness indentation is required. Samples were mounted and polished in the normal way before testing and a minimum of ten readings taken per sample.

During testing it was noticed that quite different hardness values could be achieved when different loads were used to make the impressions. Using a standard hardness block, measurements were taken over a range of loads from 10g to 200g,

and then at 1 kg on a normal Vickers Hardness machine. The results, plotted in Figure 28, show quite clearly that hardness readings can vary by up to 200 hardness points, depending on which load is used. The 1 kg load measurements agreed with those made at 200g. Caution must be exercised when evaluating micro-hardness readings and published results which are made without reference to the load employed. Loads of 100g were used throughout this work. This required slightly thicker coatings than would be necessary for say 20g load, however as the coatings were generally quite hard this was not a problem.

5.6.3 Heat Treatment of Electroless Nickel-Graphite Coatings

The literature review showed how hardness and wear resistance of electroless nickel can be increased by heat treatment of the coating. The as-plated hardness of around 500 Hv_{100} can be increased by up to 1100 Hv_{100} by heat treatment under the correct conditions. The usual heat treatment for electroless nickel is for 1 hour at 400°C. To ensure the full hardness was being reached in this work, electroless nickel coatings plated at 90°C and pH 5.00 (approximately 9% phosphorous), were heated over a range from 100°C to 700°C to confirm the full hardening temperature. The heat treatment was carried out in an air circulating furnace for 1 hour. This confirmed 400°C for one hour as the correct heat treatment for the electroless nickel and furnace used. All subsequent heat treatments unless stated were carried out in the air circulating furnace at 400°C for 1 hour.

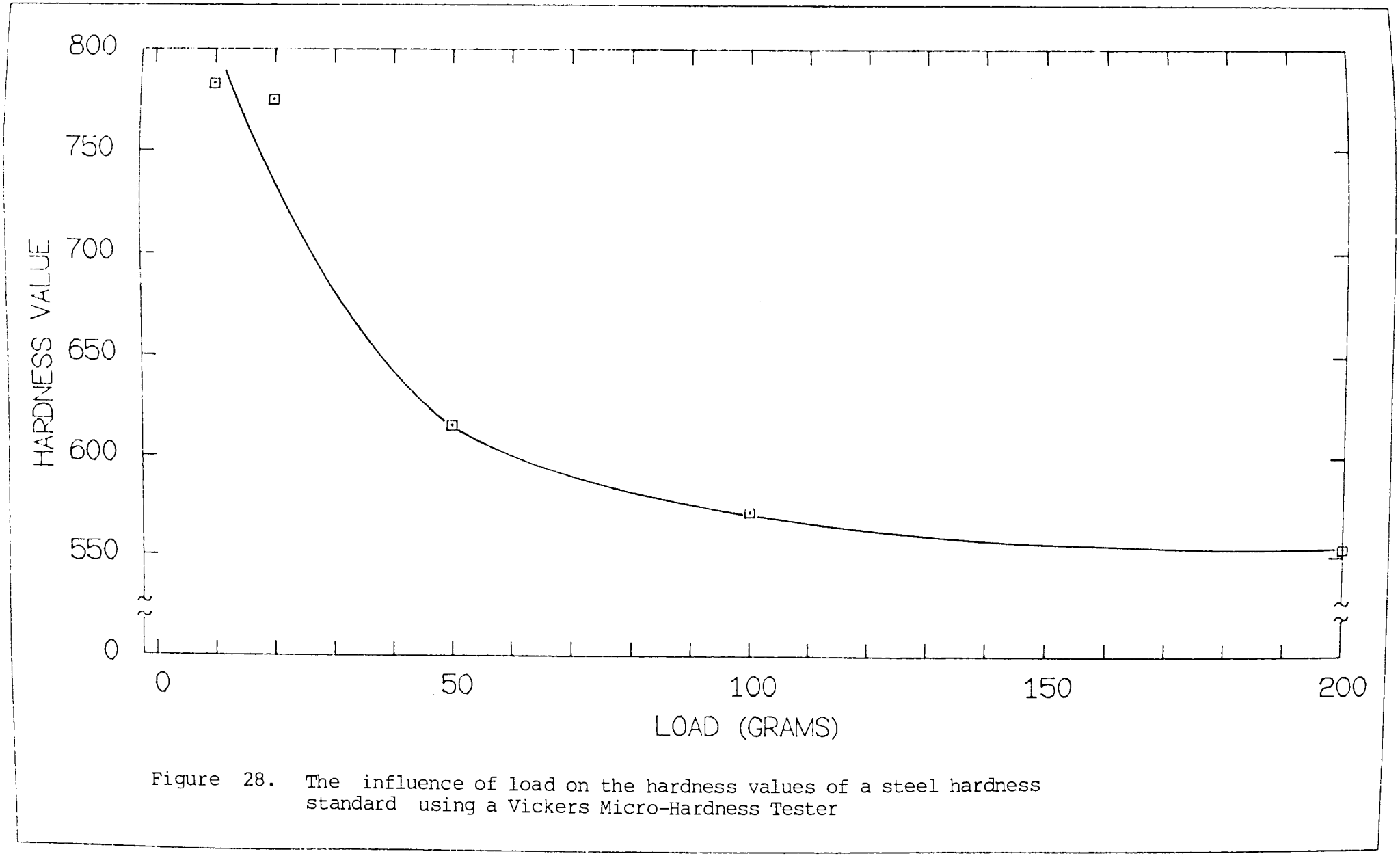

Figure 28. The influence of load on the hardness values of a steel hardness standard using a Vickers Micro-Hardness Tester

5.6.4 Heat Treatment of Electroless Nickel-Chromium Coatings

To produce a nickel-chromium-phosphorous alloy coating heat treatment at temperatures higher than those normally used for the heat treatment of electroless nickel was required to produce the inter-diffusion of the elements. A study of the nickel-phosphorous diagram, figure 19, showed that at the phosphorous content of the deposit, approximately 8%, the highest temperature that could be safely tolerated was 850°C. Coatings were therefore heat treated at a temperature of 850°C for periods of 8 and 16 hours. After heat treatment micro-sections of the coatings were produced and the inter-diffusion of the elements studied by x-ray mapping using the S.E.M. and quantitatively by E.P.M.A. analysis.

5.6.5 Internal Stress Measurement

Internal stress was measured using a Brenner and Senderoff Contractometer[176], figure 29. The basis of the contractometer is a coil of copper or stainless steel, which contracts or expands depending on the stress induced by the coating as it is plated onto the coil. This movement is converted into a reading on a dial from which stresses can be determined once calibrated.

A stainless steel coil was used, suitably stopped off on the inside with lacquer. The coil was weighed before plating to enable coating thickness to be determined after the test. The

coil was given a hot alkaline soak and an acid dip and then introduced to the electroless solutions. Plating was then initiated by making the coil cathodic and deflection readings were taken after 30 minutes.

Internal stress was measured in two solutions: conventional electroless nickel and electroless nickel plus 30 g/l of graphite with suitable addition agents. Two readings were taken from each solution.

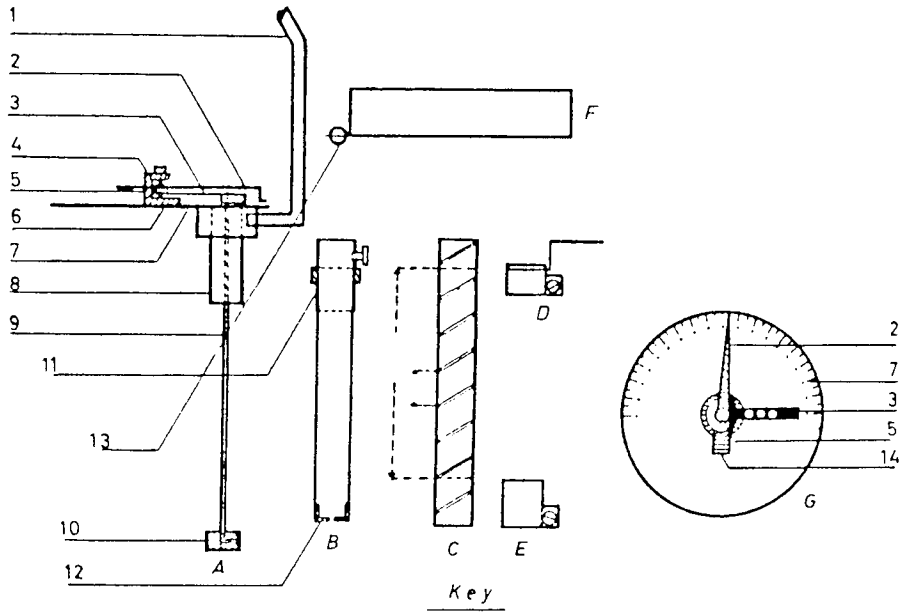

Figure 29. Schematic drawing of the spiral contractometer(176)

Internal stress was then calculated from the equation:

$$\text{Interal Stress} = S \cdot D/d \qquad (52)$$

Where S, the stress factor = 9.13×10^{-2} g/deg-cm, d is the thickness of the deposit and D is the defection of the pointer.

5.6.6 Wear Testing

As was seen in the literature review there are numerous methods of evaluating the wear and frictional properties of materials. Also as mentioned, each of these methods measures wear and friction in the individual context of that particular test, and as such, the results cannot be directly related to each other or wear situations. Much useful wear and fictional data can however be obtained by using a particular method and comparing the relative performance of different materials or coatings. Under these conditions the various test methods, which all have their own individual advantages and disadvantages, are all then comparable in perfomance at evaluating wear and friction and no one test is superior to another in this respect.

For the purposes of this study then, the pin and disc method was initially used. To further evaluate the wear and frictional performance of the coatings under different conditions the crossed cylinder test was also used. Some comparative measurements were also made using the Falex method. Each of these test methods has been widely used throughout the literature and were readily available.

(i) Pin and Disc Wear Testing

The pin and disc wear test equipment is shown in figure 30 (a) and (b). The pin under test was clamped in a rigid arm which was free to move in the vertical and horizontal planes. Transducers measured the wear of the pin and frictional forces produced at the pin and disc interface. These were calibrated before testing began. The load was applied to the end of the arm, a counter weight compensating for the natural weight of the arm.

The pins were cut from EN 31 rod, 6mm in diameter, to a length of 60mm. The pins were hardened but not tempered if the coatings were to be heat treated. The pins were ground flat, ensuring that the face was perpendicular to the long axis of the pin and polished to approximately a 6 μm finish. Discs were also made from EN 31, 12.5cm in diameter and 1.5cm thick, hardened and tempered by suitable heat treatment and then surface ground and polished again to approximately 6 μm finish. The hardnesses of the discs were in the range 738-778 Hv. Both pins and discs were plated to enable combinations of surfaces to be tested.

To carry out the test the pins were clamped in the arm, taking precautions that the arm remained horizontal during clamping to ensure the pin face remained flat to the surface of the disc. A special jigging arrangement ensured this. Before the start of the test the disc was carefully degreased to remove contamination. The arm was then loaded and the disc set in

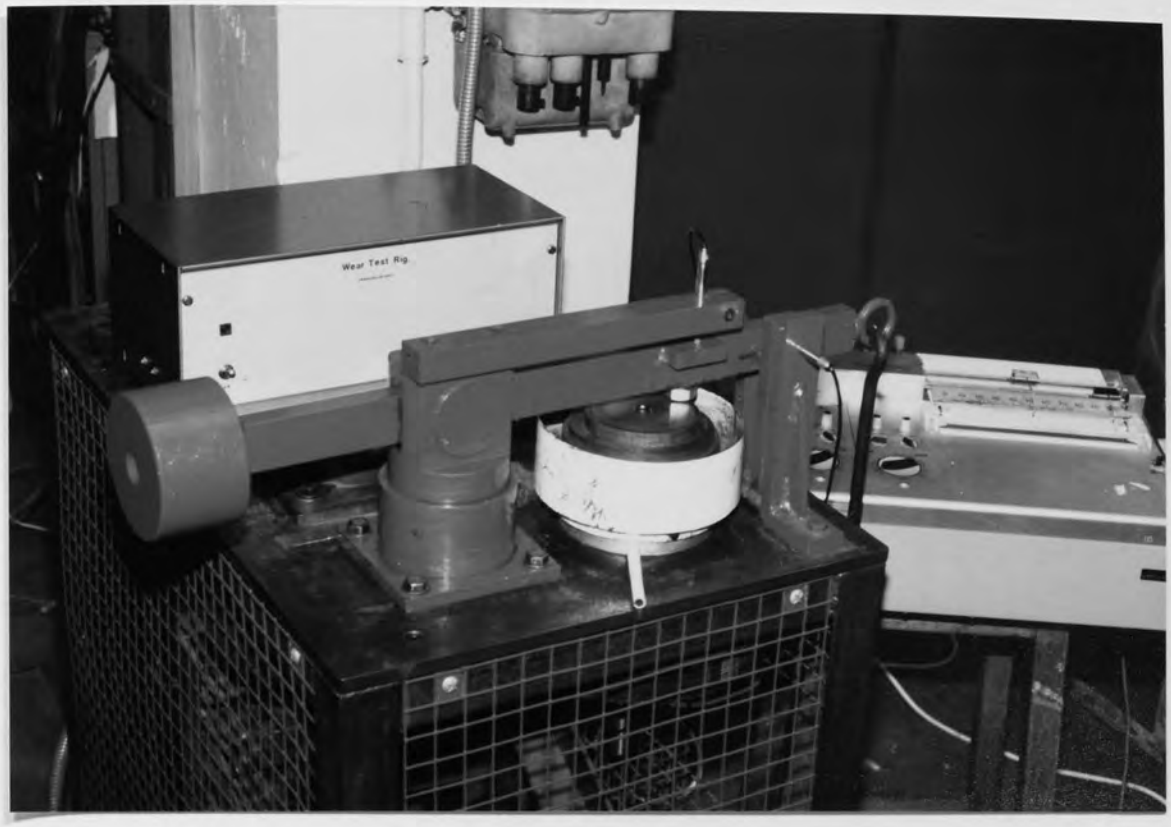

Figure 30a. Pin on disc wear test machine

Figure 30b. Close-up view of the pin on disc wear tester

motion. The results from the transducers measuring wear and frictional forces were recorded on a suitable chart recorder.

After a pre-selected time (1 hour) the test was stopped. From the wear trace the change in length of the pin was measured. This was checked by measuring the actual change in the length of the pin with a micrometer in conjunction with the disc wear measured by Talysurf equipment. The wear on the pin was then expressed in relation to the distance travelled on the disc surface. The distance travelled by the disc was equal to - DRT, where D = wear track diameter (cm), R = speed of rotation (rpm) and T = time of the test in minutes. The coefficient of friction was calculated by dividing the measured frictional force by the applied load to the pin i.e. $\mu = F/N$. Each results was the mean of a minimum of four results. The tests were carried out un-lubricated as the aim was to investigate the lubricating ability of the graphite.

(ii) **Crossed Cylinder Wear Testing**

The crossed cylinder wear test machine consists of a rotating cylinder (rotator) and a fixed counterface cylinder (stator) mounted perpendicular to each other. The rotational speed was fixed at 100 rpm, with the cylinder diameters at 17mm this gave a sliding speed of 70 cm/s. The frictional force was measured by means of a strain gauge attached to a bar which was positioned to prevent the rotator from moving from its set position. The rotating shaft was attached to the motor through a

universal joint. Several wear tracks were possible on each specimen by adjusting the position of the counterface cylinder. Five test were carried out on each cylinder, making each result a mean of five tests. The load applied was 700g . Coated cylinders were run as rotator and stator against mild steel, stainless steel and like-coated cylinders. Frictional values were measured continuously during the test by chart recorder. Wear was measured from the wear grooves produced on the rotator by using a Talysurf. A travelling microscope was used to measure the wear scar produced on the stator.

(iii) Falex Wear Testing

The falex wear and friction testing machine is normally used to evaluate the load carrying capacity and lubricating effectiveness of lubricants. However, it has proven successful in assessing the wear performance of coatings and materials in either dry or lubricated conditions. The Falex tester can be seen diagramatically in figure 12 and pictorially in figure 31. Essentially a cylindrical sample was loaded against two V-blocks and rotated, figure 12 and 31. The load was applied to the V-blocks through lever-arms and a spring gauge. The load was actuated by means of a ratchet wheel mechanism which squeezes the pin into the vertical grooves of the V-blocks. Wear took place as the pin rotated under the applied load, causing a decrease in the pin diameter, the load was maintained by means of the ratchet wheel mechanism.

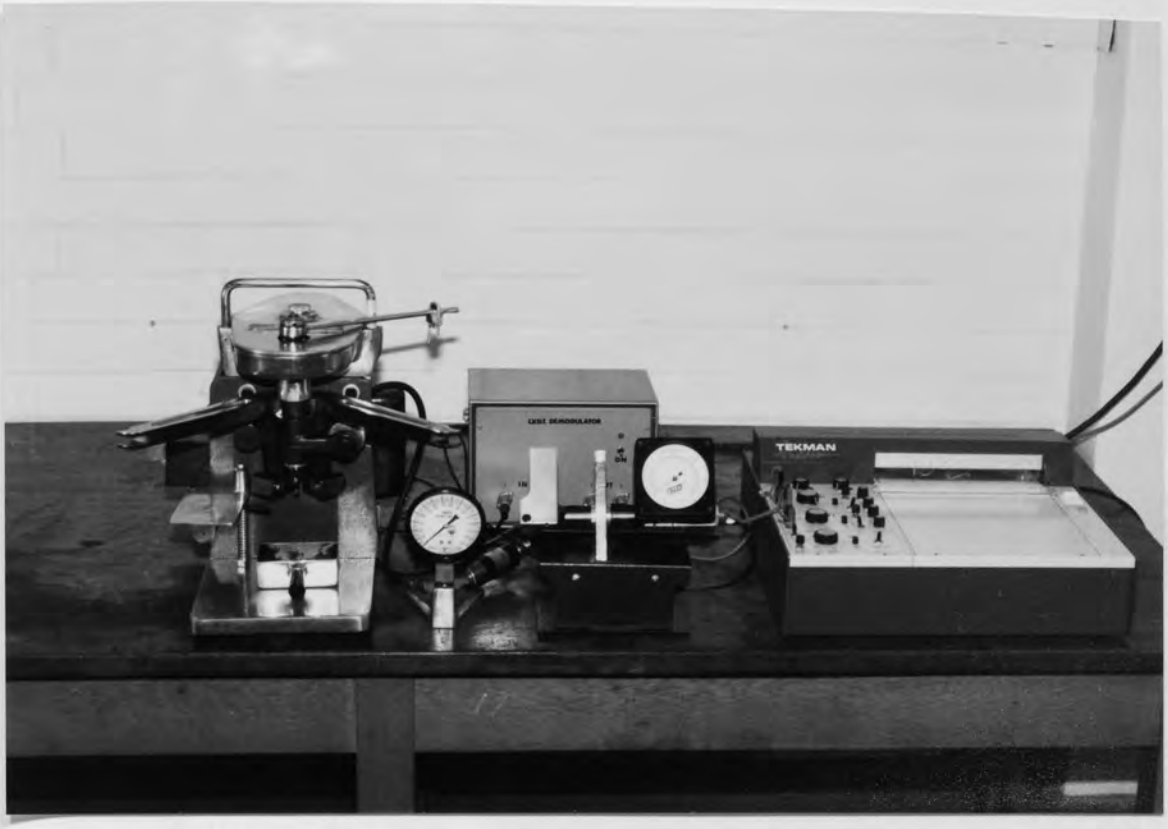

Figure 31a. Falex wear test machine

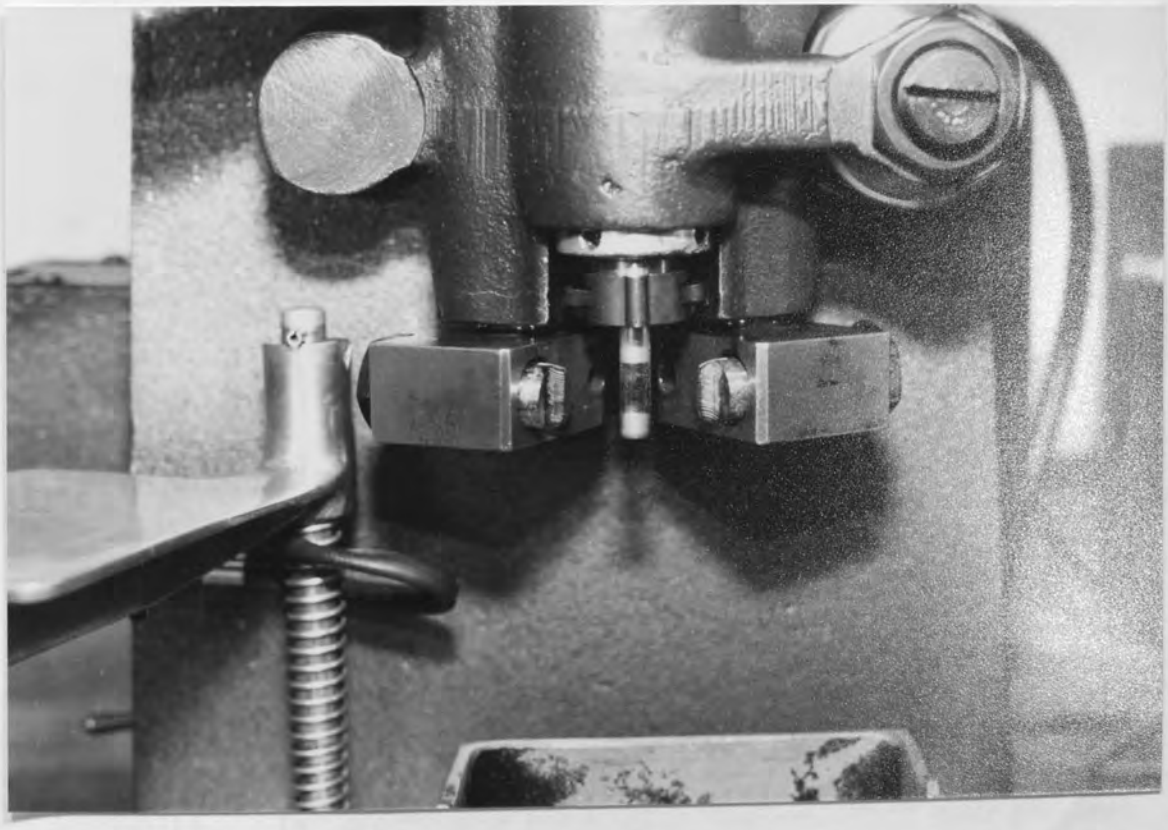

Figure 31b. Close-up view of the pin and v-blocks used in the falex wear tester

Prior to testing, the load gauge was calibrated as instructed by ASTM D2625-69. Pins and blocks made from EN 31 were ultrasonically cleaned in acetone and then weighed to an accuracy of + or - 10ug. An average of ten readings was taken for each pin weight resetting to zero for each reading. The pin and V-blocks to be tested were then located into the machine and loaded to 200 lbs (91kgs); this was the minimum load that could be applied to this machine. As with the pin on disc tester, un-lubricated conditions were used. Trials showed that un-lubricated, and with the high load, the wear rates were high in comparison to the pin on disc. This meant that samples could be safely run for a period of only 6 minutes before the coating would almost certainly be nearing depletion. After testing, pins were ultrasonically cleaned and re-weighed. Wear rate was then expressed as weight loss and the coefficient of friction, calculated from the measured torque on the pin.

After wear testing from all methods surfaces were examined with the aid of optical and S.E.M. microscopy.

5.6.7 Experimental Procedure for Wear Testing of Electroless Nickel-Graphite Composite Coatings

Experiments for plating rate showed that a high plating rate was desirable to incorporate a high concentration of graphite. In practice a compromise was necessary over the last point. If a temperature of 90^{o}C and a pH of 6.0 had been used to give maximum plating rate, then because of the relationship

between pH and phosphorus, the phosphorus content would have been low. In order to give high hardness and good wear resistance, high phosphorous contents are required, thus the pH was reduced to 5.0, this gave satisfactory phosphorous content whilst still giving acceptable plating rates. All subsequent coatings for wear testing electroless nickel-graphite were plated under these conditions.

The programme of testing electroless nickel-graphite composites for friction and wear properties was as follows:

5.6.7.1 The Effect of Graphite on the Hardness of Electroless Nickel

To compare the hardness of the electroless nickel/graphite coatings to plain electroless nickel coatings, hardness measurements were taken for the two systems in the as-plated and heat treated condition. For the electroless nickel/graphite coatings, hardness measurements were taken over the range of volume percentages of graphite obtained.

5.6.7.2 Pin and Disc Wear Testing

The prime objective was to evaluate how the coatings would perform in wear situations. To do this the following experiments were carried out with the pin and disc wear tester.

(i) The Effect of Graphite Content on Wear Rate and Coefficient of Friction against EN 31

Pins made from EN 31 steel were plated with electroless nickel/graphite, the graphite content increasing with each set of pins. The conditions for plating were 90°C and pH 5.0. Each set of pins consisted of 3 samples which gave 6 end surfaces for wear testing at each graphite content. One set of electroless nickel and one set of electroless nickel-graphite pins, containing 5% by volume graphite, were left un-heat treated, the remainder were heat treated at 400°C for 1 hour. Each set of pins was then tested against an EN 31 disc at 2 kg load on the pin and 50 cm/sec sliding speed. Coefficient of friction and wear rate were then calculated from the results.

(ii) The Effect of Graphite Content on Wear Rate and Coefficient of Friction against an Electroless Nickel-Graphite Coated Counter Face

As above, pins were plated with increasing contents of graphite. Also the disc was plated with electroless nickel-graphite from a solution containing 50 g/l graphite, this gave an approximate content of 6% by volume graphite. The conditions of plating were 90°C and pH 5.0. Both pins and disc were then heat treated at 400°C for 1 hour. The pins were then run against the disc in the wear tester under a 2 kg load and a sliding speed of 50 cms/s.

(iii) The Effect of Load on Wear Rate and Coefficient of Friction

To study the effects of increased load on friction and wear of electroless nickel-graphite, pins and discs were plated in one batch from an electroless nickel-graphite solution containing 50 g/l graphite, so as to give a constant graphite content of the coating. The conditions were as before 90°C and pH 5.0. Both pins and disc were heat treated at 400°C for 1 hour and were run against each other. A constant sliding speed was maintained throughout the work of 50cms/s, however the load which had a much greater effect on conditions than sliding speed was gradually increased from 2kg to 8kg, 7kg/cm^2 to 28.2kg/cm^2. Coefficient of friction and wear rate were then calculated for each different load on the pin.

5.6.7.3 Crossed Cylinder Wear Testing

The crossed cylinder wear test was also used to examine the wear behaviour of nickel-graphite deposits. Stainless steel cylinders were coated with electroless-nickel graphite coatings containing 6.9 volume per cent graphite and electrolytic nickel-graphite coatings containing 7.1% volume per cent graphite. The coated cylinders were run against similar coated cylinders and also against stainless steel and mild steel cylinders. Nickel-graphite coated cylinders were tested as both rotator and stator against the two steels. The electroless nickel coatings were tested in the heat treated condition. Wear testing conditions were as in section 5.6.6 ii.

5.6.7.4 Falex Wear Testing

As a further test of the coating under different wear conditions, a comparison was made between electroless nickel and an electroless nickel-graphite coating using the Falex wear tester. The nickel-graphite coating was plated from a solution containing 45g/l graphite, and both the nickel and nickel-graphite solutions were operated at 90°C and pH 5.0. All pins were heat treated at 400°C for 1 hour. A total of ten pins were tested, five electroless nickel and five electroless nickel-graphite (6.5 volume per cent graphite), and were run against hardened and tempered EN 31 steel V-blocks.

5.6.8 Experimental Procedure for Wear Testing of Nickel-PTFE Composite Coatings

The ultimate aim in the development of the electroless nickel-graphite coating was to be comparable, if not better, in terms of friction and wear properties than electroless nickel-PTFE. In order to be able to make this comparison wear tests on electroless nickel-PTFE coatings were carried out using the pin on disc machine and cross cylinder wear test.

5.6.8.1 Pin on Disc Wear Testing

A quantity of pins and a disc made from EN 31 were commercially plated with 25 μm of electroless nickel-PTFE deposit (source one). The average PTFE content of the deposits

was 18 volume per cent but varied considerably around the pin. The following combinations were then tested using the pin and disc tester:

(i) Electroless nickel-PTFE pins against an EN 31 disc.

(ii) Electroless nickel-PTFE pins against an electroless nickel-PTFE coated disc under increasing load.

(iii) Electroless nickel-PTFE pins heat treated at 400^{o}C for 1 hour against an EN 31 disc.

The same wear testing parameters were used as with electroless nickel-graphite, ie. sliding speed of 50cm/s and a load of 2 kg unless stated. The tests were run un-lubricated and a minimum of two pins, ie. four tests, were used for each result.

5.6.8.2 Crossed Cylinder Wear Testing

For crossed cylinder wear testing stainless steel cylinders were coated with two different nickel-PTFE systems. These were plated from systems developed by BAJ Ltd. (source two); one was based on electroless nickel and used 0.75 µm PTFE particles while the other was based on electrolytic nickel and used 10 µm PTFE particles. Coated cylinders were run against similar coated cylinders and also stainless and mild steel cylinders as both the rotator and stator. The electroless nickel coatings were un-heat treated and the wear test conditions were as in section 5.6.6 ii.

5.6.9 Experimental Procedure for the Wear Testing of Electroless Nickel-Chromium Composite Coatings

Electroless nickel-chromium composite coatings were assessed for wear and frictional properties using the pin on disc wear tester. Pins made from EN 31 were coated with an electroless nickel-chromium composite containing 15 volume per cent chromium. Pins were then heat treated for 1 hour at 400°C and 8 and 16 hours at 850°C. These were run against EN 31 discs. The sliding speed was 50cm/s and a load of 2 kg applied to the pin. The tests were run un-lubricated with four tests carried out for each result.

CHAPTER VI

EXPERIMENTAL RESULTS

6.1 BALL MILLING

The range of material produced by ball milling, as decribed in section 5.1.1, for experiments on particle size are shown in figures 32 and 33. These results were obtained by using Coulter analysis. Subsequent analysis of 2, 6, and 20 micron grades, by Malvern Laser analysis, showed a somewhat different range of particle sizes, figure 34. These results reflect some of the problems experienced in measuring particle size by using different methods of analysis and with powders that are not spherical.

Using Coulter analysis, the volume of the particle is measured by the change in voltage across a gap through which the particle passes. The volume is then converted to diameter assuming the particle is spherical. As the graphite particles are flake-like, the volume registered will reflect a particle diameter of a smaller spherical particle than the major dimension of the flake. A further problem measuring graphite particles with Coulter analysis is that, unless the graphite is suitably wetted by the electrolyte used in the analysis, the individual flakes will not be separated and dispersed in the solution. The analysis will then give particle sizes larger than actual size. However, S.E.M. examination of 2 micron powder, prompted by the

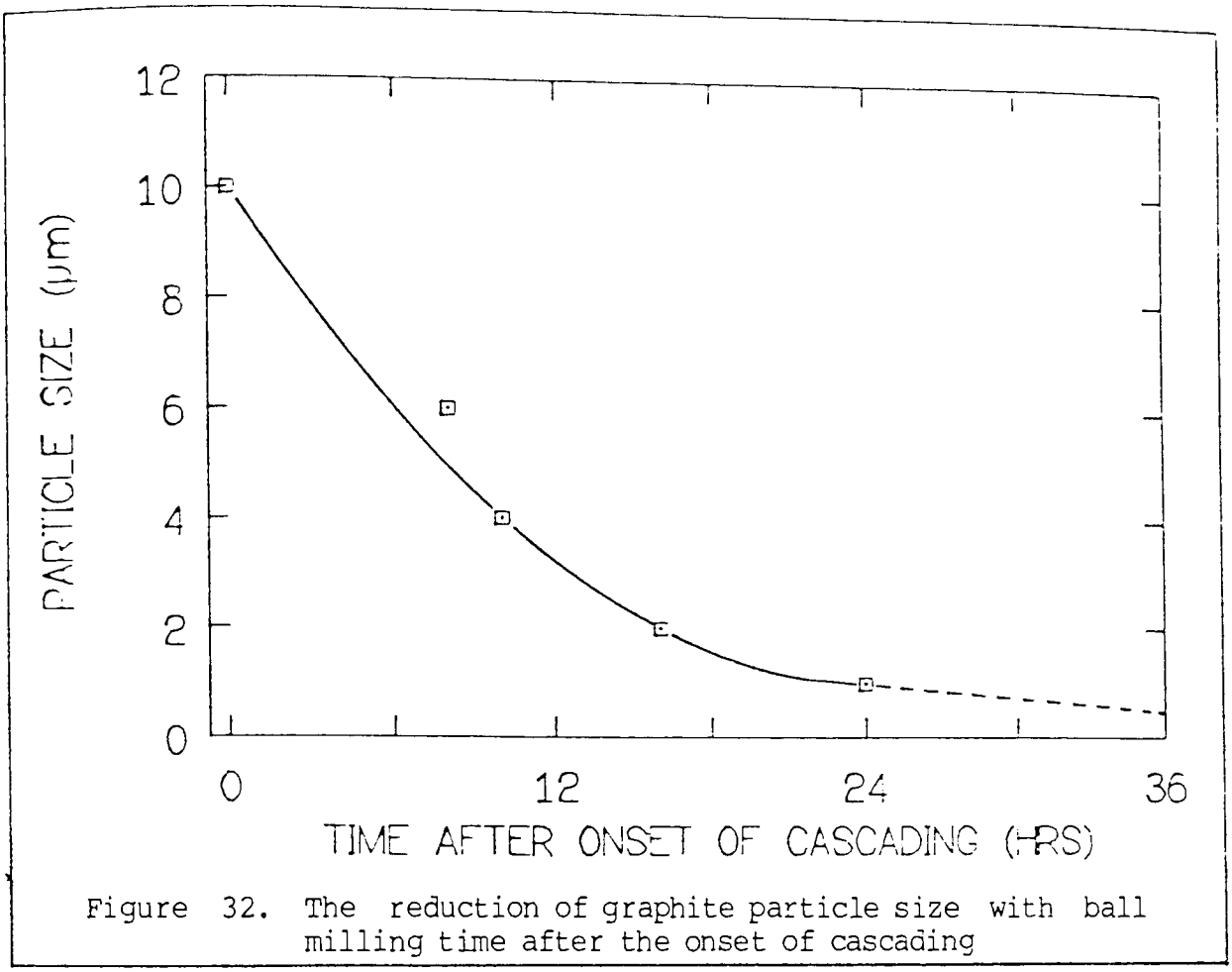

Figure 32. The reduction of graphite particle size with ball milling time after the onset of cascading

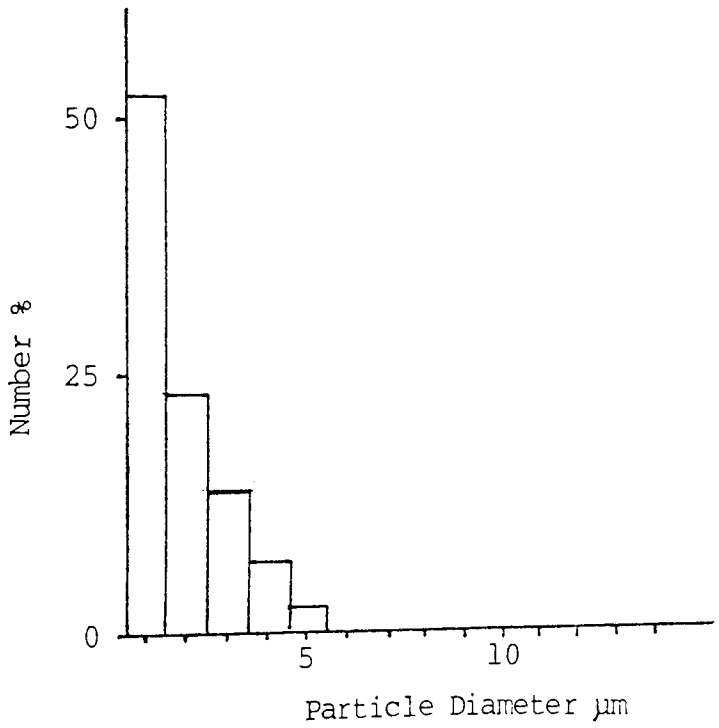

Figure 33a. Coulter analysis of the graphite particle size range produced by ball milling. 1 μm graphite powder

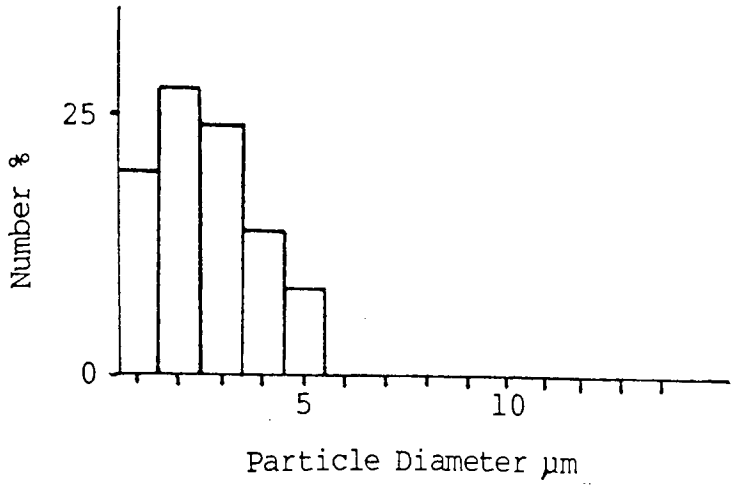

Figure 33b. 2 µm graphite powder, Coulter analysis

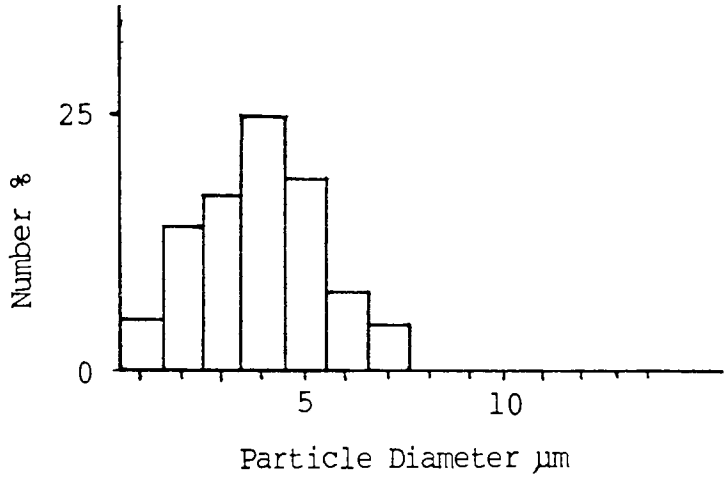

Figure 33c. 4 µm graphite powder, Coulter analysis

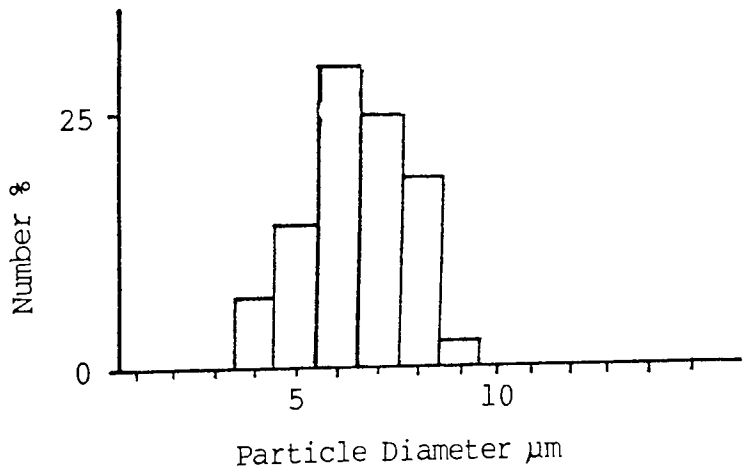

Figure 33d. 6 µm graphite powder, Coulter analysis

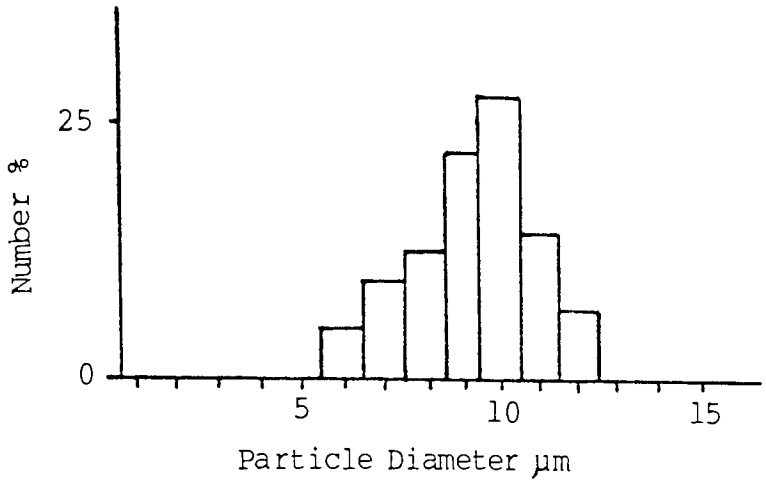

Figure 33e. 10 µm graphite powder, Coulter analysis

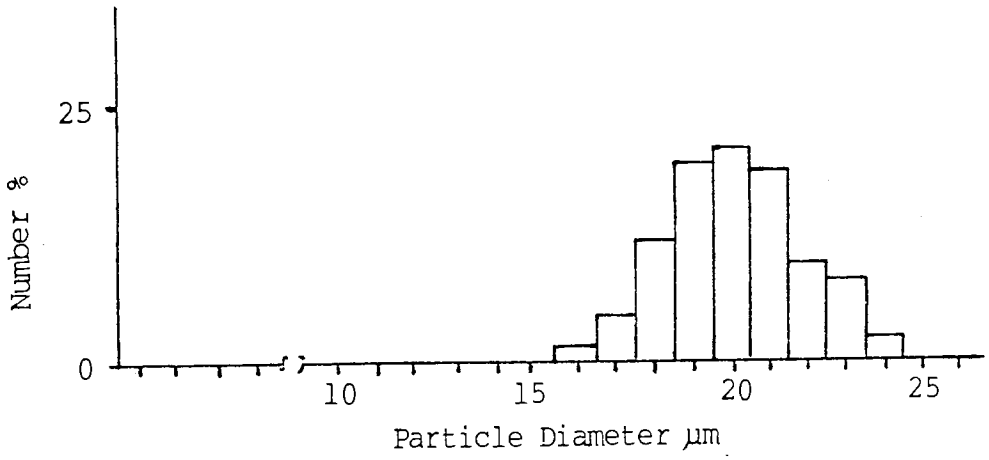

Figure 33f. 20 µm graphite powder, Coulter analysis

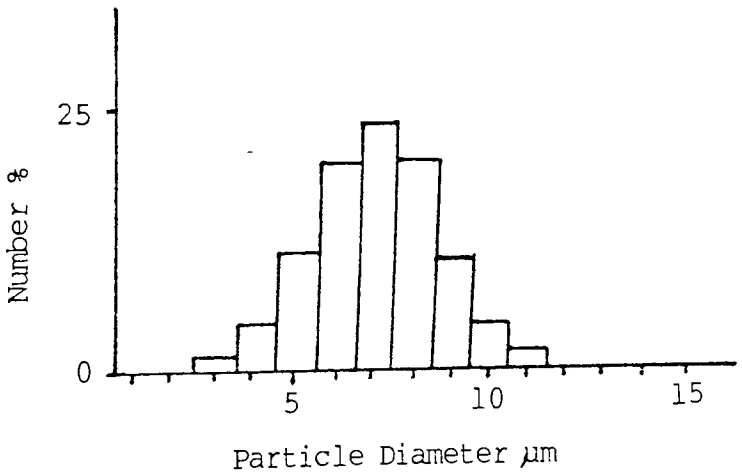

Figure 34a. Graphite particle size by Malvern Laser analysis, 2 µm graphite powder by Coulter, 7 µm by Malvern

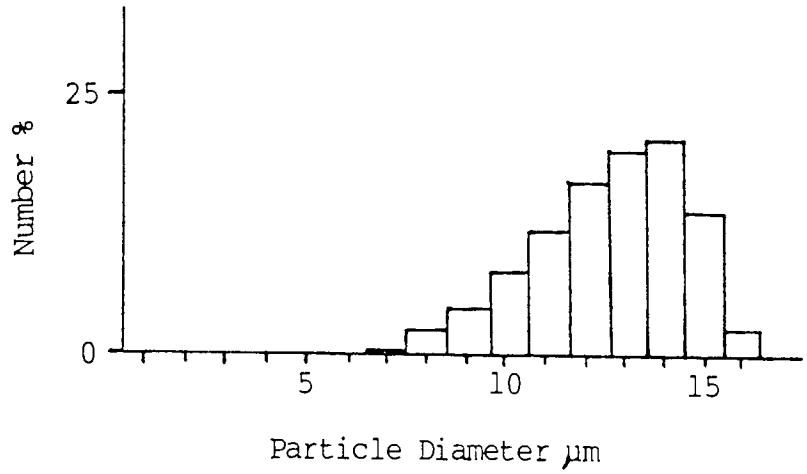

Figure 34b. 6 µm graphite powder by Coulter, 14 µm by Malvern

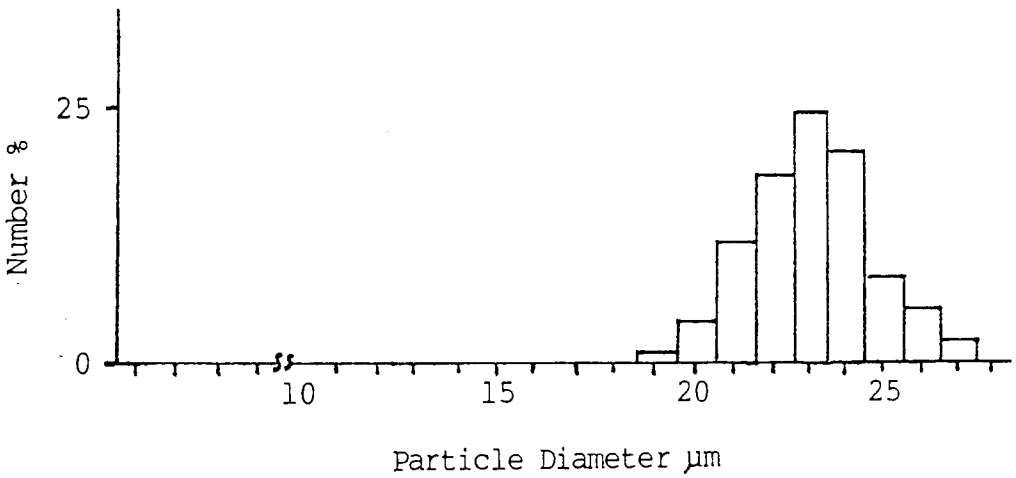

Figure 34c. 20 µm graphite powder by Coulter, 23 µm by Malvern

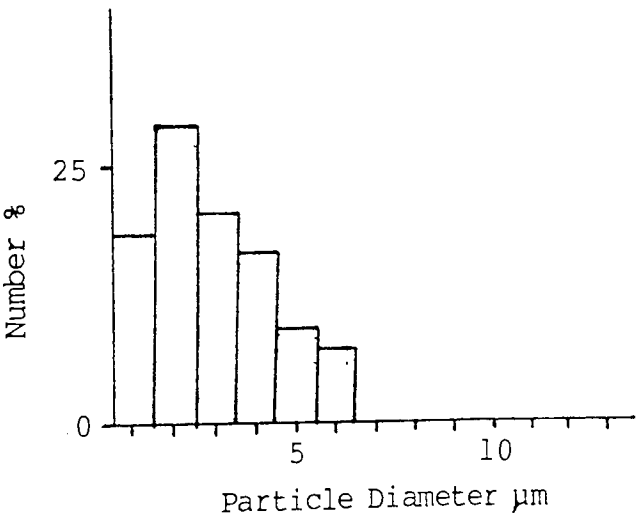

Figure 35. 2 µm graphite powder by S.E.M. analysis

difference in results, showed the graphite particle size to be similar to those results obtained by the Coulter analysis, as can be seen in figure 35. A number of S.E.M photographs were taken and particles measured, over 500 values were taken. The Malvern Laser analysis was unsuitable for flake material and so data from Coulter analysis was used throughout the work.

The chromium powder supplied by Johnson Matthey Ltd was used for all the work on electroless nickel-chromium composite coatings. The particle size range, as produced by Coulter analysis, is shown in figure 36. This showed the particle size to be nearer 4 micron nominal particle size not 2 micron as quoted by Johnson Matthey, S.E.M. examination confirmed this. Ball milling of a crushed chromium ingot was attempted in order to try and produce a range of particle size. However, this proved too difficult with the equipment available.

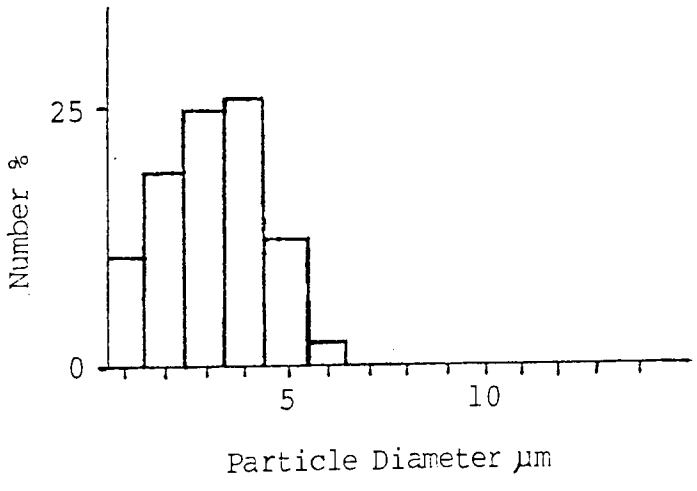

Figure 36. Chromium particle size analysis by Coulter analysis, 4 micron nominal particle size

6.2 ELECTROLESS NICKEL-GRAPHITE SOLUTION DEVELOPMENT

6.2.1 Solution Stability

The addition of graphite to the electroless nickel solution, as expected, adsorbed all the organic stabilisers present in the solution. This resulted in spontaneous decomposition of the electroless nickel solution.

To compensate for this effect organic stabilisers, supplied by Cannings, were added until stability of the solution could be found, as indicated by potential measurements. The solution was intially over-stabilised and then carefully diluted, whilst measuring the potential to give a solution which just plated. Results showed that up to ninety times the original stabiliser content was required before the electroless nickel-graphite solution could be stabilised. Subsequent analysis of the solution by polography gave a quantitative figure for the amount of stabiliser not adsorbed onto the graphite and present in the solution. The stabiliser addition could then be adjusted to give the correct level for organic stabilisers in the Nifoss 3000 electroless nickel solution for subsequent graphite containing solutions.

Unfortunately, these solutions quickly became unstable, despite correct maintenance additions of stabiliser to replace that lost during normal plating. Analysis by polography of electroless nickel-graphite solutions, containing free organic

stabiliser showed that after initial saturation of graphite and apparent stability, the organic stabilisers were then gradually adsorbed, even when the solution was cold and with no plating carried out.

To produce a stable solution it would therefore have been necessary to make up a solution with additional stabilisers and allow it to stand for a period of time to reach true stability. Regular analysis of the solution was required and the free stabiliser in solution maintained at the correct level. However, before the true stability of the organically stabilised solution was ever found, stabilisation by heavy metal ions was investigated. This proved to be a more satisfactory method of achieving stability.

The literature review showed that heavy metal ions are effective, electroless stabilisers, however are not normally added in large amounts as they can cause increased internal stress, porosity and reduce ductility of the deposit[46,47,60]. They do, however, have the advantage that they should not be adsorbed onto the graphite in any significant quantities to provide stability.

A suitable heavy metal ion was selected and a solution containing the ion was supplied by Cannings. The approximate addition of metal ions, as with organic stabilisers, was found by measurement of potential. Subsequent polography analysis showed that none of the added heavy metal ions appeared adsorbed by the

graphite. This produced a stable, predictable plating solution. A summary of the performance of the two stabiliser types can be seen in table 3.

Table 3. A Summary of the Relative Performances of the Stabilisers Used.

Stabiliser	Stability	
	Initial	Long Term
Organic	Satisfactory	Decomposition of solution
Heavy Metal Ions	Satisfactory	Satisfactory

As with organically stabilised solutions the metal ions are also plated out with the deposit. This then proved the only means by which metal ions were lost from the solution, the rate of which, was the same as for the normal electroless nickel solution. The stabiliser content could easily be maintained by correct Nifoss 3000 maintenance additions.

Data relating to the type and levels of stabiliser in solution were not reported in order to maintain confidentiality of formulations relating to Cannings solutions. The same limitations were also applied to the surfactant additions.

6.2.2 Surfactant Additions

Graphite powders added to electroless nickel solutions were not readily wetted by the solutions. To achieve better

wetting characteristics of the graphite, surfactants were added to the solution.

The adsorption properties for each surfactant were first determined by surface tension measurements. This gave a surfactant addition per gram of graphite and proved successful in keeping the free surfactant in solution to a minimum. Experience showed however, that most of the surfactants used did not have any adverse effects on plating rate or cause excessive foaming, this included those surfactants found suitable for graphite deposition. As most surfactant additions were not critical this made solution development considerably easier.

A non-ionic surfactant was first evaluated. Deposits plated from this solution showed no sign of codeposition. Observation of the solution suggested that although wetted, the graphite had a tendency to agglomerate and settle out of suspension relatively quickly on removal of the source of agitation. The fact that the graphite particles were present in the solution as groups, and not individual particles, probably prevented them from being incorporated into the deposit.

To ensure that the particles were present as separate particles, and not as agglomerated groups, a charged surfactant was required. Surfactants are bi-polar molecules, one end attaches itself to the graphite surface whilst the other charged end, is soluble in solution. This wets the particles and also produces a charged surface on the particle. The similarly

charged particles then oppose each other and so particles remain separate within the solution.

To produce such a dispersion, both anionic and cationic surfactants can be used. Cationic surfactants tend to have a much greater effect on plating rate and adhesion and are less effective dispersing agents than anionics. An anionic surfactant was therefore evaluated first.

The anionic surfactant was added in conjuction with the non-ionic surfactant to ensure complete wetting and dispersion of the graphite particles. It was found that as well as visibly providing wetting and dispersion of the graphite, this combination of non-ionic and anionic surfactants was also capable of producing codeposition of graphite with electroless nickel from a suitably stabilised solution, figure 37.

Although anionic surfactants produced satisfactory deposits, in an attempt to increase the levels of graphite codeposited, cationic surfactants were also evaluated.

As previously suggested cationic surfactants had a much greater effect on plating rate. Also in the levels that could be added to the solution without affecting plating rate, cationics appeared less efficient at maintaining a dispersion of the graphite particles. Some of the cationics tried also had a much greater tendency to foam than the non-ionic and anionic surfactants when used with air agitation.

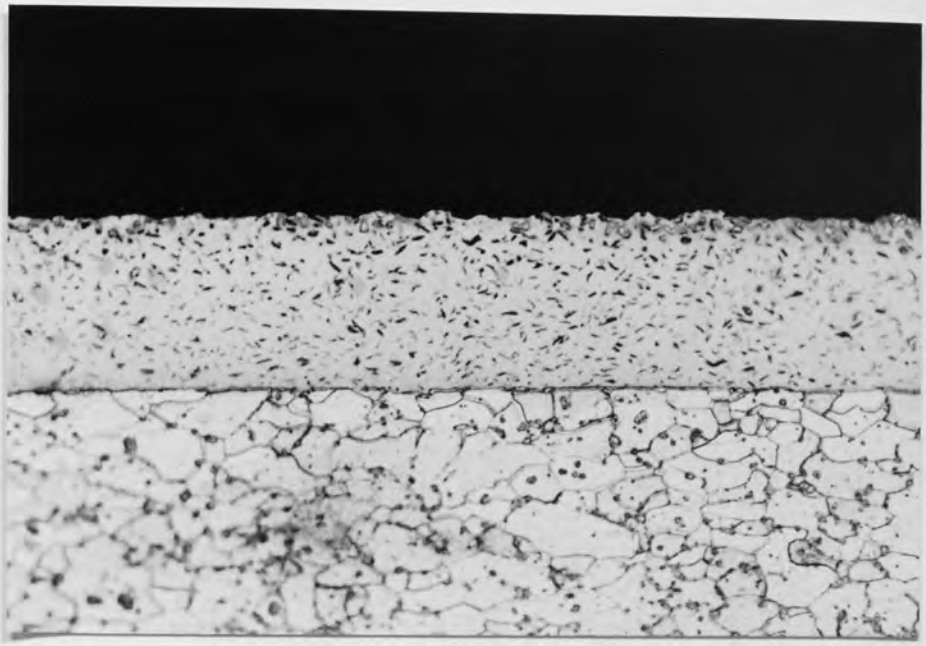

Figure 37. Electroless nickel-graphite composite coating produced from solution containing a non-ionic and anionic surfactant to provide wetting and dispersion, 40 g/l graphite, 90 ^{o}C pH 5

Because of these problems a number of cationic surfactants were tried. The more suitable of these were capable of producing wetting and dispersion and as with anionics appeared to produce considerable adsorption of graphite onto the plating surface. This gave the appearance of a thick black layer of graphite on the surface. However, unlike anionic based solutions codeposition of the graphite did not occur with cationic solutions. Although the surface appeared saturated in graphite, normal plating occurred through the adsorbed graphite layer, to produce electroless nickel deposits at normal plating rates, but

with no codeposition of graphite. In these cationic based solutions the graphite appeared to ride ahead of the plating surface without ever being codeposited, unlike the anionic solutions where codeposition occurred.

A summary of the surfactants used and their effect on the electroless nickel-graphite solution can be seen in Table 4.

Table 4. A summary of the results for the performance of the different surfactants used

Surfactant	Plating Rate	Dispersion	Codeposition
Nonionic	Unaffected	No Dispersion	None
Anionic	Unaffected	Dispersion	Yes
Non+anionic	Unaffected	Dispersion	Yes
Cationic(1)	Unaffected	Dispersion	None
Cationic(2)	Unaffected	Poor	None
Cationic(3)	Poisoned reaction	Poor	None
Cationic(4)	Unaffected	Dispersion	None
Cationic(5)	Poisoned reaction	Dispersion	None

As a result of these experiments, only the anionic based solution was found suitable for the production of electroless nickel-graphite composite coatings.

6.3 ELECTROLESS NICKEL CHROMIUM SOLUTION DEVELOPMENT

6.3.1 Oxidation of Chromium

Chromium powder was oxidised as described in section 5.4.1. (i). The weight gain of 25 grams of 4 micron chromium powder as a result of oxidation is shown in table 5, and plotted in figure 38 against oxidation time for heat treatment temperatures of 400°C and 600°C.

Table 5. Oxidation of Chromium Powder

	400°C	600°C
Time (mins.)	Weight gain (grams)	
5	-	0.03766
10	0.00572	0.05602
20	0.01012	0.06498
30	0.01435	0.07952
40	0.01762	0.08643
60	0.02230	0.10334
120	0.03284	0.14513

The results plotted in figure 38 show the oxidation of the powder to be of a parabolic nature, ie. $W \propto T$. If W^2 is plotted against t (time), very good fit straight lines, (correlation coefficient 0.99, 400°C and 0.99, 600°C), are produced confirming the parabolic nature of the growth. The parabolic rate constant can then be found from the gradient.

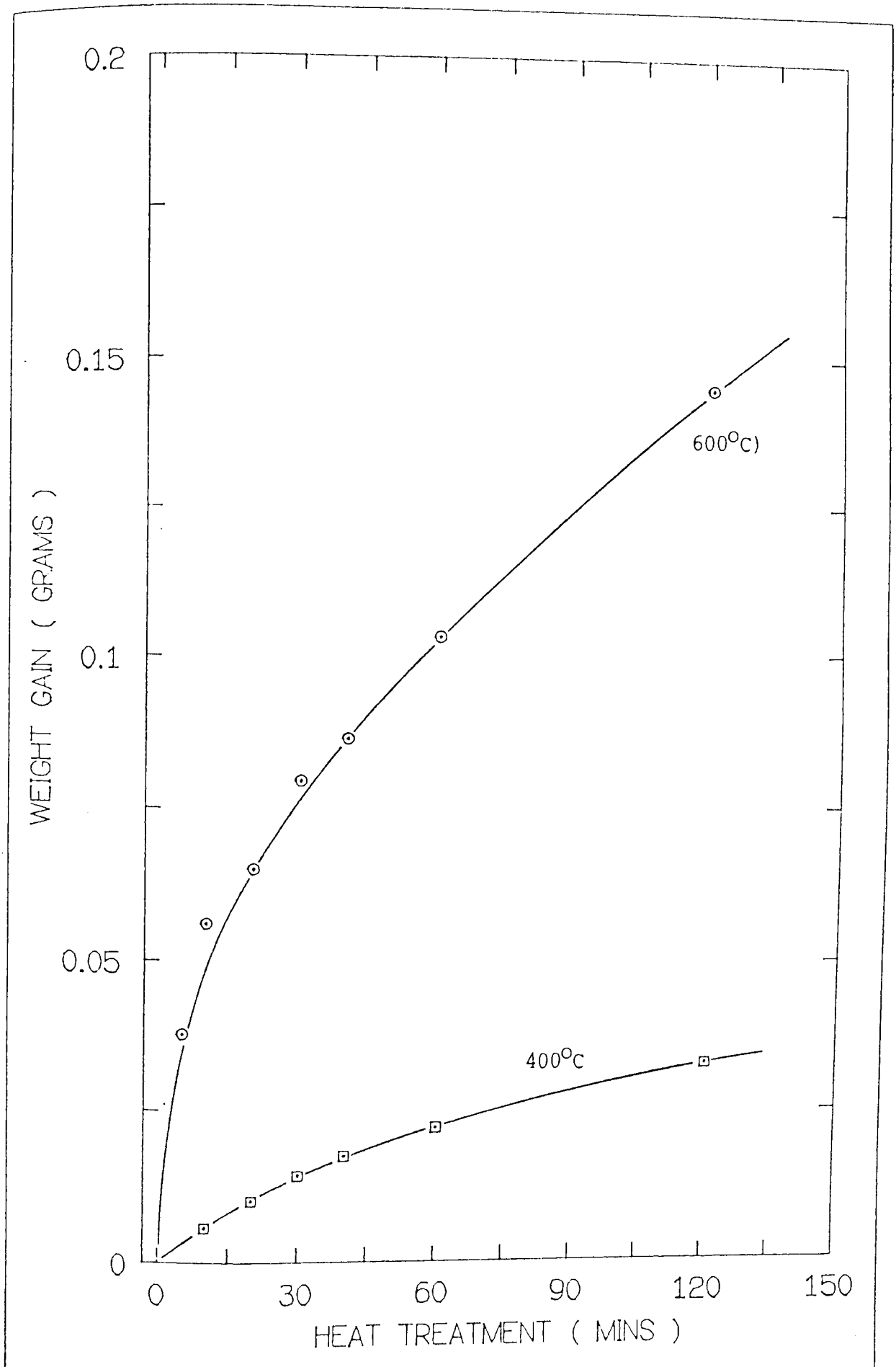

Figure 38. The oxidation of chromium powder with temperature and time. The weight gain of 25g of chromium powder, 4 µm nominal particle size

At $400^{o}C$ $W^2 = 0.0000097\ T + 0.0000823$

At $600^{o}C$ $W^2 = 0.0001611\ T + 0.0011057$

From the weight gain figures in table 5 for 25 grams of powder, it is possible to become more specific and calculate the thickness of the oxide film on the particles.

Calculating the weight gain per particle:

Weight gain (Wg) = Weight of oxidised particle (Wo) - weight of original particle (W)

The original particle weight W can be found from:

W = Density of chromium (D) * Volume of a particle (V)

Assuming a spherical particle of 4 microns, $V = 4/3\ r^3$

The weight of an oxidised particle can be found from:

$$Wo = Wt * V * D /25$$

Where Wt is the weight of 25 grams of oxidised chromium powder.

V the volume of the particle,

D the density of chromium.

If the weight gain of an oxidised particle is divided by the surface area of a 4 micron spherical particle, the degree of oxidation can be expressed as the weight gain per unit area, $\mu g/cm^2$, and the thickness in nanometers, nm. The calculated results for the weight gain per unit area and the thickness of the film are shown in table 6 for each oxidation temperature and time.

Table 6. Weight Gain per Unit Area and Oxide Layer Thickness

Oxidation Time (mins)	400°C		600°C	
	$\mu g/cm^2$	nm	$\mu g/cm^2$	nm
5	-	-	0.673	404
10	0.102	62	1.001	601
20	0.181	108	1.161	697
30	0.256	154	1.421	853
40	0.315	189	1.544	927
60	0.398	239	1.846	1108
120	0.587	352	2.593	1556

The calculated oxide films are very thin. The rate of oxide formation and the resultant film thicknesses are, however, in close agreement with the results of Gulbransen and Andrew[176], who reported on the kinetics of the oxidation of chromium.

6.3.2 Stability of Oxidised Chromium Powder in Electroless Nickel Plating Solution

Having produced an oxide layer around the chromium metal particles, powders were then added to a hot electroless nickel solution, (90°C,pH5), to assess the degree of oxidation required to prevent reaction with the solution.

The results for the stability of the chromium powder and plating solution are shown in table 7 and figure 39. The results are expressed as the amount, in ml/l, of electroless nickel base solution removed from the plating solution in one hour. The initial content of the nickel base solution was 100ml/l. This then gave a figure for interaction between the powder and solution.

Table 7. The Stability of Oxidised Chromium Powder in Electroless Nickel Plating Solution

Oxidation Time 400°C minutes	Nickel base solution removed ml/l*
0	71.05
5	16.56
10	4.7
20	1.5
40	0.0
60	0.0
120	0.0

* Initial base solution 100 ml/l.

Figure 39 shows that without oxidation interaction between the chromium powder and electroless nickel solution occurs, resulting in almost complete decomposition of the solution onto the large surface area of the powder. However, after only five minutes at 400°C a significant improvement in

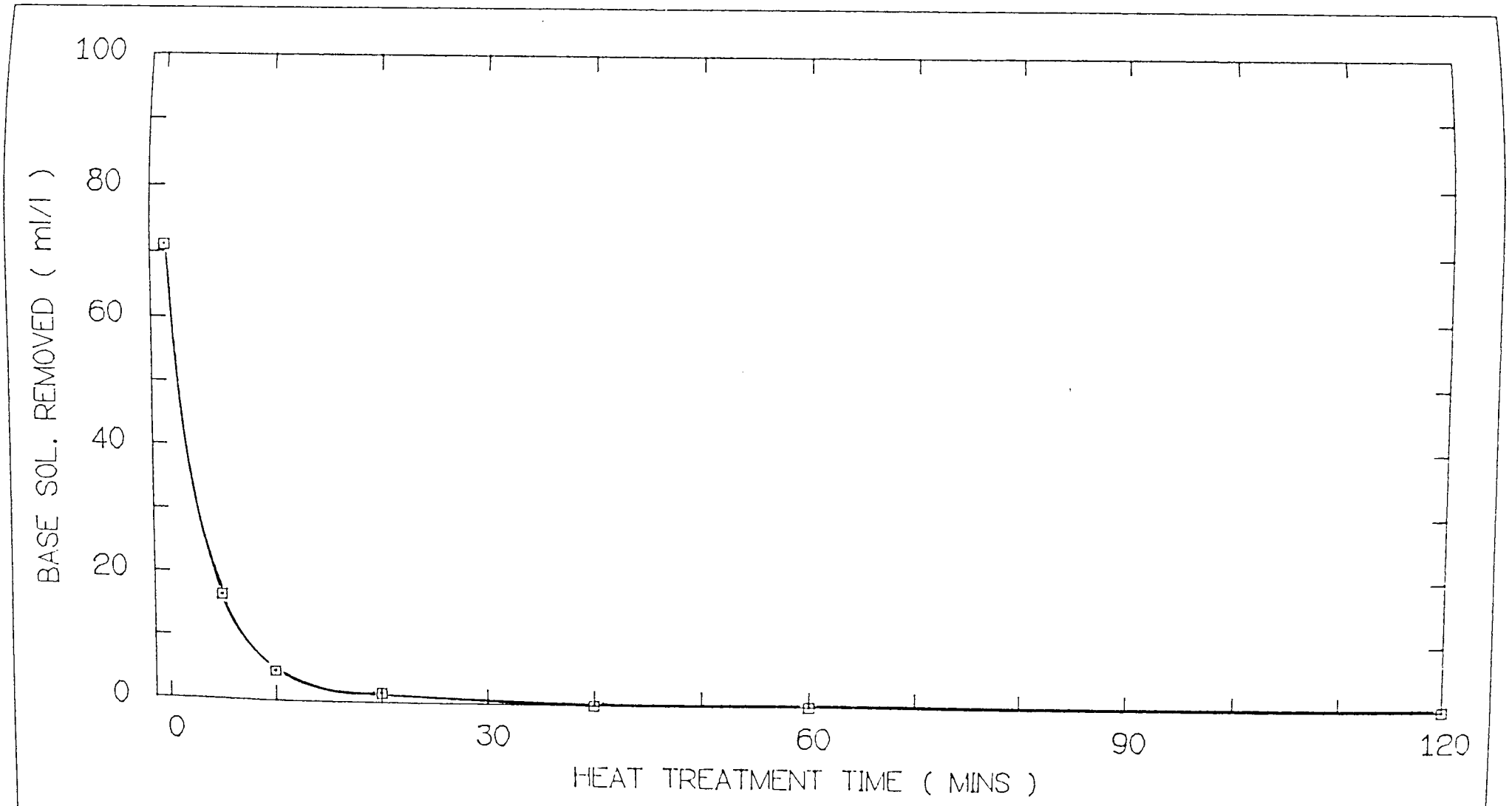

Figure 39. The stability of oxidised chromium powder in electroless nickel plating solution. Solution temperature 90°C, pH 5. Initial base solution 100 ml/l, period of immersion 1 hour

stability occurs, until after forty minutes no reaction at all was detected between the powder and solution. From figure 38 equivalent protection would also be produced by heat treatment at 600^{o}C for two minutes.

From Table 6, a film thickness of just two hundred nanometers is sufficient to cover the surface and prevent the chromium from reacting with the solution. It could be concluded, that this film must have very good integrity and adherence to provide such protection. This method appeared a simple and effective way of stabilising the chromium powder in solution. It was also found, by plating a component, that composite electroless nickel coatings containing chromium could easily be produced.

Over a period of plating longer than one hour, however, gradual instability occurred. This was as a result of adsorption of organic stabilisers onto the chromium particle and by codeposition into the deposit. Regular maintenance of the solution was just insufficient to maintain the stability and so an extra initial stabiliser addition was necessary. This then accounted for the stabiliser adsorbed onto the chromium powder. Again it was found heavy metal ions best suited the job however, in much smaller amounts than in the case of graphite.

6.4 FACTORS AFFECTING PARTICLE INCORPORATION

6.4.1 Agitation

During plating trials prior to starting the proposed investigation programme, agitation effects were noticed in samples produced from both graphite and chromium based solutions. This took the form of areas of the deposit with reduced numbers of particles codeposited. If specimens were placed close to the source of agitation two distinctly different deposits could be produced on either side of the specimen. Figures 40a - d illustrate an example of this effect.

Figures 40a and 40b show that the side of the plate specimen facing the agitation has a smoother, thinner coating and has a low graphite content of 2.5 volume per cent. The source of the agitation, the air stream, is close enough to the specimen surface to produce excessive fluid movement. This is capable of continually sweeping away settling graphite from the surface and thus reduces codeposition. Also if the surface was in contact with the air stream, this could account for the thinner coating as the solution present for plating could be reduced.

Figures 40c and 40d, show the reverse much rougher side. Codeposition of graphite and nickel readily occurred under shielded, but effective, agitation. This allowed particles to settle and remain there until codeposited.

(1) Surface open to agitation

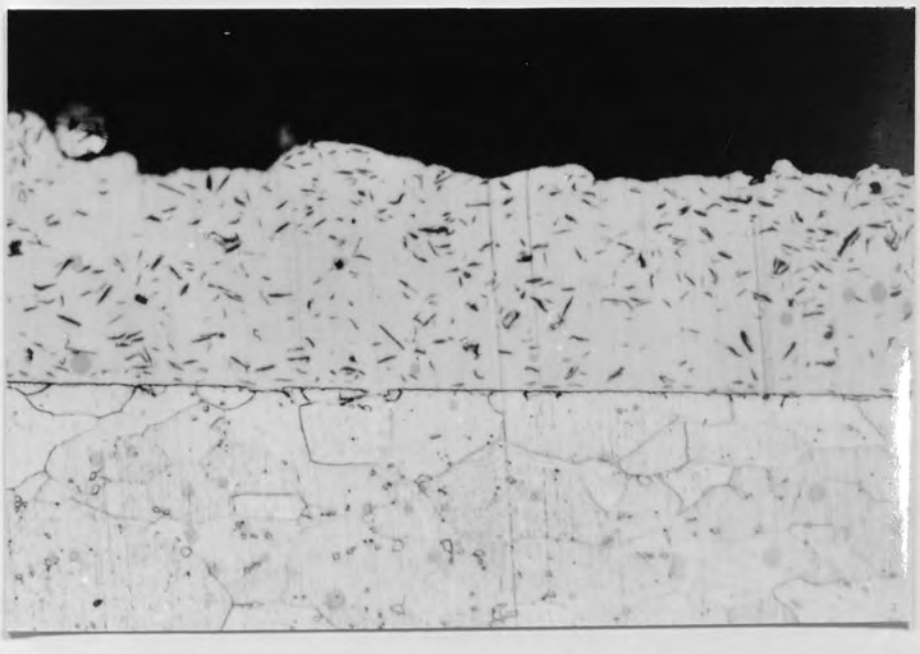

(2) Shielded surface

Figure 40a. The effect of agitation on graphite content

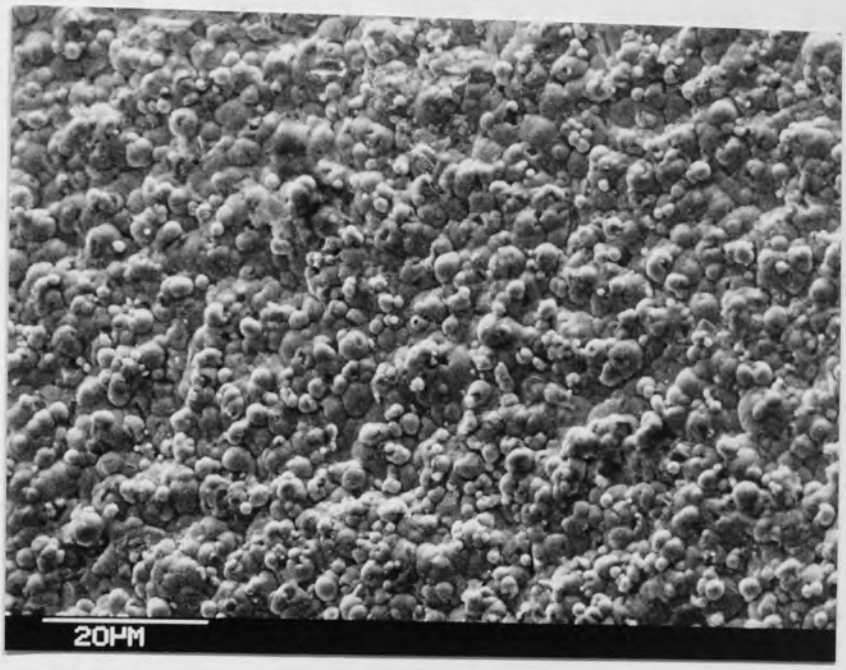

(1) Surface open to agitation

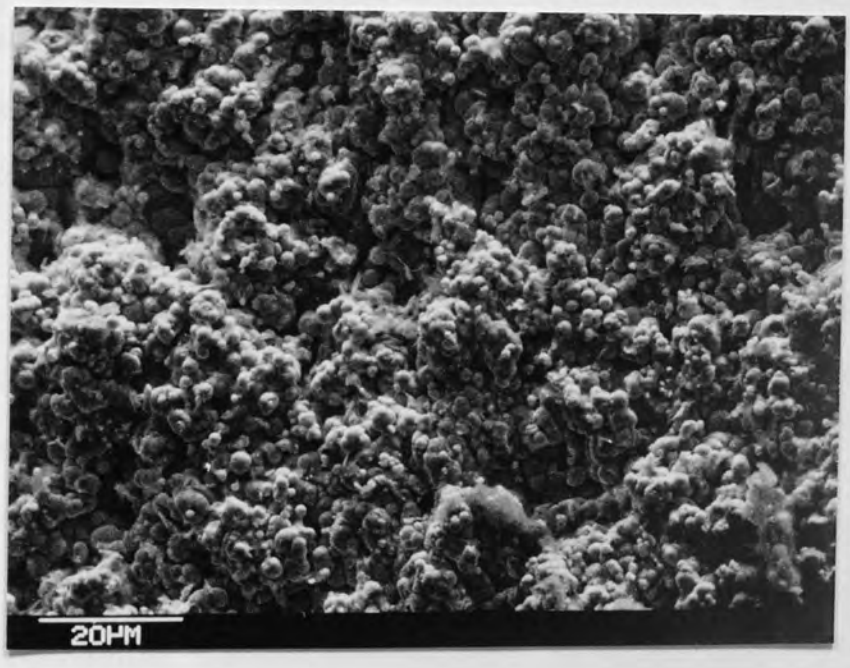

(2) Shielded surface

Figure 40b. The effect of agitation on surface roughness

If the specimens were not supported rigidly, deflection of the specimens in the air stream could also have occurred. This presented upward and downward facing surfaces which exaggerated the agitation effects, as gravity helped to prevent codeposition on the under surface, yet aided settling on the upper surface. Results of this effect contributed to figures 40a - d. Plating of right angled specimens also showed this effect.

The effects of agitation were more noticeable in the one litre container than the four litre container. This might be expected since the distance between the air source and specimen was greater in the four litre container, so that more uniform agitation was experienced by the specimen. However, the effects of settling on the upper surface was still noticed with graphite up to saturation and could still be noticed in chromium composites even when saturation had appeared to have occurred on the vertical faces.

To minimise the effect of agitation, specimens for plating were clamped vertically in a jig and wherever possible plating was carried out in the four litre container. This kept agitation effects to a minimum.

Agitation was noticed to have a significant effect on codeposition as particle size was varied. As particle size was increased so agitation effects became more noticeable even when samples were clamped rigidly and the larger, four litre container

used. The larger graphite flakes 6 to 10 μm size were much more subject to agitation effects than the 2 μm particle size. To produce uniform deposits of the large flakes it was found necessary to considerably reduce the level of agitation. As graphite has a low density, only a relatively low level of agitation was actually needed to maintain the graphite in solution. Lower levels of agitation could therefore easily be tolerated. Denser chromium particles however, needed a much higher level of agitation.

In conclusion, to produce the most uniform deposits, specimens were required to be clamped vertically and subject to just sufficient agitation, in as large a container as possible, to prevent particles settling out.

Because of these effects it was considered worthwhile to briefly re-examine the alternative methods of agitation. Circulation pumping of the solution with a peristaltic pump was found to be subject to operating problems. The temperatures of the plating solution, 90^{o}C, was found to be too high for the tubes used and caused splitting of these tubes. The use of a plate pumper appeared satisfactory but was again subject to operating problems due to a poor design. Mechanical stirring was found capable of producing deposits but suffered from agitation effects in much the same way as with air agitation. Ultrasonic agitation produced sufficient agitation to suspend the graphite particles but codeposition did not occur. Ultrasonic agitation could not provide suspension of chromium particles.

None of the alternative methods investigated proved to be of any real improvement on the air agitation method. This method was simple and the associated problems realised and generally counteracted. This method was then applied throughout the work. If foaming, caused by the addition of surfactants, had been more of a problem then the most realistic alternative would have been a more suitably designed plate pumper system.

6.4.2 Concentration of Particles in Solution.

The effect of increasing particle concentration in solution was investigated for solutions containing both graphite and chromium particles. The results of increasing graphite content for two different sizes of graphite particles, 2 and 6 µm, are shown in table 8 and figure 41.

The results show that the volume of graphite incorporated, under standard conditions, for both 2 and 6 µm particles, increased with bath content. The overall volume per cent codeposited for 2 µm graphite powder, was higher, than for 6 µm particle size. For 2 µm particle size, the volume per cent codeposition increased fairly rapidly with the increase in concentration of graphite in solution up to 30 g/l.

Table 8. The Effect of Graphite Concentration in Solution on the Volume per cent Codeposited

Concentration of graphite in solution g/l	Volume per cent of graphite codeposited	
	2 micron	6 micron
5	1.7	1.5
10	3.5	2.9
15	4.2	3.4
20	4.6	4.1
30	5.9	4.5
40	6.3	4.3
50	6.6	-
60	6.7	-

Plating conditions : 90°C, pH 5.0

With a further increase the volume codeposited began to level off until a saturation point was reached at 60g/l with 6.7 volume per cent beyond which no further increase in the volume codeposited occurred. For 6 μm particle size, an increase in the volume per cent codeposited occurred up to 20g/l giving a maximum of 4.5 volume per cent. Beyond 20g/l saturation occurred and no further significant increase was observed. Figures 42a-f show photomicrographs illustrating the effect of concentration of graphite in solution and the volume per cent codeposited.

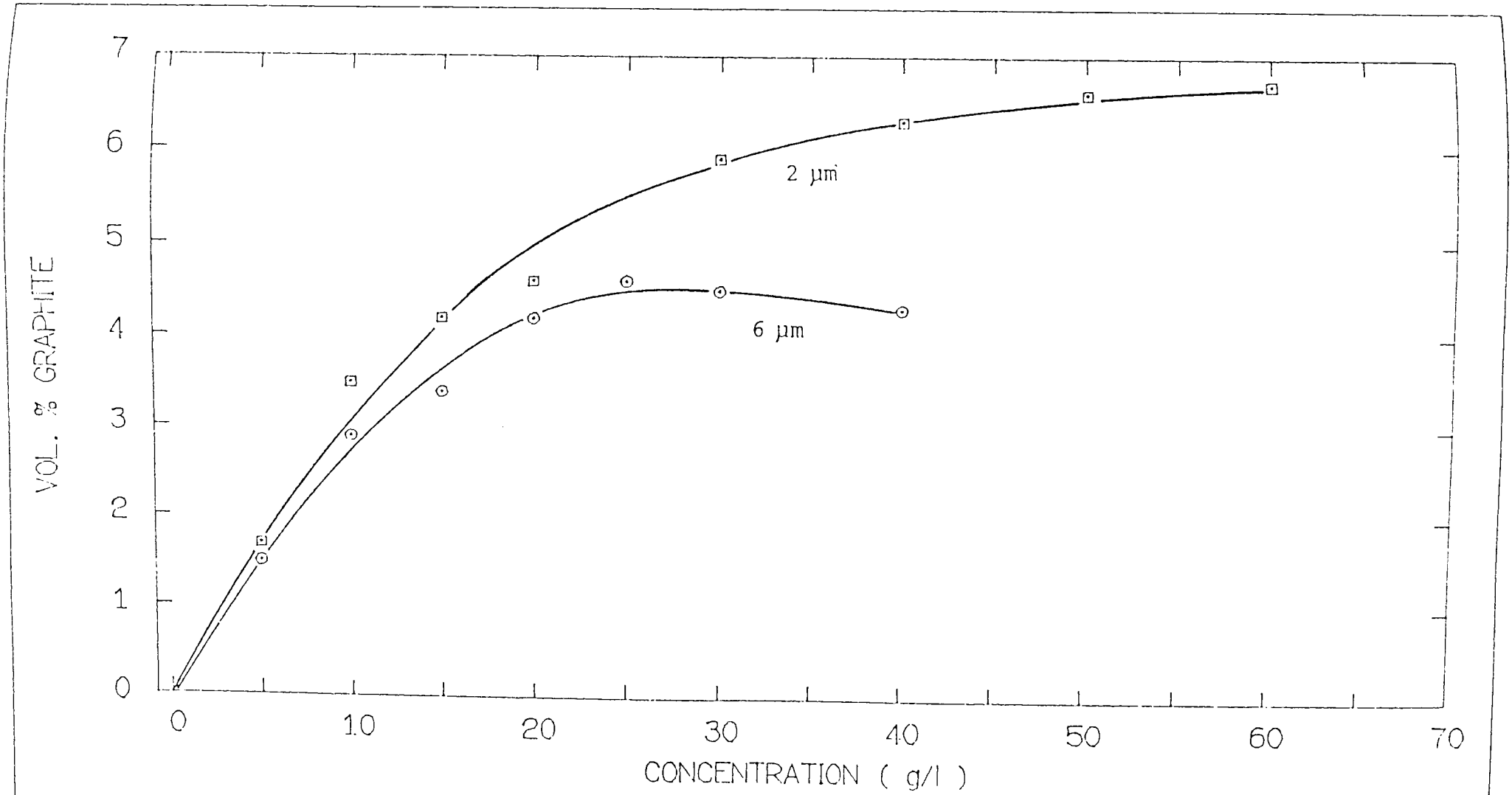

Figure 41. The effect of increasing concentration of graphite in solution on the volume per cent codeposited for 2 and 6 µm nominal particle size. Plating conditions 90°C, pH 5.0

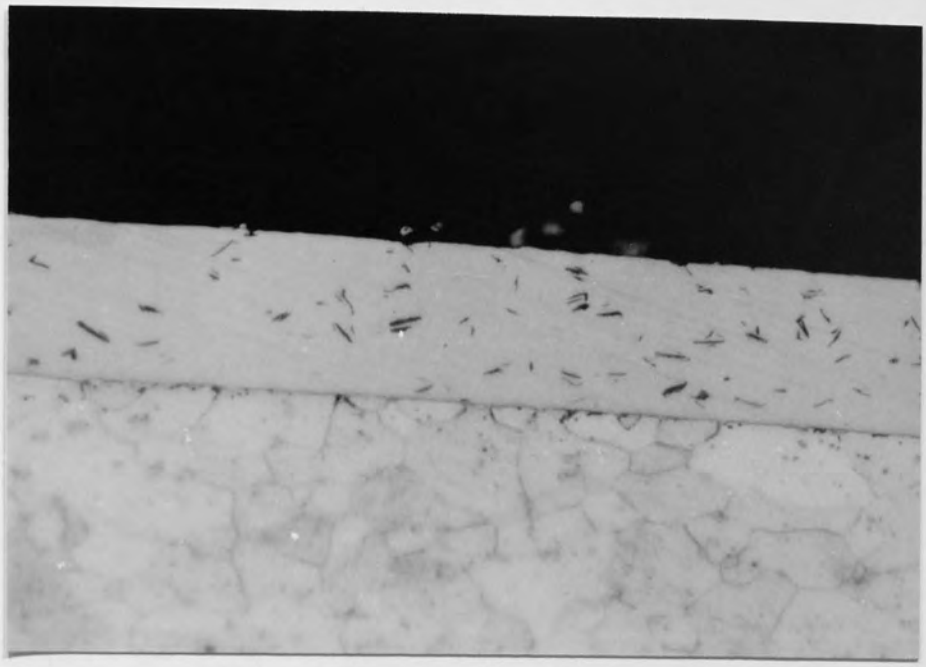

Figure 42a. Electroless nickel plus 5 g/l graphite, 90°C pH 5 (1.7 vol. % graphite) x880

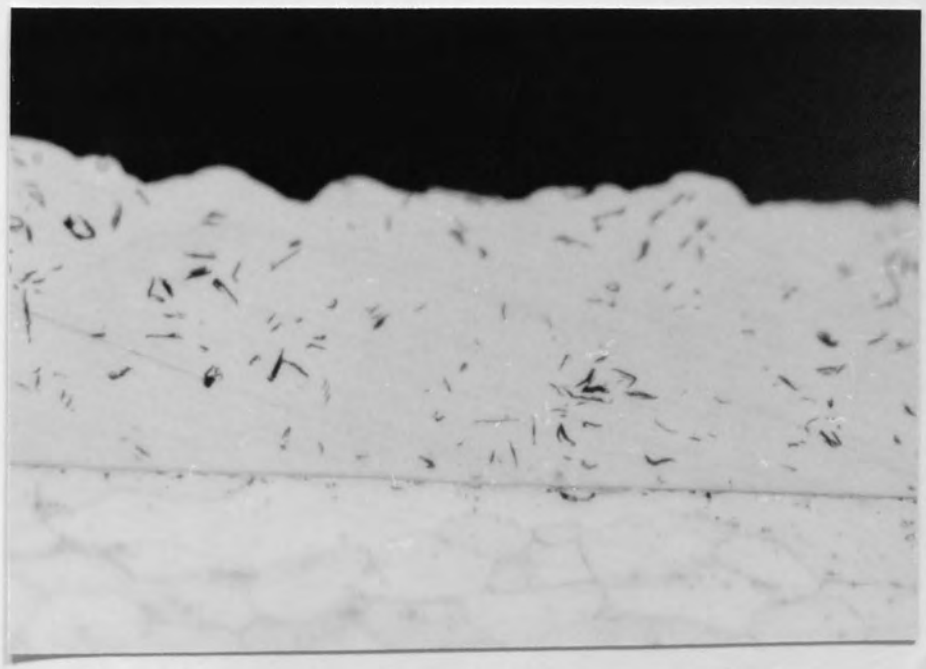

Figure 42b. Electroless nickel plus 10 g/l graphite, 90°C pH 5 (3.5 vol. % graphite) x880

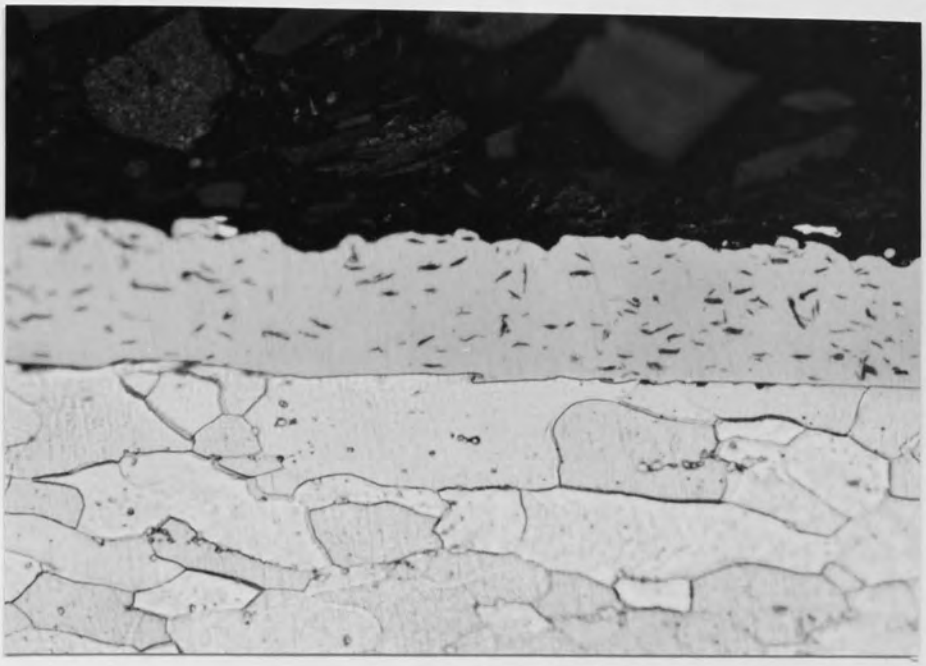

Figure 42c. Electroless nickel plus 15 g/l graphite, 90°C pH 5
(4.2 vol. % graphite) x880

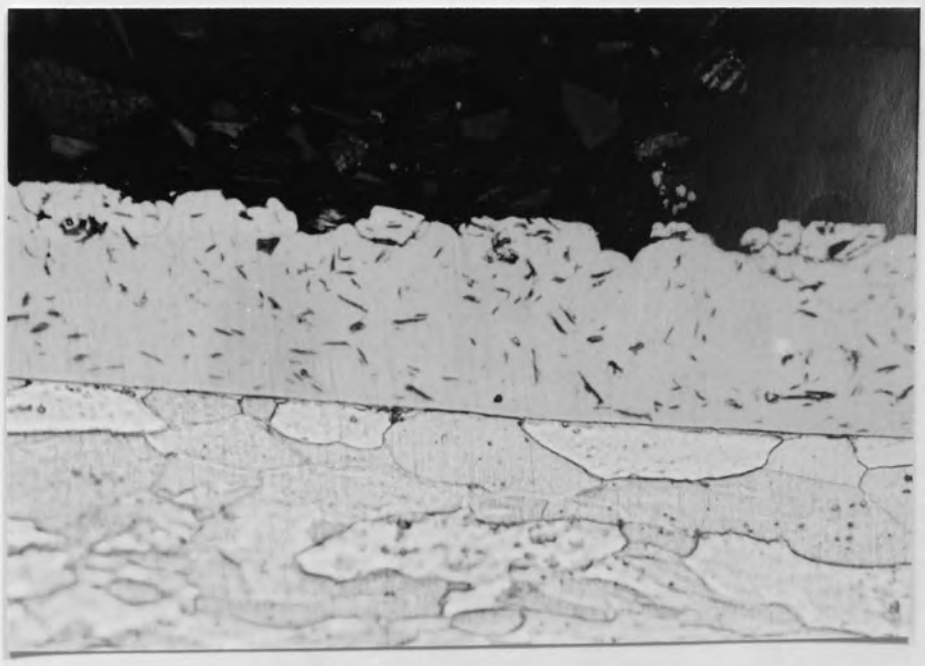

Figure 42d. Electroless nickel plus 20 g/l graphite, 90°C pH 5
(4.6 vol. % graphite) x880

Figure 42e. Electroless nickel plus 30 g/l graphite, 90°C pH 5 (5.9 vol. % graphite) x880

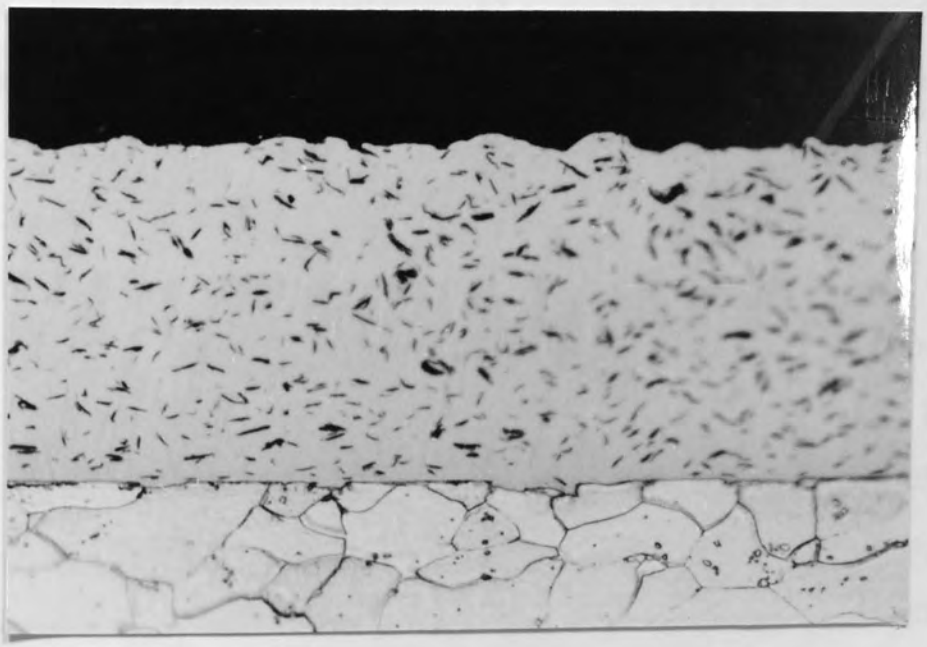

Figure 42f. Electroless nickel plus 40 g/l graphite, 90°C pH 5 (6.3 vol. % graphite) x880

The curves in figure 41 are typical adsorption isotherms for the adsorption of graphite particles onto the electroless nickel surface at a particular temperature. Figure 43 shows the isotherm plotted according to the Langmuir relationship:

$$C/\alpha = C + 1/k \qquad (53)$$

where the concentration in solution is C, α is the amount of graphite codeposited and k is a constant dependent on temperature. A straight line relationship appears to hold indicating adsorption according to the Langmuir relationship.

A study of the plating surface in the very first stages of codeposition showed some of the adsorption characteristics of the graphite flakes. Figure 44 shows the adsorption of graphite flakes onto the surface in the first 30 seconds of plating. These pictures show that initial adsorption of particles to the surface appears to have been very rapid. It can also be seen that the majority of the particles tended to adsorb onto the surface with the edge of the flake, with few particles lying flat to the surface.

The results for increasing the concentration of chromium particles in solution are shown in Table 9 and Figure 45, which also illustrate the effect of increasing solution temperature on the volume per cent codeposited. Deposits produced from increasing the particle concentration of the solution are also shown in photomicrographs, Figure 46a-d.

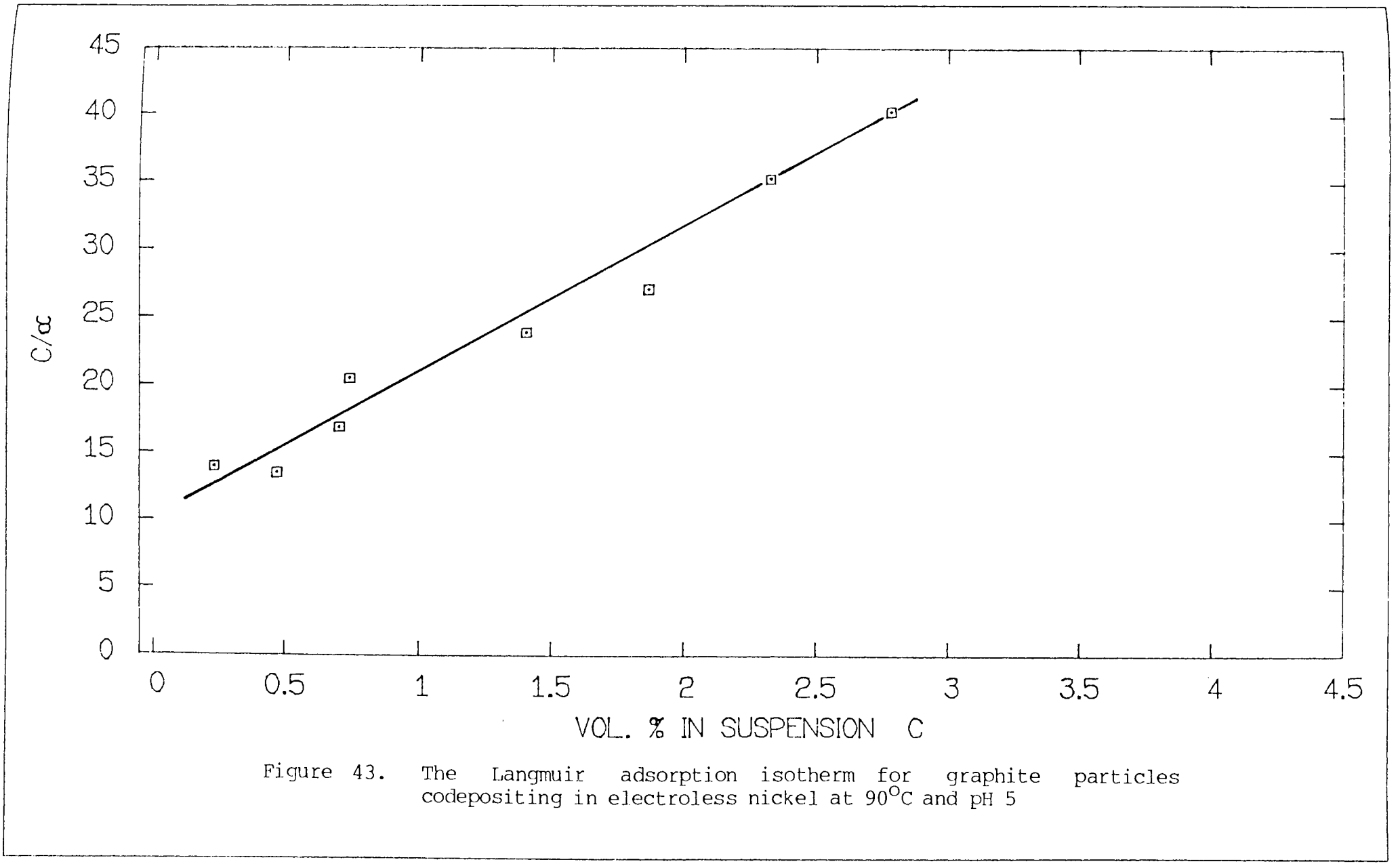

Figure 43. The Langmuir adsorption isotherm for graphite particles codepositing in electroless nickel at 90°C and pH 5

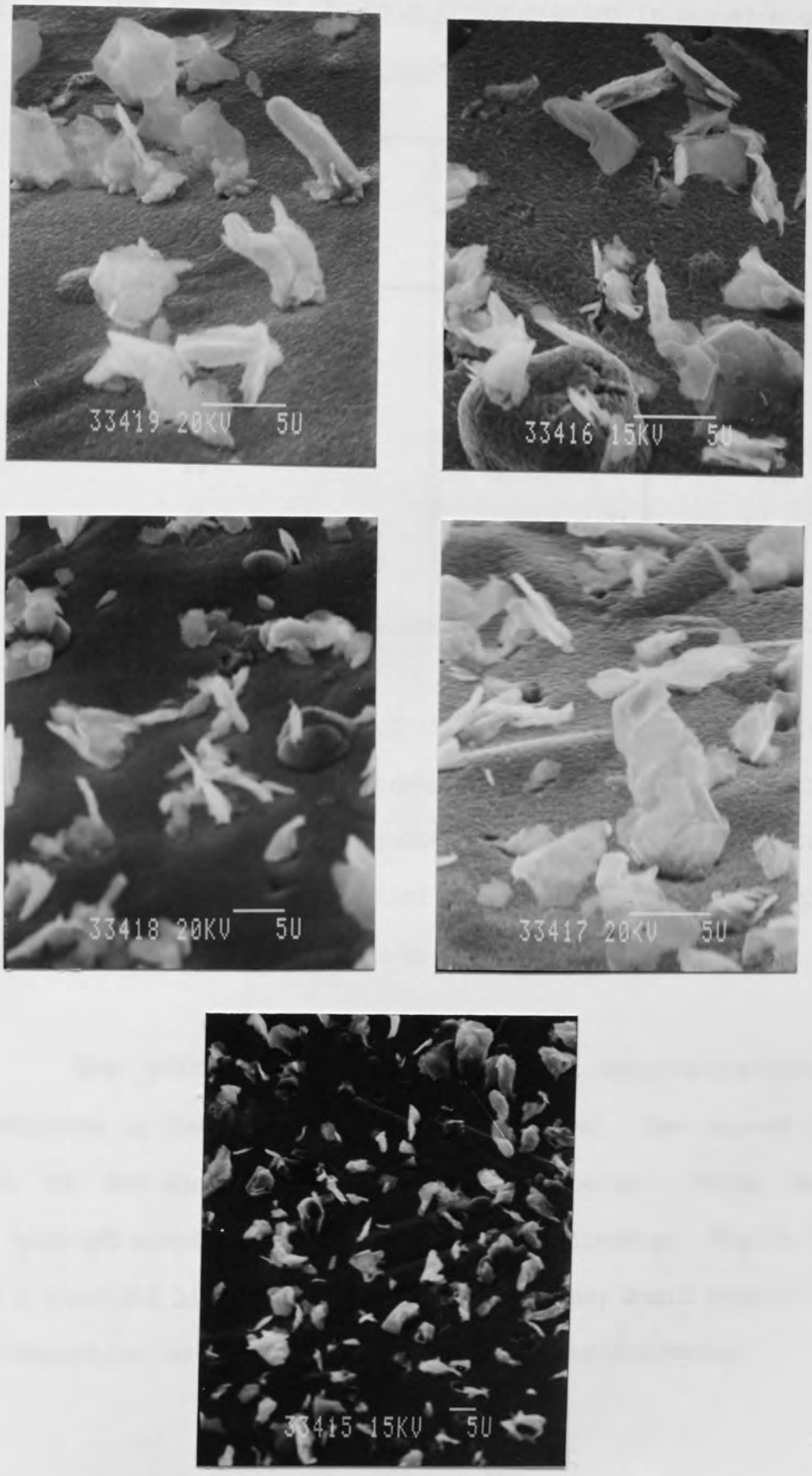

Figure 44. The adsorption of graphite flakes onto the surface during the first 30 seconds of plating from an electrolesss nickel-graphite solution.

Table 9. The Effect of Chromium Concentration in Solution on the Volume per cent Codeposited

Concentration in solution g/l	Volume per cent chromium	
	85°C	90°C
3	3.4	3.2
6	6.3	6.2
12	10.6	9.3
18	15.0	14.6
24	16.5	15.2

The volume per cent of chromium particles codeposited was seen to increase with the concentration in solution. The volume per cent codeposited increased to a maximum of 16.5 volume per cent at 24 g/l, much higher levels of codeposition than compared to graphite with 6.7 volume per cent at 60 g/l.

The effect of increasing solution temperature caused a reduction in the volume per cent codeposited. The curves in figure 45 are again typical adsorption isotherms. These were also plotted according to the Langmuir relationship, Figure 47, where a straight line relationship is also seen, again suggesting that adsorption is according to the Langmuir relationship.

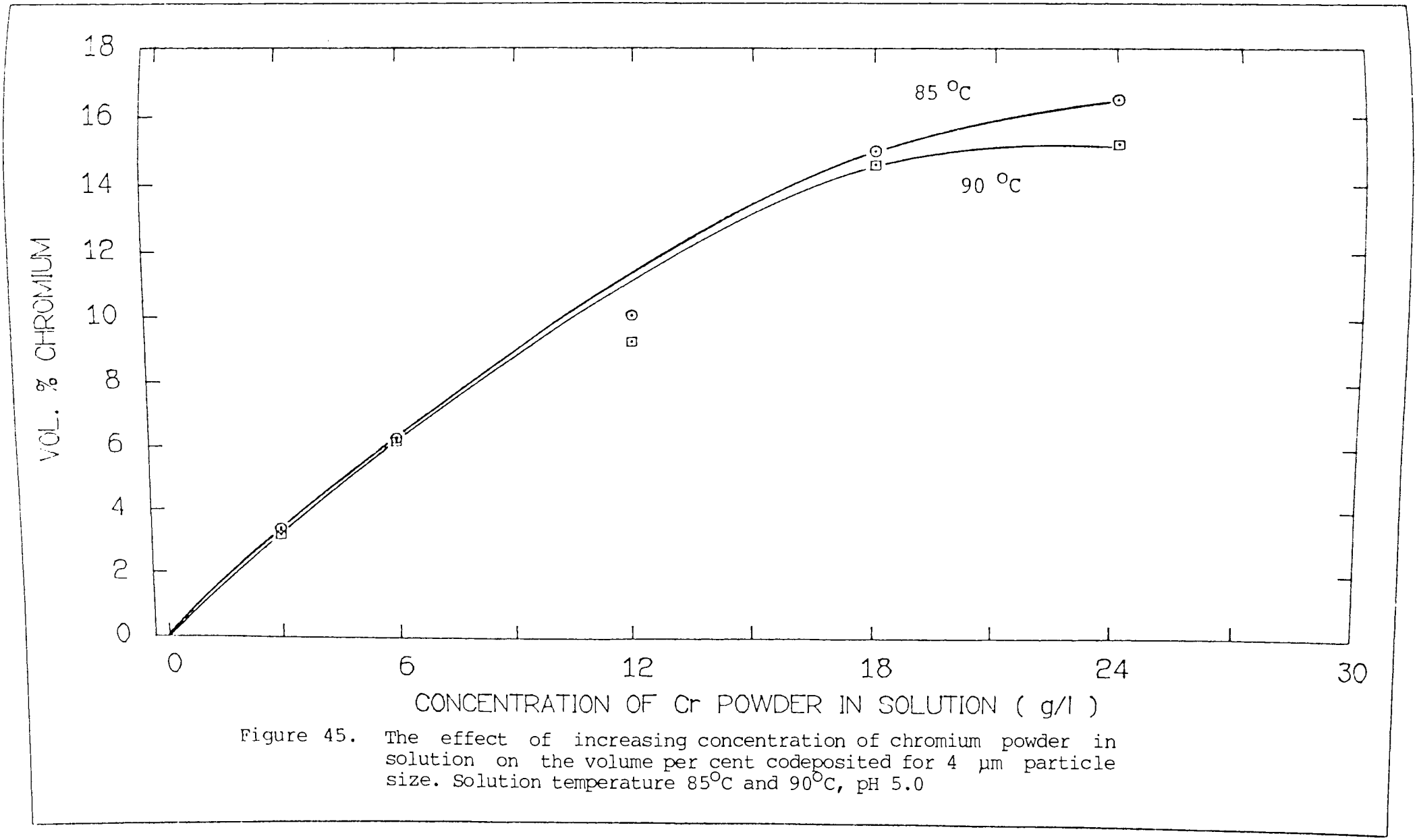

Figure 45. The effect of increasing concentration of chromium powder in solution on the volume per cent codeposited for 4 μm particle size. Solution temperature 85°C and 90°C, pH 5.0

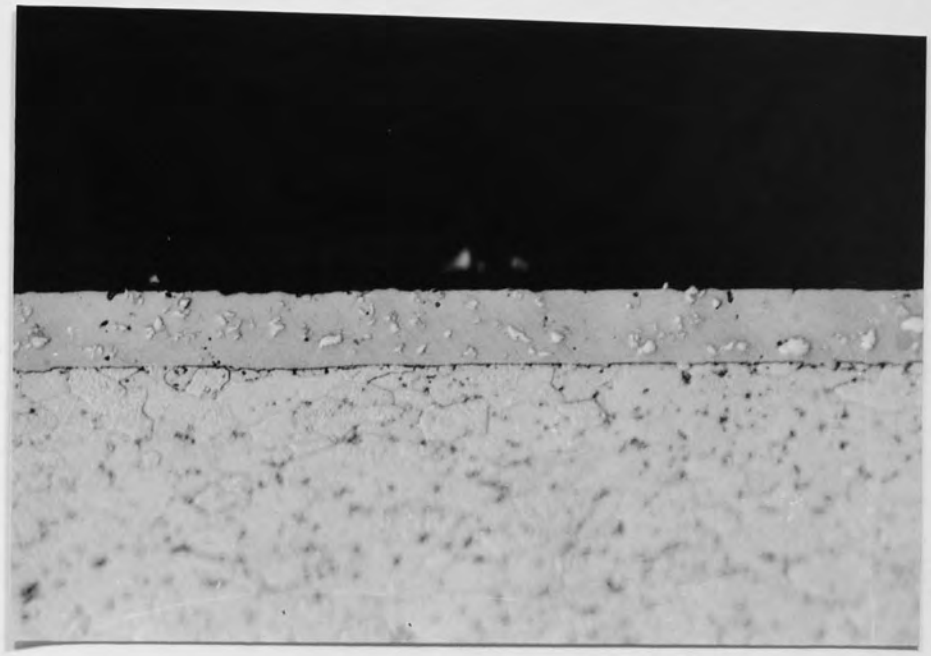

Figure 46a. Electroless nickel plus 6 g/l chromium, 90°C pH 5 (6.3 vol. % chromium) x880

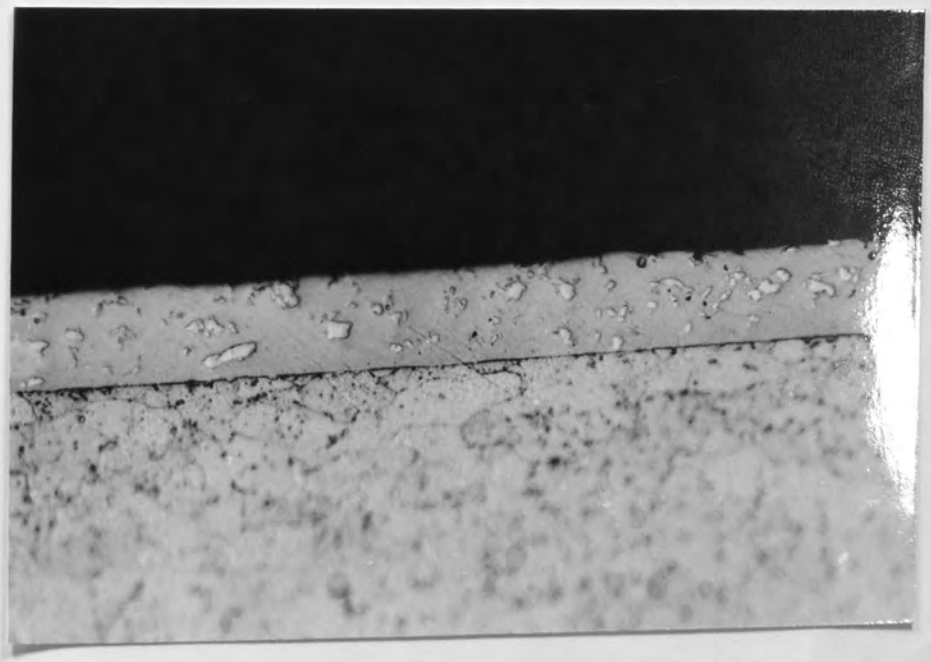

Figure 46b. Electroless nickel plus 12 g/l chromium, 90°C pH 5 (9.3 vol. % chromium) x880

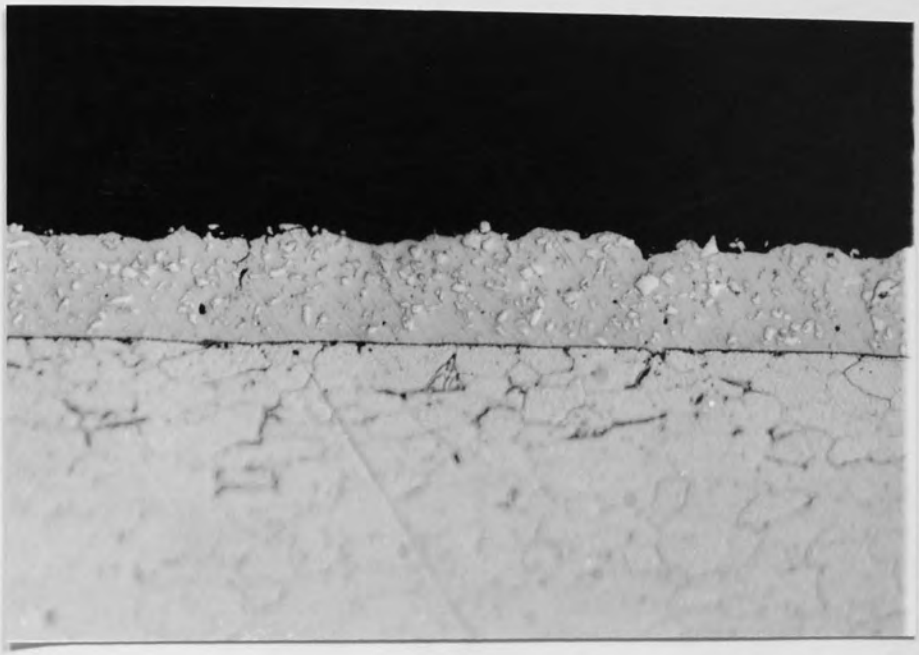

Figure 46c. Electroless nickel plus 18 g/l chromium, 90°C pH 5 (14.6 vol. % chromium) x880

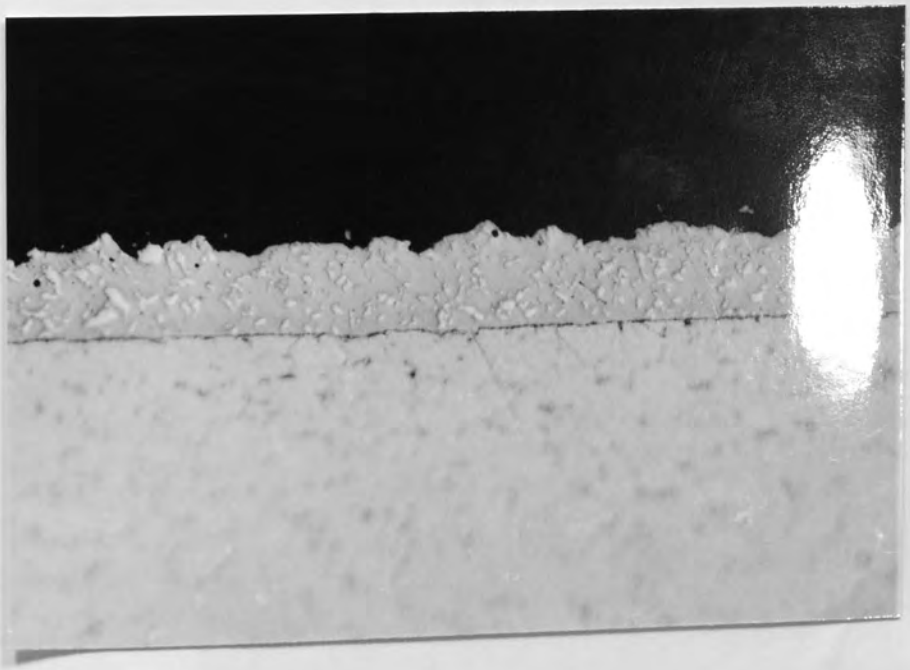

Figure 46d. Electroless nickel plus 24 g/l chromium, 90°C pH 5 (15.2 vol. % chromium) x880

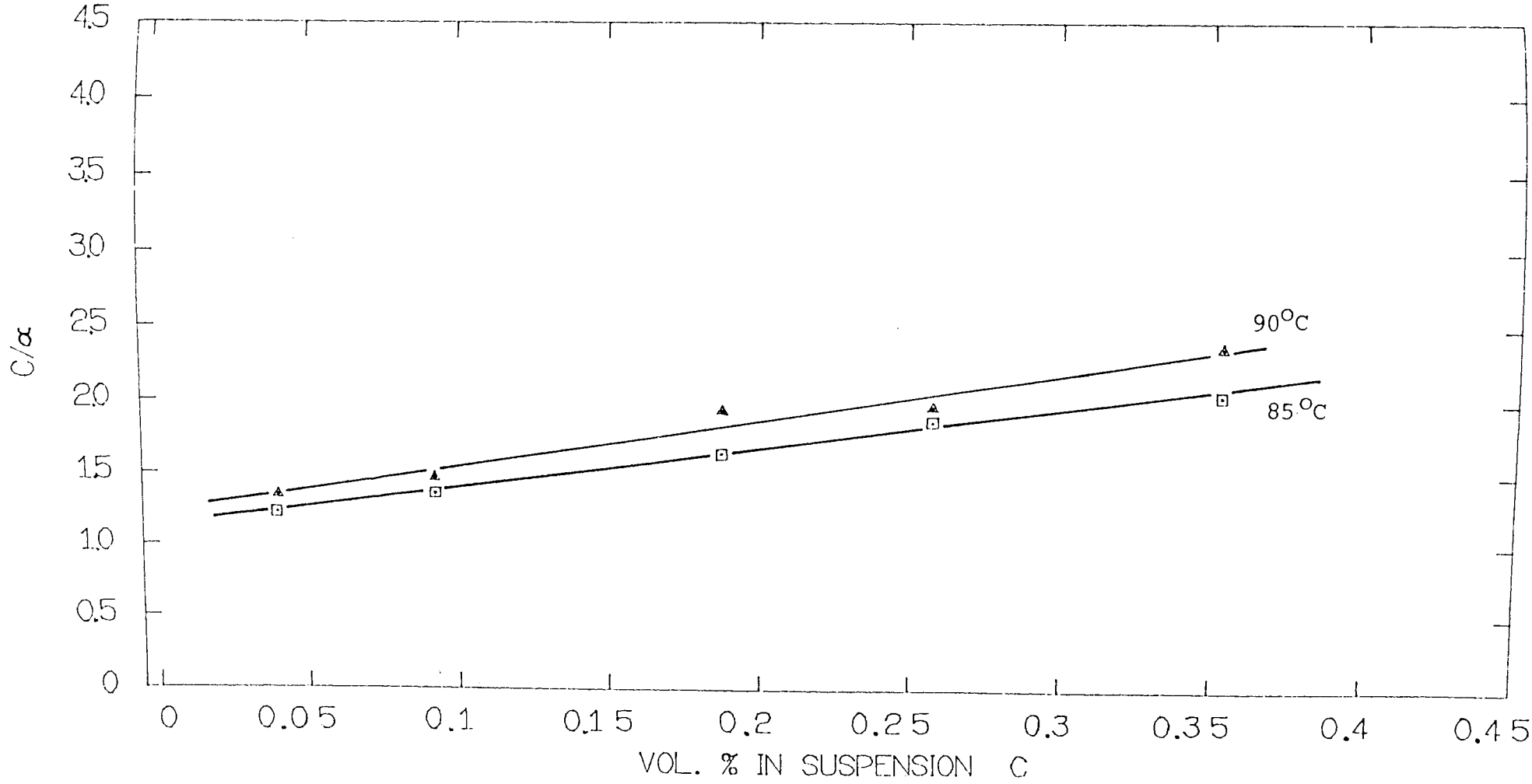

Figure 47. The Langmuir adsorption isotherm for chromium particles codepositing in electroless nickel at 85°C, 90°C and pH 5

6.4.3 Plating Rate

The effect of change in temperature and pH of the plating solution on the plating rate and particle content of the deposit is shown in table 10. The separate influences of temperature and pH are shown in figure 48, and the overall relationship with plating rate is shown in figure 49.

Table 10. The Effect of pH and Temperature on Plating Rate and Particle Incorporation.

Temperature		pH			
		4.0	4.5	5.0	6.0
75°C	Plating rate µm/hour	-	8.0	13.0	15.4
	Vol % graphite	-	2.8	4.5	5.2
80°C	Plating rate µm/hour	-	10.8	15.0	17.6
	Vol % graphite	-	3.4	4.7	5.5
85°C	Plating rate µm/hour	5.9	14.5	17.5	19.3
	Vol % graphite	2.8	3.6	5.0	5.5
90°C	Plating rate µm/hour	7.75	17.8	20.0	23.1
	Vol % graphite	2.9	4.3	5.2	5.7

Concentration in solution, 25 g/l of 2 micron particle size.

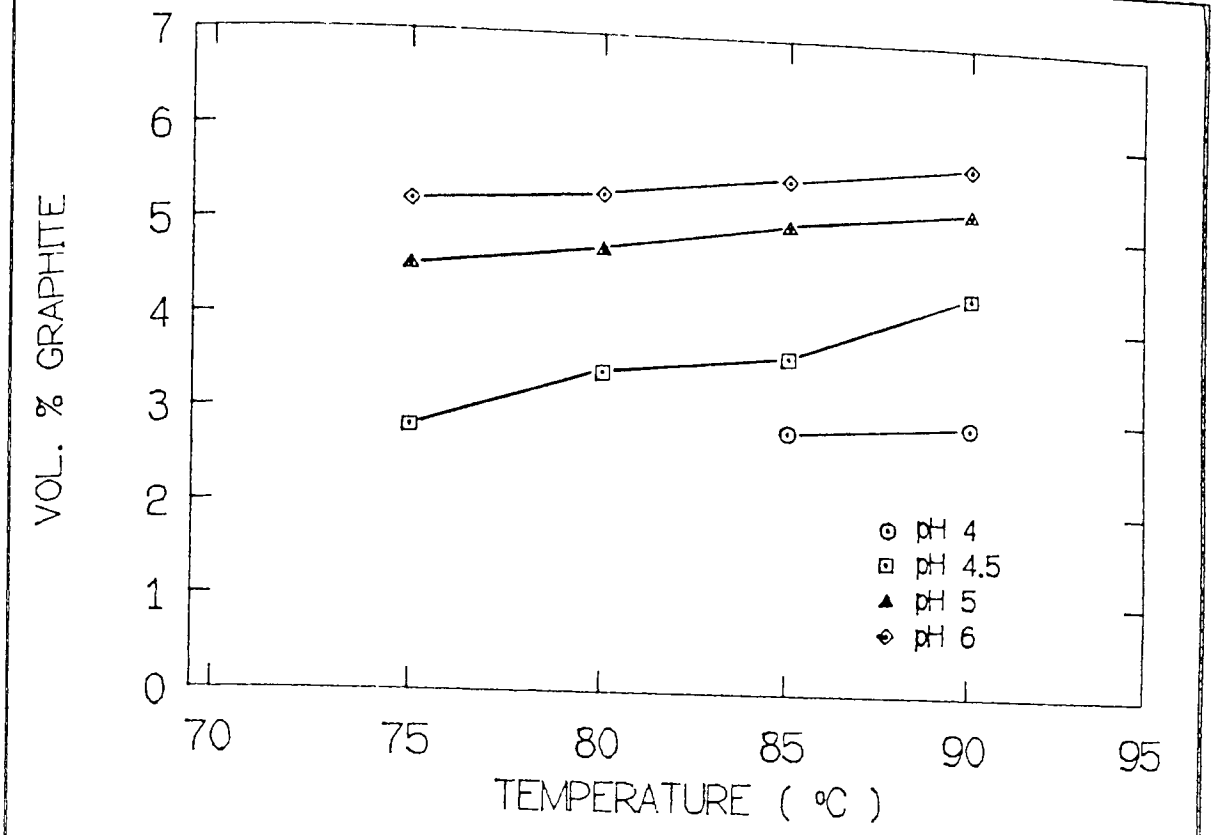

Figure 48. The effect of increasing temperature and pH on the volume per cent graphite codeposited, 25g/l graphite in solution, nominal particle size 2 µm

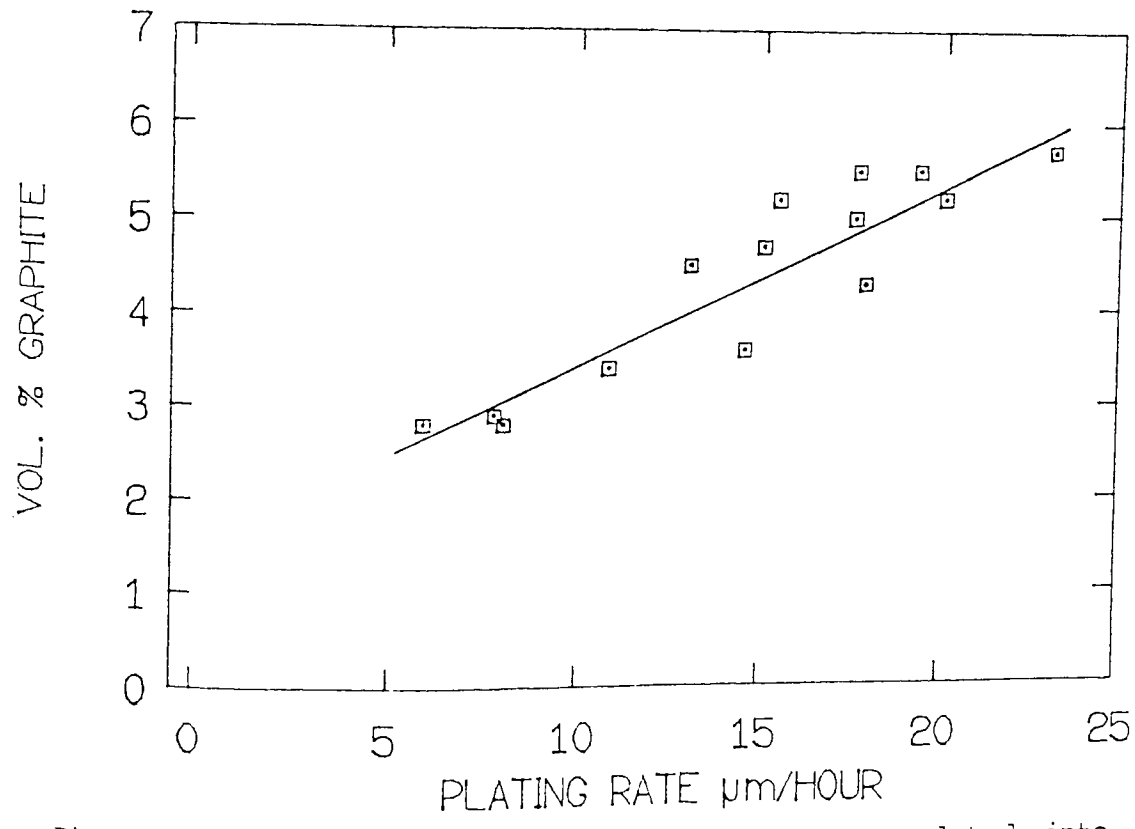

Figure 49. The effect of temperature and pH translated into plating rate and the effect on the volume per cent graphite codeposited, 25g/l graphite in solution, nominal particle size 2 µm

The results show that as expected plating rate increased with temperature and pH. Rather unexpectedly however, particle content also increased with increasing temperature and pH, and by implication plating rate. The highest volume per cent of graphite codeposited was found at the highest levels of pH and temperature and hence plating rate, 5.7 volume per cent at pH 6.0 and 90^{o}C as compared to 2.8 volume per cent at pH 4.5 and 75^{o}C.

The plating rate of 23 µm/ hour at 90^{o}C and pH 5.0 was in approximate aggreement with the manufacturer's advised plating rate for these conditions. This indicated that the surfactant and stabiliser additions were not of any significant hindrance to the plating process.

In electrolytic and electroless systems the increased plating rate has been shown to have increased metal deposition rate beyond that of the particle arrival rate, thus producing lower volume per cent codeposited[161]. Also, in the electroless system, increased hydrogen liberation with plating rate is considered to hinder particle adsorption. Hence, the unexpected result of increased codeposition of graphite with plating rate. In the case of electroless nickel-chromium codeposition however, it can be seen from figure 45 that an increase in temperature and plating rate produced a decrease in chromium particles codeposited, as expected from the literature, at 24g/l the volume per cent decreased from 16.5 % to 15.2 % as the temperature was raised from 85^{o}C to 90^{o}C and hence plating rate from 17.5 to 20 micron per hour.

6.4.4 Particle Size

The effect of decreasing graphite particle size on the volume per cent codeposited is shown in table 11 and figure 50. Examples of deposits illustrating codeposition of different particle size are shown in figures 51 a and b.

Table 11. The Effect of Particle Size on Codeposition

Particle Size Microns	Number of Particles per 1000 μm^2	Volume Per Cent Graphite
20	0	0.0
10	205	4.58
6	225	4.9
4	250	4.95
2	347	5.74
1	625	11.05
0.75	0	0.0

Plated at pH 5.00, 90^0C with 25g/l of the varying particle sizes.

As particle size was reduced so the number of particles and hence volume per cent codeposited increased, significantly at 1 µm particle size, reaching a maximum of 11.05 volume per cent. Below 1 µm and 10 µm particle size it was found that no codeposition of graphite occurred.

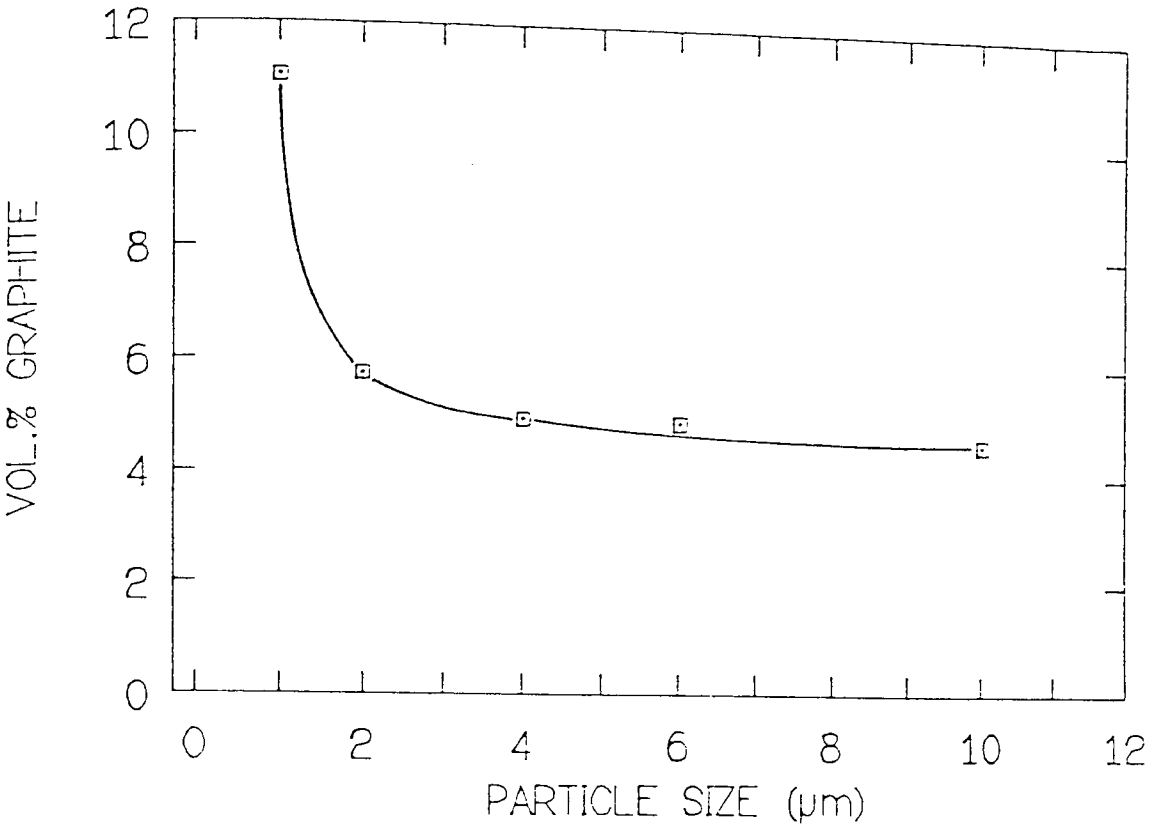

Figure 50. The effect of particle size on the volume per cent graphite codeposited.(25 g/l graphite,90 oC, pH 5.)

Factors such as agitation and surfactants were considered as possible causes for these cut off points, however, codeposition beyond 1 and 10 μm could not be induced by a variation in these factors.

Only one particle size for chromium powder was available. No experiments on the effect of chromium particle size could therefore be carried out. Attempts were made to ball mill crushed ingot material, however this proved too difficult with the facilities available.

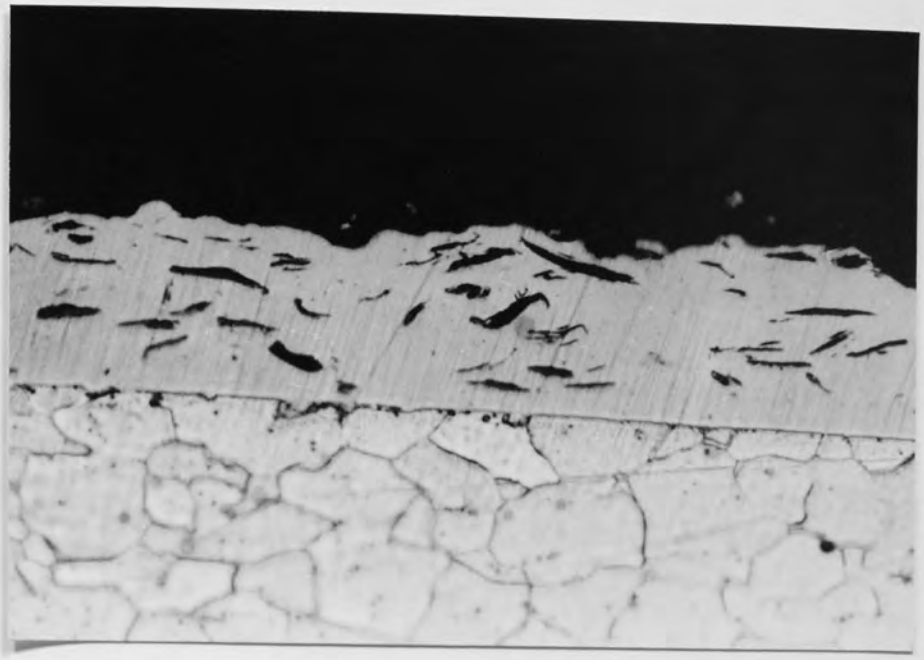

Figure 51a. Electroless nickel plus 10 µm graphite particles (4.58 vol. % graphite) x880

Figure 51b. Electroless nickel plus 2 µm graphite particles (5.74 vol. % graphite) x880

6.5 HEAT TREATMENT

6.5.1 Heat Treatment of Electroless Nickel

The heat treatment of electroless nickel deposits was carried out as a standard, and to confirm the correct heat treatment of the matrix material. The hardnesses, resulting from heat treating deposits with constant phosphorous content (8.4% P) for one hour over a temperature range from 100-800°C, are shown in figure 52.

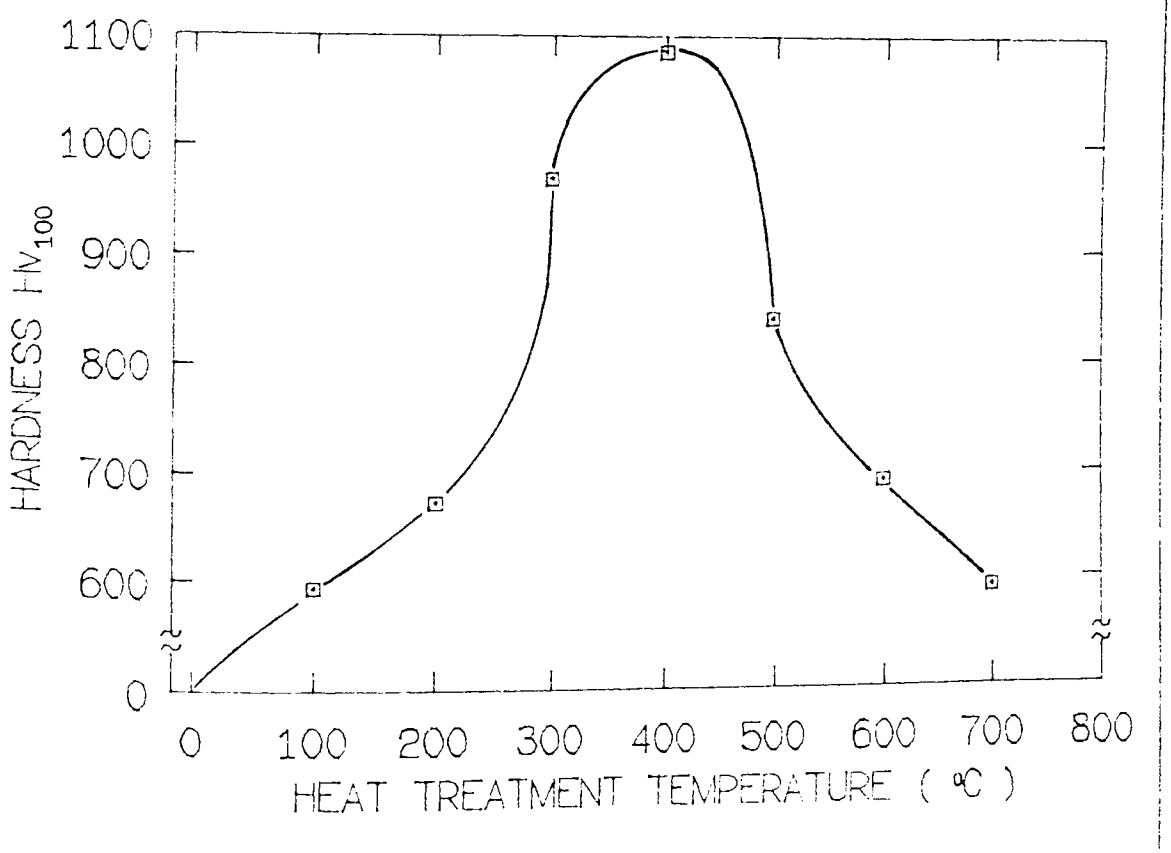

Figure 52. The variation in hardness with heat treatment temperature (8.4% phosphorus)

6.5.2. Heat Treatment of Electroless Nickel-Graphite Composite Coatings

Electroless nickel-graphite deposits, with increasing graphite volume per cent, were given a standard electroless nickel heat treatment and compared for micro-hardness against as-deposited electroless nickel-graphite deposits with a similar graphite content. Table 12 and Figure 53 illustrate these results.

Table 12. The Effect of Graphite Content on Hardness of Electroless Nickel-Graphite Composite Coatings

Volume % Graphite	Hardness Hv_{100}	
	As-Plated	Heat Treated
0.0	515	1075
3.5	495	1009
4.6	483	931
5.9	472	879
6.3	467	862
6.6	464	837

The results show that the hardness of the composite was reduced by the increasing presence of graphite, more significantly in the heat treated condition. Hardness decreased from 1075 Hv_{100} at zero per cent graphite, to 837 Hv_{100} at 6.7 volume per cent graphite in the heat treated condition.

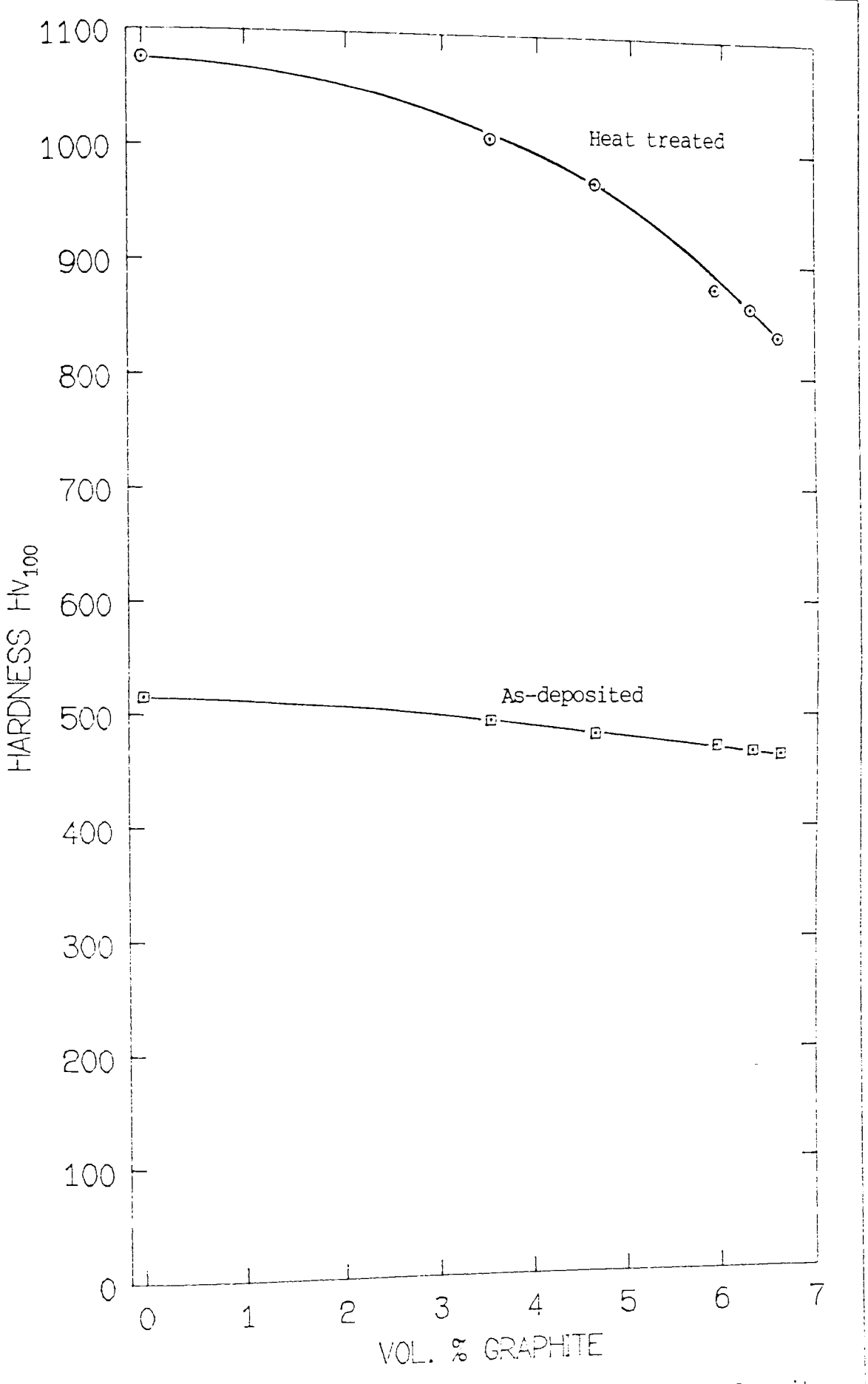

Figure 53. The effect of volume per cent graphite in the deposit on hardness. Phosphorus 8.3%, nominal particle size 2 µm

6.5.3. Heat Treatment of Electroless Nickel Chromium Composite Coatings

The object of producing electroless nickel-chromium composites, was to investigate the production of alloy coatings by heat treatment and inter-diffusion of the codeposited particles with the matrix material. Deposits were therefore assessed for the effect of inter-diffusion and the resultant effect on deposit hardness after heat treatment.

Deposits containing increasing volume percentages of chromium particles were tested for micro hardness in the as-deposited state, and after standard electroless nickel heat treatment ie. 400°C for one hour. The effect of increasing chromium content on hardness was shown as increasing the as-deposited hardness by 200 Hv_{100} yet decreasing the heat treated hardness by approximately 100 Hv_{100}. Table 13 and figure 54 illustrate this.

Examination by x-ray mapping and EPMA analysis showed that, after heat treatment for 1 hour at 400°C, no detectable inter-diffusion between the chromium and electroless nickel had occurred. Figure 55.

Heat treatment of deposits containing 15% chromium at a temperature of 850°C, for 8 and 16 hours, however, produced much more significant inter-diffusion between the elements.

Table 13. The Hardness of As-Plated and Standard Heat Treated Electroless Nickel-Chromium Composite

Chromium Content Volume per cent	As-Plated Hardness Hv_{100}	Hardness after 1 hr at 400°C. Hv_{100}
0	515	1085
6.2	547	1050
9.3	606	1025
14.6	663	995
15.2	683	986

Phosphorus content 8.7 weight per cent.

Figure 56 illustrates the line profiles produced by EPMA for the inter-diffusion which occurred by heat treatment for 8 hours at 850°C. Figure 57, a to d pictorially illustrates this by x-ray mapping. It can be seen that significant diffusion has occurred between the substrate and the coating, increasing the thickness of the coating from 30 µm to 36 µm. A study of the x-ray maps, show that diffusion has occurred between the nickel and iron from the substrate, with the chromium now distributed approximately throughout the original coating thickness. Phosphorous, originally distributed throughout the coating, had diffused to the surface of the coating and was almost totally distributed in the first 10 µm of the coating. The phosphorus level in this layer increased from 7.8% to 14.9%.

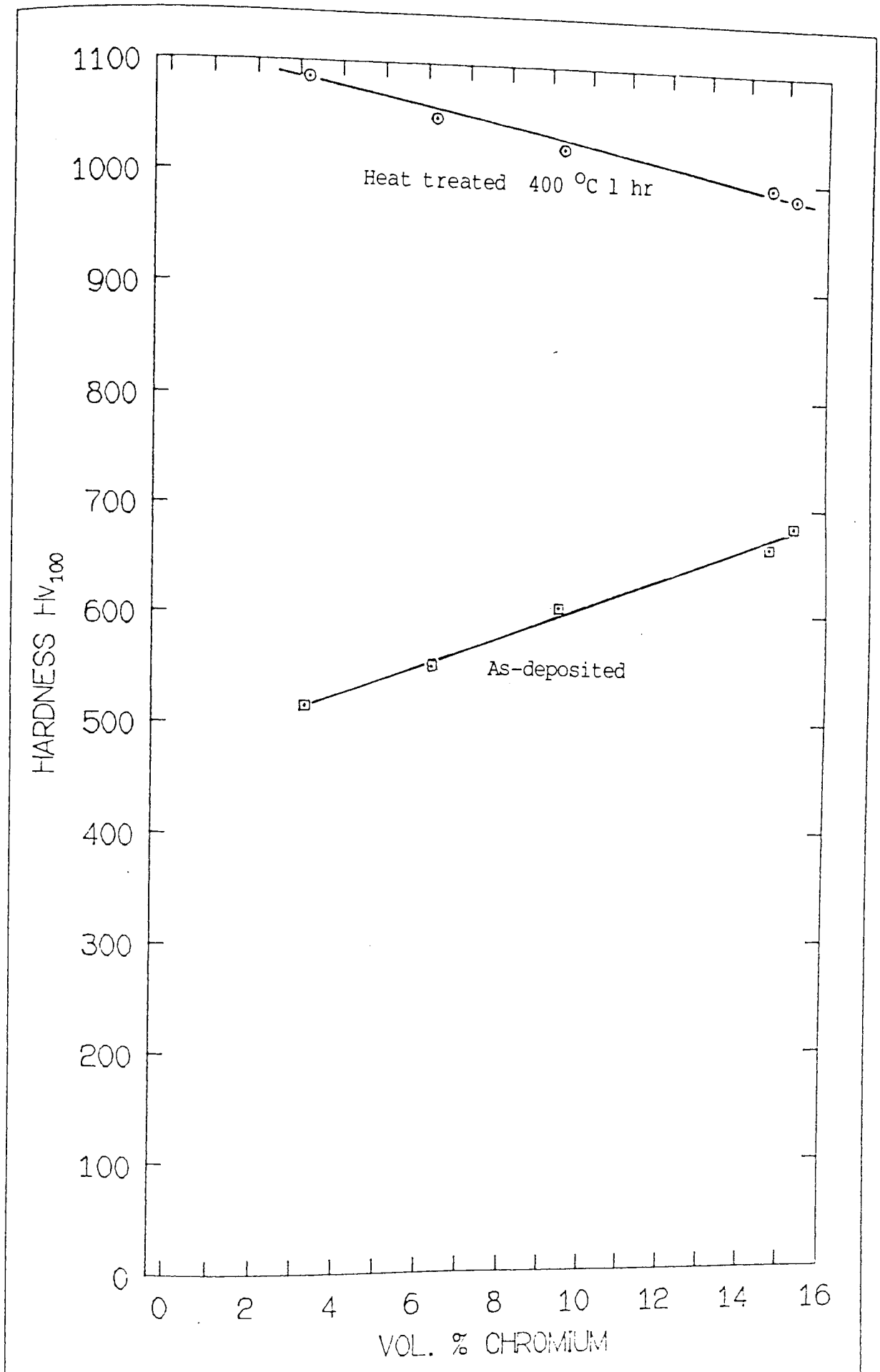

Figure 54. The effect of volume per cent chromium in the deposit on hardness. Phosphorus content 8.4%, nominal particle size 2 μm

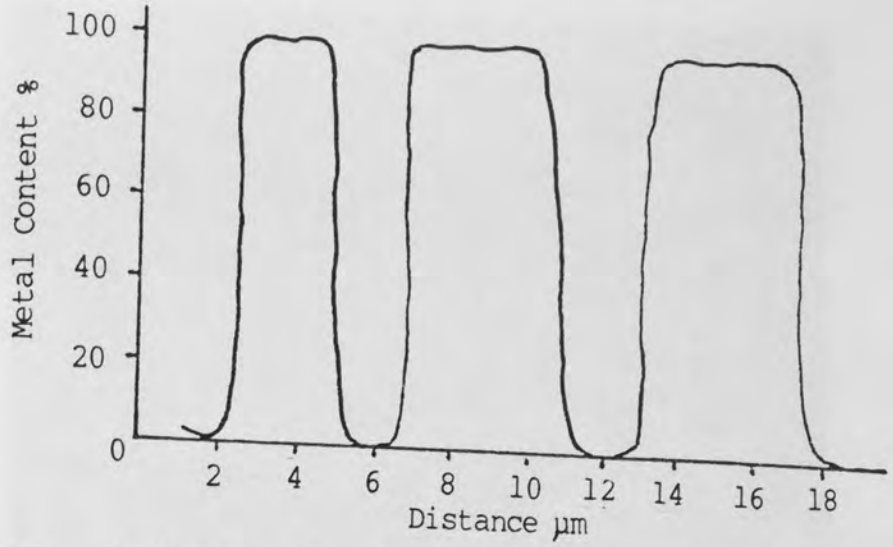

Figure 55a . EPMA trace for chromium after heat treatment for 1 hour at 400°C

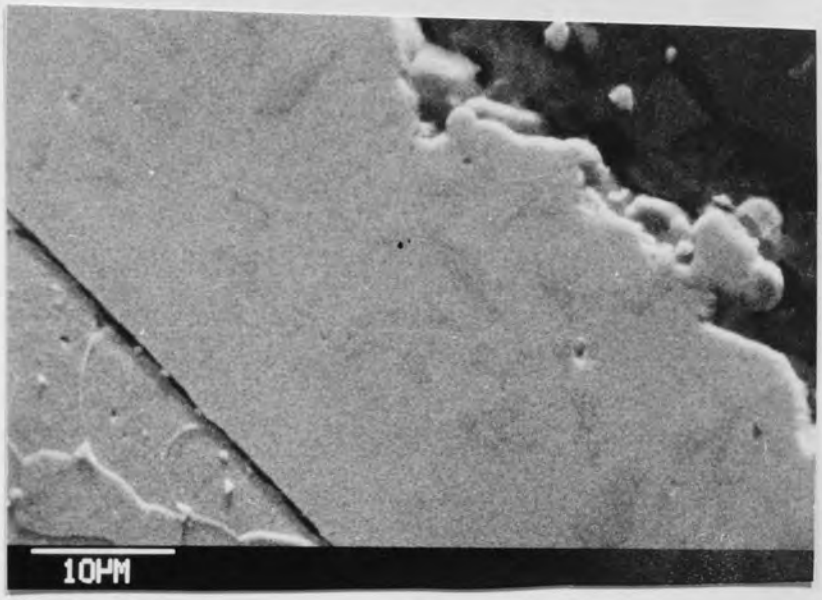

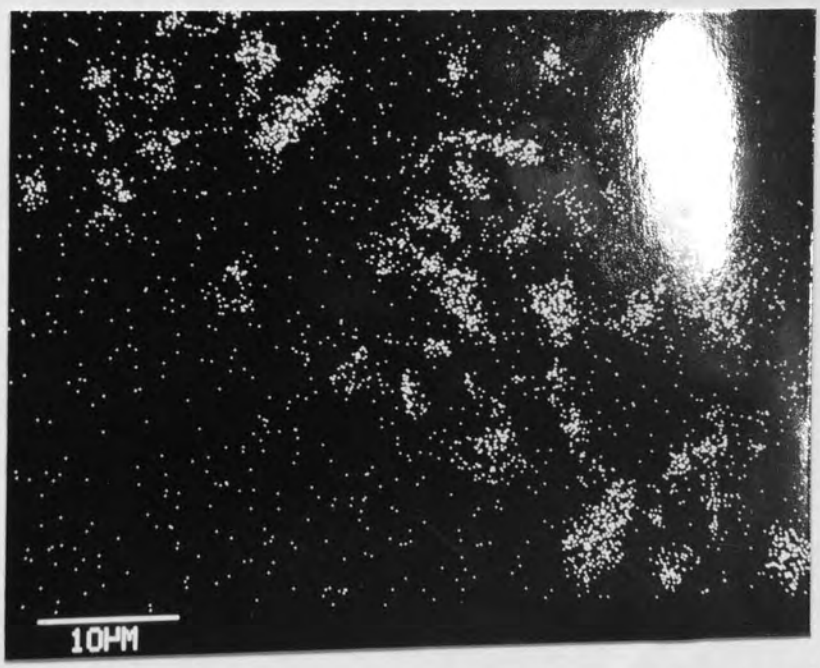

Figure 55b. S.E.M. and X-ray map of electroless nickel-chromium after heat treatment for 1 hour at 400°C

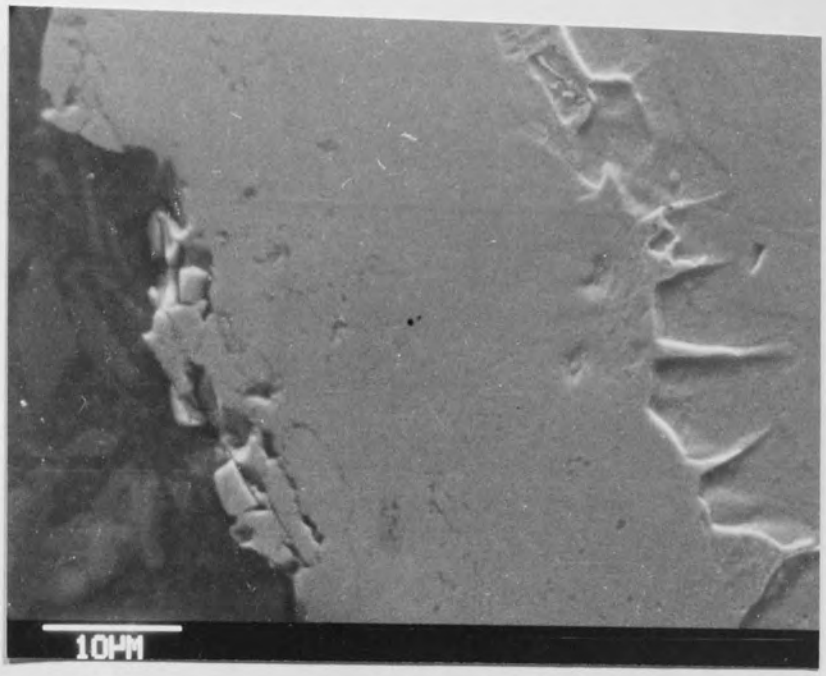

Figure 56a. S.E.M. photograph of electroless nickel-chromium after heat treatment for 8 hours at 850°C

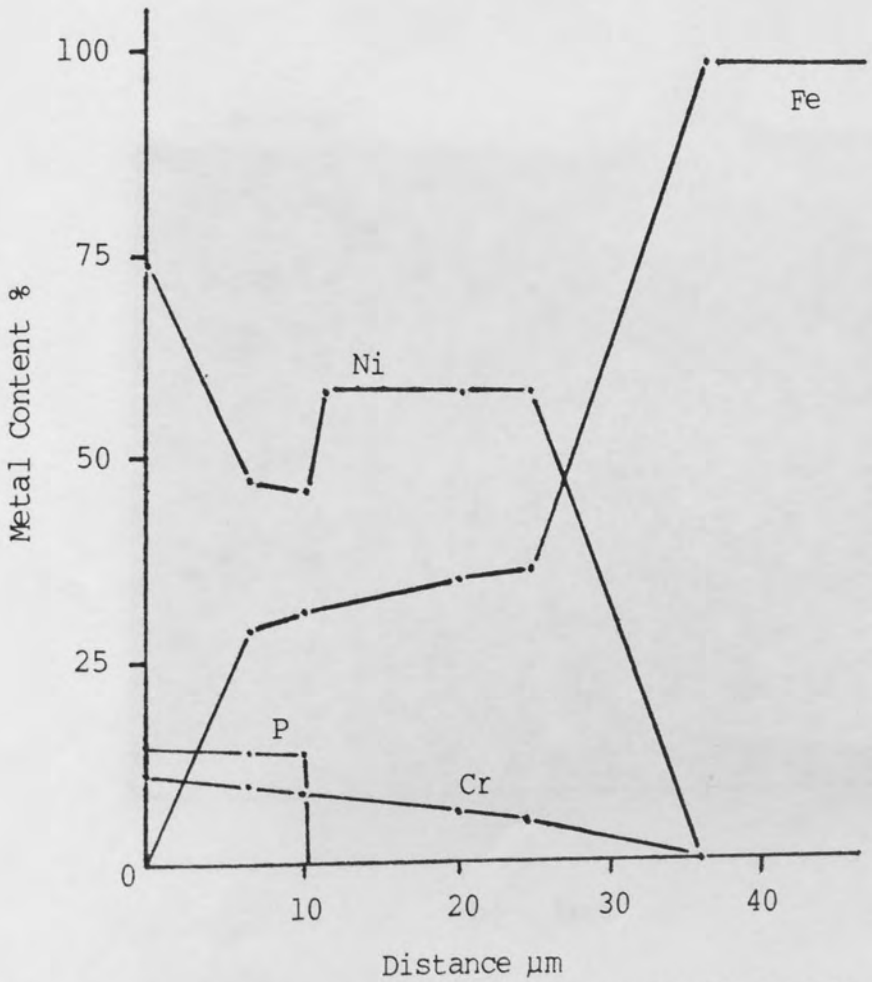

Figure 56b. EPMA trace of electroless nickel-chromium after heat treatment for 8 hours at 850°C

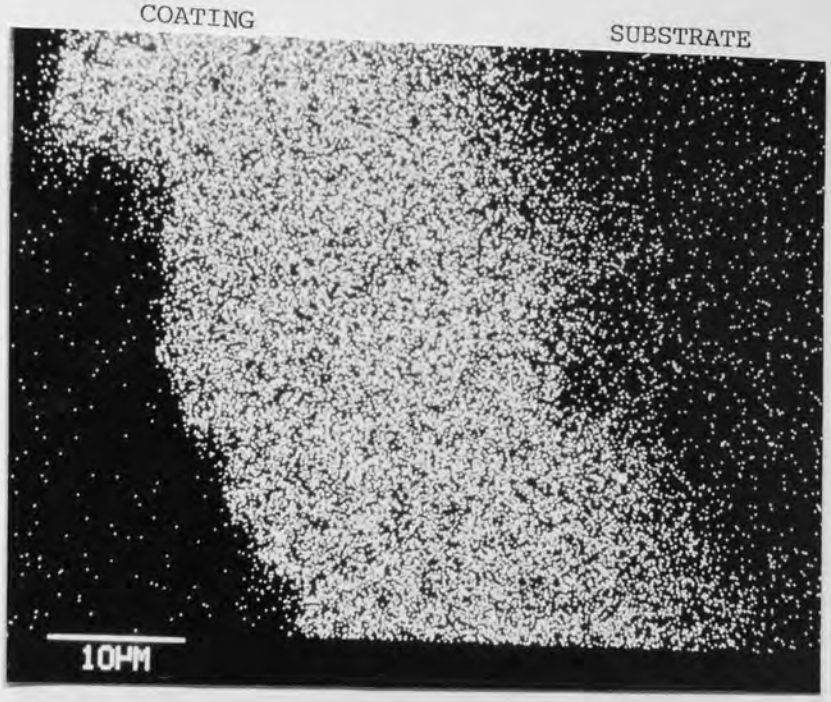

(a) Nickel

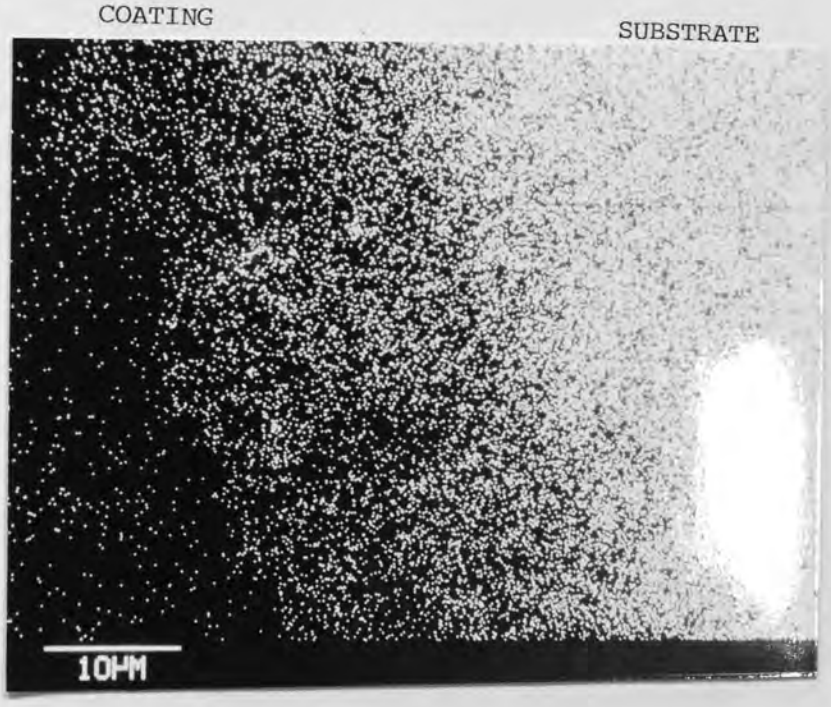

(b) Iron

Figure 57a-b. X-ray maps of electroless nickel after heat treatment for 8 hours at 850°C

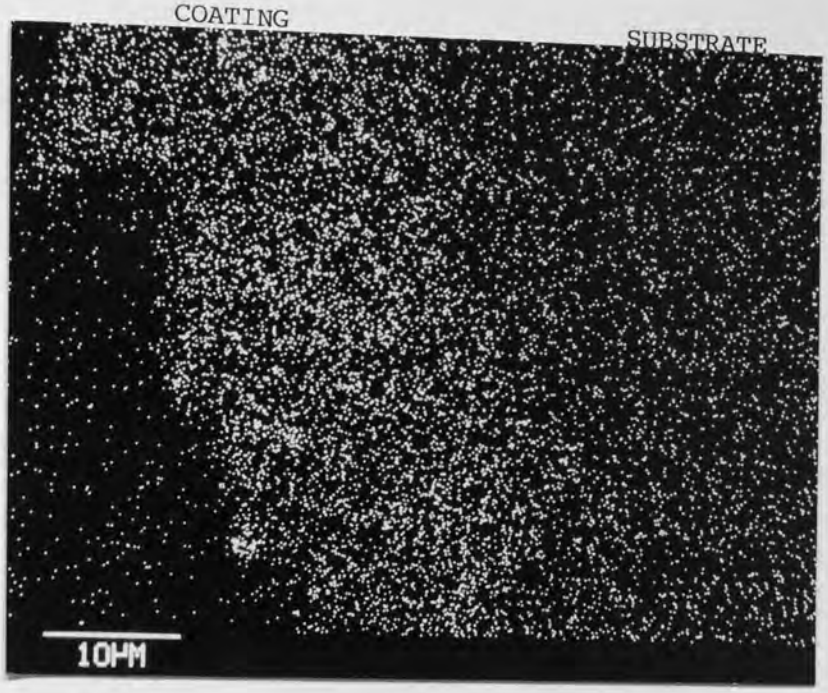

(c) Chromium

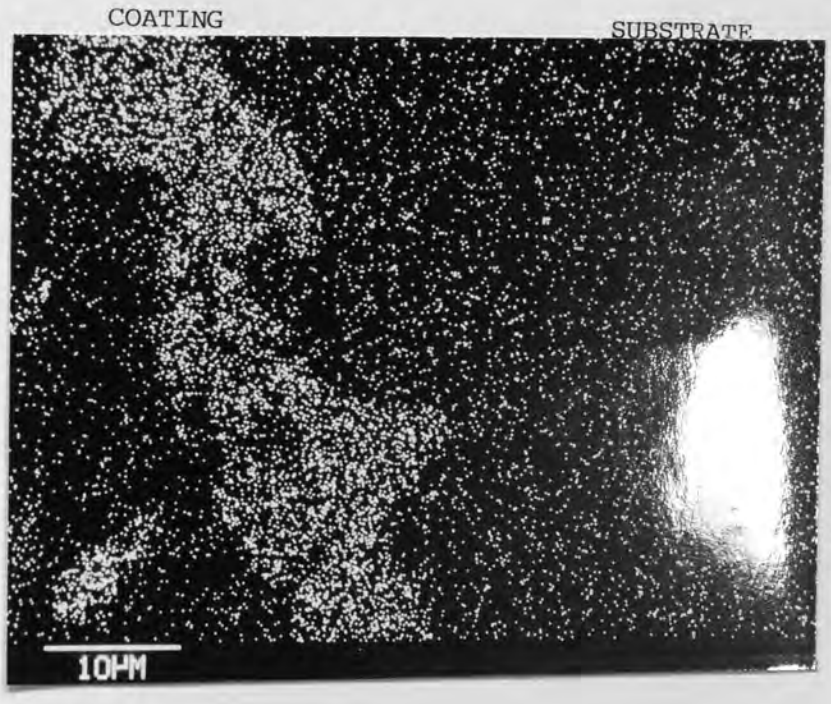

(d) Phosphorus

Figure 57c-d. X-ray maps of electroless nickel-chromium after heat treatment for 8 hours at 850°C

After heat treatment for 16 hours at 850°C, figures 58 a to d and 59, the inter-diffusion had followed a similar pattern, although inter-diffusion between nickel and iron had increased the coating thickness further to 45 μm.

The finger-like pattern of the coating reaching into the substrate would appear to be inter-diffusion and alloying down grain boundaries within the steel substrate.

From figure 58, of a 15% chromium deposit heat treated for 16 hours at 850°C, the coating principally appeared a two phase structure, with a phosphorous rich layer running along the surface and a solid solution of nickel-iron-chromium making up the majority of the coating. However evidence of possibly another phase can be seen in the phosphorus rich surface layer.

Micro-hardness measurements of the deposit showed the surface layer to have a hardness in excess of 1000 Hv_5. These readings were extremely difficult to produce due to the thickness of the layer. Loads of 5 g were required to produce readings from the deposit. The layer of nickel-iron-chromium alloy produced low hardnesses of 220 Hv_{100}.

6.6 INTERNAL STRESS

The effect of graphite inclusion on the internal stress of electroless nickel was considered by measuring the stress of

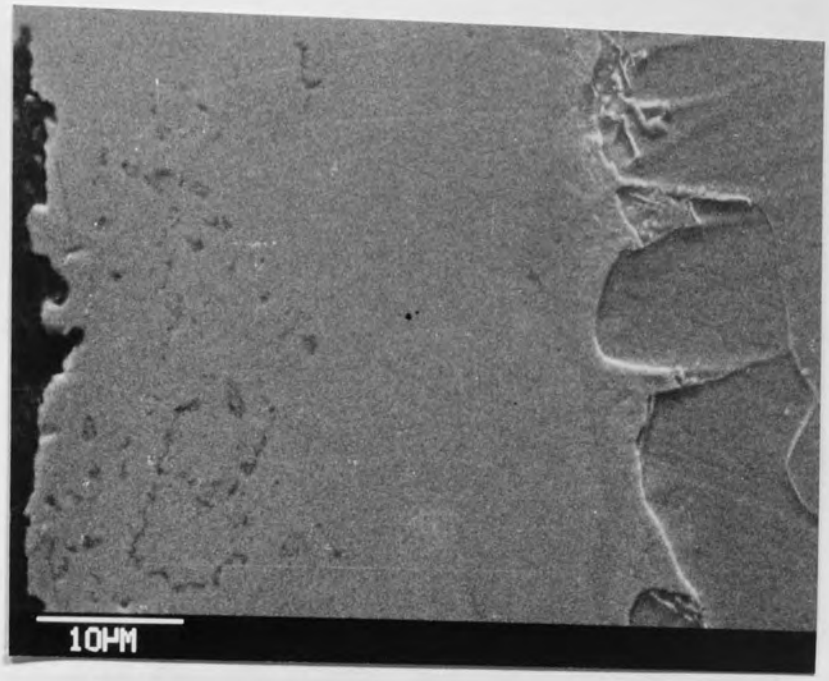

Figure 58a. S.E.M. photograph of electroless nickel-chromium after heat treatment for 16 hours at 850°C

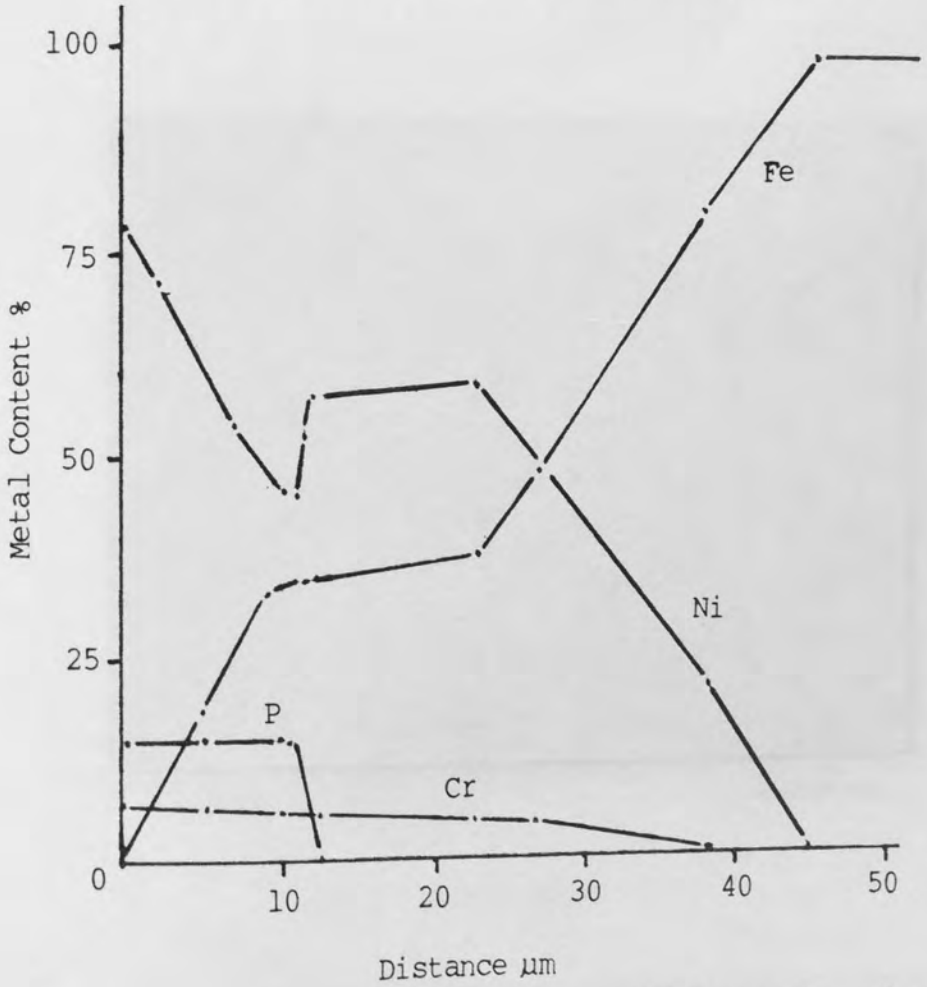

Figure 58. EPMA trace of electroless nickel-chromium after heat treatment of for 16 hours at 850°C

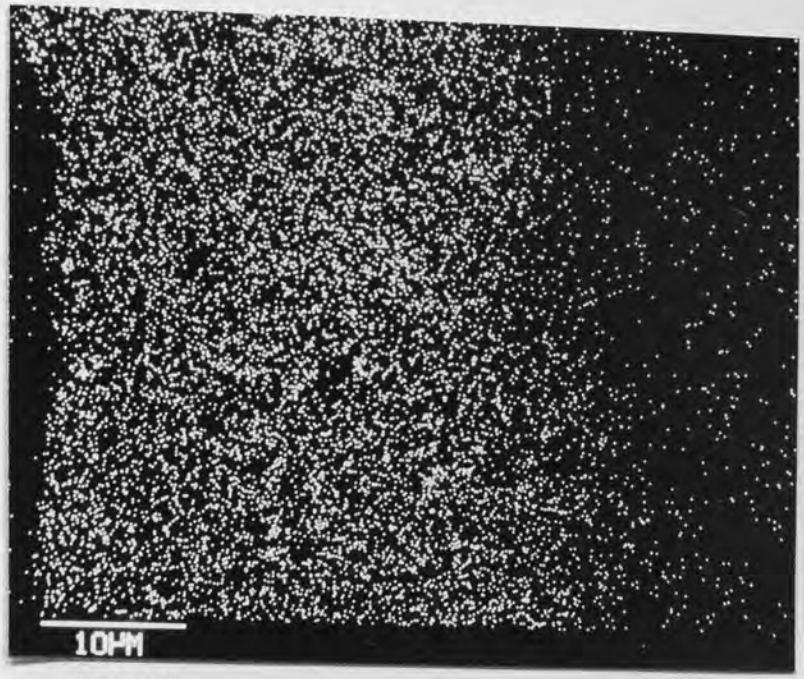

(a) Nickel

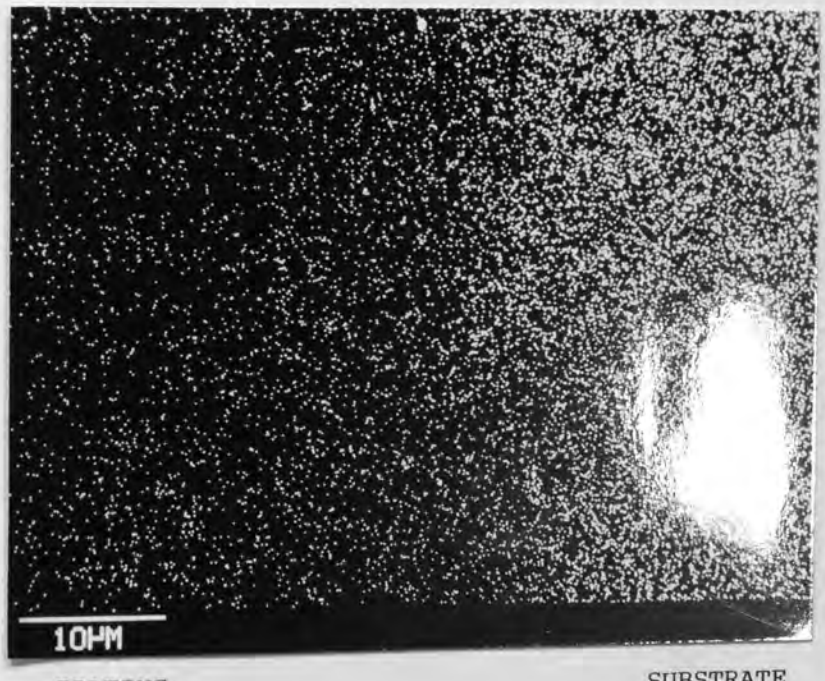

(b) Iron

Figure 59a-b. X-ray maps of electroless nickel-chromium after heat treatment for 16 hours at 850°C

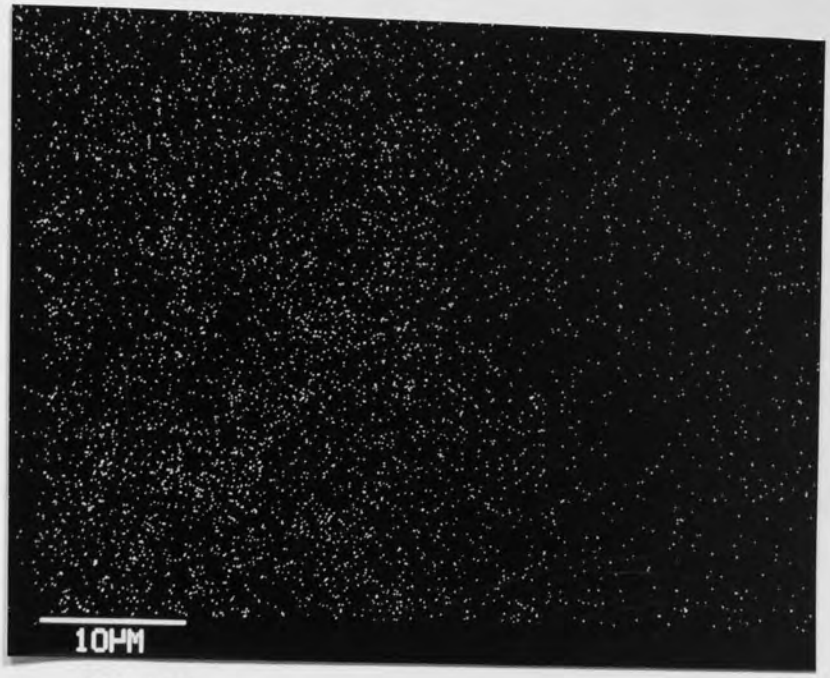

(c) Chromium

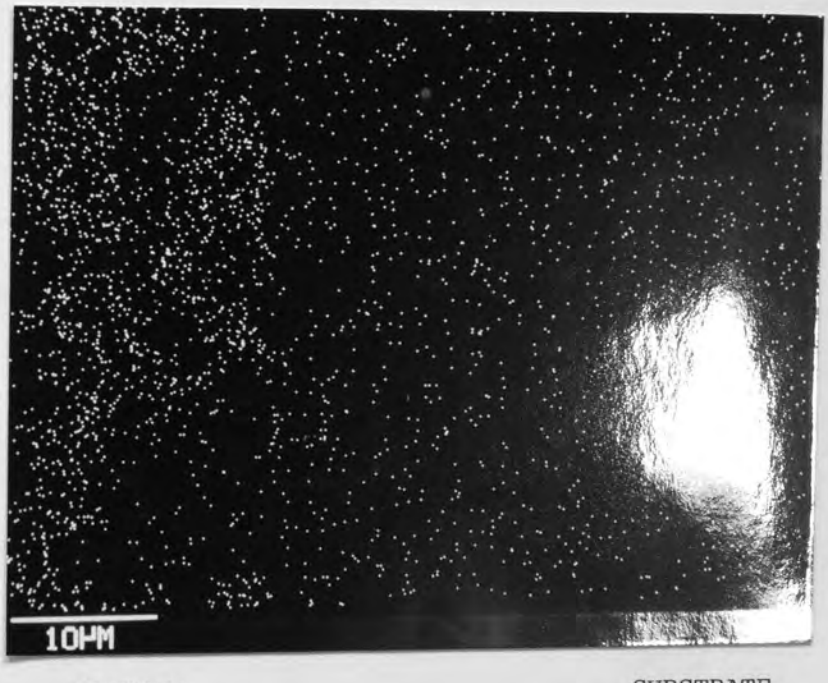

(d) Phosphorus

Figure 59c-d. X-ray maps of electroless nickel-chromium after heat treatment for 16 hours at 850°C

the two separate systems. Table 14 compares the internal stress, as measured by the Brenner and Senderoff spiral contractometer, of electroless nickel and electroless nickel-graphite deposits. A total of four readings were taken for each system as a comparison.

Table 14. Internal Stress of Electroless Nickel and Electroless Nickel-Graphite

Coating	Internal Stress N/mm^2
Electroless Nickel	47.9 44.1 42.8 49.4
Electroless Nickel-Graphite	35.1 30.4 32.6 31.9

Plated at 90°C, pH 5, graphite content-6.3 volume per cent.

Difficulty was experienced in measuring the stress using the spiral contractometer because of the agitation of the

solution. Agitation, was of course necessary to maintain the graphite particles in solution. However, if the contractometer was put in, or near the agitating air stream, deflection of the stress-reading needle could be observed. Similarly deflection would also occur on removal from the agitation. It was therefore necessary to carry out stress measurements as far removed from the agitation source as possible. Measurements were then taken using the large four-litre container with the air agitation source directed away from the contractometer.

The results of the experiment showed a similar trend to that reported in the literature for electrolytic composite systems. The internal stress of the electroless nickel-graphite composite was reduced, as compared to the values of the normal matrix material of electroless nickel, as with the electrolytic composite systems.

6.7 WEAR TESTING

Wear testing was carried out as described in the wear testing procedures. During individual wear tests however, it became obvious that excluding the overall effects on frictional force caused by load and coefficient of friction, the frictional force being measured was not constant but rather varied around a mean value. The range of the variations was dependent on the coating being tested. This range of measured force was considered to represent the stick-slipping nature of friction.

The literature review showed that the introduction of lubrication reduces the overall levels of friction and narrows the range of the measured frictional force as the sticking, static aspect of friction is reduced to that of the slipping, kinetic component.

The coefficient of friction was then recorded in these results as static and kinetic coefficients of friction as indicated by the range of frictional force measured during wear testing.

6.7.1 Electroless Nickel-Graphite Composite Coatings

6.7.1.1 Pin on Disc Wear Testing Results

a) **The effect of graphite content on the coefficient of friction and wear rate of electroless nickel-graphite coated pins against EN 31 steel disc**

Electroless nickel graphite coated pins were produced as per section 4.5.7,2a with increasing graphite content, heat treated and tested on the pin and disc wear testing machine. The effect of running electroless nickel-graphite coatings, which contained inreasing amounts of graphite, against an EN 31 steel disc are shown in Table 15 and figures 60 and 61.

As graphite content was increased so the coefficient of friction decreased. More significantly the static component of friction was reduced from 0.92 to 0.52 with the kinetic component

remaining essentially constant. The wear rate of heat treated electroless nickel was very much less than the un-coated steel. However, the introduction and increase in graphite content of the deposit increased the wear rate of the coating by a factor of 2.33 from 0.42 x 10^{-7} mm/cm to 0.98 x 10^{-7} mm/cm.

Examination of the discs by talysurf showed that, although the wear rate of electroless nickel was low, significant wear and oxidation of the EN 31 disc counterface had occurred, figure 62 and 63.

Table 15. The Effect of Graphite Content on Wear Rate and Coefficient of Friction against EN 31 steel

Vol. % graphite	Wear rate X 10^{-7} mm/cm	Coefficient of Friction	
		Kinetic	Static
un-plated	11.50	0.51	1.10
0.0 as-plated	2.69	0.71	0.99
0.0	0.42	0.50	0.92
3.5	0.67	0.46	0.62
4.6	0.77	0.47	0.58
5.0 as-plated	33.50	0.69	0.89
5.9	0.82	0.44	0.56
6.3	0.97	0.43	0.53
6.6	0.98	0.41	0.52

When this was compared to the EN 31 disc counterface after having run against electroless nickel-graphite (6.6

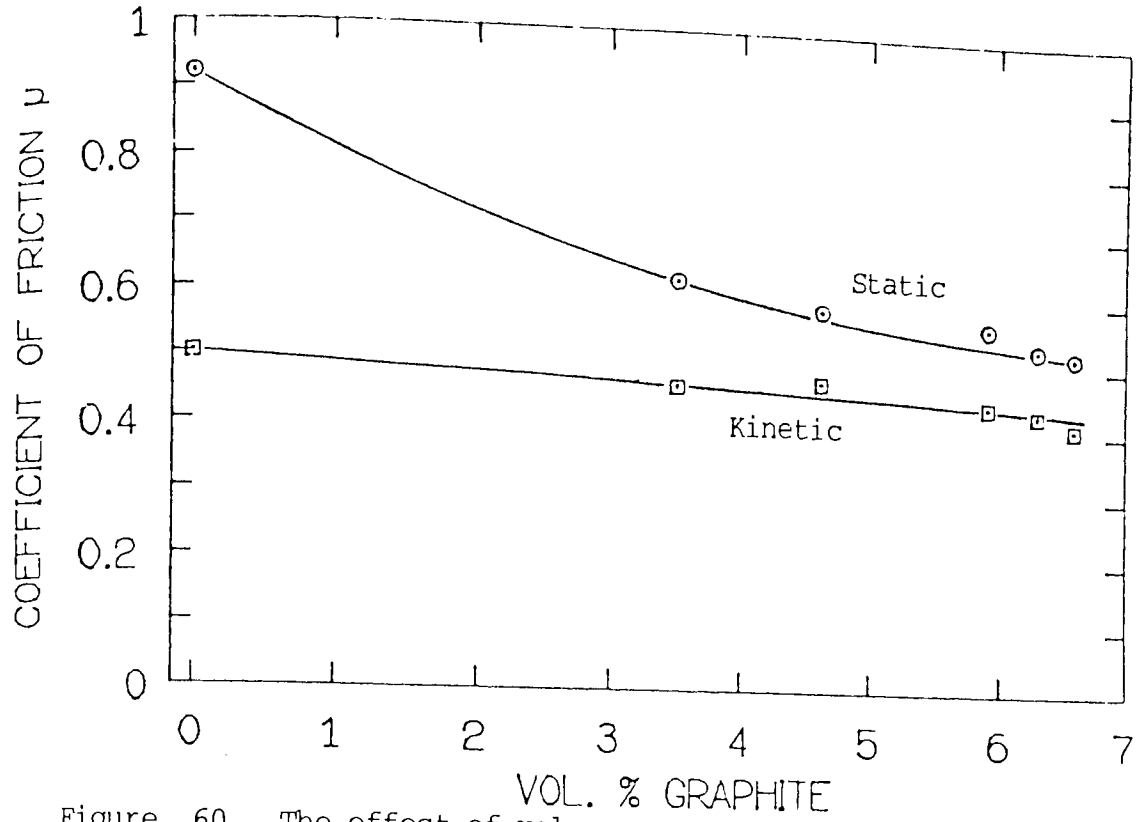

Figure 60. The effect of volume per cent graphite (2 μm nominal particle size) in the deposit on the coefficient of friction from pin on disc wear testing. Heat treated 400°C-1hr, run against an EN 31 disc, sliding speed 50 cm/s, load 2 kg

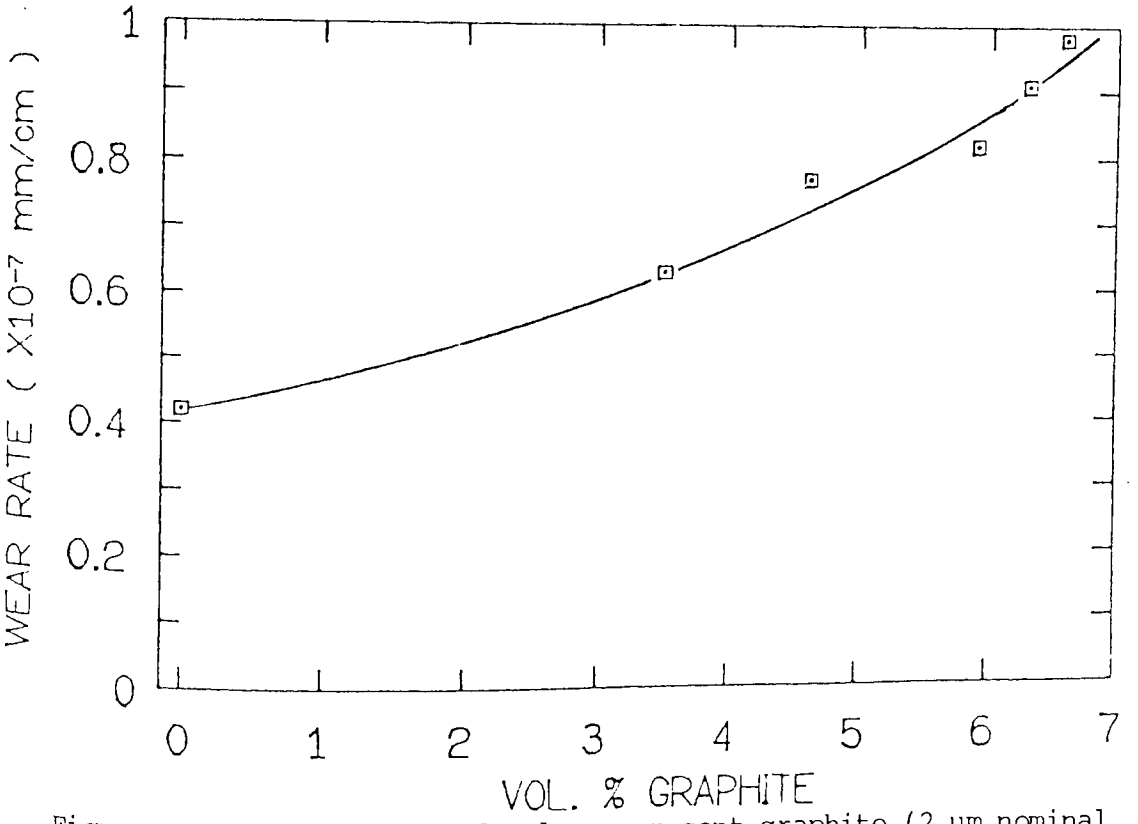

Figure 61. The effect of volume per cent graphite (2 μm nominal particle size) in the deposit on the wear rate from pin on disc wear testing. Heat treated 400°C-1hr, run against an EN 31 disc, sliding speed 50 cm/s, load 2kg

Figure 62. Profile of wear track on EN 31 disc after running for 1 hour against a heat treated electroless nickel coated pin, sliding speed 50 cm/s, load 2 Kg

Figure 63. Optical photograph of the wear track on En 31 disc after running against a heat treated electroless nickel coated pin, sliding speed 50 cm/s, load 2 Kg

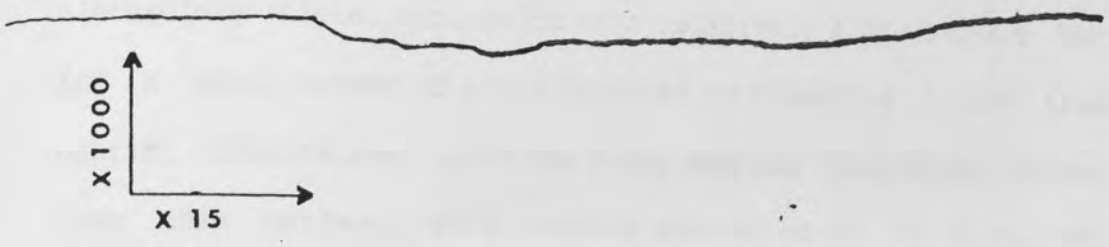

Figure 64. Profile of the wear track on EN 31 disc after running for 1 hour against a heat treated electroless nickel-graphite coated pin, sliding speed 50 cm/s, load 2 Kg

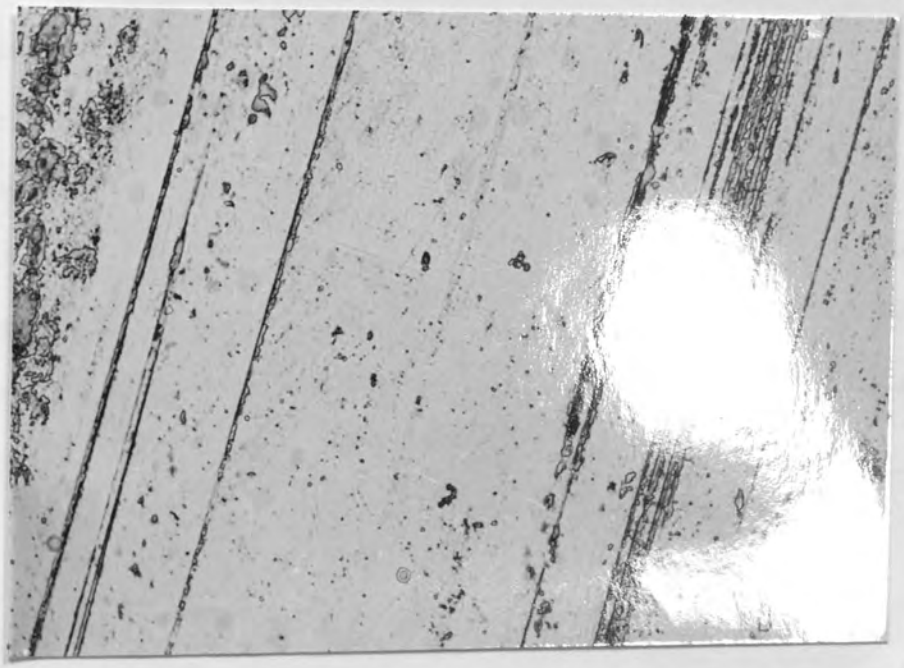

Figure 65. Optical photograph of the wear track on EN 31 disc after running against a heat treated electroless nickel-graphite coated pin, sliding speed 50 cm/s, load 2 Kg

volume per cent graphite), figure 64 and 65 it can be seen that very little wear had occurred and no signs of major oxidation were observed.

Examination by S.E.M., figure 66, showed the electroless nickel surface to be a relatively flat surface but for a small number of scars produced by ploughing action from debris. Examination using the X-ray mapping facilities showed that this surface, after running against an EN 31 disc, was covered in iron with very little nickel detected through the iron layer. This would support a strong adhesive wear mechanism.

Examination of electroless nickel-graphite coated pins run against an EN 31 counterface, figure 67 and 68 , showed a significant amount of graphite had now been exposed. Examination of an electroless nickel-graphite surface at different stages of the wear process showed a progressive flattening and smearing of the surface asperities as wear occurred, Figure 67 a through c. Eventually a relatively flat surface was produced with the graphite flakes in the deposit exposed to the surface. X-ray mapping showed that the iron transfer had now been reduced to a minimum, reflecting the low wear of the disc, figure 64, and a significant reduction in adhesive wear.

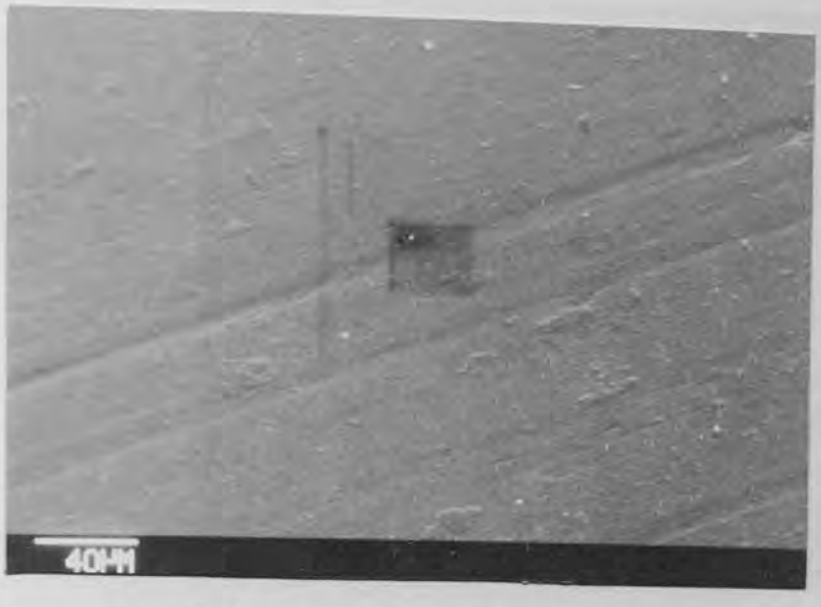

(a) S.E.M. of surface

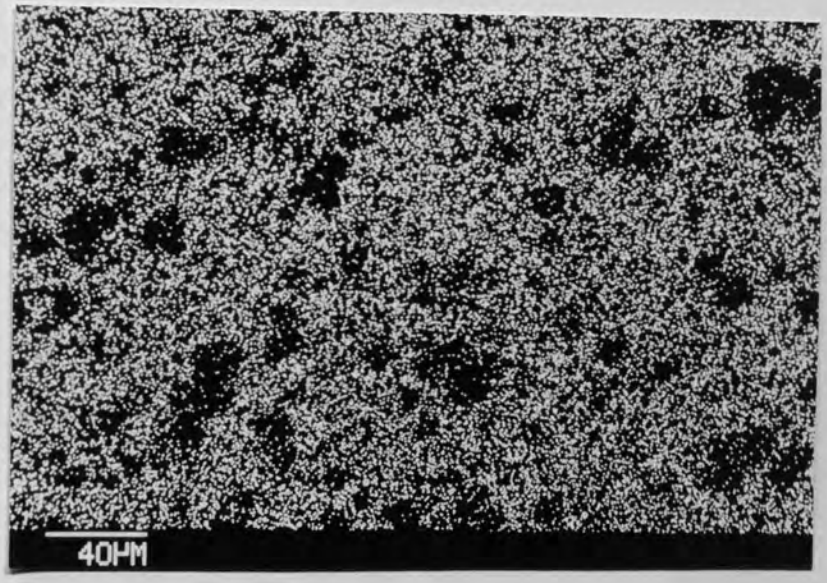

(b) X-ray map of iron

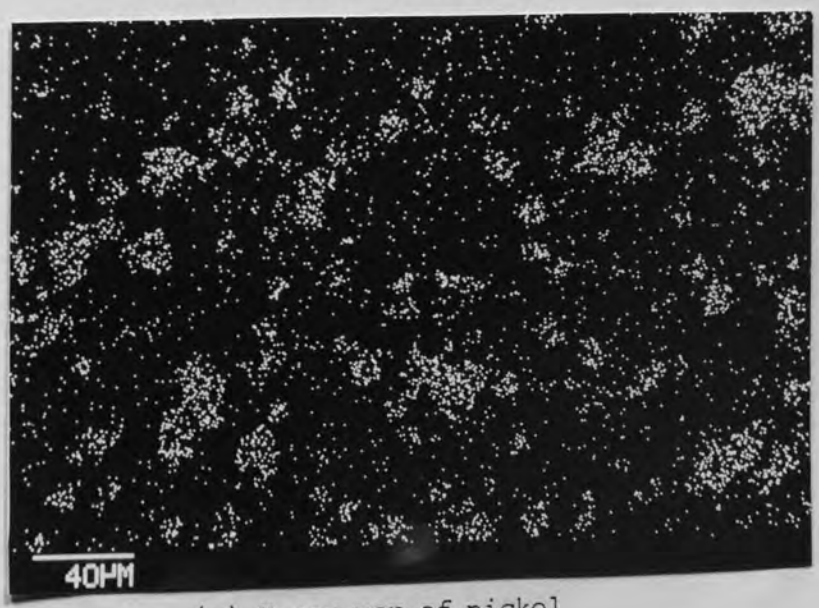

(c) X-ray map of nickel

Figure 66. X-ray maps from the surface of heat treated electroless nickel coated pin after running for 1 hour against an EN 31 disc

(a) As-deposited surface

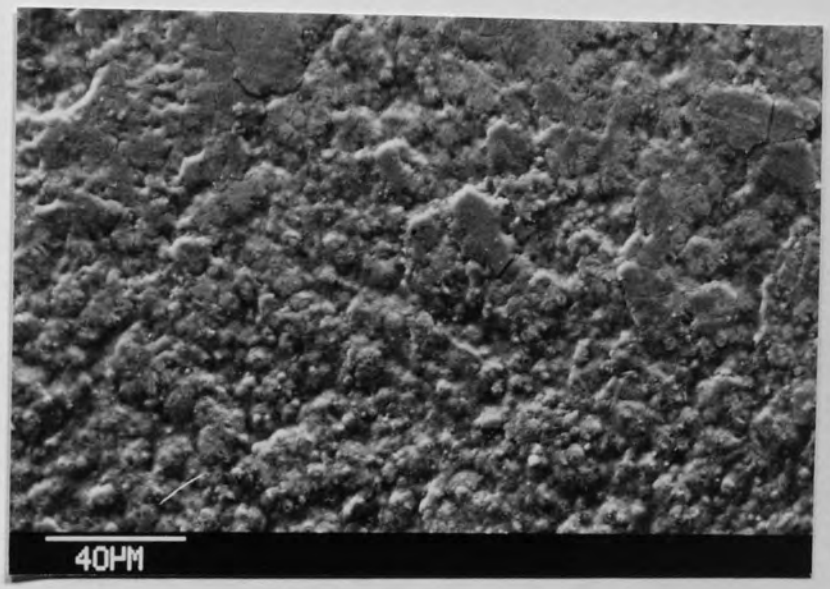

(b) Initial stages of the test

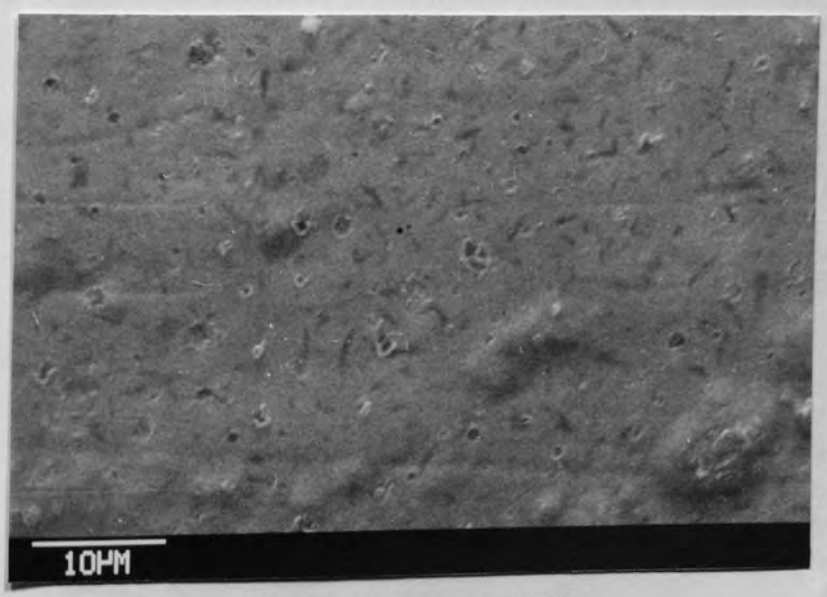

(c) Steady state conditions

Figure 67. Development of the electroless nickel-graphite wear surface of a coated pin tested in the pin on dics wear tester

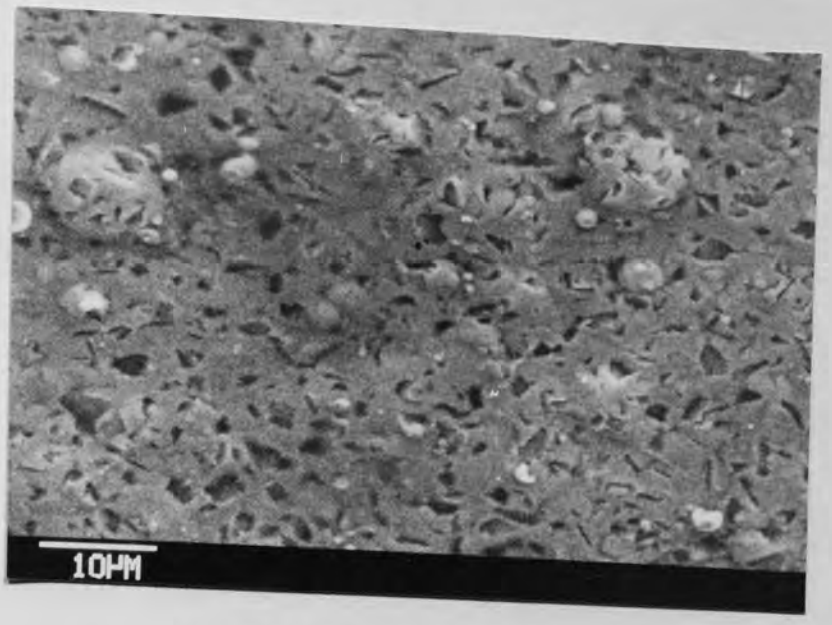

(a) S.E.M. of surface

(b) X-ray map for iron

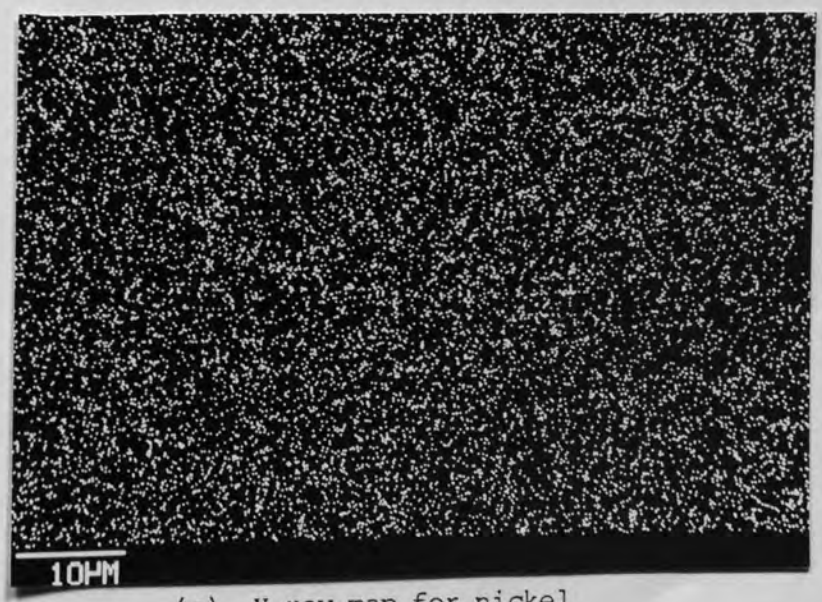

(c) X-ray map for nickel

Figure 68. X-ray maps from the surface of heat treated electroless nickel-graphite coated pin after running for 1 hour against an EN 31 disc, sliding speed 50 cm/s, load 2 Kg

b) The Effect of Graphite Content on the Coefficient of Friction and Wear Rate of Electroless Nickel Coated Pins run against an Electroless Nickel-Graphite Coated Disc

As per section 5.6.7.2(ii) pins were coated with electroless nickel with increasing graphite content and heat treated. Discs were also coated with an electroless nickel-graphite coating from a bath containing 60g/l, giving a graphite content of 6.6 volume per cent graphite and then heat treated.

The result of running an electroless nickel-graphite coated pin against a similar coated disc are shown in table 16 and in figures 69 and 70.

Table 16. The Effect of Graphite Content on the Coefficient of Friction and Wear Rate of Electroless Nickel-Graphite Coated Pins against an Electroless Nickel-Graphite Coated Disc (6.7 volume per cent graphite)

Vol. % Graphite in Pin	Wear Rate x 10^{-7} mm/cm	Coefficient of friction	
		Kinetic	Static
3.5	0.064	0.19	0.29
4.6	0.071	0.17	0.27
5.9	0.115	0.16	0.29
6.3	-----	0.15	0.22
6.6	0.136	0.14	0.20

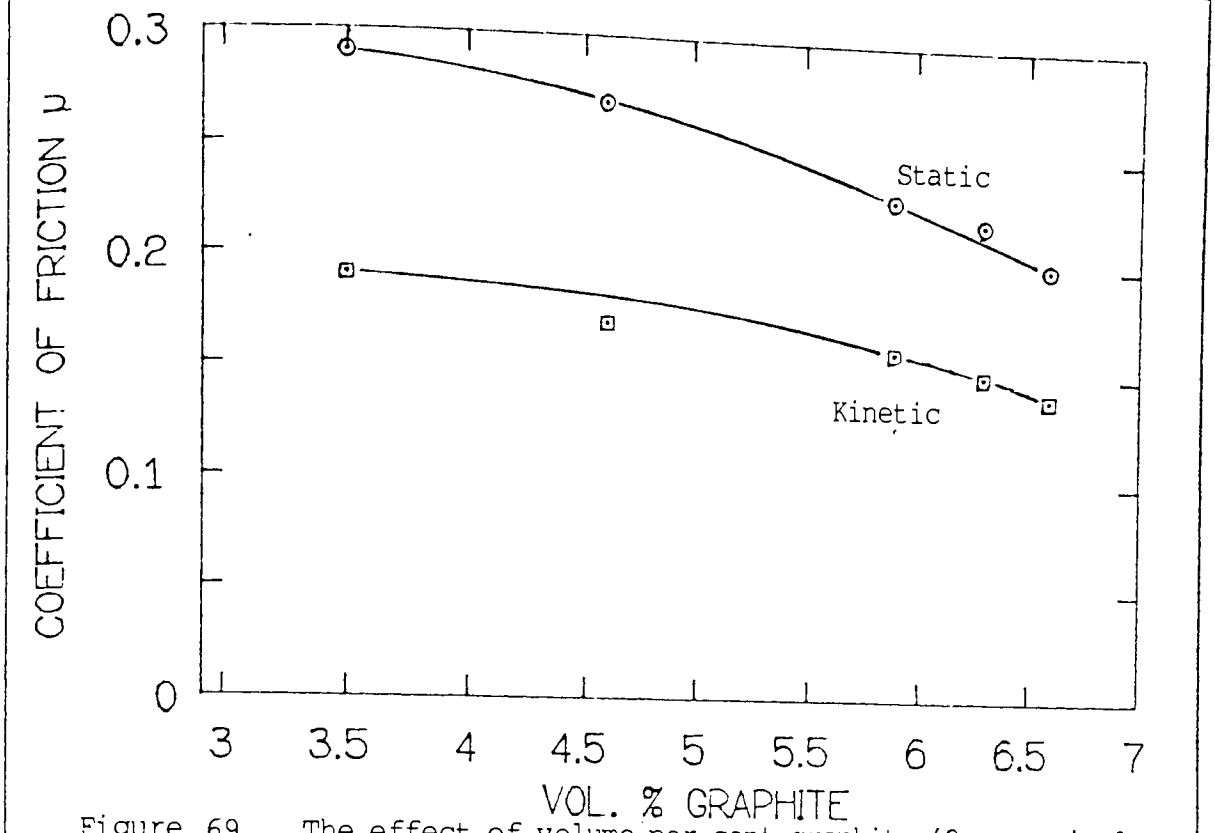

Figure 69. The effect of volume per cent graphite (2 μm nominal particle size) in the deposit on the coefficient of friction. Heat treated 400°C-1hr, run against heat treated electroless nickel-graphite coated disc (6.1 vol.% graphite). Sliding speed 50 cm/s, load 2 kg

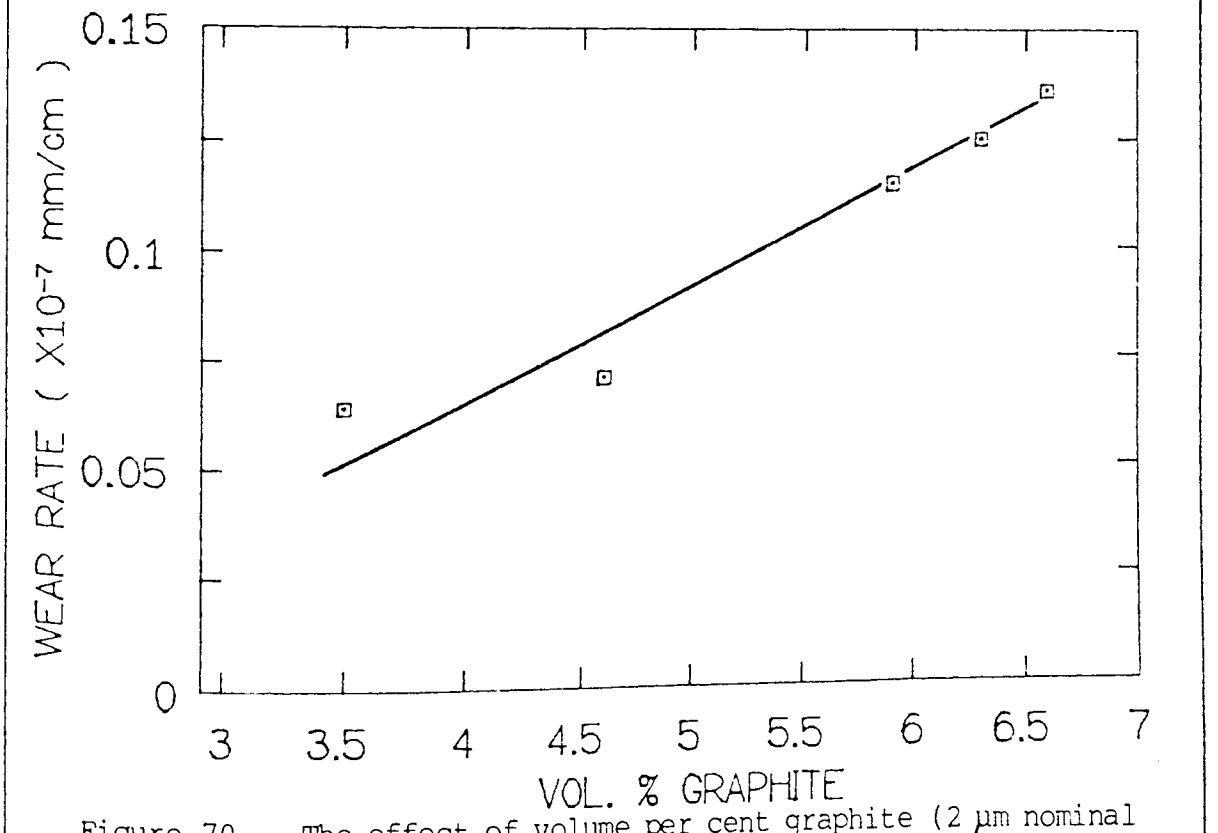

Figure 70. The effect of volume per cent graphite (2 μm nominal particle size) in the deposit on wear rate. Heat treated 400°C-1hr, run against heat treated electroless nickel-graphite coated disc (6.1 vol.% graphite). Sliding speed 50 cm/s, load 2 kg

Again increasing amounts of graphite in the coated pins reduced the coefficients of friction, in this case both static and kinetic components of friction were reduced, thus reducing the stick-slip nature between the surfaces.

The coefficients of friction were significantly lower at 0.14-0.2 than for electroless nickel-graphite coated pins run against an EN 31 discs, at 0.35-0.45. The wear rates were also much lower run like against like, at 0.136×10^{-7} mm/cm, as compared to 0.98×10^{-7} mm/cm for electroless nickel-graphite 6.6 volume per cent against an EN 31 disc.

An overall comparison of results for the average coefficients of friction and wear rates against sliding distances is shown in figures 71 and 72.

c) **The Effect of Increasing Load on the Coefficient of Friction and Wear Rate of Electroless Nickel-Graphite Coated Pins and Discs**

Pins and discs were plated as per section 5.6.7,2(ii) and heat treated. Analysis of the deposit showed a graphite content of 6.5 volume per cent for both pins and discs. The pins were then run against the discs on the wear tester under increasing loads. The results for the effect of load on the coefficient of friction and wear rate of electroless nickel-graphite coated pins running against electroless nickel-graphite coated discs are shown in table 17 and in figure 73 and 74.

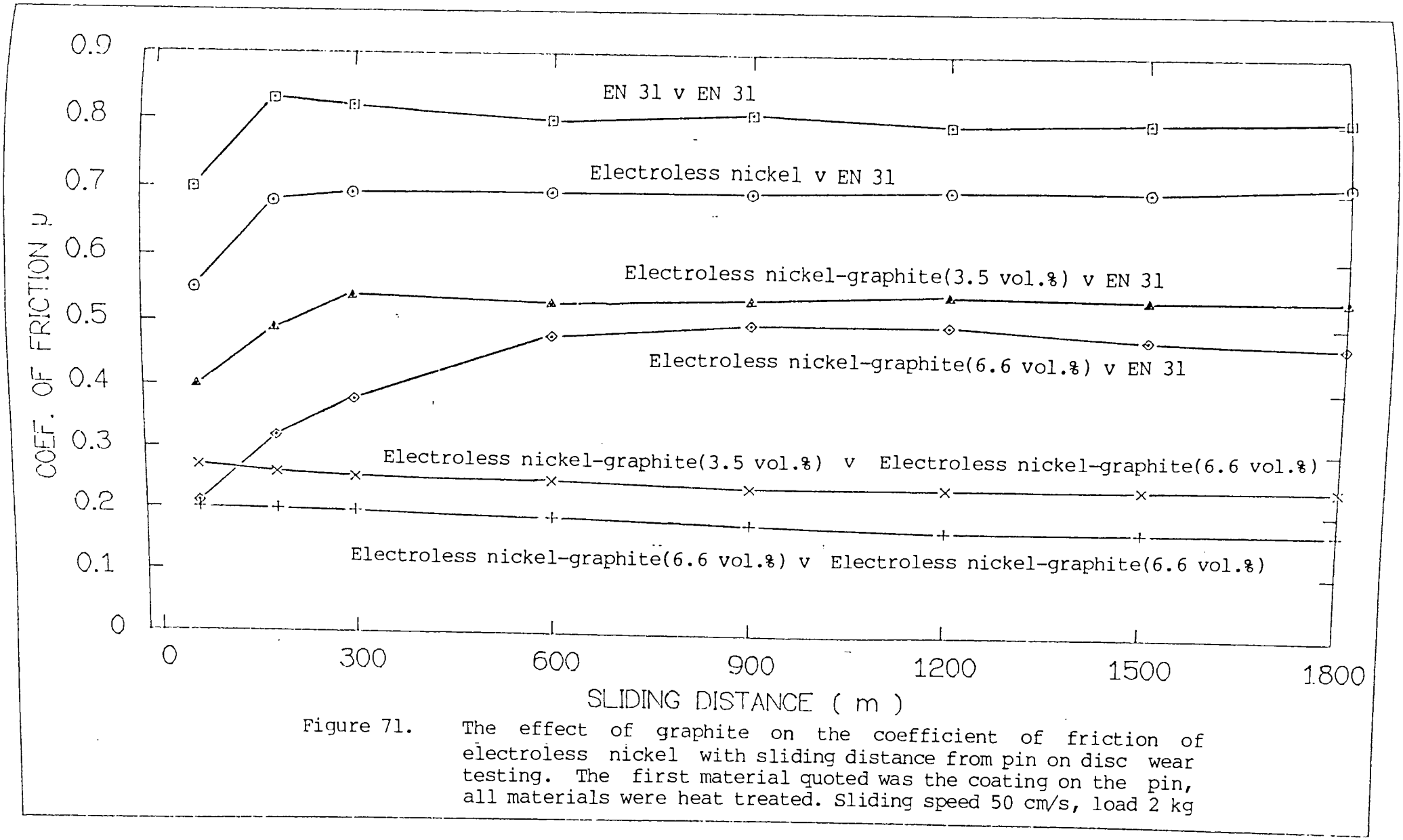

Figure 71. The effect of graphite on the coefficient of friction of electroless nickel with sliding distance from pin on disc wear testing. The first material quoted was the coating on the pin, all materials were heat treated. Sliding speed 50 cm/s, load 2 kg

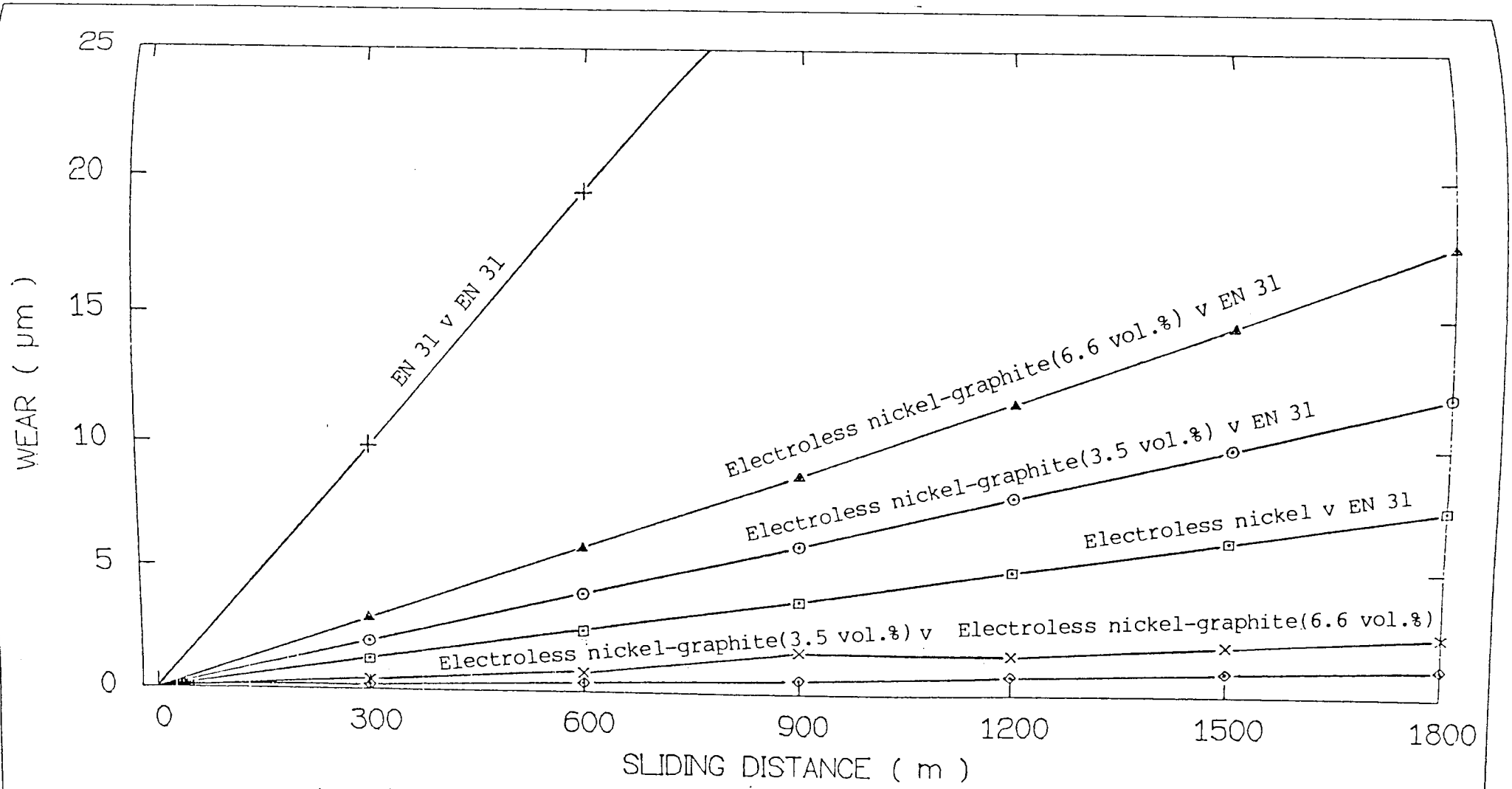

Figure 72. The effect of graphite content on the wear rate of electroless nickel with sliding distance from pin on disc wear testing. The first material quoted was the material on the pin, all materials were heat treated. Sliding speed 50 cm/s, 2 kg load

◇——◇ Electroless nickel-graphite(6.6 vol.%) v Electroless nickel-graphite(6.6 vol.%)

Table 17. The Effect of Increasing Load on Wear Rate and Coefficient of Friction. Electroless Nickel-Graphite against Electroless Nickel-Graphite

Load Kg	Wear Rate x 10^{-7} mm/cm	Coefficient of Friction	
		Kinetic	Static
2	0.115	0.18	0.27
4	0.128	0.24	0.34
6	0.199	0.28	0.53
8	0.241	0.40	0.65

The results show that as load increased both wear rate and coefficient of friction also increased, with the kinetic and static components diverging at increased loads, to significantly high levels of 0.4 to 0.65 coefficient of friction. It could possibly have been expected that wear rate and coefficient of friction would increase as load was increased. However, it could also have been hoped that if the graphite had been acting as a solid lubricant it could also act as a high pressure lubricant, maintaining a low coefficient of friction and wear rate even as load was increased.

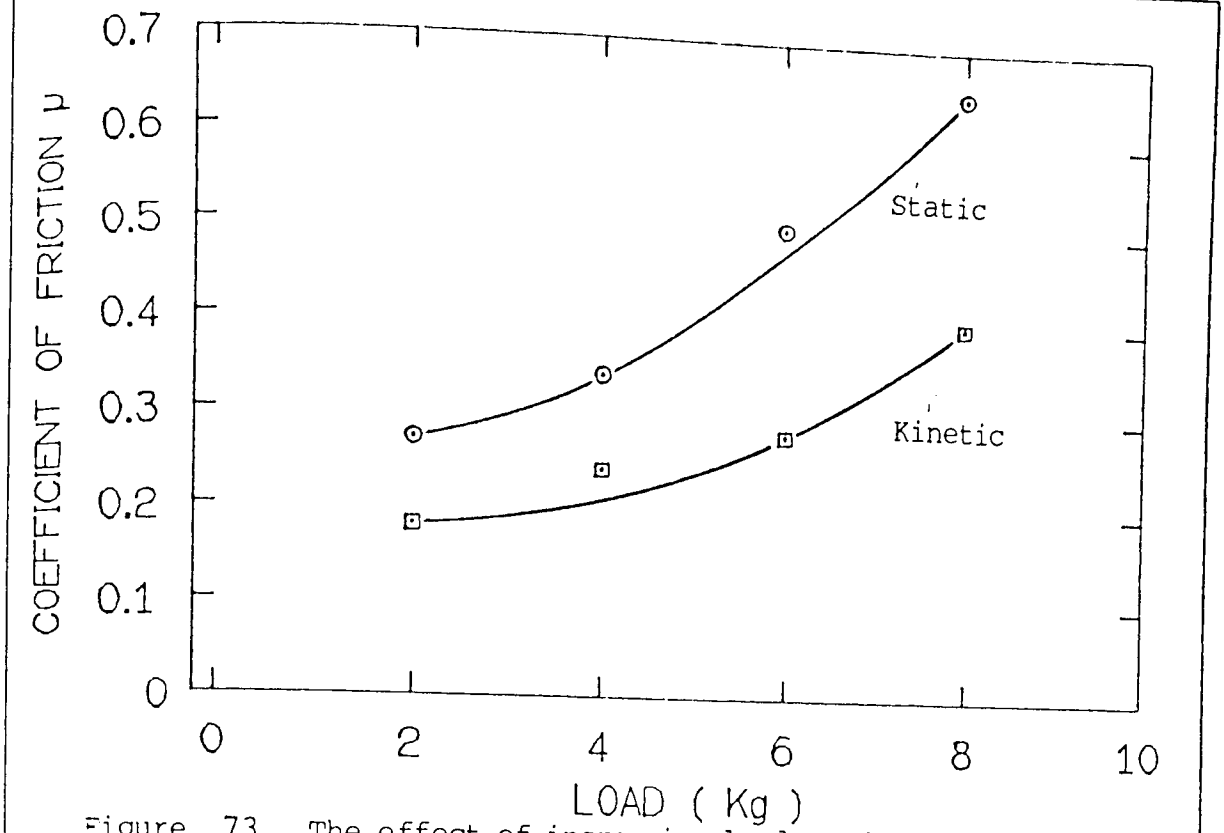

Figure 73. The effect of increasing load on the coefficient of friction of heat treated electroless nickel-graphite coated pins(6.3 vol.% graphite) when run against an heat treated electroless nickel-graphite coated disc(6.7 vol.% graphite), pin on disc wear test

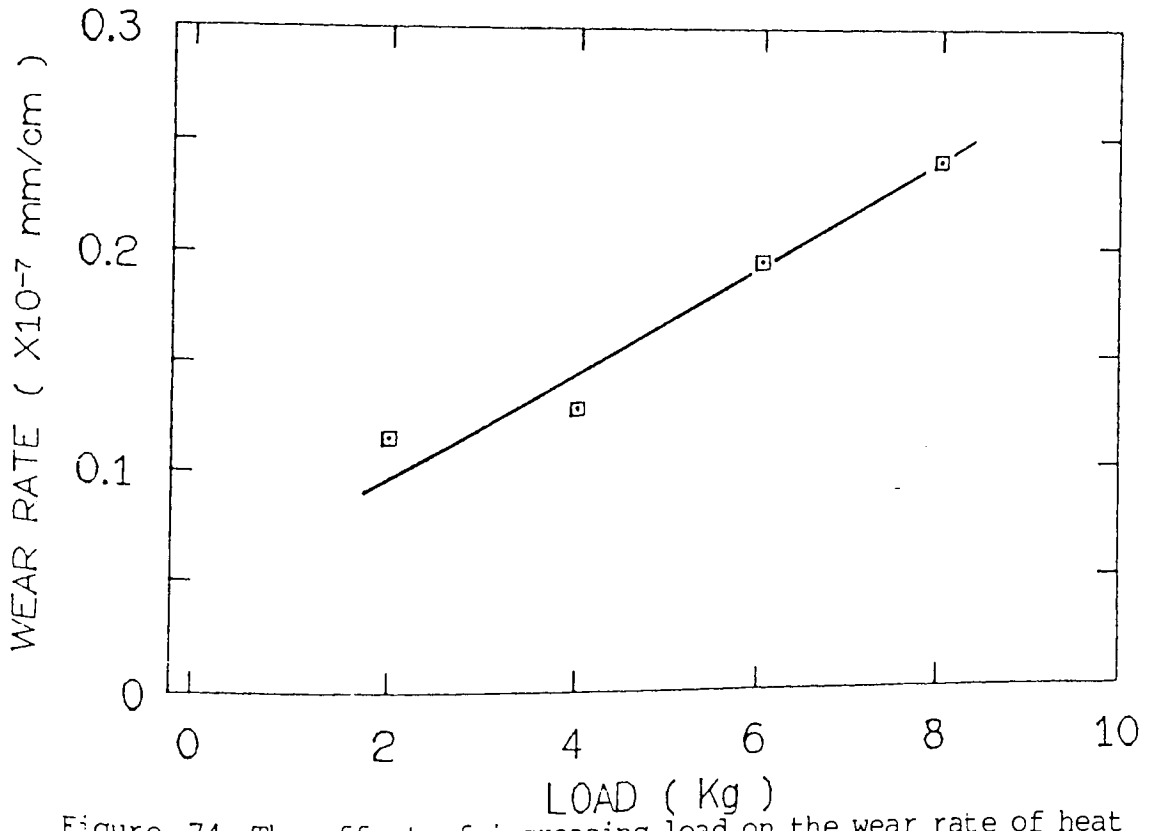

Figure 74. The effect of increasing load on the wear rate of heat treated electroless nickel-graphite coated pins (6.3 vol.% graphite) when run against an heat treated electroless nickel-graphite coated disc(6.7 vol.% graphite), pin on disc wear test

6.7.1.2 Crossed Cylinder Wear Testing Results

Cylinders for wear testing were produced as described in section 5.6.7.3 Electroless nickel deposits were heat-treated before testing, the procedure for testing was as per section 5.6.6(ii). The results for the coefficients of friction and wear rates for these deposits, tested by the crossed cylinder method, are shown in table 20 and figure 75.

A study of the results showed that the introduction of graphite into both electroless and electrolytic nickel produced a significant reduction in the coefficient of friction and wear rate. When run against stainless steel stators values of 0.07-0.12 coefficient of friction were easily produced for nickel-graphite coated rotators with the same levels of graphite content as with the pin on disc. These values were also maintained well beyond the duration of the test with no sign of any change in the value.

When run like against like, slightly higher values for the coefficient of friction were experienced, 0.15-0.24, and also the wear increased slightly.

If the stator and rotator were reversed such that a stainless steel cylinder was rotated against a nickel-graphite coated stator, initial values of friction would be low, in the order of 0.1. This value however would increase after a very

short period of time to much higher levels, 0.43-0.58. Wear of the stainless steel rotator was moderate but with much higher wear taking place on the nickel-graphite stator.

Table 18. The Coefficient of Friction and Wear Rate of Electroless Nickel-Graphite using the Crossed Cylinder Wear Tester

Rotator	Stator	Coefficient of friction		Rotator	Stator
		kinetic	static	Wear Profile μm^2	Wear Profile μm^2
ELN	ELN	0.29	0.45	53.4	45.1
ELN	MS	0.30	0.45	25.5	57.3
ELN	SS	0.43	0.58	23.9	21.7
ELN-G	SS	0.09	0.12	6.2	4.2
ELN-G	MS	0.10	0.14	9.3	7.3
ELN-G	ELN-G	0.15	0.24	13.1	11.5
ELN-G (Machined)	SS	0.27	0.55	24.1	25.1
Ni-G	MS	0.12	0.15	9.6	6.8
Ni-G	SS	0.06	0.07	6.1	3.1
Ni-G	Ni-G	0.14	0.21	11.1	8.2
SS	Ni-G	0.43	0.58	18.7	42.1
Ni-G (Machined)	SS	0.35	0.51	25.2	19.3

ELN = Electroless nickel, heat treated, 400°C 1hr.
ELN-G = Electroless nickel-graphite, heat treated, 400°C 1hr.
Ni-G = Electrolytic nickel -graphite.
MS = Mild steel.
SS = Stainless steel.

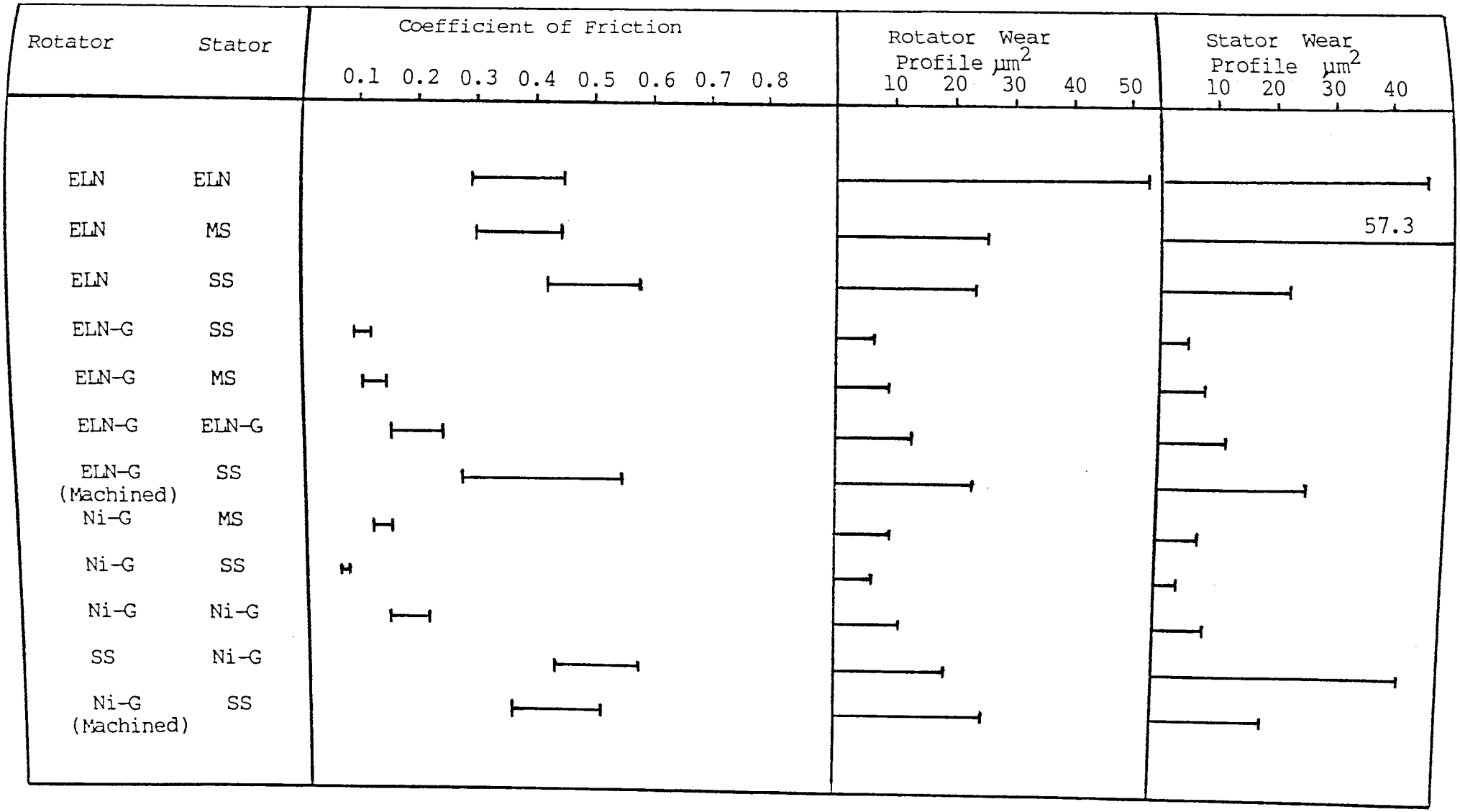

Figure 75. The coefficients of friction and wear rates of electroless nickel-graphite deposits from crossed cylinder wear testing

If the surface of a nickel-graphite deposit was polished with 500 grade emery paper before wear testing and then rotated against a stainless steel stator a much different result was obtained compared to an un-machined surface. The initial coefficient of friction, μ=0.15, was seen to gradually rise, figure 76, until a dramatic increase took place with values of 0.3-0.6 being experienced and a corresponding rise in the wear rate. The graphite content was the same as with the un-treated surfaces run against stainless steel.

S.E.M. photographs of a nickel-graphite surface, run against a stainless steel stator in the as-deposited, and surface polished condition, are shown in figure 77. In the as-deposited condition, figure 77a , deformation of the surface asperities had occurred producing a wear scar of flattened asperities which supported the load. Little subsequent wear had occurred once these flat regions had been established. Study of the deformed regions showed a mixture of nickel, possibly nickel oxide and graphite. Overall damage of the surface can be seen to be minimal. In the surface ground condition all evidence of the surface features had been removed but some graphite flakes were now exposed. Primary surface contact then appeared to be between the stainless steel and the nickel with some possible influence from the exposed graphite flakes.

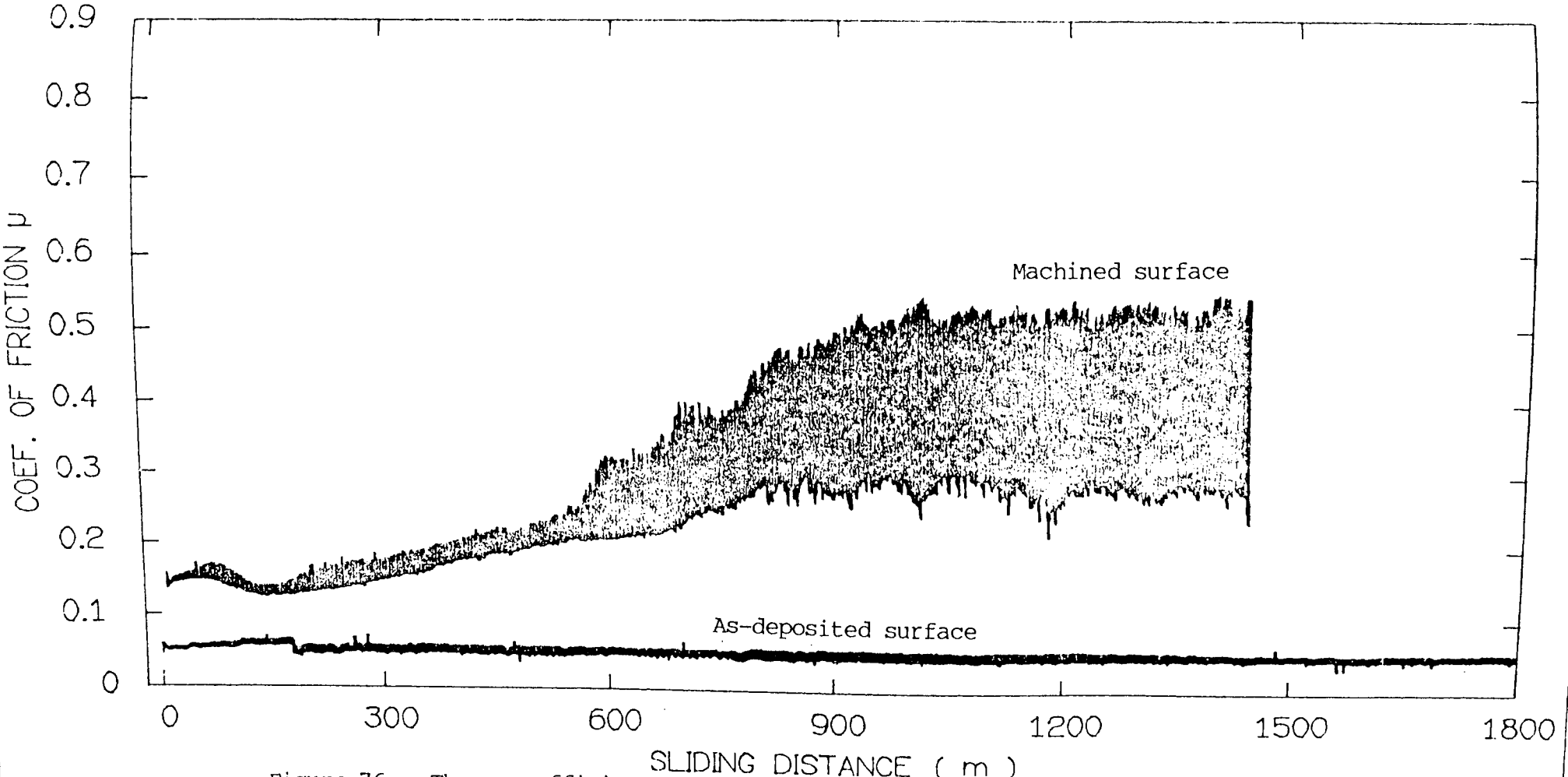

Figure 76. The coefficient of friction for as-deposited and machined electroless nickel-graphite surfaces from crossed cylinder wear tests. Coatings were heat treated and run as the rotator against a stainless steel stator. Sliding speed 70 cm/s, load 700g, 7.0 volume per cent graphite for both cylinders

(a) As-deposited surface

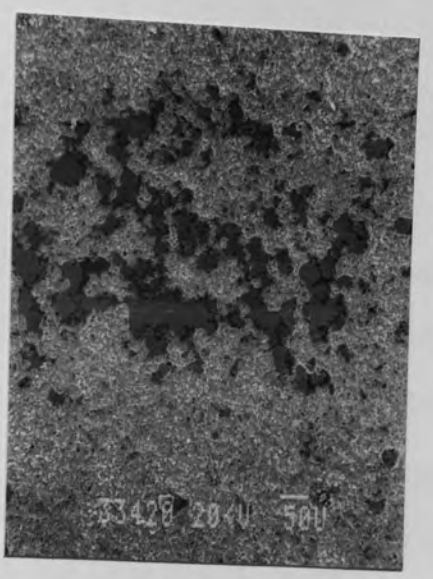

(b) Wear scar of as-deposited surface

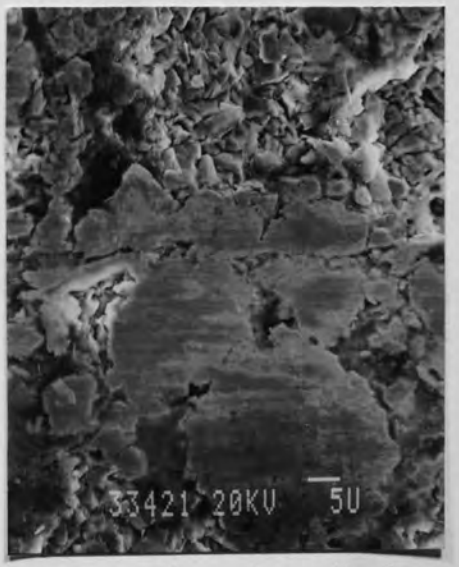

(c) Wear scar of as-deposited surface

(d) Wear scar of machined surface

(e) Edge of wear scar from as-deposited surface

Figure 77. S.E.M. photographs of the electroless nickel-graphite wear surface from a coated rotator run against a stainless steel stator

6.7.1.3 Falex Wear Testing Results

The results in table 19 show that under the much higher loads of the Falex wear tester the overall coefficients of friction of both electroless nickel and electroless nickel-graphite were reduced as compared to the results from the pin on disc tests. The results show that the presence of graphite again reduced the coefficients of friction for electroless nickel. With these results the frictional force did not vary in range during the test as with the pin on disc. In the case of the Falex tester the speed of rotation, and hence sliding speed, is very high and therefore stick-slipping is unable to take place. The coefficient of friction then measured is the kinetic component of friction.

Table 19 . A Comparison of the Coefficient of Friction and Wear Rate of Electroless Nickel and Electroless Nickel-Graphite Coatings using the Falex Wear tester

Sample No.	Electroless Nickel		Electroless Nickel-Graphite	
	μ	W.R. $x10^{-6}$g/min	μ	W.R. $x10^{-6}$g/min
1	0.31	0.23	0.20	0.50
2	0.33	0.64	0.20	0.82
3	0.35	0.52	0.25	0.61
4	0.34	0.62	0.27	0.74
5	0.33	0.78	0.21	0.59

Although the coefficients of friction for either of the deposits was not particularly high, the wear rates of the deposits were very high, with the 25μm coating being completely worn through after only an average of 10 minutes.

6.7.2 Electroless Nickel-PTFE Composite Coatings

6.7.2.1 Pin on Disc Wear Testing Results

As stated in the experimental procedure, pins and discs were commercially plated from source one with electroless nickel-PTFE and tested on the pin and disc wear test machine. The results obtained for these coatings are shown in table 20. The number of pins available for testing was slightly restricted, however, each figure is an average of at least four results all of which were in close agreement with each other. The PTFE content of the deposits was 19.4 volume per cent.

In the as-plated condition and after one hour at 200°C, as a de-embrittlement treatment, the hardness of the composite was 216 Hv_{100}. After heat treatment at 400°C for one hour hardness had increased to 389 Hv_{100}.

The wear test results for the electroless nickel-PTFE coatings show a similar pattern to electroless nickel-graphite. When run against EN31, the static component of friction was again more significantly reduced than the kinetic component, with final kinetic-static coefficients at 0.36 and 0.44. The wear rates

for electroless nickel-PTFE were however much higher than for electroless nickel-graphite deposits.

Table 20. The Coefficient of Friction and Wear Rate of Electroless Nickel-PTFE Coatings from Pin on Disc Wear Testing

Coating/Material		Load	Coefficient of Friction		Wear Rate
Pin	Disc	Kg	Static	Kinetic	x 10-7mm/cm
Ni HT	EN31	2	0.5	0.92	0.42
Ni-PTFE	EN31	2	0.36	0.44	3.33
Ni-PTFE (HT)	En31	2	0.4	0.75	1.6
Ni-PTFE	Ni-PTFE	2	0.3	0.36	0.39
		4	0.36	0.52	0.85
		6	0.38	0.62	2.15

Ni = Electroless Nickel, HT = Heat Treated, 400^{o}C for 1 hour.

When heat-treated and run against EN31 the kinetic and static coefficients were only slightly reduced from those of electroless nickel against EN31. Heat treatment did, however, reduce the wear rate of the electroless nickel-PTFE deposit.

Electroless nickel-PTFE coated pins run against electroless nickel-PTFE coated discs showed a lowering of both the static and kinetic component of friction and a more significant reduction of the wear rate to below levels for heat-treated electroless nickel.

As load increased coefficients of friction and wear rate increased as with electroless nickel-graphite, with static and kinetic coefficients increasing and diverging with load.

S.E.M. examination, figure 78 , again showed a similar pattern to electroless nickel-graphite with reference to adhesive metal transfer. When run against an EN31 disc little iron transfer was again seen to occur onto the electroless nickel-PTFE coated pin surface as compared to electroless nickel, figure 66. S.E.M. examination also showed that the structure of the deposit, figure 78a, appeared to have suffered badly from hydrogen pitting during plating. Examination of nearly all the samples showed this to be a common feature of the coating and was not particulary satisfactory from a commercial supply.

Examination of the heat-treated electroless nickel-PTFE surface showed evidence of iron transfer, figure 79. This reflected increased adhesive interaction between the surfaces, which is also indicated by the higher static component of friction. As was identified in the literature, heat treatment appeared to decrease the lubricating ability of the PTFE.

Figures 80 and 81 illustrate the overall results of coefficient of friction and wear rate from the pin on disc wear test for electroless nickel-PTFE deposits from source one plotted against sliding distance. Figures 82 and 83, compares these results against electroless nickel-graphite deposits.

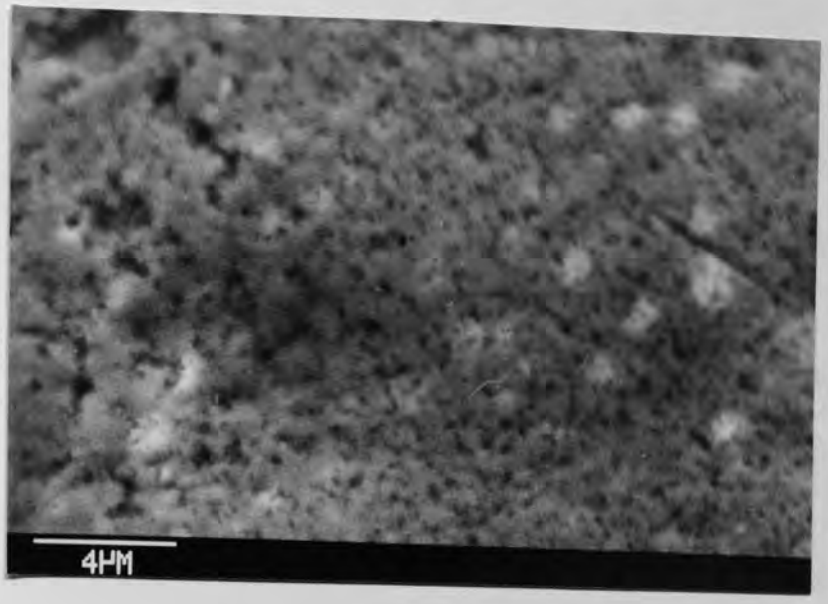

(a) Worn surface

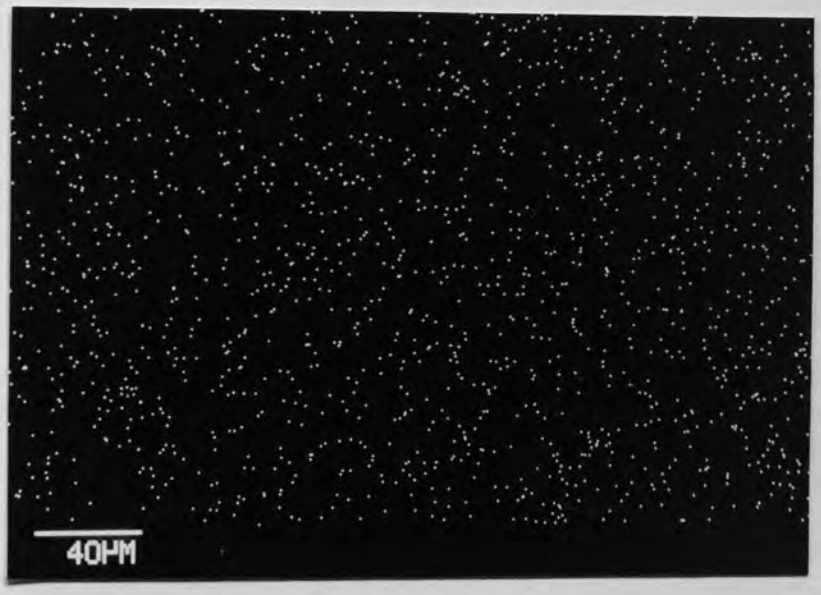

(b) X-ray map for iron

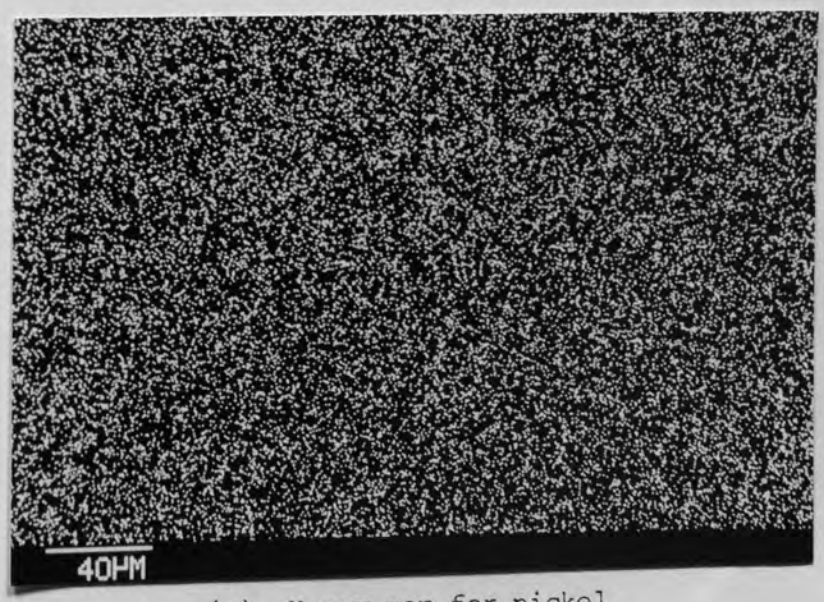

(c) X-ray map for nickel

Figure 78. The surface of electroless nickel-PTFE coated pin after running against an EN 31 disc for 1 hour, sliding speed 50 cm/s load 2 Kg

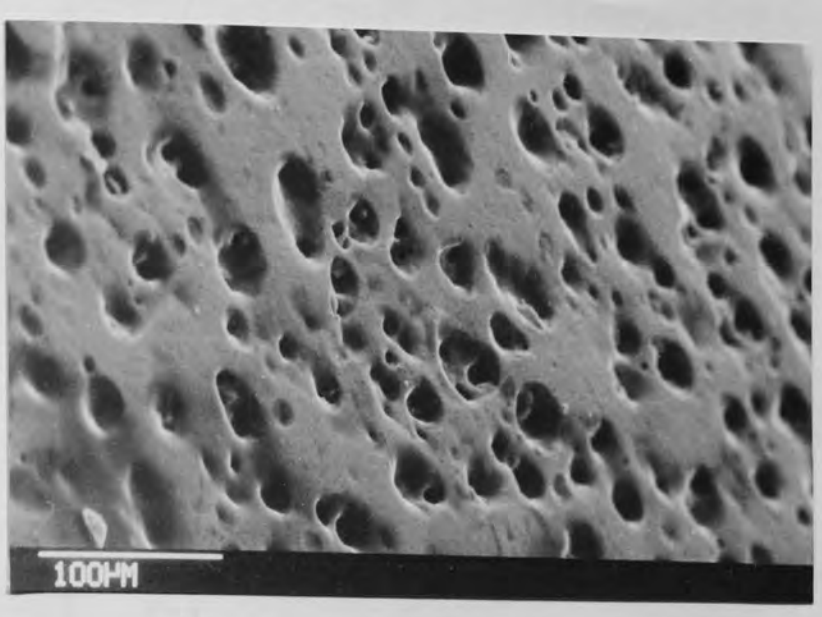

(a) Initial surface

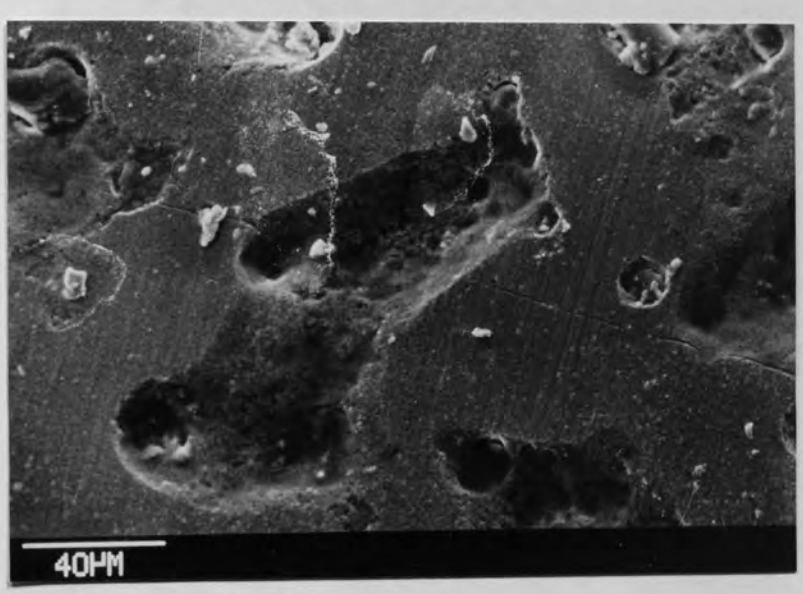

(b) Worn surface

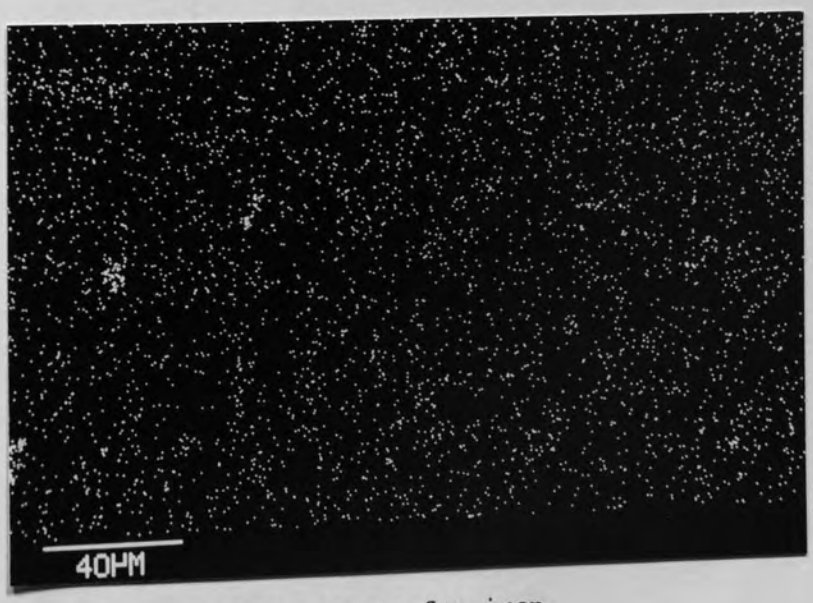

(c) X-ray map for iron

Figure 79. The surface of heat treated electroless nickel-PTFE after runnung against an EN 31 disc for 1 hour, sliding speed 50 cm/s load 2 Kg

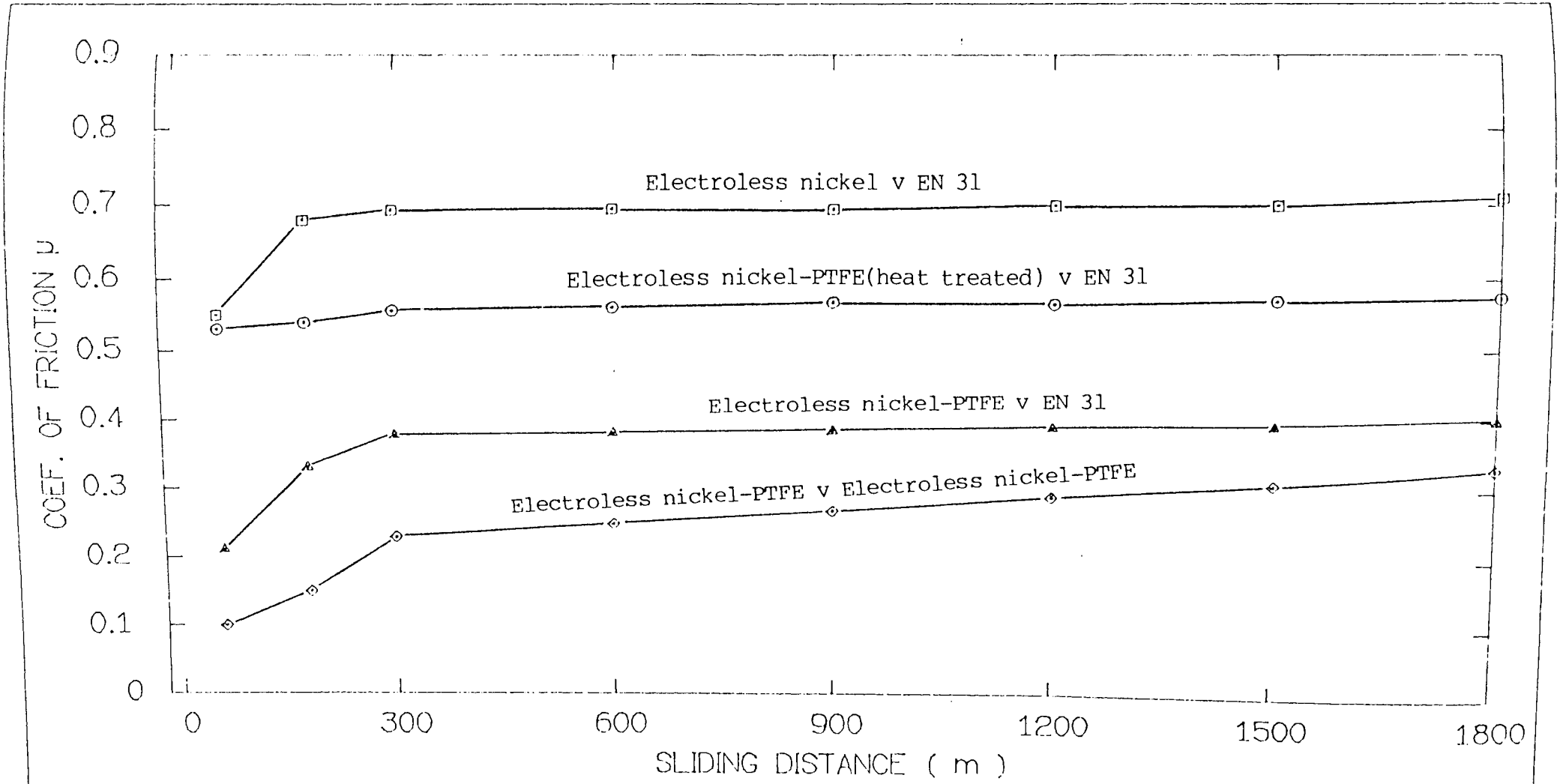

Figure 80. The effect of PTFE on the coefficient of friction of electroless nickel with sliding distance from pin on disc wear testing. The first material quoted was the coating on the pin, electroless nickel-PTFE was from source one. Sliding speed 50 cm/s, load 2 kg

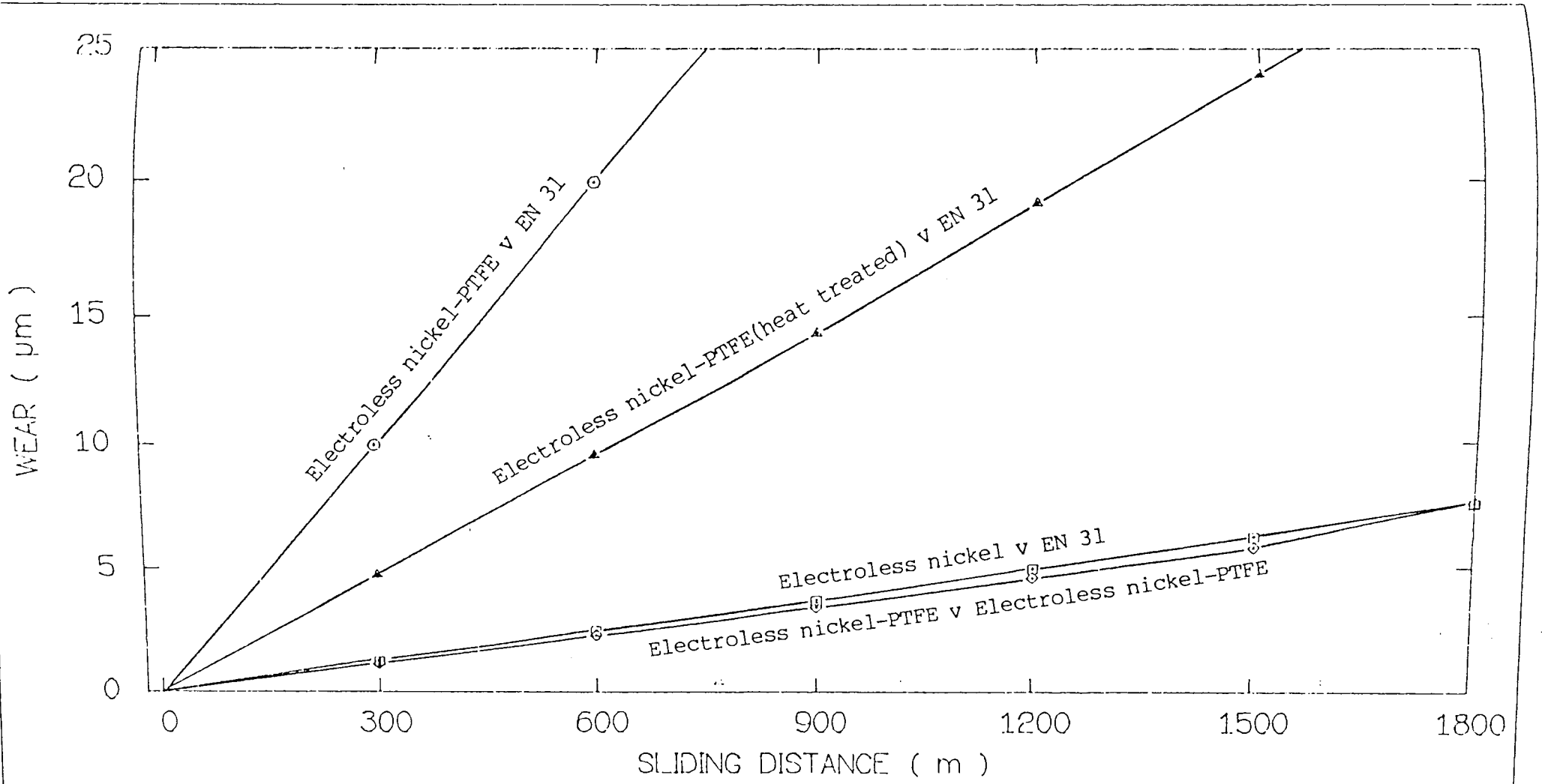

Figure 81. The effect of PTFE on the wear rate of electroless nickel with sliding distance from pin on disc wear testing. The first material quoted was the material on the pin. Sliiding speed 50 cm/s, load 2 kg

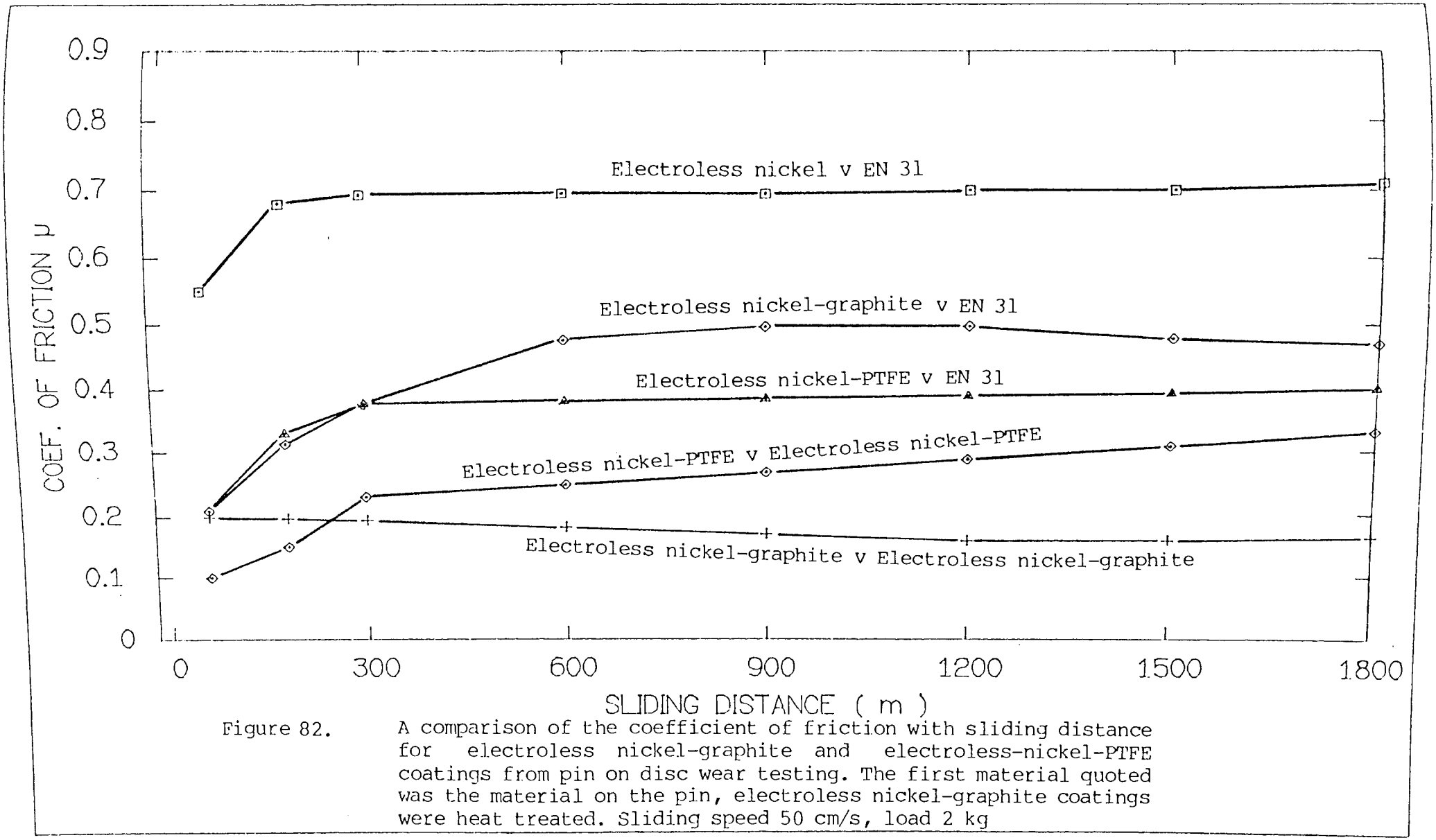

Figure 82. A comparison of the coefficient of friction with sliding distance for electroless nickel-graphite and electroless-nickel-PTFE coatings from pin on disc wear testing. The first material quoted was the material on the pin, electroless nickel-graphite coatings were heat treated. Sliding speed 50 cm/s, load 2 kg

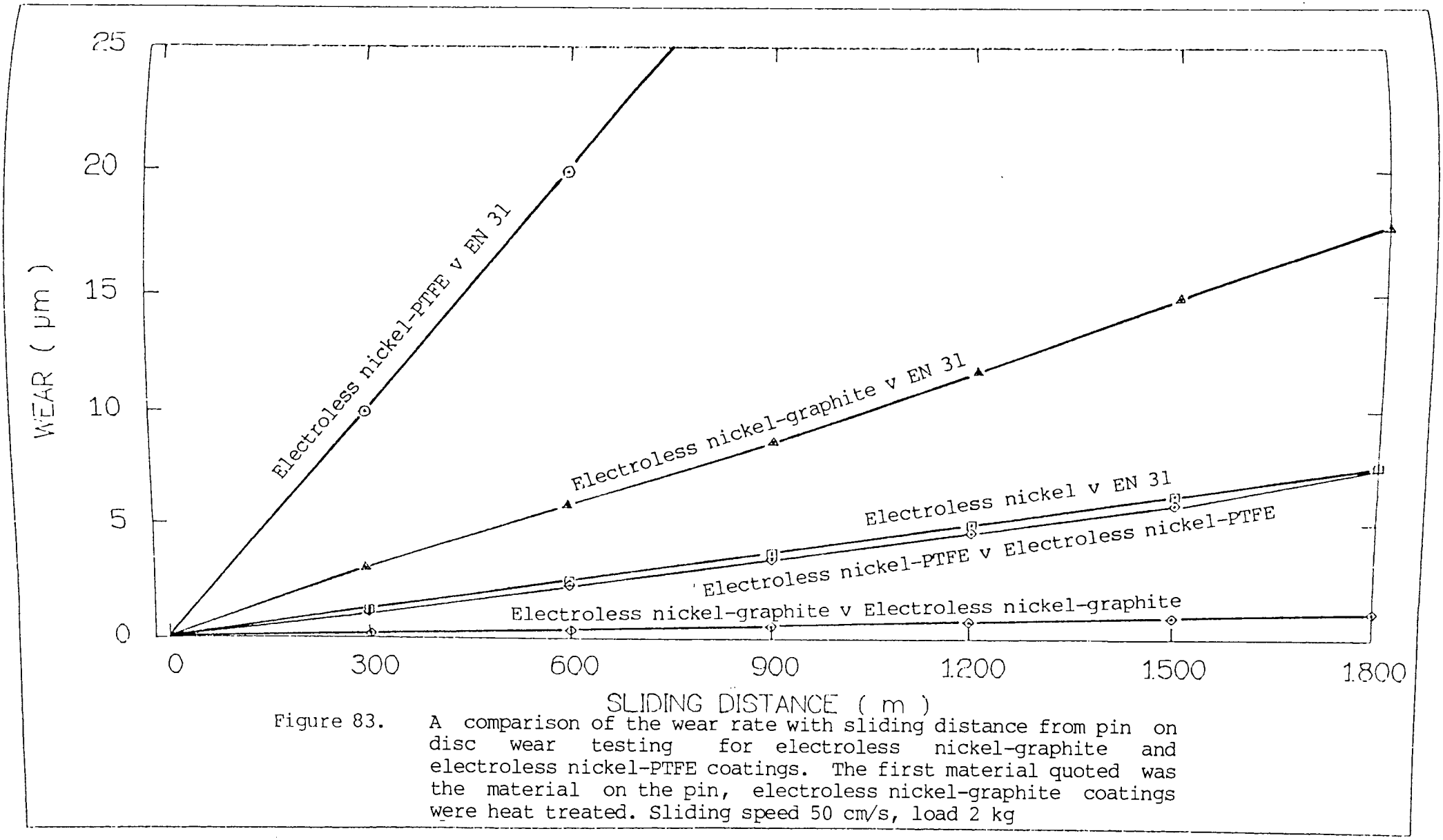

Figure 83. A comparison of the wear rate with sliding distance from pin on disc wear testing for electroless nickel-graphite and electroless nickel-PTFE coatings. The first material quoted was the material on the pin, electroless nickel-graphite coatings were heat treated. Sliding speed 50 cm/s, load 2 kg

6.7.2.2 Crossed Cylinder Wear Testing Results

The results for electroless and electrolytic nickel-PTFE deposits from BAJ Ltd when tested as the rotator and stator against a combination of different counterfaces are shown in table 21 and figure 84.

Table 21. Electroless and Electrolytic Nickel-PTFE Friction and Wear Results

Rotator	Stator	Vol.% PTFE	Coefficient of friction		Rotator Wear Profile μm^2	Stator Wear Profile μm^2
			Kinetic	Static		
ELN	SS	-	0.42	0.58	23.9	21.7
ELN-PTFE	SS	3.0	0.30	0.42	25.0	20.1
ELN-PTFE	SS	6.4	0.31	0.43	28.9	22.1
ELN-PTFE	SS	13.8	0.40	0.49	26.0	21.5
ELN-PTFE	SS	18.0	0.42	0.56	29.5	23.3
ELN-PTFE	SS	25.0	0.35	0.46	24.8	20.7
ELN	ELN	-	0.25	0.35	53.6	45.1
ELN-PTFE	ELN-PTFE	3.0	0.24	0.43	25.6	22.9
ELN-PTFE	ELN-PTFE	6.4	0.19	0.36	18.9	15.7
ELN-PTFE	ELN-PTFE	13.8	0.24	0.36	19.3	15.5
ELN-PTFE	ELN-PTFE	18.0	0.14	0.17	9.2	8.4
Ni-PTFE	SS	7.2	0.12	0.18	9.3	7.1
Ni-PTFE	SS	14.5	0.12	0.12	8.1	5.4

Table 21. Continued

Ni-PTFE	SS	24.5	0.10	0.12	6.1	2.0
Ni-PTFE (Machined)	SS	24.5	0.10	0.12	5.8	3.9
Ni-PTFE	MS	7.2	0.17	0.29	12.2	9.1
Ni-PTFE	MS	14.5	0.13	0.15	11.4	10.1
Ni-PTFE	MS	24.5	0.13	0.15	9.0	7.3
Ni-PTFE	Ni-PTFE	7.2	0.12	0.14	11.1	10.1
Ni-PTFE	Ni-PTFE	14.5	0.11	0.13	9.7	6.2
Ni-PTFE	Ni-PTFE	24.5	0.10	0.11	6.9	4.2
SS	Ni-PTFE	7.2	0.71	0.79	19.6	37.2
SS	Ni-PTFE	14.5	0.67	0.78	18.6	36.3
SS	Ni-PTFE	24.5	0.56	0.64	16.2	39.8

ELN-PTFE = Electroless nickel + 0.75 μm PTFE, un-heat treated.
Ni-PTFE = Electrolytic Nickel + 10 μm PTFE.
SS = Stainless Steel.
MS = Mild Steel.

Electroless nickel-PTFE deposits, produced with 0.75um PTFE and when run as the stator against mild steel and stainless steel stators, experienced reduced initial values of the coefficient of friction. The greatest reductions were achieved with the highest levels of PTFE within the deposit. As the test proceeded however, these levels were not maintained and quickly increased to levels equivalent to electroless nickel against stainless steel.

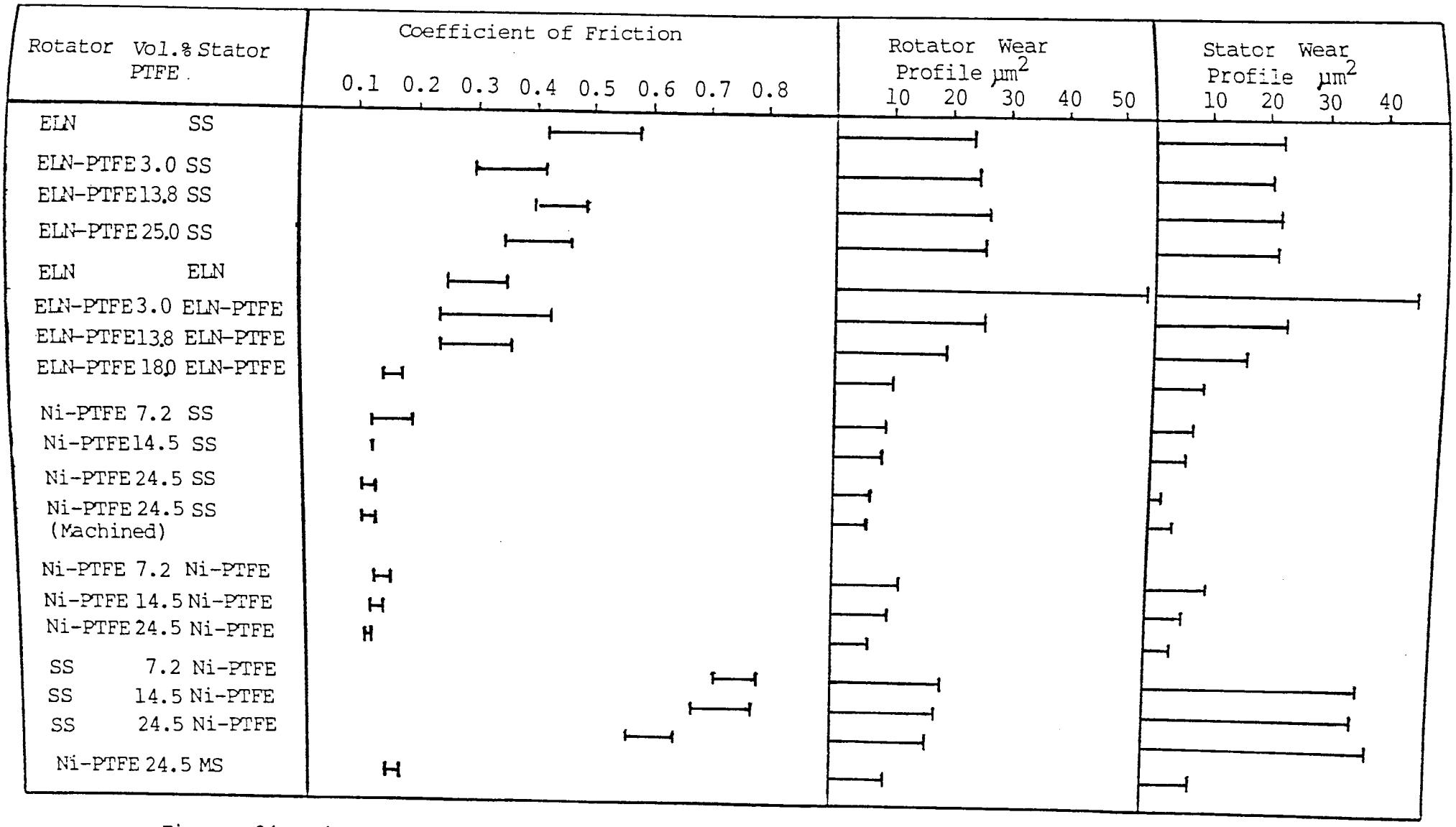

Figure 84. The coefficients of friction and wear rates of electroless-PTFE deposits from crossed cyinder wear testing

The overall wear rates were slightly less for PTFE-containing deposits than electroless nickel deposits. This could be explained by reduced initial wear rates when the coefficient of friction was low.

Electroless nickel-PTFE coated rotators run against electroless nickel-PTFE coated stators produced lower or equivalent values of friction to the above. These initially low values increased to that of electroless nickel against electroless nickel with sliding distance except with the highest PTFE levels which produced a significantly reduced final value of 0.17, as compared to 0.35 for electroless nickel against electroless nickel. Wear rates were also significantly reduced from 5.3 for electroless nickel against electroless nickel to 0.72 for electroless nickel-PTFE against electroless nickel-PTFE at the highest PTFE content.

Electrolytic nickel-PTFE deposits, produced with 10 µm PTFE, showed a significant improvement in coefficient of friction and wear rates. Introducing PTFE into the deposit on the rotator reduced the initial values of friction and also significantly reduced the final values of the coefficient of friction even at the lowest levels of PTFE in the deposit. At the maximum levels of PTFE in the deposit initial low levels of friction could be maintained through out the test, showing no signs of increasing even after extended periods of testing, ie 4 hours.

Against a mild steel stator nickel-PTFE deposits gave low values for the coefficient of friction throughout the period of the test. The best results were again produced with the highest levels of PTFE within the deposit. Overall the values for friction were slightly higher against mild steel stators than stainless steel stators and this was also reflected in the higher levels of wear against mild steel.

When run against themselves nickel-PTFE deposits produced low initial values of friction which could be maintained throughout the test even at the lowest levels of PTFE contents. Wear rates were slightly higher than against stainless steel.

When nickel-PTFE deposits were used as the stator and stainless steel cylinders used as the rotator a low initial period of friction could be achieved . This was however short, with deposits containing the lowest levels of PTFE . This period of low friction increased with PTFE levels in the deposit, final values of friction were however high. Wear of the stainless steel rotator was moderate as most of the wear took place on the nickel-PTFE stator.

When a surface ground nickel-PTFE deposit with 10 μm particle size PTFE, was run as a rotator against a stainless steel stator the coefficient of friction and wear rate were of a similar result to that of an unground coating; quite unlike the results for nickel-graphite which could not reproduce the unground results and gave much higher values of friction.

6.7.3 Electroless Nickel-Chromium Composite Coatings

6.7.3.1 Pin on Disc Wear Testing Results

Electroless nickel-chromium composite coatings, with an average of 15.8 volume per cent chromium content, were tested on the pin on disc machine. Before wear testing deposits were heat-treated for 1 hour at 400°C and also 16 hours at 850°C. The results of the wear tests of these deposits, run against an EN 31 disc, are shown in table 22 and figures 85 and 86.

Table 22. Coefficient of Friction and Wear Rate of Heat Treated Electroless Nickel-Chromium Coated Pins against an EN 31 Disc

Pin	Vol.% Cr	Initial μ		Final μ		Mean wear rate x10-7mm/cm
		Kinetic	Static	Kinetic	Static	
ELN	-	0.49	0.90	0.50	0.92	0.42
ELN-Cr (400°C,1hr)	15.5	0.56	0.88	0.58	0.73	1.24
ELN-Cr (850°C,16hrs)	16.1	0.32	0.46	0.58	0.74	0.82

Disc = EN 31, ELN = Electroless nickel, heat treated 400 °C 1hr.

Deposits heat treated at 400°C for 1 hour showed high levels of friction and wear rates from the beginning of the test, and were maintained at these levels throughout the test. When heat treated at 850°C for 16 hours however, the initial values of

friction were moderate, μ = 0.39. This value was maintained for a sliding distance 300m, figure 86, before the coefficient of friction increased sharply to a much higher value of 0.66. In this initial low friction period, wear rates were also low, before rising in conjunction with the increase in the coefficient of friction.

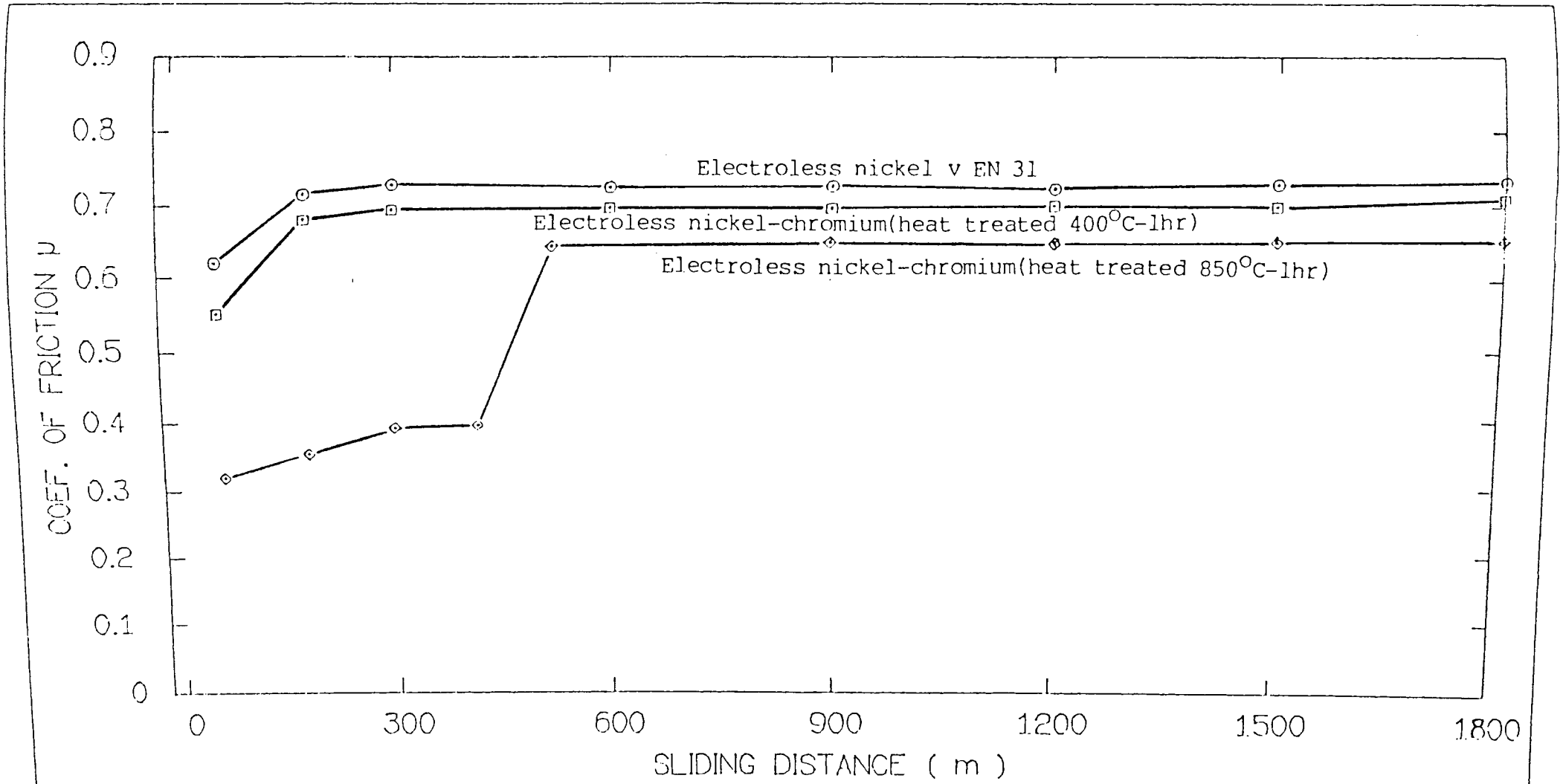

Figure 85. The effect of codeposited chromium (4 μm nominal particle size) on the coefficient of friction of electroless nickel with sliding distance from pin on disc wear testing. Sliding speed 50 cm/s, load 2 kg, disc material EN 31

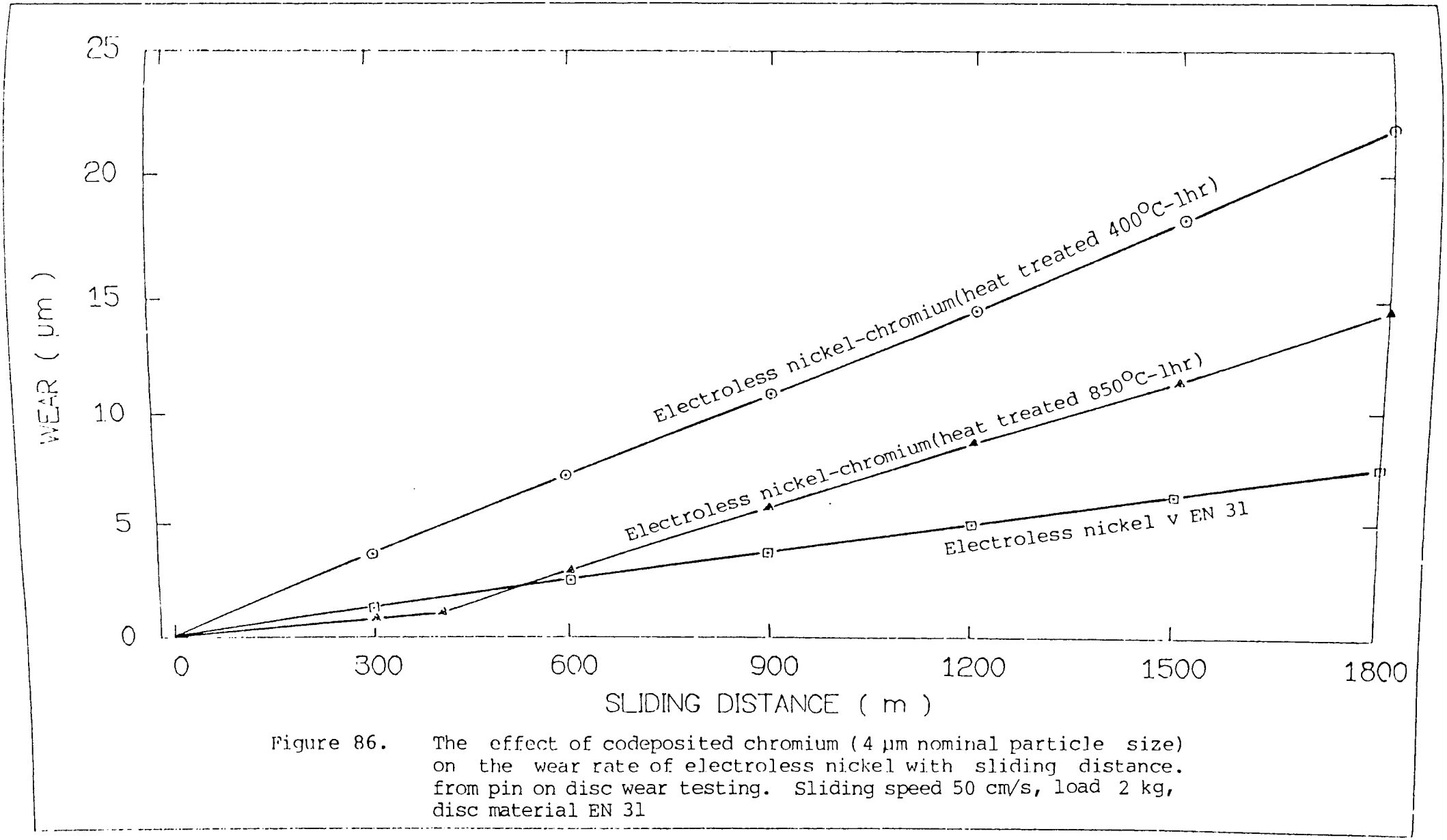

Figure 86. The effect of codeposited chromium (4 µm nominal particle size) on the wear rate of electroless nickel with sliding distance. from pin on disc wear testing. Sliding speed 50 cm/s, load 2 kg, disc material EN 31

CHAPTER VII

DISCUSSION

7.1 SOLUTION STABILITY

One of the first objectives of this work was to produce stable, particle containing, electroless nickel solutions. The experimental results showed that the most suitable method of stabilising such solutions was by the addition of heavy metal cations.

Stabilisation by organic stabiliser relied on complete coverage of the surface of the particles to provide stability. If not completely covered, the graphite particles were able to initiate the electroless reaction. Because of the very large surface area of the particles, 412 m^2/g for graphite, a high concentration of organic stabiliser was required to cover this area. Adsorption of the stabilisers also followed an exponential adsorption curve, with a rapid initial adsorption providing near stabilisation but with complete saturation taking much longer as the adsorption rate slowed down.

Particles added to an organic stabilised solution rapidly adsorbed all organics present in solution until the surface area of the particles was completely covered. A critical amount was then required to remain in solution to maintain overall stability of the solution. If this was not maintained, as

was the case, with stabiliser still being slowly adsorbed to obtain complete saturation according to the exponential adsorption rate, the critical stabiliser concentration of the solution could not be maintained and instability again resulted.

Stabilisation by heavy metal ions provided a much simpler, and more effective, stabiliser system. Heavy metal ions conferred stability by having a high overpotential for hydrogen[178]. This inhibited the hydrogen reaction within the electroless nickel reaction chain and thus prevented deposition of the nickel. A solution stabilised by heavy metal ions appeared not to rely on adsorption and complete coverage of the particle but rather on stabilisation within the solution; therefore much less stabiliser needed to be added to the solution.

When particles were added to this type of electroless nickel solution, stability was therefore maintained by the prevention of the hydrogen reaction occurring on the particle surface. The solution remained unreactive until an additional catalytic surface was created to initiate the hypophosphite reaction which was capable of overcoming the higher hydrogen overpotential.

This system was the most successful at stabilising graphite containing solutions. It also proved useful with chromium containing solutions where primary stability was provided by the chromium oxide layer around the particle. This layer, although very thin, prevented the chromium metal from

catalysing the hypophosphite reaction, however organic stabilisers were still adsorbed with time from the solution. This lost stabiliser had to be replaced to maintain the overall stability of the solution. As additional organic stabilisers would also have been adsorbed, heavy metal ions were again used to provide the long-term stability within the solution.

7.2 SURFACTANTS ADDITIONS

The addition of graphite to electroless nickel solutions showed that the graphite was difficult to wet by the solution. To overcome this problem surfactants were used to promote wetting; the most successful being a blend of non-ionic and anionic surfactants.

Surfactants consist of a large non-polar group and a polar group. The lyophobic non-polar portion is usually a hydrocarbon that may also be a fluorocarbon and can be aliphatic or aromatic. The lyophitic group is usually an ionic group. Ions have a strong affinity for water owing to their electrostatic attraction to the water dipoles and draw fairly long hydrocarbon chains into the solution with them.

Surfactants are classified as anionic, cationic or non-ionic according to the charge carried by the surface active part of the molecule. Sodium stearate is an example of an anionic surfactant.

$$CH_3\,(CH_2)_{16}\,COO^-\,Na^+$$

non polar hydrocarbon — polar ion

This type of surfactant is used to produce an emulsion of oil in water. The large non-polar hydrocarbon will dissolve in the oil, and the polar sodium atom will dissolve as a cation in the water, leaving a negatively charged oxygen anion atom "wetted" by the attraction of the polar water molecules. The fatty acid anion becomes adsorbed to the oil/water interface and lowers its interfacial tension.

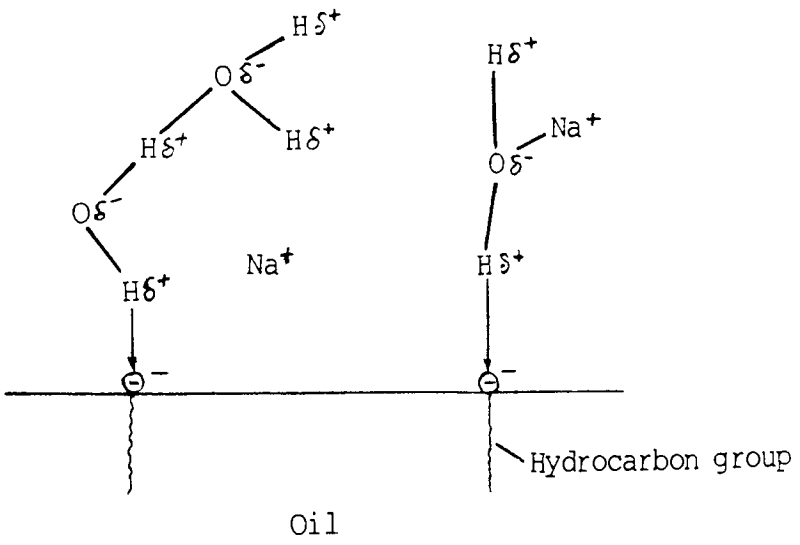

Figure 87. The wetting action of Sodium Stearate between oil and water

With this work anionic, cationic and non-ionic surfactants were used. A graphite particle in a solution of anionic and non-ionic surfactant will have the non-polar hydrophobic parts of the surfactants adsorbed onto the particle. The dissolving of the cation will leave a negatively charged anion group on the surface in the case of anionic surfactants and an uncharged group in the case of non-ionic surfactants. Cationic

surfactants will give a net positive charge as a result of the dissolving polar ion.

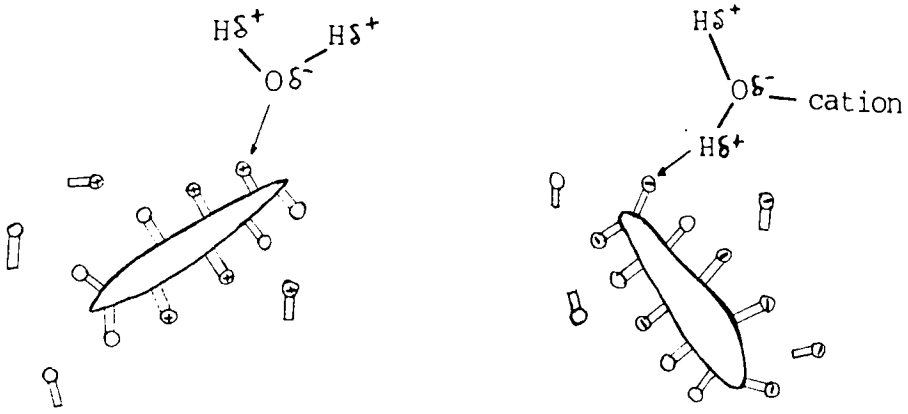

Cationic-Nonionic wetted particles

Anionic-Nonionic wetted particles

Figure 88. The adsorbtion of surfactants onto particles

The particles were subsequently wetted by the attraction of the polar water molecules. The resultant charge on the particle surface also maintained the particles as a dispersion throughout the solution.

A system in which charged particles are dispersed must contain equivalent amounts of oppositely charged ions (counter ions) to satisfy an overall condition of electro-neutrality. Ions of similar charge to that of the particles (co-ions) may also be present. To maintain electro-neutrality there must be a neutralising excess of counter ions over co-ions in the locality of each charged particle.

For a negatively charged particle in an electroless nickel solution electro-neutrality is most likely maintained by specific ion adsorption of the counter ions of nickel and also hydrogen depending on the pH. This gives a compact (Stern) layer of counter ions attached to the surface by electrostatic and Van der Waals forces[179]. In the locality of the charged particle there is a balance between electrical forces which are tending to attract counter ions and repel co-ions. Excess counter-ions near to the charged particle surface screen the electrostatic attraction for counter-ions further away from the particle surface. This gives an initially rapid drop off in electrical potential. With increasing distance the potential continues to fall, but much more slowly, becoming zero at an infinite distance from the particle surface where the distribution of ions is uniform. The effect of the electrical forces is to create a diffuse double layer referred to as the Gouy-Chapman double layer[180], figure 89. For cationic charged graphite particles with a positively charged surface electro-neutrality would be expected to be balanced by sulphate ions and hypophosphite ions.

The zeta potential of a particle is the potential at the surface of shear between the charged surface and the electrolyte solution. This is usually located just outside of the Stern layer. Graphite particles wetted with cationic surfactants therefore had net positive zeta potentials while particles wetted with anionic surfactants had net negative zeta potentials.

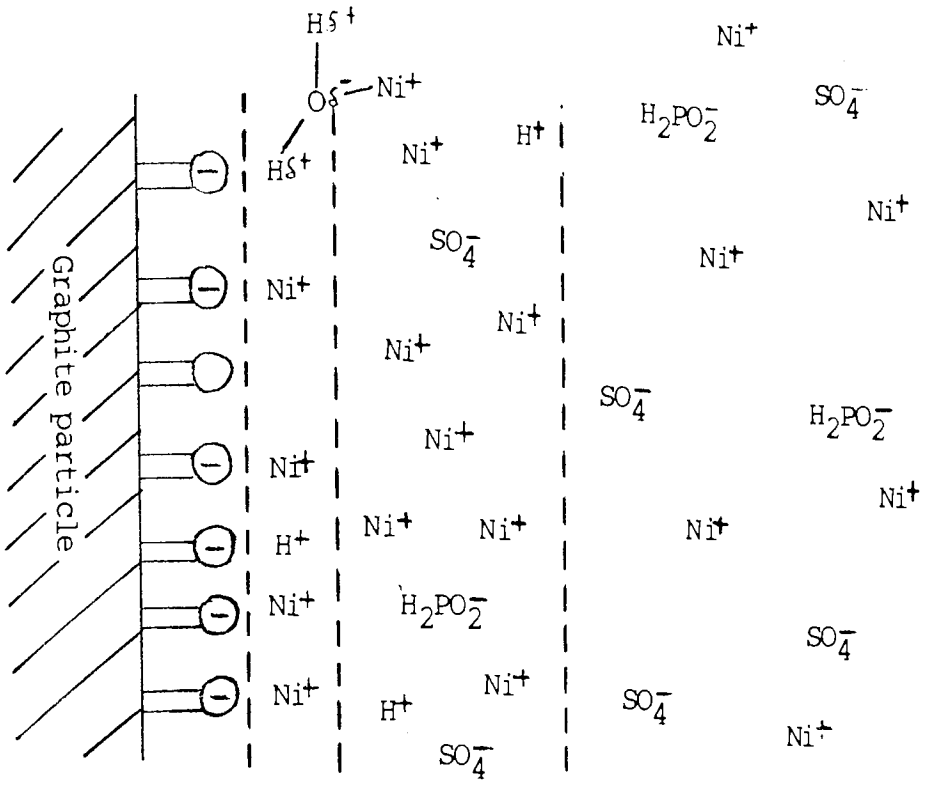

Figure 89. A schematic diagram of the diffuse double layer created on the surface of graphite particle in an electroless nickel solution wetted with anionic and nonionic surfactants

7.3 PARTICLE CODEPOSITION

The theory is widely held that for codeposition of PTFE particles with electroless nickel, a cationic surfactant is required to produce a positively charged particle which can be electrostatically adsorbed onto the negatively charged plating surface. If the above models are correct, this would seem an over simplification of PTFE adsorption.

The use of cationics and anionics in this work showed that both particles charged positively and negatively were adsorbed onto the plating surface. If adsorption were by electrostatic adsorption then particles with a net positive charge from the initial cationic surfactants could well be expected to have adsorbed onto the plating surface. However, particles with a net negative charge from the initial anionic surfactant would not be expected to have adsorbed onto the plating surface, something which clearly did occur.

Adsorption of the particles could theoretically occur by either electrostatic attraction or physical adsorption. The electrostatic attraction of a particle for the plating surface at its plating potential is quite feasible and supported by data. Fuks et al[181], have found that adhesion of a number of particles to various surfaces in aqueous solution is affected by the metal ion concentration and valency. Similarly, Zimon et al[182] also found metal ion concentration and valency to significantly affect adhesion of glass particles to a glass

surface in aqueous solution. Adhesion of particles was shown by Koros et al[183] to be dependent on dielectric constant of the medium further demonstrating the probability of electrostatic attraction.

Van der Waals forces alone have been shown to result in the attraction of solid to solid in an electrolytic medium. Isreala et al[184] measured the force between two mica sheets in aqueous potassium nitrate solution and found that under certain conditions, as the similarly charged sheets approached, the onset of repulsion was preceded by a period of attraction. This attraction was of the order expected for Van der Waals forces. The interaction of the mica sheets was interpreted in terms of the combined effects of attractive Van der Waals forces and repulsive electrostatic forces. Similarly Deryagen et al[185] interpreted experiments involving the approach of two crossed wires within an electrolyte in terms of these combined attractive and repulsive forces.

The interaction between a positive charged particle and a negatively charged surface may therefore be expected to be attractive at any distance, taking into account both electrostatic and Van der Waals forces. However, for a particle and surface of similar charge, as the particle approaches the surface it may be expected to experience an initial (secondary) attractive force, followed by a repulsive (electrostatic) force and then a second (primary) attractive force.

For graphite particles with a positive Zeta potential electrostatic forces could be held responsible for adsorption but for negatively charged particles adsorption onto the negatively charged plating surface then only Van der Waals forces could be responsible for the observed adsorption by electrostatic methods.

In this work both positive and negatively charged particles were observed to be adsorbed onto the negatively charged plating surface. White[161] also observed positively charged alumina particles could be adsorbed onto both anodically and cathodically polarised surfaces. This would suggest that electrostatic forces play no real significant part in the codeposition of particles. The adsorption of the graphite particles onto an electroless nickel plating surface may then be interpreted in terms of physical adsorption.

Once particles have been adsorbed onto the plating surface formation of a particle-surface bond may result, ultimately leading to codeposition of the particle. Adsorption of a particle onto the surface does not, however, automatically lead to codeposition. This was illustrated by graphite particles dispersed with cationic surfactants. These particles appeared to be adsorbed onto the plating surface yet were not codeposited. Plating however, occurred through the adsorbed particles. This produced a standard electroless nickel deposit without codeposition of particles, but with the particle riding ahead of the plating surface.

White and Foster[161] also observed this effect with alumina on a copper plating surface. They concluded that the adsorption of metal ions onto the particle was of major importance for codeposition of particles. For codeposition, a particle must have a layer of solution metal ions adsorbed to its surface. The importance of these metal ions is based on their ability to be reduced to form a particle-surface bond between the physically adsorbed particle and the plating surface. If these metal ions were not adsorbed onto the particle or were tied up on the surface by combination with other elements, the ions could not be reduced and thus could not form a particle-surface bond preventing codeposition.

Graphite particles dispersed with anionic surfactants have been considered to have a negative surface to which nickel ion can be adsorbed. According to the above model such particles should be satisfactorily adsorbed with the reduction of nickel ions unhindered to form a particle-surface bond and codeposition should occur. The results showed that anionic dispersed graphite particles were in fact codeposited.

With cationic dispersed graphite particles a positive surface charge is produced. This can only be electrically balanced in solution by adsorption of negatively charged ions from solution. These ions are unreducable ions at the plating surface and therefore do not promote surface-particle bonds. It would therefore not be expected for cationic dispersed graphite particles to be codeposited. The results again showed this to be

the case with particles appearing to be adsorbed onto the surface but riding ahead of the advancing metal surface without codeposition. Codeposition of PTFE dispersed by cationic surfactants has, however, been well reported[37]. If the above theory is correct, particles must also have associated nickel ions capable of producing a particle-surface bond.

References[37,135,186] show that the dispersion of PTFE is actually maintained by a blend of non-ionic and cationic surfactants and in some cases a blend of non-ionic, cationic and anionic surfactants as per the British Patent 1,511,109[135]. It may therefore be possible for nickel ions to adsorb onto the non-ionic sites and any remaining anionic sites or even the PTFE. Nickel ions may also be adsorbed onto the surface in conjuction with water molecules. Also despite coulombic repulsion co-ions can be incorporated into the Stern layer by Van der Waals attraction, thus nickel ions may be incorporated though the water negative layer of SO_4^- and $H_2PO_2^-$ ions. A second effect is that the addition of potential determining ions, or counter ions which are readily incorporated into the Stern layer can lead to a reversal of the double layer charge and a second region of stability, again posssibly containing nickel ions. A further possiblity is that of hypophosphite ions being adsorbed onto the particle. These ions may be able to reduce nickel ions onto the particle surface and thus form a bond from the particle to the surface.

Accepting that cationic surfactants can be used to codeposit particles, then the cationics used in this work may have been unsuitable for codeposition. The dispersion produced may have been too stable or may have prevented the correct form of adsorption such that one of the above mechanism could not operate. Also if the balance of cationic to non-ionic surfactant was important, as indicated in the patent 1,511,109[135], it is likely that the correct balance was not found in this work.

The adsorption of chromium particles may also be expressed in similar fashion. As no surfactants were added to the solution there will not have been any superimposed charge from this source. Particles covered in a layer of chromium oxide will most likely have adsorbed nickel ions from the plating solution onto their surface to give a positive Zeta potential for each particle. The degree of adsorption being dependent on pH and temperature. Particles may then have been physically adsorbed onto the surface, where the nickel ions could have been reduced to form a particle surface bond. White and Foster[161] showed this bond to occur very quickly for electrolytic nickel alumina with roughly 75% of the adsorbed particles being firmly attached by deposition of 500 nm of nickel.

Particle-surface bonds are most likely to occur by the formation of a number of solid-solid bonding sites. High metal ion adsorption may lead to a relatively high number of solid connections whereas low nickel ion adsorption may result in the formation either of a reduced number of bonds or weaker bonding

sites. Once sufficient connections have formed the displacement of the remaining solvent molecules, anions and unreducable cations may occur. The particles will then be encapsulated by metal deposition.

For chromium and in the specific case of graphite, adsorbed surfactants, and possibly other molecules, such as hydrogen ions, will become included into the deposit. These may have adverse effects if say sulphur is incorporated from the surfactants. Support for the inclusion of impurities is given by Chen[89] who found that gold-alumina composites expand on heat treatment and attributed this to gassification of impurities that were adsorbed onto the particles. The inclusion of impurities may also have occurred if the particle-surface connections formed only at specific sites and was followed by submersion of the particle by depositing metal, so encapsulating impurities between the connections.

There has been no serious attempt to explain codeposition of particles in electroless deposits in comparison to the many detailed studies of codeposition from electrolytic systems. The model proposed in this current work was based on the observations that both positively and negatively charged particles could be adsorbed onto the plating surface, yet only negatively charged particles were codeposited. Although no quantitative results were obtained this made it clear that codeposition was not simply by mechanical entrapment, as often quoted, but comparisons were instead found with those models

proposed for electrolytic systems[161,162]. To shed more light on this area a more detailed study of surfactants, ion adsorption and the corresponding zeta potentials in respect to particle adsorption is required.

7.4 CONCENTRATION OF PARTICLES IN SOLUTION

The curves illustrated in figures 41 and 45 showed the effect of concentration of particles in solution on the volume per cent codeposited. As the concentration was increased more particles were present in the solution so increasing the incidence of particles striking the plating surface in unit time. Consequently the number of particles available for incorporation increases and is thus the rate determining step at this stage.

The growing nickel deposit is able to accept this increase in particles up to the point where the number of particles arriving at the growing surface is equal to the number that can be accepted onto the surface. Any further increase in the number of particles arriving at the surface will have no effect as the surface is completely covered and effectively saturated. Thus the graph of particle concentration in solution against volume per cent codeposited levels out as the saturation point is reached. As concentration increases beyond saturation the volume per cent codeposited may even decrease as arriving particles now collide with particles that have already been adsorbed onto the plating surface. This may result in the displacement of the adsorbed particles. These particles may be

replaced, but could just as quickly be displaced again, especially as concentration increases further. The net result is a reduction in the number of particles codeposited. In particular this may be the case for chromium particles which are more dense than graphite flakes and, coupled with the effects of gravity and solution movement, could provide sufficient force to displace adsorbed particles. Evidence of this displacement with increased concentration of particles in solution was shown by Gawrilov[167] using electroless nickel-alumina.

The maximum concentration of particles codeposited was found to be 6.7 volume per cent for 2 micron graphite powder at 60 g/l, and 16.5 volume per cent at 24 g/l for 4 micron chromium powder. The results for graphite were comparatively low for codeposited volumes as compared to the chromium and the relevant literature for alternative materials[37] [164]. Figure 44 shows that the plating surface was uniformly covered in graphite flakes. A closer examination of the particles adsorbed to the surface showed that the graphite particles had a tendency to be attached by one end of the flake or by its "tail". This is understandable as graphite flakes fall through the solution oscillating from edge to edge (ie. falling leaf-like). The probability of a settling flake landing on an edge is therefore higher than its settling on either of the two flat surfaces. A less likely alternative is that adsorption of nickel ions was most likely to occur preferentially on the higher free energy surfaces of the edges. It is therefore possible that a stronger particle surface bond could have been formed at the edges of the

flakes promoting adsorption of particles landing on an edge rather than particles landing on the flat surfaces of the flakes.

Figure 44 also showed that there was a considerable area of the surface that could be considered suitable adsorption sites unoccupied by particles. Some explanation must then be considered for this less than complete coverage even though saturation appeared to have been achieved. The upright particles may have tended to shield adjacent surface areas making it difficult for additional particles to leave the solution and settle in these areas. Especially if the flakes settled "leaf-like" making it difficult for them to slot into the spaces. Nickel would then have deposited in the shielded areas and would not have received a particle until the shielding effect was reduced by coverage of the adsorbed particles by the depositing nickel.

The deposition of the flakes in an upright fashion and a filling in of the areas around the flakes would have prevented the flakes packing flatly and thus produced a very open structure of graphite flakes within the deposit. This open structure would explain the relatively low volume per centage of graphite codeposited. This effect can be expressed in terms of a low packing density of particles, a factor reported as an important control of particle content by Newnham and Foster[143]. Plating may also have occurred on the graphite flakes themselves again promoting a more open structure and the rougher surfaces experienced.

When graphite was codeposited with electrolytic nickel the volume per cent codeposited was also a maximum at approximately 7 per cent. This also demonstrated how the flake nature of the graphite was instrumental in determining the content of the composite irrespective of the solution.

If the particle-surface bond was produced preferentially on the edge of the flakes, then the number of flakes adsorbed may then simply reflect the number of particles settling on an edge over the surface. All other particles which settled did not produce a strong bond and were removed by solution leaving a blank area to be filled with nickel. The total volume of graphite codeposited would then be low. A saturation point was still reached by complete coverage of adsorbing and non-adsorbing particles. This explantion is less likely.

For the more equi-axed chromium particles such orientation effects were not so predominant and therefore a more closely packed particle structure was produced with higher volume per centages codeposited. The deposit content was dependent on reaching saturation of the surface in particles and the packing density of the adsorbed particles.

Figure 43 and 47 show graphite and chromium adsorption isotherms plotted according to the Langmuir relationship. The straight line would indicate that particle adsorption could be considered to have followed the Langmuir model. This model assumes that the adsorbed species do not interact with the

surface and this seems reasonable for physical adsorption of particles as the mechanism for codeposition.

Although the straight line relationship for the Langmuir isotherm appears to hold, the slope of the line should be unity for the isotherm to be fully obeyed. This was clearly not the case but may be explained by the mutual interference of particles during the adsoption process.

7.5 TEMPERATURE AND pH

Figure 48 shows that as pH and temperature were increased, so the volume per cent graphite codeposited also increased. In their work, White and Foster[161] showed that as pH and temperature were increased so the metal ion adsoption on the particles was found to increase. Bond strength also rose with pH and temperature and hence implied a strong dependence of bond strength on metal ion adsoption. Figure 48 could then be interpreted in the same fashion. As pH increased the concentration of hydrogen ions in the solution decreased. There was then reduced competition between hydrogen ions and metal ions for adsoption sites on the particle resulting in increased adsorption of metal ions. A greater number of nickel ions was now available on the surface of the particle to be reduced by the hypophosphite to form the particle-surface bond. High hydrogen adsorption at lower pH would have resulted in reduction of hydrogen which did not promote bond formation. As indicated increased temperatures also promoted the adsorption of metal ions

and hence bond formation. Overall this increased ability in bond formation may result in a greater number of particles being codeposited.

An increase in pH and temperature also resulted in an increase in plating rate, this can also be used to explain the increased particle codeposition. The straight line produced in figure 49 shows that an increased plating rate gave a greater codeposition rate.

Experiments for examining plating rates were carried out at 25 g/l, below the saturation at 60 g/l. Particles were therefore likely to be arriving at a surface with excess adsorption sites for the graphite particles. It is also likely that, because strong agitation was used for this work, particles were arriving at the surface and not remaining there long enough to allow bond formation. An increase in plating rate promoted faster and stronger bond formation by easier reduction of adsorbed nickel ions. This bond formation therefore captured a greater number of the particles adsorbing onto the surface before they could be swept away by solution movement and particle collisions. Also, with increased burial rate, there was a greater chance of an adsorbing particle colliding with the metal surface rather than another particle so increasing adsorption rate. This would explain the increased volume per cent codeposited with increased plating rate and is more likely to be the dominant affect of increased pH and temperature. At the saturation level of 60 g/l particle arrival rate is at a maximum. If nickel

deposition rate was to have exceeded this rate then it would have been more likely that the codeposited volume would decrease. This is the more commonly reported result.

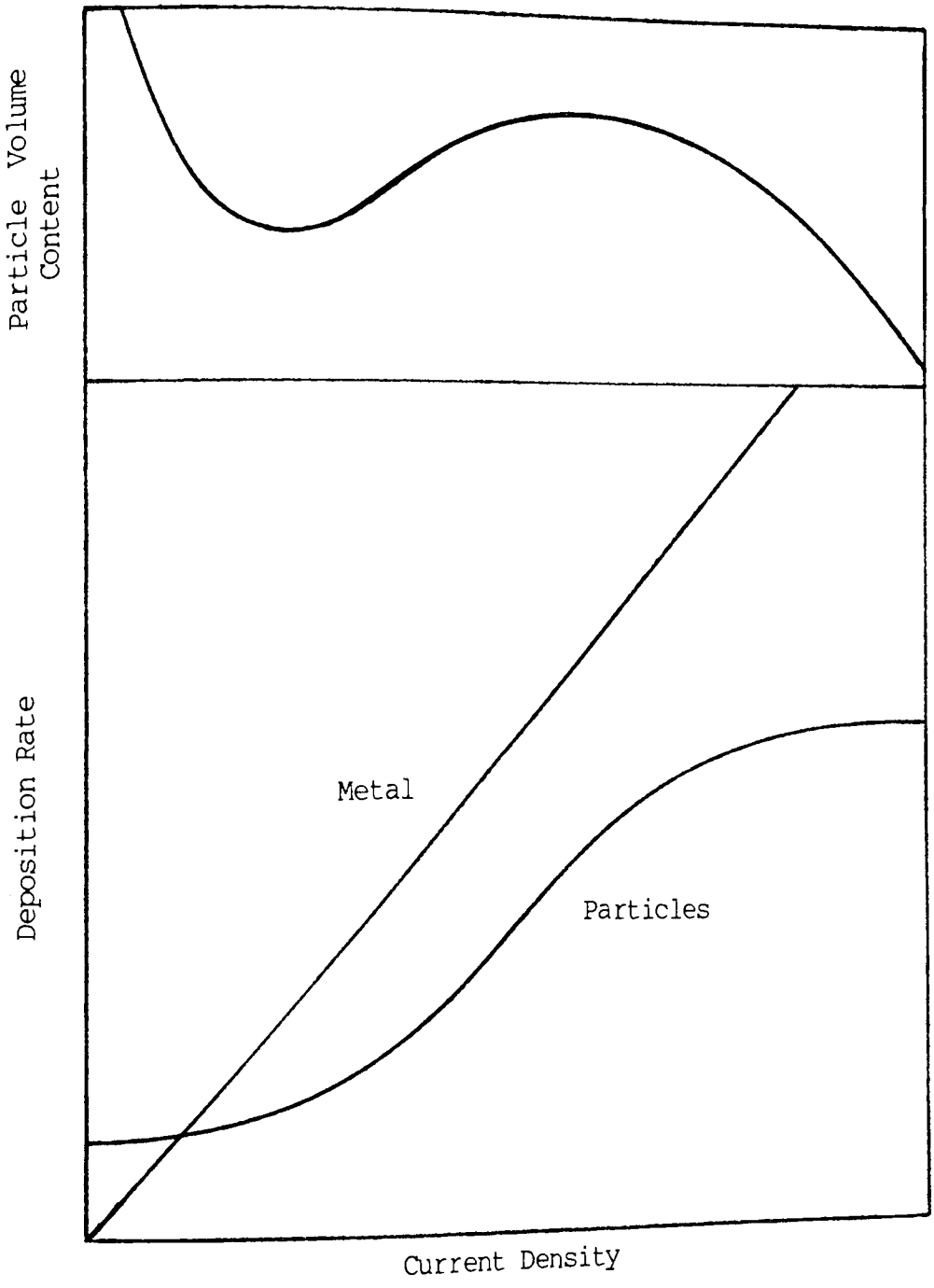

Figure 90. The effect of particle arrival rate and plating rate on particle codeposition[161]

The codeposition of chromium particles behaved in the more "conventional" manner as observed by Gawrilov[167] and for most

electrolytic systems. As plating rate was increased so the particles content of the deposit decreased. This was due to an increase in deposition of nickel at a preferential rate to the particle arrival rate.

The difference between the two systems is due to the number of particles present in solution. At 25g/l for both graphite and chromium the number of particles present was many times higher for graphite than chromium because of the difference in density and volume of the two particles. The maximum particle arrival rate was then lower for chromium than graphite and could potentially be overtaken by the metal deposition rate.

The increased hydrogen evolution with increased electroless nickel plating rate has also been reported as a mechanism for the reduction of particle codeposition. The hydrogen bubbles produced at an increased rate may have interfered with the particle arrival rate allowing metal to deposit preferentially to the particles. At saturation however, particle arrival rate most likely overcame this effect and excessive metal deposition rate was the more dominate factor.

For the surfactant covered surface of the graphite, the adsorption of metal ions onto the particle surface may have occurred more strongly on the charged surface of the anionic surfactant covered graphite than on the chromium particle. This strong adsoption may have required a greater plating rate to provide the reduction of the metal ion to produce the particle

surface bond. Particle codeposition would then have increased with plating rate as was seen.

Temperature may have a further effect on particle codeposition through the ability of temperature to reduce boundary layers which retard the approach of particles to the surface.

When a fluid flows over a solid surface a velocity gradient is set up at right angles to the direction of flow. This is due to the viscous forces acting within the fluid. The fluid in contact with the surface must necessarily be brought to rest since, otherwise, the velocity gradient and the shear stress at the surface would be infinite. The drag force resulting from the retardation of the fluid at the surface is transmitted throughout the whole of the fluid and hence the velocity gradient. For all practical purposes however, at great distances the effect of drag becomes very small and it can be regarded as being confined to a region close to the surface and is known as the boundary layer. The whole of the velocity gradient is assumed to lie within the boundary layer and, outside it, the velocity is assumed to remain constant figure 91.

For adsorption to occur particles must leave the solution and penetrate this boundary layer. Once adsorbed onto the surface they are in a region of virtually stagnant solution and can remain there undisturbed by the solution until codeposition occurs. Factors which effect the boundary layer are therefore important.

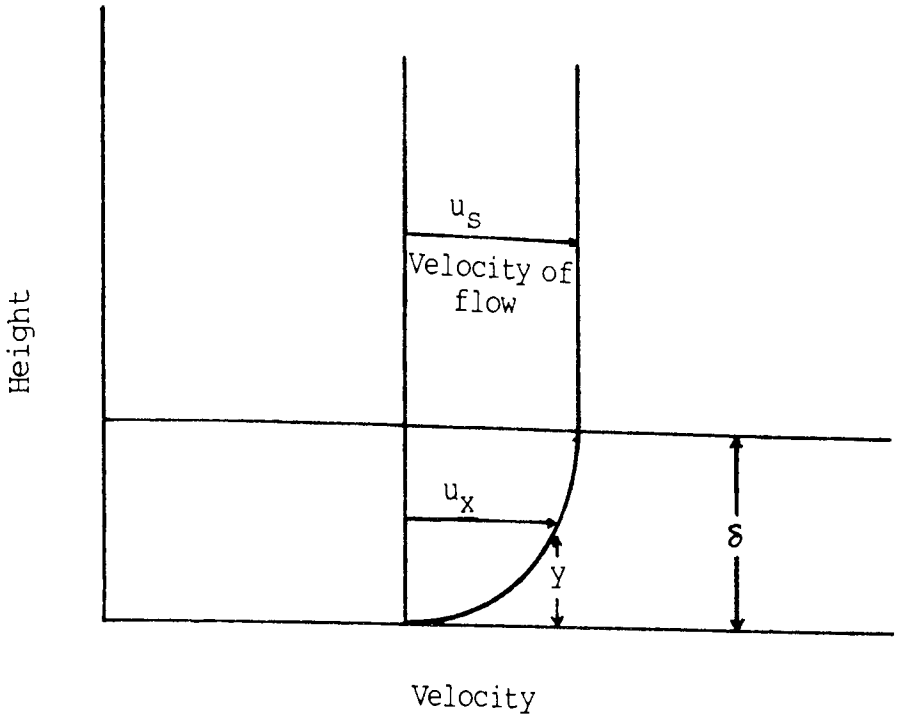

Figure 91. Velocity distribution gradient in a streamline boundary layer

The thickness of the boundary layer, developed when a fluid flows over a flat plate, is inversely proportional to the square root of the Reynolds number and therefore directly proportional to the square root of the viscosity of the liquid.

$$\frac{\delta}{x} = 4.64\sqrt{\frac{\mu}{x\rho u_s}} = 4.64\ R\ e_x^{-1/2} \qquad (54)$$

Where δ = boundary layer thickness

μ = viscosity of the liquid

ρ = density of the liquid

u_s = velocity of the bulk solution

x = distance from the leading edge of the surface

$R\ e_x$ = Reynolds number at x

An increase in temperature will reduce the viscosity of the solution and thus the boundary layer. The boundary layer thickness for an electroless nickel solution can be calculated to be reduced from approximately 1800 μm at 80^{o}C to 1000 μm at 90^{o}C. This could increase the number of particles able to leave the solution and collide with the surface, increasing the number of particles available for codeposition.

As velocity of the solution increases the boundary layer decreases. This can also have a negative effect if particles are so large as to stick out into the main solution as a result of reduced boundary layer thickness. This would increase the chance of particle removal by solution movement.

The reduced viscosity of the solution at higher temperatures may also result in a less aggressive dislodging action of the particles on the surface; this perhaps is less likely.

7.6 PARTICLE SIZE

From the curves of figures 50, it can be seen that for graphite, an increase in particle size decreased the volume per cent codeposited. As particle size increased so the number of particles for a given bath loading, ie. 25 g/l decreased. There were therefore less particles available for codeposition because of reduced arrival rate. Also if the open structure suggested was the reason for low codeposited volumes by interaction of the

flakes, i.e. low packing density, as particle size increased this effect would have been multiplied. Large particles attached to the surface at their ends would have produced greater shielding and an even more open structure than the smaller particles, decreasing the volume per cent codeposited as was seen.

Below one micron and above 10 μm no codeposition was observed to occur. Above 10 μm this was most likely linked to agitation. As was seen, to be adsorbed onto the surface, a particle had to leave the solution and penetrate the boundary layer. For increased particle size it was progressively difficult for particles to completely leave the solution without remaining part in the boundary layer and part in the solution. Such particles were then more easily removed by the moving solution in comparison to smaller particles which completely entered the static region of the boundary layer. Thus as particle size increased less particles are able to be adsorbed onto the surface.

Below 1 μm particle size the situation was not so clear. The answer may again be associated with agitation. It is possible that the agitation was too great for the very small particles making it very difficult for them to leave the solution and penetrate the boundary layer. Hydrogen liberation combined with agitation may also have prevented the particles from settling onto the surface.

Alternatively, the surface condition of the smaller particles was different from that of the larger particles. Ball milling to this size may have altered the structure such that adsorption of surfactant and nickel ions was effected and thus adversely influenced the codeposition of this particle size.

As particle size is increased the relationship normally followed with reference to deposit content is shown in figure 92[143]. As particle size is increased, packing density of the progressively larger particles is improved until a maximum is reached. Beyond this point the particles become too big for the boundary layer and are affected by agitation. It is in this region that the graphite particle size range could be considered to fall. If smaller particles could have been codeposited it is possible from this relationship that deposits with significantly higher volume per cent graphite could have been produced as packing density was improved to its maximum.

The more equi-axed 4 micron chromium particles, with a much higher packing density, would probably have been below and to the left of the maximum peak. Had a range of particle size been available, an increase in particle size would most likely have resulted in an increase in the volume per cent codeposited. As large equi-axed particles are codeposited a greater volume of the deposit is occupied than for a number of smaller particles which pack much more openly for same volume of material.

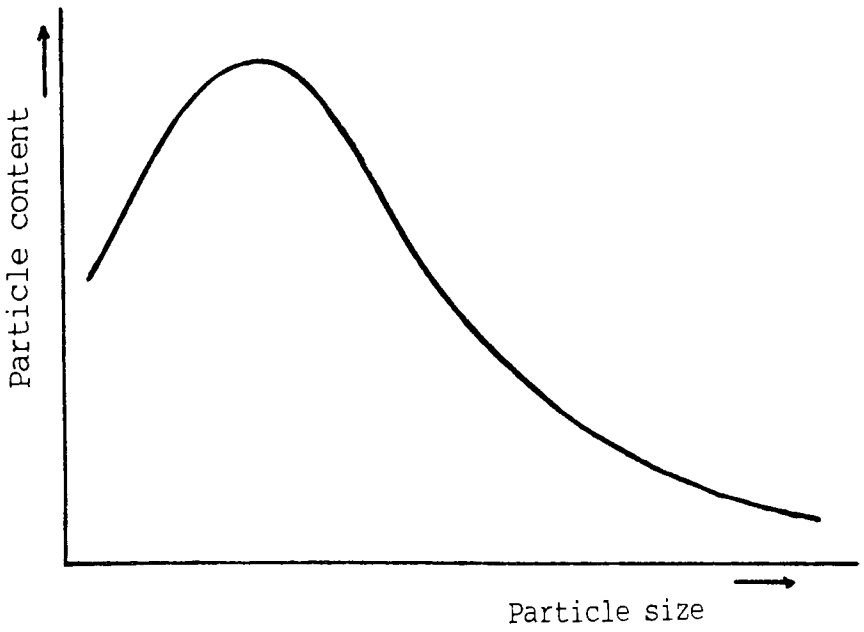

Figure 92. The variation in particle codeposition with particle size

7.7 AGITATION

In the development of the plating process it became obvious that agitation was of considerable influence in the production of composite coatings, as can be seen by reference to the results in Chapter VI, section 6.4.1.

These results showed that not only was the method of agitation important in efficiently maintaining particles in suspension but also the level of agitation, which imparted additional kinetic properties into the particle.

At 60 g/l for graphite and 20 g/l for chromium particles the number of particles available for collision with the surface was very many times more than the number incorporated, as was shown by Shiek[171]. The standard agitation used in this work was very high and thus produced high particle velocities relative to the surface. This made it very difficult for a particle to leave the solution and settle out onto the surface. The dwell time of a particle on the surface was also very low. Any factor which increased the chance of capturing a particle, ie. an increase in plating rate, would therefore have increased the volume per cent codeposited.

If however, the level of agitation was reduced, the relative velocity of the particle would alter acordingly. This in turn would enable longer dwell times of particles on the surface and easier settling from the solution. Reduced particle velocities also reduced the intensity of particle to particle collision between incoming and adsorbed particles, this reduced the dislodging effects on the adsorbed particles. A greater number of particles in solution were now able to settle on the surface and be codeposited. Thus as agitation was reduced so the efficiency of the solution producing a composite coating was increased. This was demonstrated for graphite with advanced agitation systems developed by BAJ Ltd. figure 93.

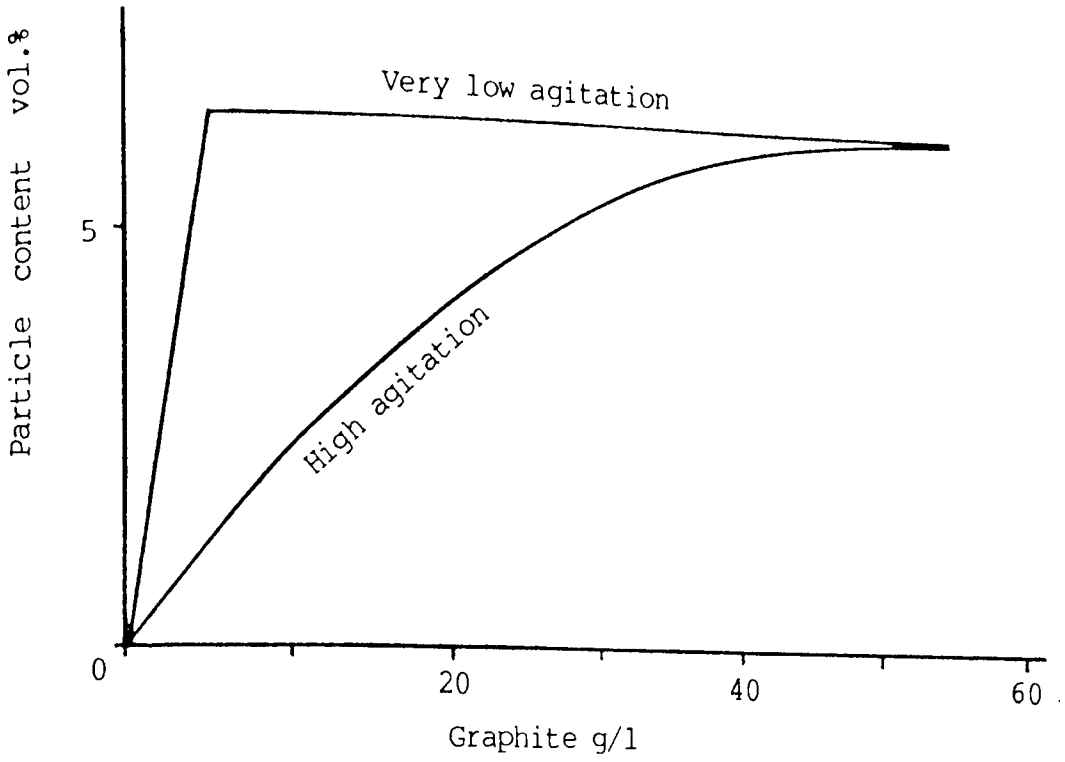

Figure 93. The effect of agitation on particle codeposition particle size 2 μm, temperature 90 °C, pH 5.0

At high levels of agitation a maximum content of 6.7 per cent was reached at 60 g/l with electroless nickel. Using a much reduced, more efficient agitation system, the same maximum content could be reached at 5 g/l. Also at reduced solution velocities and concentrations it was likely that an increase in plating rate would then decrease the volume per cent codeposited. The particle arrival rate having reached a maximum at the surface but at a much lower rate, the metal deposition rate then had the chance of overtaking the particle arrival rate diluting the particle content (Although particle arrival rate was lower this was counteracted by longer dwell times on the surface therefore the same codeposition rates were maintained).

The level of agitation and resultant solution velocity also effects the boundary layer conditions. As the solution

velocity is reduced boundary layer flow can change from turbulent to streamline flow and as a result significantly increase the thickness of the surface boundary layer as the turbulent flow is removed. The velocity gradient between the surface and bulk solution is also reduced. This enables particles to remain on the surface unaffected by solution flow for increased dwell times. Much larger particles can also be more easily adsorbed.

The uniformity of the codeposited particles was significantly influenced by the agitation of the solution. Experimental evidence showed that on upward facing surfaces particle content would be high, while on downward facing surfaces where gravity and solution movement hinder settling, low particle contents are experienced. Increased agitation could have reduced settling on upper surfaces and allowed more particles to reach downward facing surfaces. This would have produce more uniform coatings but less overall content as discussed above. Increased particle content of the bath would counteract the reduced content leading to higher bath contents ie. 60 g/l, as was eventually required for uniform coatings with the agitation used..

Alternatively, suitable rotation of the component to allow all surfaces to be upward facing at some point would have allowed unhindered settling for lower solution concentration over the complete surface.

Comparisons of electroless composite plating and electrolytic composite plating have suggested that lower

concentrations of particles can be used in electroless plating than in electrolytic plating to obtain the same concentration of particle in the deposit. This is a difficult comparison to make unless exactly the same conditions are used for both systems, ie. agitation and powder must be identical, something which is unlikely to be achieved between authors. This work also showed that for graphite the same maximum graphite content of the deposit could be obtained for both electroless and electrolytic plating at 5 g/l. However, given the same agitation and powder, electroless plating is carried out at a much higher temperature than electrolytic plating. This would significantly increase metal ion adsorption onto the particles and thus promote bond formation between particle and plating surface[161]. Increased temperatures would also significantly reduce boundary layers from approximately 5000 μm at 40°C to 1000 μm at 90°C enabling particles to make much closer approaches to the surface and increase the chance of colliding with the surface.

7.8 HEAT TREATMENT

Figure 53, shows that the incorporation of graphite into electroless nickel reduced the hardness of the coating, more significantly in the heat treated condition. This is not surprising as the value determined was a composite hardness of hard electroless nickel and the much softer graphite. The hardness of these coatings was however significant and based on hardness alone could be considered capable of producing good abrasion and adhesive wear resistant properties.

Deposits containing PTFE were also softer than conventional electroless nickel. Un-heat treated the composite hardness was lower than for graphite at approximately 200 Hv_{100}. This reflected the higher PTFE content of the deposit, approx. 25 volume per cent, than for graphite 6.7 volume per cent. Heat treated the composite hardness was again lower than for graphite for the same reason.

Heat treatment of electroless nickel chromium composites for a standard one hour at 400^0C produced little effect. In the un-heat treated condition the chromium particles produced a slight hardening effect. Heat treated hardnesses were slightly lower than for conventional electroless nickel with the chromium being softer having been annealed by the heat treatment.

When heat treated at 850^0C for 8 and 16 hours, conditions were then suitable for inter-diffusion of the elements and the production of an alloy coating. This can be readily illustrated by the x-ray maps and line profiles in figures 55-59.

As temperature increased diffusion began to take place. At 850^0C the nickel-phosphorus matrix was close to its melting point. Diffusion of chromium from the particles and iron from the substrate may then have diffused quite rapidly throughout the matrix. The net effect of the iron and chromium diffusion was to produce an Fe-Ni-Cr alloy, with the interdiffusion of nickel and iron at the interface increasing the effective thickness of the coating.

Referring to the phase diagrams figure 94 and 95 it can be seen that chromium is an α stabiliser, while nickel is a much stronger γ stabiliser and in this case was also present in greater amounts. The predominant phase present in the portion of the coating adjacent to the substrate was then γ phase Fe-Ni-Cr alloy. Phosphorus, has a maximum solubility of 0.5 per cent in γ phase and was thus rejected from the phase and pushed ahead of the growing γ phase . This increased the phosphorus content of the surface layer from 8% to 15% phosphorus. The surface layer was then predominantly nickel and phosphorus with approximately 5% chromium present. This layer was then most likely to be a nickel phosphide layer with further precipitates of Ni_5P_2 and Ni_7P_3 possible within this region.

The variation in composition across the Fe-Ni-Cr band of the coating was most likely to approximate to the line indicated on the ternary phase diagram in figure 96. At the steel substrate, ie. Fe rich portion, the composition indicated the possibility of producing ferrite. No evidence of this was found, probably because the gas quenching of the components was sufficient to prevent diffusion of the elements to produce ferrite. Any carbon diffusion into the phase would have remained in solution after quenching. This would not have revealed itself unless the coating was re-heated to allow precipitation of chromium carbides.

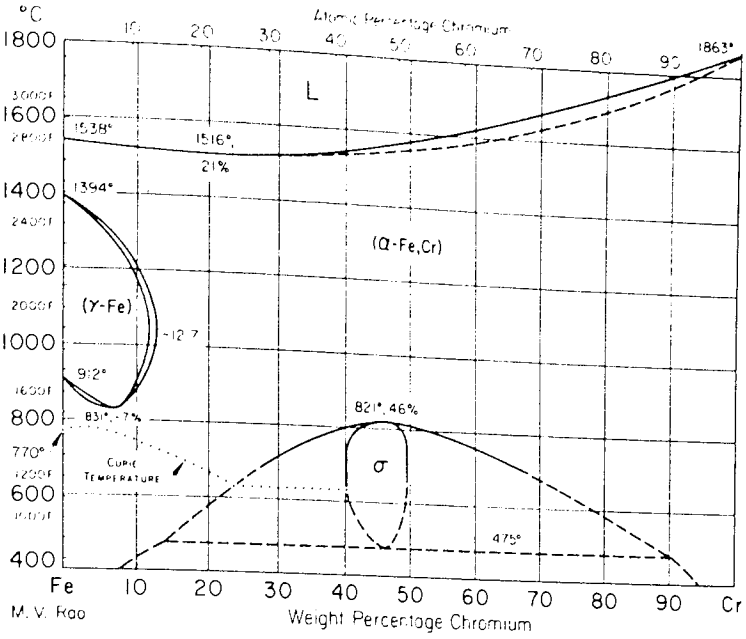

Figure 94. Iron-Chromium phase diagram

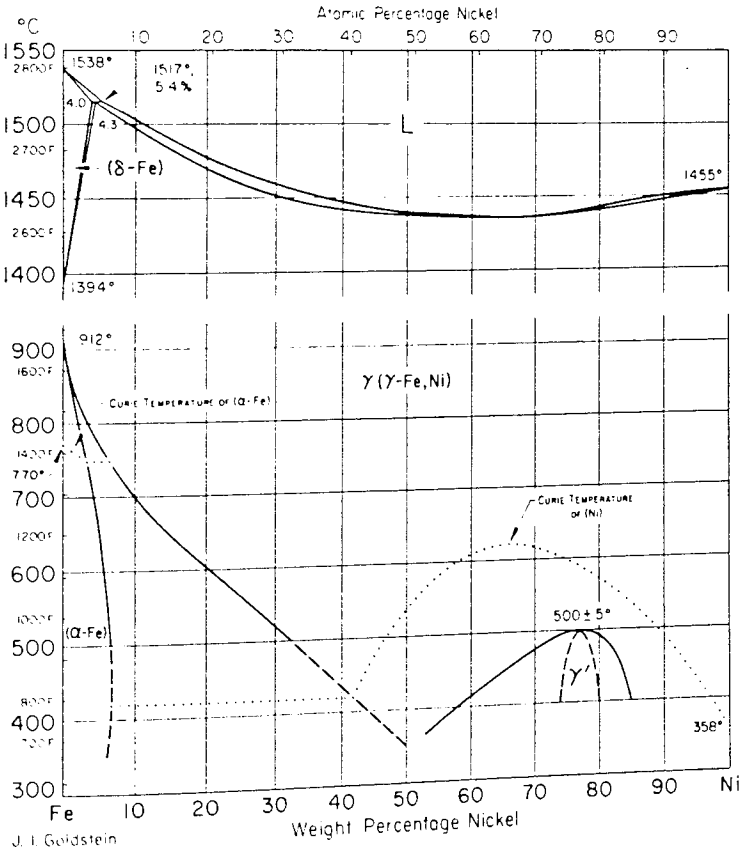

Figure 95. Iron-Nickel phase diagram

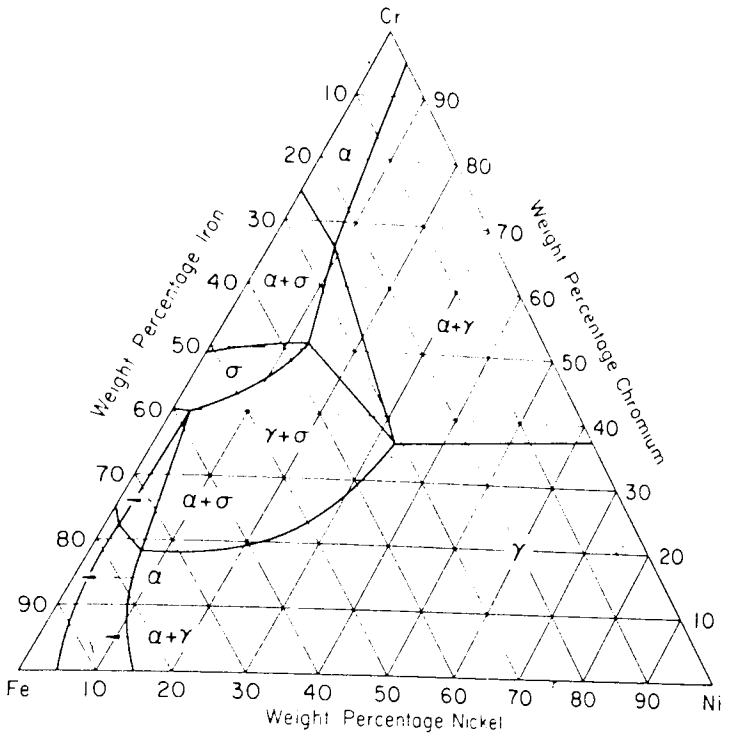

Figure 96. Ternary phase diagram for Nickel-Iron-Chromium at 600 ^{o}C

Hardness profiles across the coating showed the nickel phosphide band at the surface to be very hard with a hardness of approximately 1400 Hv_5. At the change in phase the hardness dropped to that of γ phase approximately $200Hv_{100}$.

This coating clearly showed the concept of producing alloy coatings by the incorporation of metal particles into a matrix and suitably heat treating. The combination of alloys are many and by control of the incorporated metal particles the alloy composition could be controlled and tailored to the desired requirements. The example produced in this work an Fe-Ni-Cr alloy with a hard nickel phosphide protective surface, offers potential as a corrosion and possibly oxidation resistant surface, especially if the chromium content could be increased.

The phosphorus limits the surface to a temperature of around 900^{o}C before melting and the two phase structure could produce a galvanic effect between phases increasing corrosion. Alloys such as nickel-iron-chromium may best be produced by codepositing iron-chromium particles in electrodeposited nickel and heat treating, thus eliminating any problems with the presence of phosphorus.

7.9 INTERNAL STRESS

The results in table 14 showed that the introduction of graphite particles into electroless nickel reduced the internal stress of the deposit by an average of 13.6 N/mm^2 . This result is in general agreement with other workers such as Kedward[106] who reported on the reduction of internal stress with the incorporation of chromium carbide into electrodeposited cobalt. Sadowska-Mazur[93] also showed a reduction in internal stress for the incorporation of silicon carbide into tin. No explanation was given by the authors for this effect.

The internal stress of electrolytic and electroless deposits has been attributed to a number of factors. These factors include lattice misfit between deposit and substrate, the codeposition of hydrogen, the formation of vacancies within the deposit and lattice contraction. No one universally accepted theory has however been proposed; it is more likely that stress is due to a combination of certain factors and varies from one system to another.

The incorporation of particles into the deposit may then influence one of the factors considered to produce internal stress. Particle incorporation may reduce the lattice misfit, prevent codeposition of hydrogen or the formation of vacancies and may accommodate lattice contraction, in each case a reduction in stress would result.

7.10 FRICTION AND WEAR

The curves in figure 60 and 61 show that, when run against an EN 31 disc, the incorporation of graphite into electroless nickel in increasing amounts, reduced the static component of friction from 0.7 to 0.35. The kinetic coefficient of friction however, remained essentially constant.

To explain this, the surfaces of the electroless nickel-graphite coated pins, run in the wear tester, were examined by scanning electron microscopy. Figure 40 showed the electroless nickel-graphite surface to have been quite rough in comparison to the electroless nickel surface. When this surface then came into contact with the EN 31 disc the peaks of the asperities were the first to make contact. All the load was supported on these asperities and they were subjected to a high compressive stress, beyond their yield stress. This resulted in plastic deformation of the asperities. Also, under the influence of tangential stress from the motion, juction growth of the asperities resulted in the direction of the motion, ie. smearing of the asperities, figure 67. The coefficient of friction was

low, however the wear rate, in the form of surface deformation would have been high, because of high compressive stress. Deformation continued until the gross asperities were removed and the compressive stress was more evenly distributed as the load was now supported on the true area of contact. This should then have been a steady state condition for the coefficient of friction and wear rate.

Figure 67c however, for the electroless nickel-graphite surface run against EN 31 discs, shows that steady state conditions were not reached until the surface was completely flat in comparison to the asperities of the rough surface before wear. This indicates either a high contact load causing high deformation or that significant adhesive wear had occurred.

Figure 67c also showed that the surface had a significant fraction of exposed graphite flakes prompting the question of whether this provided the solid lubrication to reduce the static coefficient of friction. Experimental evidence to support this as a possible mechanism was found by looking at the surfaces under the scanning electron microscope and analysing the surfaces by x ray mapping.

In the case of electroless nickel, running against an EN 31 disc, friction and wear could be considered a result of adhesion between asperities and the resultant shearing of material at the interface. Shearing will occur in the weaker material giving a value for friction and producing adhesive wear

as the sheared material is left adhered to the counterface. With the combination of electroless nickel and EN 31 the weaker material in shearing is proposed to be the EN 31 steel. Evidence for this can be seen in the low wear rate of the electroless nickel surface and the x ray maps of the surface which showed the nickel surface to be almost completely covered in adhered iron.

As wear continues the transferred steel will work harden and be removed as hard particles. Also, because of the increased temperatures of the surfaces in contact, these particles and the surfaces, will then oxidise. The net effect is a wear track, figure 62, produced by adhesive wear and ploughing from oxide particles. The track itself is also oxidised by the temperatures during sliding. The surface of the steel after sliding against electroless nickel can be seen in figure 63.

For electroless nickel-graphite run against an EN 31 disc, x ray maps of the coated pin showed little iron transfer, figure 68, and talysurf measurements of the disc figure 64, showed little wear or oxidation. With the combined effects of reduced disc wear and iron transfer, oxidation and static coefficient of friction , it could be concluded that the graphite had produced solid lubrication between the surfaces preventing contact between asperities and so protecting the surfaces.

However, if graphite had actually been producing solid lubrication not only would it have been expected to reduce the static coefficient of friction but the kinetic component of

friction should also have been reduced to a value approaching the kinetic coefficient of friction for graphite, approximately 0.15. Although the EN 31 disc had been protected with little wear occurring, the wear rate of the electroless nickel-graphite actually increased with graphite content. If lubrication had occurred both surfaces would have been protected.

As these factors prevented the evidence for solid lubrication from being complete it was concluded that for electroless nickel-graphite coatings on the pin, run against an EN 31 disc, solid lubrication did not occur. The exposed graphite flakes may have reduced the static coefficient of friction slightly by reducing the surface area of the pin which could be adhered to the disc surface. However, a considerable surface area of nickel remained to provide adhesion with the contacting disc, but this time shearing occurred within the deposit. The graphite had considerably reduced the shear strength of the coating so that it was behaving as a type of abradable coating. The reduced shear strength with increasing graphite content reduced the static component of friction, as shearing occurred before extended sticking could occur. This also explained the increased wear rate of the coating while protecting the disc. The static coefficient of friction then approached the kinetic component and reflected the force required to produce shearing with little sticking occurring. It is not surprising that the critical shear stress was reduced as the relatively long thin flakes produced natural planes of weakness and probably behaved as micro cracks throughout the coating. The ends of the

cracks were suitable notches for growth, however the cracks may have only extended as far as the next flake. In this way though, cracks would have linked up, promoting removal of large fragments of nickel as the coating was abraded away. A similar mechanism to the above was considered responsible for the results obtained from the falex wear results. Where lower coefficients of friction were experienced with graphite, but with increased wear rates.

When electroless nickel-graphite coated pins were run against electroless nickel-graphite coated discs the coefficient of friction was much reduced fig. 69, and very much lower wear rates were experienced, fig. 70. With both static and kinetic coefficients of friction reduced and wear also reduced it can be more realistically suggested that graphite provided solid lubrication between the surfaces.

It was most likely that in the previous case of a coated pin run against an EN 31 disc that this was a rather severe test. This could be seen when the ratio of coated pin area to uncoated disc was considered. The uncoated area was very much greater than the coated pin and it was then very difficult for the small surface area of coating to produce sufficient solid lubricant to cover this area. If the situation had been reversed, with the large suface area of the disc coated and the pin uncoated, then sufficient solid lubricant would most likely have been present to cover the disc and easily cover the area of the pin. The coefficients of friction would then have been similar to those experienced in figure 69. This effect of the

ratio of coated to uncoated area, was confirmed by experiments with the crossed cylinders for both graphite and PTFE.

The crossed cylinder wear test was used to further examine the wear mechanism of electroless nickel graphite coatings. Figure 75 showed that when run against a stainless steel stator very low coefficients of friction were experienced ie. $\mu = 0.07$. Examination of the coated cylinder before wear testing, figure 77, showed that there was a significant number of graphite flakes actually on the surface. These were particles bonded to the surface which were in the process of being covered by the growing coating. The roughness of the surface may also have indicated that some of these particles have been covered preferentially to the surface, rather like conducting particles in electrolytic composite plating. When this surface was brought into contact with the counter face, and given that the ratio of coated surface area to uncoated area was in favour of the coated surface, then the surface asperities deformed until the load was fully supported.

The surface asperities for a nickel-graphite coating from figure 77 were graphite flakes and nickel coated graphite flakes. Deformation of the graphite flakes resulted in graphite being smeared over the surface. Nickel coated graphite flakes deformed and most likely fractured to expose further graphite. The smeared graphite and wear debris filled in the surface roughness locally, producing a smooth surface in the area of contact, figure 77c and diagramatically in figure 97. The

areas of deformation on the wear track reflected the true area of contact between the surfaces.

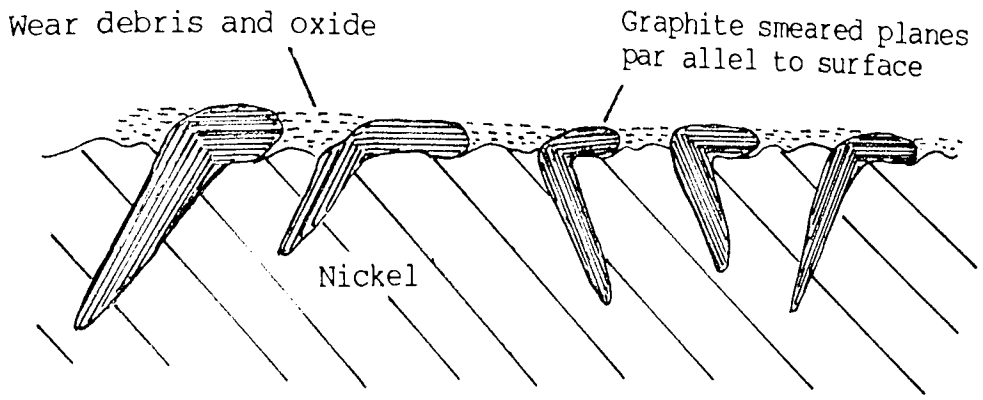

Figure 97. Schematic diagram of the wear surface of as-deposited nickel-graphite composite

The principle area of contact was a layer of graphite orientated parrallel to the surface, and intermixed with wear debris of nickel and probably nickel oxide. S.E.M. spot analysis showed the presence of nickel in what appeared to be a thick layer of graphite. The net effect of the layer was to separate the surfaces from adhesive interaction with a low shear stress layer capable of producing the very low levels for coefficient of friction by solid lubrication.

The numerous theories that have been advanced for the mechanism of lubrication of graphite were considered in Chapter II, the literature review on Friction, Wear and Lubrication.

Summarising the work, it can be seen that lubricating conditions prevail when either the shear strength of the graphite between the layered atomic planes, or the adhesion between already separated planes, is reduced and when the reaggregation of the wear debris is prevented by the absorption of oxygen or condensable vapours. It was further shown that provided the graphite was adhered securely to the surfaces, it would lubricate under atmospheric conditions even in the absence of adsorbed films of condensable gases. If the surface bond is weak then the shear strength of the graphite must be reduced by the adsorption of gases to below that of the metal/graphite interface.

Graphite is then capable of producing very effective solid lubrication when established as a surface layer. If however, the film is broken down or if the surface were to be machined before wear testing much higher coefficients of friction were shown to result, Table 18. Removal of the surface layer by machining or wear produced a surface as in figure 77d and 98. There was now no surface graphite to produce the initial solid lubricating film and therefore all rested on the exposed graphite flake from the matrix. The amount of graphite available for lubrication was significantly reduced and the orientation of the flakes was also considered non-conducive to easy shearing.

The low shear strength layers within graphite, which produce the low coefficient of friction, lie parallel to the longitudinal dimensions of the graphite flakes. As can be seen from figure 44 and 98, flakes were orientated in an upright

fashion and hence when exposed the low shear strength layers were at right angles to the direction of motion. Therefore shear did not readily occur and little graphite is smeared over the surface, even when at high contents and high ratios of coated surface to uncoated. The graphite contributed little to reduce the coefficient of friction which was essentially represented by the substrate material.

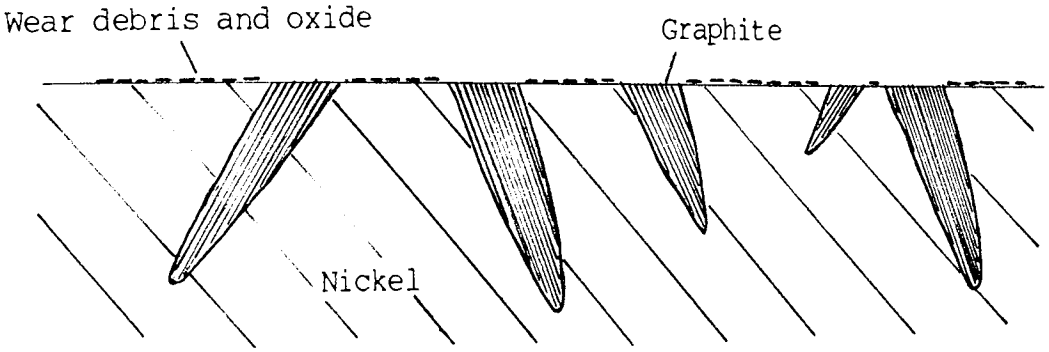

Figure 98. Surface of machined electroless nickel-graphite

An increase in the coefficient of friction and wear rate resulted if the load on the wear surface was increased. This may have been as a result of breakdown and removal of the material providing the lubricant layer by the more closely approaching surface. Once the layer had broken down the low coefficient of friction could not be restored, as was seen when the surface was removed by machining. The nickel-graphite

lubricating surface would therefore be ineffective in abrasive conditions as the solid lubricant would quickly be removed and unable to be replaced. Contact with a surface of high surface roughness would also have produced a similar result if the graphite-wear debris mix had been insufficient to "fill in" the surface depressions and cover the surface asperities.

From these results it was possible to conclude that although very low coeficients of friction could be produced, the effect was essentially a surface effect. The coating did not provide true self-lubrication throughout its life but relied totally on the intial surface layer produced.

Pin on disc results for PTFE containing electroless nickel deposits, from source one, followed a similar pattern to those of electroless nickel-graphite. Run as a coated pin against an uncoated EN 31 disc, the ratio of coated to uncoated area was again unfavourable and insufficient solid lubricant was available to prevent interaction of the surfaces.

As with nickel-graphite it was considered that the PTFE reduced the shear strength of the coating and it was this which reduced the static coefficient of friction and also increased the wear rates. Reduced metal transfer and protection of the EN 31 disc also resulted as the coating again acted as an abradable coating.

These commercially produced coatings from source one were also structurally poor. S.E.M. pictures of the surface before wear testing, figure 78, showed the surface was particularly porous, posssibly as a result of hydrogen liberation. These were then unlikely to be the most suitable coatings for wear testing.

In the heat treated condition the improved properties of the electroless nickel reduced the wear and increased the coefficient of friction slightly as the coating had become more wear resistant and less likely to be abraded. Again no lubrication of the surface occurred, the heat treatment temperature of 400^{o}C was presumed to have degraded the PTFE which has a melting point of 325^{o}C.

Also similar to results for electroless nickel-graphite were the results for electroless nickel-PTFE coated pins run against electroless nickel-PTFE coated discs. With the more favourable ratio of coated to uncoated area the volume of PTFE available for lubrication was significantly increased to the point where solid lubrication between the surface could occur. This was then reflected by the reduced coefficients of friction and wear rates.

A better understanding of the behaviour of PTFE-containing deposits was presented by the results from the crossed clyinder wear test experiments. With electroless nickel-PTFE deposits containing increasing amounts of 0.75 micron PTFE,

initial coefficients of friction were reduced, but could not be maintained throughout the test until like against like were run at the maximum content. Thus, although initial films of self-lubricating PTFE were formed insufficient PTFE was present to maintain these films and once broken they could not be reformed. A critical PTFE content is therefore required in a deposit before continuous self-lubrication can be produced throughout the life of the coating. This is in agreement with PTFE-impregnated bearings, where an optimum volume ratio of greater than 32 per cent by volume PTFE is required to produce the required self-lubricating nature.

With electrolytic nickel-PTFE coatings containing PTFE of 10um particle size the self-lubricating properties of the coating were much improved. The larger PTFE particle appeared much more efficient at producing lubricating films, even at low PTFE contents (5 volume per cent) and when run against stainless steel or mild steel counterfaces. The large PTFE particles could be considered to be much more capable of transfering large amounts of PTFE to the counterface than the smaller particles even if smaller particles were present in larger numbers. Also if such films were broken by suface grinding, the films could easily be reformed by the exposed, large PTFE particles, unlike graphite, and can be called self-lubricating coatings.

The lubricating mechanism of PTFE was considered in Chapter II, section 2.3, the literature review of Friction Wear and Lubrication. Under the conditions of wear testing used in

this work, ie. low speeds and moderate conditions, PTFE from the deposit was capable of being drawn over the counterface, for example a stainless steel stator. The transfered film would adhere to the steel with a highly orientated fibrous structure approximately 1000 to 4000 nm thick. The low friction was attributed to the easy shear of these layers under tangential movement.

Once the PTFE lubricating film had been formed contact between the counterfaces was prevented, thus reducing any possibility of adhesive wear and providing a low shear strength surface film, this then gave the low coefficients of friction. Under steady state condition, very little wear of the coating occurred unless this film was removed. This resulted in long periods of low coefficients of friction with little wear occurring until this film was removed over time. Interaction of the surfaces then exposed further PTFE to reform the film. The coating did not perform, as sometimes reported, by continual wear and exposure of PTFE particles but more on an intermittent basis. When slightly higher wear rates were experienced against other counterfaces this reflected the degree of wear necessary to expose sufficient PTFE to produce the lubricating film with the varying surface roughnesses and hardness of the counterfaces. Such self-lubricating coatings would of course be of little use in abrasive conditions where film formation would be continually prevented. This effect was also reflected when the load on the contacting surfaces was increased. This reduced the film thickness and brought asperities into contact, so increasing friction and wear.

When nickel-PTFE coated cylinders were reversed and tested as the stator, and stainless steel cylinders ran as the rotator, the effect of coated area to uncoated area was again experienced. The coated area was now small compared to the uncoated area and the PTFE volume available was insufficient to provide complete coverage of the rotating cylinder. Low coefficients of friction could then not be maintained for any period of time. Thus even with the most effective self-lubricating coating the ratio of coated to uncoated surface area must be in favour of the coated surface area.

For commercial applications electroless nickel-graphite would have little advantage over electroless nickel-PTFE coatings. Electroless nickel-graphite relies on its initial surface for low coefficients of friction. Such coatings would have to be treated with care before use and once the initial layer was removed in use or by other means the effective lubrication of the coating would be lost. Electroless nickel-PTFE deposits which offer self-lubrication throughout the coating are much more applicable as a low coefficient of friction surface. One area where electroless nickel-graphite deposits could be more applicable would be for higher temperature applications where the graphite would be far superior to PTFE.

Unlike the low coefficients of friction it is possible to experience with self-lubricating coatings, electroless nickel-chromium deposits produced much higher values of friction. Heat treatment for 1 hour at 400^{o}C produced little interdiffusion of

elements. The exposed wear surface was then one of electroless nickel and chromium metal. With the elevated temperatures that can be reached at the interface during wear with the loads used in the test, oxidation of the surface is also likely, making the contacting surface against the EN 31 disc more likely to be a mix of precipitated nickel phosphide, nickel and nickel and chromium oxide. The coefficients of friction then reflect the running of this surface against the steel disc with adhesive wear and oxidation producing the high coefficients of friction and wear.

When heat treated for 16 hours at 850^{o}C a completely new structure was produced and this was reflected in the wear test results. In the initial stages of wear testing low wear rates with relatively low coefficients of friction were experienced. This corresponded to the hard nickel phosphide layer at the surface of the deposit. As this layer was removed and the much softer Fe-Ni-Cr phase was exposed the coefficient of friction and wear rate rapidly increased. Increased adhesive wear and oxidation of the coating surface, again possible with the contacting surface temperatures, may have caused the higher coefficients of friction and wear rates.

CHAPTER VIII

SUMMARY AND CONCLUSIONS

8.1 SUMMARY

This first objective of this work was to develop solutions capable of codepositing graphite and chromium with electroless nickel. These particles had previously been considered difficult to codeposit. This was because of the instability caused by their addition to the electroless nickel solution, particularly in the case of chromium which was also capable of initiating the electroless reaction. An added difficulty in the case of graphite was its inability to be wetted by the solution.

Solution development showed that these problems could be overcome by the addition of suitable stabilisers and surfactants to the electroless nickel solution. In particular it was found that heavy metal cations produced very stable solutions with particle additions. Graphite particles could be wetted by non-ionic surfactants but required the presence of an anionic or cationic to produce a dispersion of the particles.

It was found however, that codeposition only occurred when non-ionic and anionic surfactants were used. Particles dispersed with cationic surfactants appeared adsorbed to the plating surface but rode ahead of the advancing metal surface.

This prompted the discussion of the mechanism of codeposition of particles from electroless plating solutions.

The mechanism of codeposition of particles from an electroless system is often quoted as "mechanical entrapment", this is an over-simplification. In addition the simple charge produced by surfactants does not provide a complete explanation. Particle codeposition from electrolytic systems has been shown to be essentially physical adsorption although strongly dependent on the adsorbed ions on the particle surface. It is almost certain that solution ions are also adsorbed onto the particles in electroless systems and, as adsorption to the plating surface was concluded to be physical, a mechanism of codeposition for particles in electroless systems similar to electrolytic systems was believed to occur. This would explain the results for codeposition observed in this work.

The principal factors which controlled particle content of the deposit were also considered to be similar to those factors which operate in electrolytic codeposition. Of key importance was agitation. This was required to maintain particles in solution and also to transport particles to the plating surface as efficiently as possible. It is possible to conclude that in a correctly agitated system the concentration in solution for maximum particle content of the deposit can be kept low. Uniform deposits can be produced and with the codeposition operating under saturation conditions at the plating surface particle content can be controlled by the particle size or

packing density of the particles. Plating rate also has a significant affect on particle content of the deposit when related to particle arrival rate.

Electroless nickel-graphite deposits, although containing low volume per cents of graphite, because of the low packing density of graphite, reduced the hardness of the deposit both in the as-deposited and heat treated condition. The deposit did however produced a very low coefficient friction surface. Examination of the surface showed that once established the load bearing surface consisted of smeared surface graphite and wear debris producing a low surface shear stress and low coefficients of friction and wear rates. Removal of this layer exposed codeposited graphite flakes, these however did not provide efficient lubrication because their orientation was not considered ideal for easy shear of graphite layers. The coefficients of friction and wear rates were now very much higher. Electroless nickel-graphite deposits rely on the initial surface for effective self-lubrication .

In contrast to this electroless nickel and electrolytic nickel-PTFE deposits produced effective self-lubrication throughout the thickness of the deposit. The PTFE particles were not so dependent on orientation as with the graphite particles and could reproduce a lubricating film of PTFE whenever the established film was removed.

It was shown with these coatings that a minimum content of solid lubricant was necessary in the deposit to provide continuous self-lubrication. Increased particle size of PTFE also produced significantly more efficient lubrication of the surfaces. It was also shown that the ratio of the surface area of the self-lubricating composite coating to the uncoated surface of the counterface must be in favour of the composite coating to enable sufficient lubricant to be present to cover the contacting surface area. Once established the lubricant films protect the surfaces and very little wear of either counterface occurs. Further wear and exposure of more solid lubricant eventually occurs when the smeared lubricant is removed with time.

Electroless nickel-chromium deposits were also produced once stabilisation of the powders by oxidation and heavy metal cation had been achieved. After diffusion heat treatments Ni-Fe-Cr alloys with surface layers of high phosphorus content were produced. This surface layer was very hard which combined with the stainless type substrate may offer potential as a corrosion resistant coating. The two layer structure of the coating was also reflected in the wear properties of these deposits with a transition from moderate to high friction and wear, observed as the interface between layers was crossed.

8.2 CONCLUSIONS

(1) Graphite and chromium particles could be codeposited with electroless nickel provided suitable additions of stabilisers and surfactants were made to the solution.

(2) The mechanism of codeposition of particles from electroless nickel was shown to have similarities with codeposition from electrolytic systems. The mechanism of codeposition was concluded to occur by physical adsorption onto the plating surface and to be strongly dependent on the solution metal ions, adsorbed to the particle surface, for codeposition.

(3) The volume per cent of graphite and chromium codeposited was found to be dependent on the concentration of particles in solution, the plating rate and the particle size, but agitation was an important factor in influencing all the above relationships.

(4) The coefficients of friction and wear rates for electroless nickel-graphite coatings in the as-deposited condition were very low. Removal of the as-deposited surface layer resulted in an increase in coefficients of friction and wear rates. Self-lubrication was not provided by the coating due to unfavourable orientation of the graphite flakes for easy shear of the atomic planes.

(5) Electroless nickel and electrolytic nickel-PTFE coatings produced the most effective self-lubrication and were not dependent on any initial surface layer. A minimum content on PTFE was found to be necessary for continuous self-lubrication, with the minimum content decreasing with increasing particle size.

(6) For self-lubricating coatings to be effective the ratio of coating surface area to counterface surface area must be in favour of the self-lubricating coating. If this is not the case insufficient lubricant is present to establish a lubricating film on the counterface.

(7) Heat treatement of electroless nickel-chromium deposits produced nickel, iron, chromium alloys with a phosphorus rich surface of high hardness. Coefficients of friction and wear rates were initially moderate for the phosphorus rich layer but increased for the nickel, iron, chromium region of the coating.

Further Work

Further work could be divided into two areas of research (1) the mechanism of codeposition of particles from electroless solutions and factors affecting particle codeposition and (2) the properties of electroless composite coatings.

A mechanism of codeposition, similar to that produced in electrolytic composite solutions, has been considered in order to develop a model for codeposition from electroless solutions. To examine this model a detailed study of surfactants, ion adsorption and the corresponding zeta potentials, with respect to particle adsorption, is required in conjunction with the influence of factors of particle size, concentration, plating rate and agitation. This would provide considerable information in an area of little understanding and establish the mechanism of codeposition of particles from electroless solutions.

Understanding of codeposition may enable more suitable composites to be produced, i.e. deposits of higher volume per cent graphite with improved properties as a result. The study of nickel-PTFE deposits showed particle size to be important in lubricating ability. A study of such parameters for graphite, with a better understanding of codeposition to enable larger particles to be codeposited, could also produce significant improvement in properties. The codeposition of metals and the resultant alloy coatings after heat treatment offers considerable potential for study.

APPENDIX A

SOLUTION PREPARATION AND MAINTENANCE

(1) SOLUTION PREPARATION

The required volumes of electroless nickel solution were prepared according to the manufacturers' instructions, as below:

Nifoss 3000 Base Solution N.21321	:	100 ml
Nifoss 3000 Initial Additive N.21322	:	200 ml
Distilled or deionised water	:	to 1 litre

The Nifoss 3000 Base Solution followed by Nifoss 3000 Initial additive was added to approximately half the distilled water and then made up to the final volume with the remaining water. The pH of the solution was checked using the pH meter and where required, adjusted using ammonia solution (S.G. 0.880) diluted 1:1 with water of a 10% sulphuric acid solution.

(2) SOLUTION MAINTENANCE

The electroless solution was analysed at regular intervals for the concentrations of Base Solution and Reducer Solution so that corrections could be made.

(3) ESTIMATION OF NIFOSS 3000 BASE SOLUTION

The concentration of Nifoss 3000 Base Solution was determined by titration. A 10.0 ml volume of plating solution

was diluted to 100 ml with distilled water and 5 ml of S.G. 0.880 ammonia added. This was then titrated with 0.1 M EDTA using 0.5g of Murexide (prepared by using 0.2g Murexide to 100 g No Cl) as an indicator. The amount of EDTA added in m/s, multiplied by 8.95 was equivalent to the concentration in ml/l of Nifoss 3000 Base Solution in the plating bath. Base Solution was then added to return the concentration to 100 ml/l.

(4) ESTIMATION OF NIFOSS 3000 REDUCER SOLUTION

The concentration of Nifoss 3000 Reducer Solution was determined by adding 0.5 ml of 0.2 % pallodium chloride solution to 5.0 ml of plating solution at 95-100^{0}C. The volume of hydrogen liberated was collected in a burette. The volume in ml of hydrogen is subtracted from 30 and multiplied by 3.5. This figure is equivalent to the concentration of Nifoss 3000 Reducer Solution in ml/l in the plating solution. Additions were then made to return the Reducer Solution to 200 ml/l.

Additions of Base and Reducer Solutions were made frequently, at least every hour at a bath loading of 1 dm^2/l at 95^{0}C, at lower loadings maintenance was less frequent. No more than 20 ml/l of each of Base and Reducer Solution were added in any 30 minute period, as this could cause over-stabilisation of the bath and prevent the deposition reaction.

Reference: CANNING Instruction Sheet No 1653D, W. Canning Ltd.

REFERENCES

1. Archard, J.F., "Contact and Rubbing of Flat Surfaces", J. Appl. Phys., **24**, 981-988, (1953)

2. Archard, J.F., "Elastic Deformation and the Laws of Friction", Proc. Roy. Soc., **A243**, 190-205, (1957-58)

3. Archard, J.F., "Single Contacts and Multiple Encounters", J. Appl. Phys., **32**, 1420-1425, (1961)

4. Bowden, F.P., Tabor, D., "The Friction and Lubrication of Solids", Part 1, Clarendon Press, Oxford, (1954)

5. Bowden, F.P., Tabor, D., "The Friction and Lubrication of Solids", Part 2, Oxford University Press, (1964)

6. Timashenko, S., "Theory of Elasticity", McGraw Hill, New York, (1934)

7. McFarlane, J.S., Tabor, D., "Relation between Friction and Adhesion", Proc. Roy. Soc., **A202**, 244-253, (1950)

8. Courtney-Pratt, J.S., Eisner, E., "The Effect of a Tangential Force on the Contact of Metallic oBodies", Proc. Roy. Soc., **A238**, 529-550, (1956-57)

9. Bowden, F.P., Leben, L., "The Nature of Sliding and the Analysis of Friction", Proc. Roy. Soc., **A169**, 271-391, (1939)

10. Bowden, F.P., Leben, L., Tabor, D., "The Sliding of Metals, Frictional Fluctuations and Vibration of Moving Parts", The Engineer, **168**, 214-217, (1939)

11. Bowden, F.P., Tabor, D., "The Area of Contact Between Stationary and Moving Surfaces", Proc. Roy. Soc., **A169**, 391-413, (1939)

12. Czichos, M., "Failure in Thin Film Lubrication, the Concept of a Failure Surface", Tribology, 14-20, (1974)

13. Kruschov, M.N., "Resistance of Metals to Wear by Abrasion, as Related to Hardness", Proc. Conf. Lab. Wear, I. Mech. Eng., 655, (1957)

14. Richardson, R.C., "Wear of Metals by Relatively Soft Abrasives", Wear II, 245, (1968)

15. Rabinowicz, E., "Friction and Wear of Materials", J. Wiley and Sons Inc., N.Y. (1965)

16. Welsh, N.C., "The Dry Wear of Steels", Phil. Trans. Roy. Soc., **257**, 31-70, (1965)

17. Lea, M., PhD Thesis, Brunel University, (1972), as referenced by Eyre, T.S., "The Mechanism of Wear", Tribology, 91-97, (1976)

18. Suh, N.P., "The Delamination Theory of Wear", Wear, **25**, 111-123, (1923)

19. Sarkar, A.D., "Friction and Wear", Academic Press, London, (1980)

20. Seifert, V.W., Wescott, V.C., "A Method for the Study of Wear Particles in Lubricating Oils", Wear, **34**, 372-382, (1975)

21. Johnson, W., "Impact Strength of Materials", Edward Arnold, London, (1972)

22. Vac´dma, L.E., "The Wear of Metals in the Presence of a Non-Renewable Layer of Abrasive", Friction and Wear in Machinery, (ASME), **13**, 17, (1959)

23. Waterhouse, A.B., "Fretting Corrosion", Pergamon Press.

24. Reynolds, O., "Theory of Lubrication", Phil. Trans. Roy. Soc., **177**, 157, (1886)

25. Dowson, D., Higginson, G.R., "Elasto-Hydrodynamic Lubrication", Pergamon Press, Oxford (1966)

26. Hardy, W.B., Hardy, S.K., "Static Friction and Lubricating Properties of Certain Substances", Phil. Trans Roy. Soc., 32-48, (1919)

27. Bragg, W., "Introduction to Crystal Analysis", 64, Bell and Sons, (1948)

28. Tsuzuku, A., Proc. 1957 Conference on Carbon, 434, Pergamon.

29. Amelinck, S. and Delavignette, P., "Electron Optical Study of Basal Dislocations in Graphite", J. Appl, Phys., **31**, 2126-2135, 196

30. Boswell, T., Proc. Europ. Conf. Electron Microscopy (Delf), 1960

31. Savage, R.H., " Graphite Lubrication", Gen. Electric Rev., **48**, 13, (1945)

32. Savage, R.H., "Graphite Lubrication", J. Appl. Phys., **19**, 1-10, (1948)

33. Rowe, G.W., "Some Observations on the Frictional Behaviour of Boron Nitride and Graphite", Wear, 3, 74, (1960), Campbell, W.E., Kozak, R.L., Trans. A.S.M.E., **70**, 491, (1948)

34. Deacon, R.F., Goodman, J.F., Proc. Roy. Soc., **A243**, 464, (1958) as referenced by Braithwaite, E.R., in "Lubrication and Lubricants", Elsevier Publishing, (1967)

35. Makinson, K.R., Tabor, D., Proc. Roy. Soc., **A281**, 49, (1964)

36. Tanaka, K., Uchiyama, Y., Toyooka, S., "The Mechnism of Wear of PTFE", Wear, **23**, 153-172, (1973)

37. Tulsi, S.S., "Composite PTFE-Nickel Coatings for Low Friction Applications", Trans. I.M.F. **61**, 147-150, (1983)

38. Pugh, D., "Practical Lubrication", Butterworth, London, 178, (1970)

39. Buttery T.C., Archard J.F., "Grinding and Abrasive Wear", Proc. Inst. Mech. Eng. **185**, 537-551. (1971)

40. Merritt, H.E., "Worm Gear Performance", Proc. Inst. Mech. Eng., **129**, 177-194, (1935)

41. Wurtz, A., Comptes Rendus, **18**, 702, (1844). **21**,149, (1845), as referenced by Dennis, J.K., Such, T.E., "Nickel and Chromium Plating", Butterworths, (1972).

42. Breateau, R., Societe Aluminium Francais, U.S. Patent No. 1207218, (5.12.16)

43. Brenner, A., Riddel, G.E., Proc. Amer. Electroplaters Society, **33**, 23, (1946)

44. Brenner, A., Riddel, G.E., Proc. Amer. Electroplaters Society, **34**, 156, (1947)

45. Colin, R., "Electroless Nickel Plating. Catalytic Nickel Deposition by the Kanigen Process", Galvanotechnik, **52**, 158-167, (1966)

46. Gutzeit, G., "An Outline of the Chemistry Involved in the Process of Catalytic Nickel Deposition from Aqueous Solution", Plating, **46**, (10) 1158-64, (11) 1275-8, (12) 1377-8, (1959). **47**, (1) 63-70, (1960)

47. Mallory, G.O., Electroless Nickel Conf., Cincinnati, Ohio, November 1979

48. Gutzeit, G., ASTM Tech. Pub. No. 265, (1959)

49. Machu, W., El-Gendi, S., "Effect of Heavy Metal Salts on the Brightness and Deposition Rates in Electroless Nickel Plating", Metalloberfl, **13**, 97-103, (1959)

50. Muller, K., "Electrochemical Thermodynamics of Chemical Metal Deposition", Metalloberfl, **14**, (3) 65-9, (4) 102-3, (1960)

51. Ishibashi, S., "Theoretical Considerations on Electroless Nickel-Plating Process", Himeji Kogyo Daiguku Ken Kyu Hokoku, No. 13, 68-76, (1961), Chem. Abstr. **56**, 1283, (1962)

52. Gutzeit, G., "Industrial Nickel Coating by Chemical Catalytic Reduction , Trans. I.M.F., **33**, 383-415, (1956)

53. deMinjer, C.E., Brenner, A., "Studies of Electroless Nickel Plating", Plating, **44**, 1297-1301, (1957)

54. Gorbunova, K.M., Nikiforova, A.A., "Reduction of Nickel by Hypophosphite. Conditions of Formation and Several Properties of Layers", Zhur. Fiz. Khim., **28**, 883-96, (1954)

55. Schwizgebel, K., "Phosphite, One of the Causes of the Instability of Chemical Nickel Plating Baths", Metalloberfl, **19**, 390-1, (1965)

56. Panchenko, S.M., Krokhina, M.A., "Chemical Nickel Plating", Vestnik Mashinostroenija, **34**, 68-70, (1954)

57. Lukes, R.M., "The Mechanism for the Autocatalytic Reduction of Nickel by Hypophosphite Ion", Plating, **51**, 969-71, (1964)

58. Nikiforova, A.A., Sadakov, G.A., "Mechanism Underlying the Reactions Taking Place in the Cause of Chemical Nickel Plating", Electrokhimija, **3**, 1207-1211, (1967)

59. Sutyagina, A.A., Gorbunova, K.M., Glazunov, M.P., "The Mechanism of the Chemical Nickel Plating Reaction", Dohyl. Akad. Nauk., SSSR, **147**, 1133-6, (1962)

60. Gawrilov, G.G., "Chemical Electroless Nickel Plating", Portcullis Press, (1979)

61. Graham, A.K., Lindsay, R.W., Read, M.I., "The Structure and Mechanical Properties of Electroless Nickel" and "Structure of Electroless Nickel", J. Electrochem. Soc., **112**, 401-2, (1965), **109**, 1200-1, (1962)

62. Baldwin, C., Such, T.E., "The Plating Rates and Physical Properties of Electroless Nickel-Phosphorus Alloy Deposits", Trans. I.M.F., **46**, 73-80, (1968)

63. Randin, J.P., Hintermann, H.E., "Electroless Nickel Deposited at Controlled pH; Its Mechanical Properties as a function of the Phosphorus Content", Plating, **54**, 523, (1967)

64. Gorbunova, K.M., Nikiforova, A.A., "Physio-Chemical Principles of Nickel Plating", 63-11003, U.S. Dept. Commerce, 207, (1963)

65. Gutzeit, G., Krieg, A., U.S. Patent 2, 658, 841, (1953)

66. Saubestre, E.B., "Electroless Plating Today", Metal, Finishing, **60**, (6) 67-73, (7) 49-53, (8) 45-49, (9) 59-62, (1967)

67. Safranek, W.K., "The Properties of Electrodeposited metals and Alloys - A Handbook", Ch. 22, Elsevier

68. Spencer, L.F., "Electroless Nickel Plating - A Review", Metal Finishing, **72**, (10) 35, (11) 50, (12) 58, (1974), **73**, (1) 38, (1975)

69. International Nickel Company Incorporated, "The Engineering Properties of Electroless Nickel Deposits", (1971)

70. Goldenstein, A., Rastoker, W., Schossberger, F., Gutzeit, G., "Structure of Chemically Deposited Nickel", J. Electrochem. Soc., **104**, (2) 104-110, (1957)

71. Marton, J.P., Schlesinger, M., "The Nucleation Growth and Structure of Thin Ni-P Films", J. Electrochem. Soc., **115**, 16-21, (1968)

72. Wiegand, M., Heinke, G., Schwitzgebel, K., "Properties of Chemical Nickel Deposits from the Hypophosphite Bath", Metalloberfl, **22**, (10) 304-11, (1968)

73. Pai, S.T., Marton, J.P., Brown, J., "Annealing effects on the structure of Ni-P films" J. Appl. Phys., **43**, 282-287, (1972)

74. Randin, J.P., Maire, P.A., Sawer, E., Hintermann, H.E., "D.T.A. and X-Ray Studies of Electroless Nickel", J. Electrochem. Soc., **114**, 442-5, (1967)

75. Randin, J.P., Hintermann, H.E., "Evidence of Nickel Phosphide Ni_2P in As-Plated Electroless Nickel", J. Electrchem. Soc., **115**, (5) 480-4, (1968)

76. Higgs, C.E., "The Effect of Heat Treatment on the Structure and Hardness of an Electrolessly Deposited Nickel Phosphorus Alloy", Electrodeposition and Surface Treatment, **2**, 315-326, (1974)

77. Spahn, H., "Corrosion Fatigue of Metals VII, Internal Stresses in Electro and Chemically Plated Nickel Deposits and their Influence on the Behaviour of Steel under Corrosion Fatigue Conditions", Metalloberfl, **17**, (1) 1-9, (1963)

78. Johnson, C. E., Ogburn, F., "Hardness of Heat Treated Electroless Nickel", Surface Technology, **4**, (2) 161-172, (1976)

79. Parker, K., Shah, M., "Residual Stresses in Electroless Nickel Plating", Plating, **58**, (3) 230-235, (1971)

80. Duncan, R. N., "Performance of Electroless Nickel Coatings in Oil-Free Environments", Corrosion '82 Conf. National Assoc. of Corrosion Engineers, Houston, March, 1982

81. Spahn, H., "The Effect of Internal Stresses on the Fatigue and Corrosion Fatigue Properties of Electroplated and Chemically Plated Nickel Deposits",Trans. I.M.F. **42**, 364-369, (1964)

82. Turns, E.W., Browning, J.W., "Properties of Electroless Nickel Coatings on High Strength Steels", Plating, **60**, 463, (1973)

83. Parker, K., "Hardness and Wear Resistance Tests of Electroless Nickel Deposits", Plating, **61**, 834-840, (1974)

84. Tope, N.A., Baker, E.A., Jackson, B.C.,"Wear Resistance of Electroless Nickel", Plating and Surface Finishing, **63**, (10) 30-34, (1976)

85. Gould, A.J., Bowden, P.J., Harris, S.J., "Fretting Wear and Fretting Fatigue of Electroless Nickel-Phosphorus Coatings", Trans. I.M.F., **61**, 97-104, (1983)

86. Duncan, R.N., "Properties and Applications of Electroless Nickel Deposits", Finishers Management, **26**, (3) 5-8, (1981)

87. Celis, J.P., Roos, J.R., " Kinetics of the Deposition of Alumina Particles from Copper Sulphate Plating Baths", J. Electrochem. Soc., **124**, 1508-11, (1977)

88. Brown, D.S.R., Gow, K.V., "The Composition, Tensile Strengh and Hardness of Electrodeposited Iron Alumina Dispersion Strengthened Alloys", Plating, **59**, 437-441 , (1972)

89. Chen, E.S., Sautter, F.K.,"Porosity in Electrodeposited Gold Alumina Alloys", J. Electrochem. Soc., **117**, 5, 726-728, (1970)

90. Saifullin, R.S., Metallou No. 2,3, 215-8, (1967)

91. Waterman, W.J., British Patent No. 1,032,899, June 1966

92. Withers, J.C., Wright Air Development Division, Tech. Dept. WADD-TR-60-718, 1961

93. Sadowska-Mazur, J., Warwick, M.E., Walker, R.,"Electrodeposition and Properties of Tin/Nickel-Silicon Carbide Composite Coatings", Trans. I.M.F., **64**, 142-148, (1986)

94. Kedward, E.C., Gibson, I.H., Kiernan, B., British Patent. 1,218,179, Jan. 1971, Bristol Aerojet Ltd.

95. Metzger,W., Florian, T.,"The Deposition of Dispersion Hardened Coatings by Means of Electroless Nickel", Trans. I.M.F., **54**, 174-7, (1976)

96. Parker, K., "Hardness and Wear Resistance Tests of Electroless Nickel Deposits", Plating, **61**, 834-841, (1974)

97. Fink, C.G., Prince, J.D., " The Codeposition of Copper with Graphite", Trans. Am. Electrochem. Soc., **54**, 315, (1928)

98. Brown, H., Tcmaszewski, T., Proc. Surface, 88, (1966)

99. Grazen, A. E., U.S. Patent No. 3,061,525

100. Simions, A., U.S. Patent 2,571,772, (1951)

101. Kishi, M, et al, J. Metal Fin. Soc. Japan, No. 10,16, 453-62, (1965)

102. Aguese, G.H.L., Belgian Patent No. 506,837, (1951)

103. Metzger, W., et al, Galvanotechnik, 998 , (1970)

104. Kedward, E.C., "Electrodeposited Composite Coatings for Tribological Applications", Metallurgia, 225-228, (1969)

105. Kedward, E. C., "Electrodeposited Composite Coatings", Cobalt, **66**, 3, 53-59, (1973)

106. Kedward, E.C., "The Development of Wear Resistant Electrodeposited Composite Coatings for Use in Aero Engines", Trans. I.M.F., **54**, 8-16, (1976)

107. Kedward, E.C., Wright, K.W., "The Wear Control of Aircraft Parts Using a Composite Electroplate" Plating and Surface Finishing., 38-41, Aug. (1978)

108. Cameron, B.P., Foster, J., Carew, J.A., "The Effect of Carbide Content and Pre-Heat Treatment on the Oxidation of Cobalt-Chromium Carbide Electrodeposits in Air at 1000^0C", Trans. I.M.F., **57**, 113, (1979)

109. Hubbel, F.M., "Chemically Deposited Composites - A New Generation of Electroless Coatings", Trans. I.M.F., **56**, 65-69, (1978)

110. Sinha, P.K., " Electrodeposited Nickel Alumina Codeposition", Plating, **64**, 55, (1973)

111. Sautter, F.K., "Electrodeposition of Dispersion Hardened Ni-Al_2O_3 Alloys", J. Electrochem. Soc., **110**, 557-560, (1969)

112. Pushpovanom, M. et al, "Nickel Alumina Oxide Composite Coatings", Metal Finishing, **75**, (4), 38-43, (1977)

113. Williams, R.V., Martin, P.W., "Electroplated Composite (Metal/Non-Metal) Coatings", Trans. I.M.F., **42**, 182-187, (1964)

114. Vishwanathan, W., "Occlusion Plating to form Nickel Cermets", Metal Finishing, **71**, (1), 38-43, (1973)

115. Brandes, E.P., et al, "Electrodeposition of Cermets", Metallurgia, **76**, (11) 195-197, (1967)

116. Gillann, E., McVie, K.M., Phillips, M., "Electrodeposited Composite Coatings", J. Inst. Metals, **94**, 228, (1966)

117. Ishimori, et al, Suzuki Motor KK, Japanese Patent 5311131 (1976)

118. Vishwanathan, M., Doss, A., "Occlusion Plating of Nickel Cermets", Metal Finishing, **70**, 83-84, (1972)

119. Bristol Aerojet, British Patent No. 1,224,166

120. Murphy, R.J., American Soc. of Metals Trans., **60**, (1) 29, (1967)

121. Safranek, W.K., "Fibre Reinforced Electroforms", Plating, **55**, (6) 605, (1968)

122. Sautter, F.K., "Electrodeposition of Dispersion Ni-Al_2O_3 Alloys", J. Electrochem. Soc., **110**, 6, 557-68, (1963)

123. Roberts, B.L. et al, French Patent No. 1,578,551

124. Foster, J., Kariappar, A.M., "A Study of the Mechanism of Formation of Electrodeposited Composite Coatings", Trans. I.M.F., **51**, 27, (1973)

125. Kedward, E.C. et al, British Patent No. 1,214,166

126. Vest, L.E., Bazarre, D. F., "Codeposited Nickel Molybdenum Disulphide", Metal Fin., **65**, (11), 52, (1967)

127. Tomaszewski, T. W., Tomaszewski, L., Brown, H., "Co-deposition of Finely Dispersed Particles with Metal", Plating, **50**, 1234-1239, (1969)

128. Schwedhelon, A.E., et al, U.S. Patent, 3,342,566

129. Mitchell, D.C., Proceedings of Conference on Lubrication and Wear, Inst. Mech. Eng. 396, (1958)

130. Williams, R.V., Martin, P.W., Proc. 6th Int. Conf. on Electrodep. and Metal Fin. 182-187, (1964)

131. Faust, L.C., "The development of Porous Metal", Trans. I.M.F. 31, 517-526, (1954)

132. Donakowski, W.A., Morgan, J.R., "Zinc/Graphite-A Potential Substitute for Anti-Galling Cadmium" Plating and Surface Finishing, **70**, 48-51, (1983)

133. Ghouse, M., Viswanathan, M., Ramachandran, E.G., "Friction and Wear Characteristics of Electrodeposited Nickel-Graphite and Nickel-MoS_2 Composites", Metal Finishing, **78**, 57-63, (1980)

134. Yukotsuya, et al, Trans. A.S.L.E., **3**, (17), 229-235, (1973)

135. AKZO N.V. British Patent 1,511,109 (1978)

136. Plastiques, S.A., French Patent 1,316,700 (1963)

137. Boyer, J.J., French Patent 1,319,408 (1962)

138. Vandervell Products Ltd., British Patent 1,032,899 (1966)

139. Schwedhelon, A.E., U.S. Patent 3,342,566

140. Bazzard, R., Boden, P.J., "Nickel Chromium Alloys by Codeposition: Part Two, Diffusion Heat Treatment of Codeposited Composites", Trans. I.M.F. **50**, 207-210, (1972)

141. Wearmouth, W.R., "Nickel Alloy Electrodeposits for Non-Decorative Applications", Trans. I.M.F., **60**, 68-73, (1982)

142. Sova, V., "Electrodeposited Composite Coatings for Protection from High Temperature Corrosion", Trans. I.M.F., **65**, 21-23, (1987)

143. Newnham, M., Foster, J., "The Production and Evaluation of Electrodeposited Cobalt Alloys Containing Chromium, Tungsten and Carbon", Technical Publications, BAJ Ltd.

144. Honey, F., Kedward, E.C., Wride, V., "The Development of Electrodeposits for High-Temperature Oxidation/Corrosion Resistance", J. Vac. Sci. Technol. A 4 (6), 2593-7, Nov/Dec, (1986)

145. Varadi, P.F., et al, "Simultaneous Catopheretic and Electrolytic Deposition of Nickel for Cathode Bases of Reliable Electron Tubes", J. Electrochem., **109**, (4), 292-296, (1962)

146. Guglielmi, N., "Kinetics of the Deposition of Inert Particles from Electrolytic Baths", J. Electrochem. Soc., **119**, 1000-1012, (1972)

147. Snaith, D.W., Grooves, P.D., "A Study of the Mechanism of Cermet Electrodeposition", Trans. I.M.F., **50**, 95-101, (1972)

148. Lakshminarayanan, G.R., Sautter, F.K., "Technical Report," WVT 7024, Watervliet Arsenal, Watervliet, New York. (1970)

149. Kariapper, A.M.J., Foster, J., "Further Studies on the Mechanism of Formation of Electrodeposited Composites", Trans. I.M.F., **52**, 87-91, (1974)

150. Foster, J., Cameron, B., "The Effect of Current Density and Agitation on the Formation of Electrodeposited Composite Coatings", Trans. I.M.F., **54**, 178-183, (1976)

151. Brands, E. A., Goldthorpe, D., "Electrodeposition of Cermets", Metallurgia, **11**, 195-198, (1967)

152. Sykes, J.M., Alner, D.J., "Mechanism for the Formation of Electrodeposited Composite Coatings", Trans. I.M.F., **52**, 28-31, (1974)

153. Martin, P.W., "Electrodeposition of Composite Coatings", J. Metal Fin., **11**, 339-403, (1965)

154. Roos, J.R., Celis, J.P., Kelchtermans, H., "Dispersion-Hardened Electrolytic Copper-Alumina Coatings", Thin Solid Films, **54**, 173-182, (1978)

155. Bazzard, R., Boden, P.J., "Nickel Chromium Alloys by Codeposition: Part One, The Effect of Current Density", Trans. I.M.F., **50**, 63-67, (1972)

156. Williams, R.V., Martin, P.W., Pro. 6th. International Conference on Electrodeposition and Metal Finishing, 182-187, (1964)

157. Foster, J., Cameron, B., " The Effect of Cermet Density and Agitation on the Formation of Electroplated Composite Coatings", Trans. I.M.F., **54**, 178-183, (1976)

158. Lakshminarayanan, G.R., Chen, E.S., Sautter, F.K., "The Effect of Oxide Dissolution on the Electrodepositing of Dispersion-Hardened Co and Ni-Al_2O_3", Plating, **63**, 35-39, (1976)

159. Celis, J.P., Roos, J.R., "Kinetics of the Deposition of Alumina Particles from Copper Sulphate Plating Baths", J. Electrochem. Soc., **124**, 1508-11, (1977)

160. Tomaszewski, T.W., "Effect of Anions on the Formation of Electrodeposited Composite Coatings: Some Experimental Evidence", Trans. I.M.F., **54**, 45-48, (1976)

161. White, C., Foster, J., "A study of Particle Cathode Adhesion During the Formation of Electrodeposited Composite Coatings", Trans. I.M.F., **56**, 92-96, (1978)

162. Roos, J.R., celis, J.P., Helson, C, "Codeposition of Alpha and Gamma Alumina with Copper from Copper Sulphate Baths", Trans. I.M.F., **55**, 113-116, (1977

163. Foster, J., Walton, P., To be published.

164. Metzger W., Galvanotechnik, **63**, 722, (1970); Blasberg Bull **25**, (1973); Oberflachentechnik **51**, 510, (1974); VDI-Berichte, 242, 39, (1975)

165. Metzger, W., U.S. Patent 3,617,363

166. Parker, K., Interfinish 72 202, (1972)

167. Gawrilov, G., Galvanotechnik, **65**, 858, (1974)

168. Lukschandel, J., "Diamond-Containing Electroless Nickel Coatings", Trans. I.M.F., **56**, 118-120, (1978)

169. Parker, K., U.S. Patent 3,562,000

170. Shiekh, S., PhD Thesis, Aston University, (1979)

171. Kiowa, I., Osaka, T., "Codeposition of Cr Powders into Electroless NI-B Films" Journal Metal Fin. Soc. of Japan, **35**, 155-159, (1984)

172. Pratt, G.C., "Material for Plain Bearings", International Metallurgica Reviews, **18**, (1973)

173. Takeuchi,E., "The Mechanisms of Wear of Cast Irons in Dry Sliding", Wear, II, 201-211, (1968)

174. Channell, D., "The Operation of Ball Mills", The Industrial Chemist, Feb., (1951)

175. Hankin, J., PhD Thesis, Exeter University, (1957)

176. Brenner, A., Senderoff, S., "Calculation of Stress in Electrodeposits from the Curvature of a Plated Strip" Journal of Research, **42**, 105-123, (1949)

177. Gulbransen, E., Kenneth, E.,"Kinetics of the Oxidation of Chromium", J. Electrochem. Soc., **104**, 334-338, (1957)

178. Gould, A.J., W. Cannings, Private Communications

179. Stern,O., Z.Elektrochem,**30**, 508, (1924) as referenced by Adamson, A., "Physical Chemistry of Surfaces", Interscience Publisers, (1967)

180. Gouy,.G., J. Phys, **9**, 457 (1910), Chapman, D.L., Phil. Mag, **25**, 475 (1913) as referenced by Adamson, A., "Physical Chemistry of Surfaces", Interscience Publisers, (1967)

181. Fuks, G. et al., Kolloid. Zhur., **21**, 718-730, (1959)

182. Zimmon, A., Deryagin et al., Kolloid. Zhur., **27**, 685-689, (1965)

183. Koros, E., et al, Hiradastech. Ipari. Kutatuo. Int. Kozlemeny, 6 (1), 71-77, 89 (1966)

184. Isrealachvili, J., Adams, G., Nature, 262, (1966)

185. Deryagin, B. et al., Kolloid Zhur., **31**, 47-52, (1969)

186. Pearce, C., "Polytetrafluoroethylene-Electroless Nickel Composite, Product Finishing, **37**, 6,(1984)